ELECTROCHEMICAL DETECTION OF CERTAIN SPECIFIC POLLUTANTS FROM WATER USING NANOSTRUCTURED CARBON-BASED COMPOSITE ELECTRODES

Teză destinată obţinerii
titlului ştiinţific de doctor inginer
la
Universitatea "Politehnica" din Timişoara
în domeniul Inginerie Chimica
de către

Ing. Anamaria Simona SCHEAU

Conducător ştiinţific:	prof.univ.dr.ing. Georgeta BURTICĂ
Referenţi ştiinţifici:	prof.univ.dr.dr.h.c. Joop SCHOONMAN
	prof.univ.dr.ing. Carmen TEODOSIU
	conf.univ.dr.ing. Andrea KELLENBERGER

Ziua susţinerii tezei: 06 decembrie 2012

Seriile Teze de doctorat ale UPT sunt:

1. Automatică
2. Chimie
3. Energetică
4. Ingineria Chimică
5. Inginerie Civilă
6. Inginerie Electrică
7. Inginerie Electronică şi Telecomunicaţii
8. Inginerie Industrială
9. Inginerie Mecanică
10. Ştiinţa Calculatoarelor
11. Ştiinţa şi Ingineria Materialelor

Universitatea „Politehnica" din Timişoara a iniţiat seriile de mai sus în scopul diseminării expertizei, cunoştinţelor şi rezultatelor cercetărilor întreprinse în cadrul şcolii doctorale a universităţii. Seriile conţin, potrivit H.B.Ex.S Nr. 14 / 14.07.2006, tezele de doctorat susţinute în universitate începând cu 1 octombrie 2006.

România, 300159 Timişoara, Bd. Republicii 9,
tel. 0256 403823, fax. 0256 403221
e-mail: editura@edipol.upt.ro

Foreword

The PhD thesis has been developed during of my activity at the „Departament of Applied Chemistry and Engineering of Inorganic Compounds and Environmental" of University „Politehnica" of Timisoara.

I tank to God, for letting me through all the difficulties. I have experienced Your guidance day by day. You are the one who let me finish my thesis. I will keep on trusting You for my future. Thank You, Lord.

I would like to express my sincere gratitude to my advisor **Prof.dr.eng. Georgeta Burtica** for her guidance, support, help, advice, immense knowledge and she is trust in me.

It would not have been possible to write this doctoral thesis without the help, support and guidance of the **Assoc.prof.dr.eng. Florica Manea**, who have been a tremendous mentor for me. I would like to thank you for encouraging my research and for allowing me to grow as a research scientist. I am also extremely indebted for her valuable advice, constructive criticism and her extensive discussions around my work. It has been an honour to be in your research group and I appreciate all your contributions of time, ideas and funding to make my PhD. experience productive and stimulating. The joy and the enthusiasm she has for her research was contagious and motivational for me, even during tough times in the PhD. pursuit. She is an inspiration.

I would like to thank the rest of my thessis committee: **Prof.dr.h.h.c. Joop Schoonman,** from Technical University of Delft, Holand, **Prof.dr.eng. Carmen Teodosiu**, from University „Gheorghe Asachi", Iasi, and **Conf.dr.eng. Andrea Kellenberger**, from University „Politehnica", of Timisoara for their encouragements, insightful comments and valuable suggestions. I would also like to thank to the **Prof.dr.eng. Rodica Pode** for her advice, time, and helpful comments.

I would also like to thank my colleague's research group. The group has been a source of friendships as well as a good advice and collaboration. To my special friend, **Sorina Motoc**, she was always beside me during the happy and hard moments to push me and motivate me; thank you for the support, encouragement, and care, understanding and precious friendship. I gratefully acknowledge to **Aniela Pop, Corina Orha, Adriana Remes, Agnes Jakab, Liliana Colar, Magdalena Ardeleanu**, **Laura Cocheci**, for their precious times to help me in this project, love, care, support and creating a pleasant atmosphere for me here.

Last but not least, I would like to thank my family for all their love and encouragement and their constant moral support; **my parents** who raised me with a love of science and supported me in all my preoccupations; to my sister **Sonia**, and **my in-laws**, for the moral support. And most of all for my loving, supportive, encouraging, and patient husband **Marius** whose faithful support during the final stages of this Ph.D. is so appreciated. Thank you.

I would like to thank all those who contributed in many ways to the success of this study, those people who made this thesis possible and made it an unforgettable experience for me.

This research would not have been possible without the financial support of the strategic grant **POSDRU/88/1.5/S/50783 (2009)** of the Ministry of Labor, Family and Social Protection, Romania, co-financed by the European Social Fund – Investing in people within the Sectoral Operational Programme Human Resources Development 2007-2013 and the **PN-II-ID-PCE 165/2011**.

Timişoara, decembrie 2012 Anamaria Simona SCHEAU

Scheau, Anamaria Simona

ELECTROCHEMICAL DETECTION OF CERTAIN SPECIFIC POLLUTANTS FROM WATER USING NANOSTRUCTURED CARBON-BASED COMPOSITE ELECTRODES

Teze de doctorat ale UPT, Seria 4, Nr. 65, Editura Politehnica, 2012, 169 pagini, 79 figuri, 22 tabele.

ISSN: 1842-8223

ISBN: 978-606-554-584-7

Cuvinte cheie: electroanalysis, electrochemical detection, carbon-based composite electrodes, persistent organic polltants, heavy metals pollutants

Rezumat,

This research aimed the elaboration and manufacturing of some carbon based composite electrode materials with useful properties for the electrochemical detection of persistent organic pollutants from water. Also, the elaboration and manufacturing of silver-(doped zeolite)-modified carbon based composite electrodes suitable for the electrochemical detection of arsenic from water was aimed. Morphological, electrical and electrochemical characterization of the electrode materials was investigated. The electrode materials behaviour in different supporting electrolytes and in the presence of the target analyte, to establish the relationship between obtained electrode material and reaction type was assessed. The detection protocols for both the individual electrochemical determination of pentachlorophenol, arsenic (III) and simultaneous electrochemical determination of arsenic (III) and lead (II) from water were elaborated based on the assessment of the detection experiments performance. Specific informations regarding the voltammetric/amperometric detection type, detection potential value, concentration ranges, electrode sensitivity, stability, reproducibility and lifetime, detection limits, calibration were provided. Exploitation of the specific features of the pulsed voltammetric/amperometric techniques allowed improving the electroanalytical performance for the detection of the pollutant from water. The specific compositions of the unmodified/silver-modified carbon-based composite electrodes were selected to elaborate the detectors characterized by the real utility potential for pentachlorophenol, arsenic (III) and lead (II) detection from water.

TABLE OF CONTENTS

NOTATIONS, ABBREVIATIONS, ACRONYMS

AAS - atomic absorption spectroscopy
AFS - atomic fluorescence spectrometry
ASSWV - anodic stripping square-wave voltammetry
ASV - anodic stripping voltammetry
ATSDR - agency for Toxic Substances and Disease Registry
CA - chronoamperometry
CE - capillary electrophoresis
CL - chemiluminescence
CME - chemically modified electrode
CNF - carbon nanofiber
CNF-Ag - chemically-decorated carbon nanotubes
CNF-EG-Epoxy - carbon-nanofiber expanded graphite-epoxy
CNF-Epoxy - carbon nanofibers-epoxy
CNF-Epoxy (Ag) - silver-electrochemically decorated carbon nanofibers
CNF-ZNAg-Epoxy - silver-doped natural zeolite-modified carbon nanofibers-epoxy
CNT - carbon nanotube
CNT-Epoxy - carbon nanotubes-epoxy
CNT-Epoxy (Ag) -silver-electrochemically decorated carbon nanotubes zeolite-modified carbon nanotubes-epoxy
CNT-ZAAg-Epoxy (Ag) - silver-electrochemically decorated silver-doped synthetic carbon nanotubes-epoxy
CNT-ZN/ZA-Ag - epoxy-silver-doped natural or synthetic zeolite-modified carbon nanotubes-epoxy
CRQL - Contract Required Quantitation Levels
CSV - cathodic stripping voltammetry
CV - cyclic voltammetry
DMA - dimethylarsinate
DMAA - dimethyl arsenic acid
DMF - dimethylformamide
DNA - deoxyribonucleic acid
DPP - differential-pulsed polarography
DPV - differential-pulsed voltammetry
ECD - electron capture detection
EG-Epoxy - expanded graphite epoxy
EPA - United State Environmental Protection Agency
ETAAS - electrothermal atomic absorption spectrometry
ETV - electrothermal vaporisation
EU - European Union
FI - flow injection technique
FIA - MIMS-flow injection analysis coupled with the membrane introduction mass
FPP - four-point probe resistance measurements

GC - glassy carbon
GFAA - graphite furnace atomic absorption
GFAAS - graphite furnace absorption spectrometry
HGAAS - hydride generation atomic absorption spectroscopy
HMDE - hanging mercury drop electrode
HPLC – high performance liquid chromatography
HS-LPM - headspace liquid-phase microextraction
HS-SPME - headspace solid-phase microextraction
ICP - inductively coupled plasma
ICP-AES -inductively coupled plasma-atomic emission spectrometry
IUPAC - International Union of Pure and Applied Chemistry
LC - liquid chromatography
LIBS - laser induced breakdown spectroscopy
LLE - liquid–liquid extraction
LPME - liquid-phase microextraction
LOD - the lowest limit of detection
LSV - linear-sweep voltammetry
LQ - limit of quantification
MIMS - membrane introduction mass spectrometry
MMA - monomethylarsonate
MMAA - monomethyl arsenic acid
MPA - multiple-pulsed amperometry
MS - mass spectrometry
MWCNTs - multiwalled carbon nanotubes
NADH - nicotinamide adenine dinucleotide
NPL - National Priority List of hazardous substances
PAD - pulsed amperometric detection
PCBs - polychlorinated biphenyls
PCDFs - polychlorodibenzenzofurans
PCDDs - polychlorodibenzodioxins
PCP - pentachlorophenol
PDMS - polydimethylsiloxane
PEO - polyethylene oxide
ppb - parts per billion
ppm - parts per million
PS - polystyrene
PVC - polyvinyl chloride
RCRA - Resource Conservation and Recovery Act
RP - reversed-phase
RSD - relative standard deviation
SCE - saturated calomel reference electrode
SDME - single-drop microextraction
SEM - scanning electron microscopy
SERS - surface-enhanced Raman spectroscopy
SPE - solid-phase extraction
SPME - solid-phase microextraction
SWCNTs - single-walled carbon nanotubes

SWV - square-wave voltammetry
THF - tetrahydrofuran
TRM - two roll mill procedure
UV-VIS - ultraviolet–visible spectroscopy
Z-Ag - silver-modified zeolite
ZMEs - zeolite-modified electrodes
ZN/ZA - natural / synthetic zeolite
WHO - World Health Organization
wt – weight.

LIST OF TABLES

LIST OF FIGURES

CHAPTER 1. WATER QUALITY MONITORING

1.1. The presence of the organic pollutants in water

Considerable ecological problems with severe impact for all existing organism has been produced, in the last period, due to the huge quantities of synthetic chemicals, such as solvents, plasticizers, insecticides, herbicides, and fungicides discharged into the environment through industrial, agricultural, medical, and domestic activities [1].

These substances include phenolic compounds and its derivates, which have been classified as priority pollutants by the US Environmental Protection Agency [2]. This Federal Register List includes eleven substituted phenols that are considered hazardous for human health and depending to their toxicity degree, and the maximum admissible concentration ranged between 60-400 μg/l. Thus, for some phenolic compounds the maximum admissible concentration in drinking water, according to the World Health Organization (WHO), must be of 200 μg/l for 2,4,6-trichlorophenol, 9 μg/l for pentachlorophenol, 10 μg/l for 2-chlorophenol and 40 μg/l for 2,4-dichlorophenol [3, 4].

In agricultural practice, phenolic compounds are used as pesticides, herbicides, insecticides or, may be obtained from the degradation of the chlorophenoxycarboxylic herbicides and organophosphorous insecticides [5]. In addition, they are used as disinfectant and reagent in chemical analysis, and furthermore the alkylphenols can develop from alkylphenol polyethoxylates transformation, present in detergents as non-ionic surfactants. They can arrive in the water environment through industrial and domestic wastes and through treated sewage discharges [6].

The concentrations of phenol in surface water are different, *e.g.*, in natural waters its amounts are between 0.01 – 2.0 μg/L. River water polluted with sewage derived from petrol processing plants contained the concentration of phenol over 40 mg/L [7].

One of the most important and widespread groups of phenols are chlorophenols. They are found in wastewater, sludge products, surface waters, and groundwater [8-10]. Other sources of contamination are accidental spills, hazardous waste disposal sites, storage tanks, or municipal landfills.

These synthetic organic compounds are formed in the environment on widely industrial and commercial scales by chlorination of mono and polyaromatic compounds present in soil and water, or hydrolysing chlorobenzenes, or as a result of the use and degradation of phenolic pesticides [11, 12]. The chlorophenols are frequently used as precursors in the production of dyes or pharmaceuticals, and also are used as bactericides, insecticides, herbicides, fungicides, wood preservatives [2, 13-16], or as by-products of other industrial operations, such as pulp bleaching with chlorine, water disinfection or even waste incineration [28]. The chlorophenols are very toxic, the noxious produced by these compounds can cause genotoxicity, mutagenicity, and carcinogenicity [18, 19].

In the aquatic environment, chlorophenols exist as dissociated, non-dissociated or adsorbed onto suspended matter. The forms of occurrence of

chlorophenols depend on pH of the environment, as well as on physical and chemical properties of the particular compounds. The concentrations of chlorophenols in oceanic waters are of 5-10 ng/L. The highest concentrations are noted for river waters and are in the range of 2-2000 μg/L. Also, it was reported that Canadian drinking water was contaminated, about 20% of the samples containing PCP [20].

Chlorophenols are chlorinated aromatic ring structures consisting of the benzene ring, –OH group and atoms of chlorine. From the selected group of chloroderivatives, the methyl- and ethyl-phenols are also considered as chlorophenols. However, each other chloroderivatives, from the whole group of tens of chlorophenols compounds are considerably differing with their molecular structure, and therefore with their physical and chemical properties. All chlorophenols are solids at room temperature, except one, *i.e*. 2-chlorophenol which is a liquid. In general, these compounds dissolve weakly in water, but well in organic solvents. Their water solubility decreases with increasing number of chlorine atoms in a molecule. They are weakly acidic, their acidity is slightly lower than that of phenols. In reactions with alkaline metals (sodium, potassium) in the aquatic environment, they yield salts highly soluble in water [21, 22]. Toxicity of chlorophenols depends on the degree of chlorination and the position of chlorine atoms relative to the hydroxyl group.

Toxicity of chlorophenols decreases with the number of chlorine substituents. Also, toxicity of chlorophenols increases if chlorines are substituted at the 3-, 4- and 5- positions. This regularity may account for higher toxicity of 3, 4, 5-trichlorophenol compared to other chlorophenols. In contrast, lowering of toxic properties is due to simultaneous occurrence of chlorine atoms substituted at the positions 2- and 6- or only at the position 2-.This proposition may be confirmed by comparing toxicity of 2,6-dichlorophenol and 3,5-dichlorophenol and it was demonstrate that 2,6-dichlorophenol is less toxic than 3,5-dichlorophenol. These facts may suggest that PCP is more toxic than other chlorophenols [23-27].

Pentachlorophenol is a synthetic substance, made from other chlorophenols and chlorophenoxyphenols, and depending on the manufacturing method contain a large number of microcontaminants, mainly, polychlorodibenzodioxins (PCDDs), polychlorodibenzenzofurans (PCDFs), polychlorophenoxyphenols, hexachlorobenzene and polychlorinated biphenyls (PCBs), and does not occur naturally in the environment [28].

Pure pentachlorophenol exists as needle-like crystals, consists of light tan to white, and is relatively volatile; impure pentachlorophenol is dark to brown and exist as dust or flakes. It is soluble in most organic solvents but only slightly soluble in water, it can be found like pentachlorophenol itself or like as the sodium salt of pentachlorophenol [29].

Pentachlorophenol has become one of the most versatile and widely used biocides due to their efficiency, broad spectrum, and low cost. The total world production of pentachlorophenol it has been estimated to be of the order of 30 000 tons per annum. Among its many and varied applications in the industrial, agricultural, and domestic fields, pentachlorophenol has been used extensively in water systems as a molluscicide for bilharzia control, as a fungicide for wicker products such as baskets, as indoor disinfectant for cleaning floors, leather and textile application, as an ingredient in antifouling paint, as an insecticide (termiticide), herbicide, algicide. However, the principal use of pentachlorophenol is as a wood preservative, particularly on a commercial scale. The domestic use o pentachlorophenol is of minor importance in the overall pentachlorophenol market,

but has been of particular concern because of possible health hazards associated with the indoor application of wood preservatives containing pentachlorophenol; for example, it has been reported that the measured concentration of pentachlorophenol in the indoor air of an treated log-cabin brushed with pentachlorophenol is in the range of 0.5-10 parts per trillion. [30]

However, in recent years most developed countries have been restricted the use of pentachlorophenol as product in wood preserving solutions or insecticides and herbicides available for home and garden because of increasing concern about the potential health and environmental hazards of this compound and its impurities [30].

Pentachlorophenol is widely distributed in all environmental media – air, soil, and water due to its past use in various fields. Therefore, pentachlorophenol has been broadly detected in surface water, sediments and groundwater because of discharge from factories, wood-treatment installation, and hazardous waste sites. As well, it enters in the soils as a result of its past use as a pesticide, spills at industrial facilities using PCP, disposal at hazardous waste sites, and solubilisation from treated wood products. However, the pentachlorophenol may be released in the air by evaporation from treated wood surfaces, and from chemical and/or wood preservation plants that disposal the waste. Moreover, it has been detected in human urine, human milk, blood, and adipose tissue [31].

PCP is very toxic to all forms of life, and the compound is quickly photolyzed by sunlight and can be metabolized by microorganisms, animals, and plants, but the levels of PCP in water and food are low, so that the ingestion of contaminated groundwater used as a source of drinking water, ingestion of contaminated food and soils, contributes in a small proportion of the human body weight. Pentachlorophenol is known to volatilize from treated wood products, from painted surfaces and the levels of the PCP in room air varied very much with temperature and ventilation, for example in older residences constructed with treated wood products, inhalation of contaminated indoor air may be an important source of exposure, or from painted wood within an enclosed indoor swimming area may be other source of exposure by evaporation of PCP from them. By coating the treated wood surfaces with varnishes and epoxy coatings, it may reduce the volatilization of pentachlorophenol [32].

Therefore, there is no question that PCP it may be considered dangerous under any conditions such as: medicinal use, air in treated buildings, or on indoor wood surfaces where it is not matter to photochemical or microbial degradation, and itself can represent a severe toxic hazard to expose.

The adsorption or mobility of pentachlorophenol onto soils is controlled primarily by environment pH, and also, the degradation and its tendency to disperse by solubilisation is affected by the degree of adsorption of PCP. The amount of pentachlorophenol adsorbed increases with increasing organic content of the environmental media, but also, the PCP is strongly adsorbed by volcanic ash soil [33, 34]. Pentachlorophenol is adsorbed to a moderate degree to environmental media under acidic conditions, but the compound moves quite rapidly in ionized form under neutral or alkaline conditions [35]. In addition, it has been reported that the adsorption is maximum at a media pH of 4.6—5, and no adsorption occurs above pH 6.8 [36]. Moreover, the presence of cosolvents such as alcohols or petroleum hydrocarbons decreases the adsorption of pentachlorophenol in soils by increasing its solubility in the soil solution [37]. This may also be important at spill, storage, and hazardous waste sites, where a large amount of cosolvent would be estimated. In addition, in the presence of methanol in contaminated soils, the

pentachlorophenol was desorbed more readily and presents an affirmative correlation with increasing methanol concentration [38]. Furthermore, the mobility of pentachlorophenol, pentachlorodibenzodioxins, and pentachlorodibenzofurans in soils contaminated with wood-preserving oil, decreases the adsorption of the compounds in soil as a result of the presence of a subsurface, contaminated oil phase [39].

Pentachlorophenol releases to surface water occur through direct discharge and direct entry from numerous sources, including treated wood. In surface waters, pentachlorophenol undergoes biotransformation and photolysis, and is adsorbed to sediments. Hydrolysis, oxidation, and volatilization do not considerably affect surface water concentrations. In addition, pentachlorophenol is transported to surface waters from the atmosphere by wet deposition and from soil by overspill and leaching. Most of the pentachlorophenol removed from effluent streams by wastewater treatment processes is adsorbed to sludge solids.

Chlorination of phenolic compounds during water treatment has been reported to produce detectable levels of pentachlorophenol [40]. In addition, common pesticides such as lindane, hexachlorobenzene, pentachlorobenzene, and pentachloronitrobenzene are known to be metabolized to pentachlorophenol by plants, animals, and/or microorganisms [41]. Approximately 90% of wood-treatment plants evaporate their waste water and, consequently, have no direct discharge to surface waters. The remainder of the plants discharges to municipal wastewater treatment facilities [42].

Concerns regarding contamination of environmental media, the natural waters and effluents, plants, and animals, with hazardous waste, in particular, pentachlorophenol and substituted phenols, and due to their appearance from wide range of activities have led to the developing new and more efficient and at the same time more rapid, sensitive and selective methods of analysis. Therefore, many phenolic compounds have been included in the environmental legislation. So, in this context, the pentachlorophenol is one of the eleven phenol compounds cited in the List of Priority Pollutants of the United State Environmental Protection Agency (EPA). Under EPA's regulation the maximum contaminate level for semivolatiles such as pentachlorophenol in water is 50 mg/L, in low soil sediments is 160 mg/kg, in drinking water is at 1 ppb; while under European Union (EU) legislation regarding this hazardous substance, PCP, the Contract Required Quantitation Levels (CRQL) for drinking water has to be 0.5 ppb. [43-45].

1.2. The presence of the heavy metals in water

Metals are inorganic substances that occur naturally in geological formations. Their presences in water are normally and, in small quantities are not harmful for the health. In fact, some heavy metals are nutritionally essential for a healthy life.

Such inorganic substance essential for life and that existing for normal body functions are calcium, magnesium, potassium, and sodium, and also are metals in our body that, at low levels help the activities of enzyme to be more rapid, such metals are cobalt, copper, iron, manganese, molybdenum, selenium, and zinc. But, in addition to these metals essential in our body and that are normally available in our chain food and water, the drinking water contains metals, which cause acute or chronic poisoning [46, 47].

Otherwise, these heavy metals are considered ones of the most persistent and dangerous pollutants in water, because they are difficult to degrade, have the

ability to persist in natural ecosystems for an extended period, and can accumulate throughout the food chain, producing potential human health risks and ecological disturbances [48, 49]. Their presence in water is due to two pathways, the first is natural geochemistry, meaning that the trace amounts of metals presence in soil or rocks are percolates of rain through rocks and enter naturally in water supplies. The second way is own to human activities, including discharges from residential dwellings, and also, because of the industrial wastes and agriculture activities that have released these toxic materials in the groundwater and in that way led to the contamination of drinking water [50, 51].

Actually, there is are list containing certain metals that are considered very hazardous and that may have negative effects on the plants and animals but, may also cause health hazards to human. Such metals include arsenic, lead, mercury, aluminium, barium, cadmium, chromium, nickel, selenium, thallium, beryllium, copper. Based on the above presented consideration, these heavy metals are monitored frequently by the public water supplies [52-54].

To reduce pollution sources, to remedy polluted water resources, and to minimize the effects of the presence of heavy metals that can affect the quality of drinking water supply, it is necessary the implementation of standards regarding the maximum contaminated levels for these heavy metals and also, the promulgation of several legislation and worldwide directive. Therefore, to achieve unpolluted drinking water distribution and waste water discharge is a nationally and internationally challenge and concern [55, 56].

The need for environmental sustainability and for the minimization of the health and environmental impacts of the presence of heavy metals in aquatic systems that preserves precious natural resources and biological lives requires an economically viable and effective technology [57, 58].

In general, a single technology for the treatment of the water and for detection of the heavy metal presents both the advantages and disadvantages [59]. Due to the enormous benefits and drawbacks of each of the existing treatment technologies/processes, there is a need for the implementation of an integrated treatment technology which can have great potential [60].

The most ubiquitous of toxic metals in drinking water is arsenic. Arsenic is a metalloid with the atomic number 33, atomic weight 74.9216, symbol As and placed in the group Va of the periodic table of elements together with nitrogen, phosphorus, antimony and bismuth. Arsenic is a redox-sensitive element, which means that can gain of an electron by reduction and loss of an electron trough oxidation.

It has been reported that the occurrence, source distribution, mobility, and forms of arsenic in water depend on the interaction of some factors such as pH conditions, adsorption-desorption, precipitation-dissolution, oxidation-reduction reactions, ion-exchange of other ion species, particle size, organic contents, and biological activity and aquatic characteristics [61, 62].

Arsenic is an omnipresent element, which occurs naturally in the earth's crust. In the literature is cited as the 20th most abundant element in the earth’s crust, 14th in the seawater and 12th in the human body, and it is found in areas with active volcanism, geothermal waters, and sedimentary rocks and in soils with a high concentration of sulphides. In fact, it is now acknowledged that the drinking water is the major source of human intake of arsenic in its most toxic (inorganic) forms. Although, elemental arsenic is not soluble in water, and arsenic salts exhibit a wide range of solubility depending on pH and the ionic environment. Thus, it is considered one of the most toxic elements meeting in the environment, especially

that the presence of arsenic, even at high concentrations, is not accompanied by any change in taste, odor or visible appearance of water. The presence of arsenic in drinking water is therefore difficult to detect without complex analytical techniques [63, 64].

Arsenic is largely distributed in the environment throughout earth crust, soil, sediments, water, air, and living organism. Arsenic is usually found in the environment associated with other elements such as oxygen, chlorine and sulfur and has as result the inorganic form of arsenic. But also, it can be found in combination with carbon and hydrogen forming the organic form of arsenic. Arsenic cannot be destroyed in the environment. It can only change its form, or become attached to or separated from particles. It may change its form by reacting with oxygen or other molecules present in air, water, or soil, or by the action of bacteria that live in soil or sediment [65, 66].

Toxicity is expressed as the number of milligrams of the compound per kilogram of body weight that will result within a few days in the death of half of those who ingest it in a single dose. Arsenic toxicity strongly depends on the form in which arsenic is present. Inorganic arsenic forms, typical in drinking water, are much more toxic than organic ones that are present in sea food. Inorganic arsenic compounds in which arsenic is present in trivalent form are known to be the most toxic [67].

The toxicity and mobility of arsenic varies with its valency state and chemical form. As (III) is generally more toxic to humans and four to ten times more soluble in water than As (V) [68, 69]. The valency state of an element plays an important role for the behaviour of the element in the aqueous system. Thus, the toxicity of As (III) is higher than that of their pentavalent species. The valency state of an element also determines the sorption behaviour and consequently the mobility in the aquatic environment. The toxicity of different arsenic species varies in the order: arsenite > arsenate > monomethylarsonate (MMA) > dimethylarsinate (DMA). The concentration of arsenic in natural waters depends on the geological composition and the degree of pollution of the environment [70-73].

Arsenic is perhaps unique among the heavy metalloids and oxyanion-forming elements (*e.g*. arsenic, selenium, antimony, molybdenum, vanadium, chromium, uranium, and rhenium) maybe due to it exists in nature in the five oxidation states (+V (arsenate), +III (arsenite), 0 (arsenic) and -III (arsine)) and all the form of arsenic are different not only by their physical and chemical forms but also vary in toxicity and mobility. The valency and species of inorganic arsenic are dependent on the redox conditions and the pH of the water.

Based on the redox conditions, in the aquatic media inorganic arsenic appears commonly in the oxidation states +V and +III. As arsenous acid (As (III)), the reduced trivalent form, which is the dominant form under reducing conditions, and normally is found in groundwater, under oxidizing conditions, in surface water, the stable species is arsenic acid (As (V)), which is strongly sorbed onto clays, iron and manganese oxides/hydroxides and organic matters [74-79].

Based on pH, As (III) exists in five forms: $H_4AsO_3^+$, H_3AsO_3, $H_2AsO_3^-$, $HAsO_3^{2-}$, and AsO_3^{3-}. Similarly, As (V) exists in four forms in aqueous solution H_3AsO_4, $H_2AsO_4^-$, $HAsO_4^{2-}$, and AsO_4^{3-}. As (III) is neutral at pH <9 and ionic at pH >9, and at pH>3 the dominate ionic forms is of As (V) [80].

Consequently, growing interest in the determination of different species of arsenic in environment is caused due to the fact that physiological and toxic effects of arsenic are related with its oxidation state, which influences also the degree of bioavailability. Thus, knowledge of the speciation of arsenic in the environment is

importance for remedy decisions. Speciation analysis of environmental samples involves both the identification and the quantification of the total quantity of arsenic and also, the different physico-chemical forms of the element. However, the predominant reason for speciation studies is to measure the toxic part of the arsenic [81, 82]. Total arsenic is the sum of both particulate arsenic, which can be removed by a 0.45- micron filter, and soluble arsenic. Soluble arsenic occurs in two primary forms: inorganic and organic. Inorganic arsenic can occur in the environment in several forms and valences, but in natural waters, and thus in drinking-water, it is mostly found as trivalent arsenite (As (III)) or pentavalent arsenate (As (V). Organic arsenic species are abundant in seafood, and include such forms as monomethyl arsenic acid (MMAA), dimethyl arsenic acid (DMAA), and arseno-sugars. They are very much less harmful to health, and are readily eliminated by the body [83-85].

Arsenic in its most recoverable form is found in various types of metalliferous deposits. In the major deposits of this type the arsenic is common in iron pyrite, galena, and chalcopyrite and less common in sphalerite. The most common arsenic mineral is arsenopyrite. Volcanic eruptions and other natural processes are sources of high arsenic concentrations in the environment [86].

There is a variety of sources of As in the environment, and drinking water perhaps is the most danger to human health. Drinking water is derived from a diversity of sources depending on local availability: surface water (rivers, lakes), groundwater and rain water. Beside noticeable point sources of As contamination, high concentrations are mostly found in groundwater. The presence of arsenic in natural water is related to the process of leaching from the arsenic containing source rocks and sediments [87].

The occurrence of arsenic in natural water is generally related with the geochemical environments such as catchments deposits, volcanic deposits, and inputs from geothermal sources, mining wastes and wastes deposits. The presence of arsenic in natural water depends on the local geology, hydrology and geochemical characteristics of the aquifer resources [88].

Furthermore, the geochemical characteristics of the aquifer material and their interactions with the aqueous media also play an important role in controlling retention and/or mobility of arsenic within the underground environment [89].

Arsenic is concentrated in some reducing marine sediment, and it might be co-precipitated with iron hydroxides and sulphides in sedimentary rocks. Iron deposits, sedimentary iron ores and manganese piles were abundant in arsenic. Arsenic naturally occurs in many different mineral forms, of which arsenates are in the highest proportion, followed by the sulfides and sulfosalts which are in the same percentage, and the remaining amount includes arsenides, arsenites, oxides, silicates and elemental arsenic (As) [90].

Although arsenic occurs naturally in the earth' crust, but, the anthropogenic sources exceed the natural sources regarding arsenic contamination of the environment. Mainly contamination source are owed the human activities by their utilization of natural sources releasing the arsenic into the air, water and soil. The source that arise from the hand-made activities may include the disposal of industrial and animal wastes, the burning of fossil fuels, the smelting of arsenic bearing minerals, and also, the application of arsenic compounds in many products, for example, the widely use of arsenic compounds for the preparation of pesticides and insecticides for agricultural activities, the extensively use of inorganic arsenicals as weed killers, or broadly use of arsenic acid as a cotton desiccant, and also many arsenic compounds are used for feed additives [91, 92].

It has been reported in literature that, the concentration of arsenic is usually less than 2 μg L^{-1} in seawater, in unpolluted surface water and groundwater the levels of arsenic vary typically from 1–10 μg L^{-1}, in freshwater, the variation is in the range of 0.15–0.45 μg L^{-1} and in thermal waters, concentrations of arsenic is up to 8.5 mg L^{-1} and 1.8–6.4 mg L^{-1}. [93-95].

The World Health Organization (WHO) has establishing a new arsenic standard for the drinking water at 10 μgL^{-1} down from the current 50 μgL^{-1} level (*i.e*. from 0.05 mg/l to 0.01 mg/l), to reduce public health risks from arsenic in water systems. The value of 10 μg/ was set as reasonable limit taking into account the widespread negative health effects on humans and practical problems associated with its removal at lower levels. The WHO provisional guideline of 10 μg/L has been adopted as a national standard by most countries, including Japan, Jordan, Laos, Mongolia, Namibia, Syria and the USA, and by the European Union (EU). For countries like Bangladesh and India that still retain the limits of 50 μg/L and which have a serious problem in terms with arsenic concentration in excess in their groundwater, the implementation of a lower limit of arsenic in drinking water is not practicable. Other countries like Bolivia, China, Egypt, Indonesia, Saudi Arabia, Sri Lanka, Vietnam and Zimbabwe, still keep the older standard of 50 μg/L regarding their drinking water standards.

Arsenic concentrations above accepted standards for drinking water have been regarded as a global issue due to the large number of countries on all continents that it has been reported it presence in groundwater [96-99].
Arsenic has been reported in groundwater in the following countries, among others:

Asia	Bangladesh, Cambodia, China (including provinces of Taiwan and Inner Mongolia), India, Iran, Japan, Myanmar, Nepal, Pakistan, Thailand, Vietnam
America	Alaska, Argentina, Chile, Dominica, El Salvador, Honduras, Mexico, Nicaragua, Peru, United States of America
Europe	Austria, Croatia, Finland, France, Germany, Greece, Hungary, Italy, Romania, Russia, Serbia, United Kingdom
Africa	Ghana, South Africa, Zimbabwe,
Pacific	Australia, New Zealand

Table 1.1. The presence of arsenic in groundwater from several countries [100].

1.3. References

[1] K. Furukawa, Biosci.Biotechnol. Biochem. 70 (2006) 2335.
[2] ATSDR (2007).
[3] EPA136 (1984a) 58.
[4] EPA/635/R-02/006 (2002).
[5] S. Lacorte, D. Barcelo, Environ. Sci. Technol. 28 (1994) 1159.
[6] M.L. Davi, F. Gnudi, Water. Res. 33 (1999) 3213.
[7] EPA/600/8-86/003F (1986).
[8] S.K. Samanta, O.V. Singh, R.K. Jain, Trends Biotechnol. 20 (2002) 243.
[9] C. Zhang, G.N. Bennett, Appl Microbiol. Biotechnol. 67 (2005) 600.
[10] A. Geng, A.En-WeiSoh, C.J. Lim, C.T.L. Loke, Appl. Microbiol. Cell. Physiol. 71 (2006) 728.

[11] J. Michałowicz, W. Duda, Polish. J. Environ. Stud. 18 (2009) 845.
[12] N. Schweigert, A.J.B. Zehnder, R.I.L. Eggen, Environ. Microbiol. 3 (2001) 81.
[13] M.D. Murcia, M. Gomez, E. Gomez, J.L. Gomez, F.A. Sinada, N. Christofi, Chem. Eng. 10 (2007) 2.
[14] C. Yang, C. Lee, J. Hazard. Mater. 152 (2008) 159.
[15] W.S. El-Sayed, M. Ismaeil, F. El-Beih, Res. J. Cell. Mol. Biol. 3 (2009) 20.
[16] S.E. Murialdo, R. Fenoglio, P.M. Haure, J.F. González, Water SA 29 (2003) 457.
[17] ATSDR (1999).
[18] M.M. Häggblom, I.D. Bossert, Kluwer Academic Publishers Boston Mass (2003) 3–29.
[19] Canadian Water Quality Guidelines for the Protection of Aquatic Life (1999).
[20] T. Ivanciuc, O. Ivanciuc, J.K. Douglas, Int. J. Mol. Sci. 7 (2006) 358.
[21] K. Furukawa, Biosci. Biotechnol. Biochem. 70 (2006) 2335.
[22] H. Saito, M. Sudo, T. Shigeoka, F. Yamauchi, Environ. Toxic. Chem. 10 (1991) 235.
[23] M. Czaplicka, Chromatographia 53 (2001) S470.
[24] M. Czaplicka, Sci. Total. Environ. 322 (2004) 21.
[25] A.O. Olaniran, E.O. Igbinosa, Chemosphere 83 (2011) 1297.
[26] Canadian Soil Quality Guidelines for the Protection of Environmental and Human Health (1997).
[27] J. Michałowicz, Polish. J. Environ. Stud 14 (2005) 327.
[28] Pentachlorophenol Health and Safety Guide, International Programme on Chemical Safety, Health and Safely Guide, no 19, Geneva.
[29] Environmental Chemistry of Pentachlorophenol, Pentachlorophenol in Drinking water. Guide no. 19.
[30] D.E. Boy, K. Killham, A. Meharg, Chemosphere 43 (2001) 157.
[31] J. Michałowicz, W. Duda, Polish. J. Environ. Stud. 16 (2007) 347.
[32] S. Kuwatsuka, M. Igarashi, Soil. Sci. Plant. Nutr. 21 (1975) 405.
[33] K.K.C. Tse, S.L. Lo, Water Res. 36 (2002) 284.
[34] S. Kuwatsuka M. Igarashi, Soil. Sci. Plant. Nutr. 21 (1975) 405.
[35] J. Choi, S. Aomine, Soil. Sci. Plant. Nutr. 20 (1974) 135.
[36] S.C. Tam, S.A. Johnson, A. Graham, Water Air Soil Poll. 115 (1999) 337.
[37] J.H. Kim, W.S. Shin, D.I. Song, S.J. Choi, Water Air Soil Poll. 166 (2005) 367.
[38] C. Bulle, F. Bertrand, R. Samson, L. Deschênes, Chemosphere 73 (2008) S149.
[39] G.F. Lee, J.C. Morris, Int. J. Air Wat. Poll. 6 (1962) 419.
[40] W.A. Anwar, Environ. Health Persp. 105 (1997) 801.
[41] ATSDR (2011).
[42] A.M. Awawdeh, H. J. Harmon, Sensor. Actuat. B 106 (2005) 234.
[43] C. Li, Microchim. Acta 157 (2007) 21.
[44] M.A. Quiroz, S. Reyna, J.L. Sanchez, J. Solid. State. Electr. 7 (2003) 277.
[45] H.M. Salem, E. A., Eweida, A. Farag, ICEHM Cairo University Egypt September (2000) 542.
[46] A. Martin-Gonzalez, S. Díaz, S. Borniquel, A. Gallego, J.C. Gutierrez, Res. Microbiol. 157 (2006) 108.
[47] S.M. Nomanbhay, K. Palanisamy, Electron. J. Biotechnol. 8 (2005) 43.
[48] Y. Xu, T. Xu, IEEE. Xplore. (2008) 2789.
[49] W.O. Nelson, P.G.C. Campbell, Environ. Pollut. 71 (1991) 91.
[50] J. Gardea-Torresdey, J.R. Peralta-Videa, G.D. Rosa, J.G. Parsons, Coord. Chem. Rev. 249 (2005) 179.
[51] H. Hussein, S. Farag, K. Kandil, H. Moawad, Process. Biochem. 40 (2005) 955.
[52] S.U. Khan, A. Moheman, Pollut. Res. 25 (2006) 99.

[53] D.B. Johnson, K.B. Hallberg, Sci. Total. Environ. 338 (2005) 3.
[54] R. Athar, M. Ahmad, Water Air Soil Poll. 138 (2002) 165.
[55] P. Rajendran, J. Muthukrishnan, P. Gunasekaran, Indian J. Exp. Biol. 41 (2003) 935
[56] E. Aksorn, P. Visoottiviseth, Sci. Asia 30 (2004) 105.
[57] R.F. Fuggle, M.A. Rabie, Juta Cape Town (1983).
[58] M. Humar, F. Pohleven (2006) http://www.bfafh.de/inst4/45/ppt/7bioremd.pdf.
[59] O. B. Akpor, M. Muchie, Int. J. Phys. Sci. 5 (2010) 1807.
[60] M.C. Shih, Desalination 172 (2005) 85.
[61] M.D. Safiuddin, M. Karim, Groundwater, Proc. 1st IEB Int. Conf. 7th Annual Paper Meet, Chittagong, Bangladesh 2-3 November (2001).
[62] B.K. Mandal, Kazuo T. Suzuki, Talanta 58 (2002) 201.
[63] M. Kumaresan, P. Riyazuddin, Curr. Sci. 80 (2001) 837.
[64] S. Mahimairaja, N. S. Bolan, D. C. Adriano, B. Robinson, Adv. Agron. 86 (2005) 1.
[65] J. Matschullat, Sci. Total. Environ. 249 (2000) 297.
[66] W.R Chappell, C.O. Abernathy, R.L Calderon, Proc. Third Int. Conf. Arsenic Exposure and Health Effects, 14-18 July San Diego California (1998) S.l.
[67] http://www.epa.gov/nrmrl/pubs/625r97009/625r97009.pdf, USEPA (1997).
[68] http://www.osha.gov/SLTC/healthguidelines/arsenic/recognition.html, USOSHA (2001).
[69] I. Pizarro, M. Gómez, C. Cámara, M.A. Palacios, Anal. Chim. Acta 495 (2003) 85.
[70] M. Leermakers, W. Baeyens, M. De Gieter, B. Smedts, C. Meert, H.C. De Bisschop, R. Morabito, Ph. Quevauviller, Trend. Anal. Chem. 25 (2006) 1.
[71] E. Terlecka, Environ. Monit. Assess. 107 (2005) 259.
[72] S. McSheehy, J. Szpunar, R. Morabito, P. Quevauviller, Trend. Anal. Chem. 22 (2003) 191.
[73] J.F. Ferguson, J. Gavis, Water Res. 6 (1972) 1259.
[74] N.E. Korte, Q. Fernando, Crit. Rev. Env. Cont 21 (1991) 1.
[75] R. Cheng, S. Liang, H.C. Wang, M.D. Beuhler, J. Am. Water. Work. Assoc. 86 (1994) 79.
[76] J.G. Hering, V.Q. Chiu, J. Environ. Eng. 126 (2000) 471.
[77] K. Fytianos, Speciation. J. AOAC. Int. 84 (2001) 1763.
[78] J.H. Huang, E. Matzner, Sci. Total. Environ. 377 (2007) 308.
[79] M Edwards, S. Patel, L. McNeill, H.W. Chen, M. Frey, A.D. Eaton, R.C. Antweiler, H.E. Taylor, J. Am. Water. Work. Assoc. 90 (1998) 103.
[80] A. Kot, J. Namiesnèik, Trend. Anal. Chem. 19 (2000) 69.
[81] Z. Gong, X. Lu, M. Ma, C. Watt, X. C. Le, Talanta 58 (2002) 77.
[82] S. Garcia-Manyes, G. Jimenez, A. Padro, R. Rubio, G. Rauret, Talanta 58 (2002) 97.
[83] P. Carrero, A. Malavé, J.L. Burguera, M. Burguera, C. Rondón, Anal. Chim. Acta 438 (2001) 195.
[84] K. Wrobel, K. Wrobel, B. Parker, S.S. Kannamkumarath, J. A. Caruso, Talanta 58 (2002) 899.
[85] M.E. Ortiz Escobar, N.V. Hue, W.G. Cutler, University of Hawaii Honolulu HI USA (2005).
[86] M.M. Karim, Water Res. 34 (2000) 304.
[87] P.L. Smedley, D.G. Kinniburgh, Appl. Geochem. 17 (2002) 517.
[88] A.H. Welch, R.S. Oremland, J.A. Davis, S.A. Watkins, San Francisco Estuar Water Sci 4 (2006) 1.

[89] P. Bhattacharyaa, A.B. Mukherjee, G. Jacksa, S. Nordqvist, Sci. Total. Environ. 290 (2002) 165.
[90] V.K. Sharma, M. Sohn, Environ. Int. 35 (2009) 743.
[91] M. Bissen, F.H. Frimmel, Acta Hydrochim. Hydrobiol. 31 (2003) 1.
[92] J.C. Ng, J. Wang, A. Shraim, Chemosphere 52 (2003) 1353.
[93] R.E. Stauff., J.M. Thompson, Geochim. Cosmochim. Acta 48 (1984) 2547.
[94] M. Bissen, F.H. Frimmel, Acta. Hydrochim. Hydrobiol 31 (2003) 97.
[95] B. Petrusevski, S. Sharma, J.C. Schippers, K. Shord, Ed Peter McIntyre Oxford UK (2007) 1-13.
[96] http://www.who.int/water_sanitation_health/dwq/gdwq3/en/, WHO (2004).
[97] http://www.who.int/water_sanitation_health/dwq/arsenic3/en/.
[98] http://www.epa.gov/tio/tsp/download/arsenic_issue_paper.pdf.
[99] http://www.who.int/mediacentre/factsheets/fs210/en/.
[100] E.S. Gurzau, A.E. Gurzau, Elsevier Science, New York, (2001) 181–184.

CHAPTER 2. QUANTITATIVE DETERRMINATION METHODS OF PHENOLIC DERIVATES IN WATER

The phenolic derivates can exist in water cycle in relation to the water sources and treatment. Thus, in water treatment plant, the disinfection of drinking water by chlorination, for example, produces several chlorophenols, which can give to water a specific taste and odor even at lower concentrations of 1 μg/L [1]. Acceptable levels of phenolic compounds in drinking water vary within the 1-10 μg/L range or less [2]. In addition, an important phenolic derivates source is represented by specific wastewater, which is discharged in surface water. Based on this reasons, selective and sensitive analytical techniques are used to monitor these severe water contaminants [3].

Due to its high sensitivity, the classical colorimetric method based on the red colour obtained by condensing ortho- and meta- substituted phenols with 4-aminoantipyrine (4- AAP) is extensively used to determine the total content of phenols in water. However, this method has some drawbacks, for example, it is nonselective and consequently it is not capable to distinguish the various possible phenol contaminants. Another disadvantage is the necessity of sample pretreatments by distillation to remove potential interferences, but several phenols fail to distil completely [4].

Due to their low concentration or complicated matrices in environment of the phenols and its derivates, it has been developed analytical procedures for the separation and preconcentration of these contaminants. Thus, procedures like liquid–liquid extraction (LLE) [5, 6], liquid-phase microextraction (LPME) [7, 8], headspace liquid-phase microextraction (HS-LPME) [9] solid-phase extraction (SPE) [10, 11] solid-phase microextraction (SPME) [12, 13] headspace solid-phase microextraction (HS-SPME) [14], and single-drop microextraction (SDME) [15], have been successfully employed with satisfactory results. Because these methods are time-consuming and necessitate toxic solvents, such: chlorobenzene, carbon tetrachloride, tetrachloroethylene and carbon disulfide as extraction solvents, they are not suitable for on-line or in-situ monitoring of phenols in the environment [16]. However, most of these methodologies fail when analysing both free and bound phenols, especially in the case of nitrophenols and chlorinated phenols [17, 18].

In order to enhance considerably the determination of phenols from water, comparatively with the extraction and preconcentration methods, has been employed the derivation and anhydrides methods by derivation phenols directly in water [19].

It has been reported that using the off-line acetylation of phenols in water coupled with the membrane introduction mass spectrometry (MIMS) [20] enhanced the limit of detection in the range of 0.5-10 μg/L about two times, resulting a direct, selective, sensitive method for phenol quantification [21]. Also, coupling the flow injection analysis with the membrane introduction mass spectrometry (FIA-MIMS) providing a great technique for the efficient monitoring of phenols in environmental water samples, with excellent quantitative precision and accuracy, high analytical frequency, simplicity of the experimental setup, and economy of sample [22]. The

combination of FIA coupled with MIMS with on-line acetic anhydride derivation shows major advantages, *e.g.*, detection limits in the range of µg/L, no need the extraction or preconcentration steps, a high selectivity, accuracy and rapidity for the trace level quantitation of phenolic compounds in water [23].
Another alternative analytical technique that it has also been reported for the analysis of these compounds [24], and that can provide high separation efficiency, small sample and electrolyte consumption, rapid analysis, is capillary electrophoresis (CE) [25, 26].

It has been reported that to obtain very low detection limit, with a simple instrumentation, the analytical detection method suitable is chemiluminescence (CL). This technique can be applied for the determination of phenol, but due to lack of selectivity for phenol, chemiluminescence systems cannot determine phenol in water samples directly. Phenol can be determined only when the CL system is combined with some separation procedures like liquid chromatography and capillary chromatography [27].

In addition, for the reliable identification of the environmental matrices it has been reported that the mass spectrometry is the only method that can achieved this. However, this technique has identification purposes, and in order to correct response the mass spectrometry (MS) detection was coupled with liquid chromatography (LC) method [28]. However, LC-MS still shows low sensitivity and, in order to reach the phenolic compound levels in environmental samples, extraction and enrichment steps are always necessary prior to their instrumental determination [29]. Still, the most common analytical methods described in the literature for detecting, and/or measuring, and/or monitoring of phenol and phenol derivative compounds of environmental importance are made by means of spectrophotometric and chromatographic analysis.

High-performance liquid chromatography (HPLC) combined with ultraviolet (UV) detection (HPLC/UV) was used to measure chlorinated phenols in surface-treated lumber and to distinguish the phenol derivatives [30]. It has been reported a method using gas chromatography/mass spectrometry for determination pentachlorophenol and related compound as residues in vegetable matrixes [31]. HPLC offers a rapid and sensitive method when it was used for detection of chlorophenols from comparatively clean water samples, but when a complex matrix such as municipal waste water has to be analyzed its advantages are lost.
A possible method for the detection and quantification of chlorinated phenols at trace levels in complex matrices was the choice of using capillary gas chromatography combined with the selectivity of the electron capture detection (ECD) towards halogenated compounds as a good method [32]. Good results were reported for extraction and determination of phenol in a urine sample [33, 34]. It was described a rapid screening method and developed a solid-phase microextraction method for determination of chlorophenols in wood, paper, fruits [35, 36]. However, these methods require expensive and most often laboratory complicated instruments. The specific cost of analysis can be high, and the methods are not suitable for in situ measurements.

The electrochemical techniques appear to be very attractive because offer the prospect of a reasonably good analytical performance characteristics (high sensitivity, good selectivity, rapid response), with relatively simple and low cost equipment, and regarding the possibility of miniaturization and automation which may allow obtaining an analytical devices for in situ measurement. Also, they allow detection of trace amount of such compound like pentachlorophenol with detection

limit compatible with environmental legislation, and comparable with the other methods described above at lower concentration range, and also, above of all, they are environmental friendless [37-39].

Direct anodic oxidation of pentachlorophenol is one of the most promising electrochemical methods for its detection in the aqueous solutions. The complex direct electrochemical oxidation process of such chlorophenols depends on the type of electrode employed. Thus, the improvement in chlorophenol determination by electrochemical techniques needs the development of the alternative electrode materials, which do not exhibit the hazardous potential for human health like the traditionally mercury surface, and which can avoid the negative interference that occur at the surface by the secondary products resulted from oxidation of the chlorophenol during the electrochemical oxidation process [40-43].

Therefore, it is widespread comprehension that the electrooxidation of phenolic compounds occur at various type of electrode materials, but successful results were reported on carbon based sensors, because they belong to the new generation of so-called environmentally friendly sensors. Although phenol derivates in general, can be oxidized at many electrode materials, the oxidation at carbon-based solid electrodes produces phenoxy radicals, which couple to form an insulating polymeric film fouling the surfaces of the electrodes. A simple method of renewing the electrode surfaces is based on the anodic treatment. This relies on adjusting the working electrode potential high enough to oxidize the insulating film and making it water-soluble without damaging the electrode. To avoid the electrode fouling, several variants of the chemically modified carbon based electrodes, *i.e.*, graphite, carbon fibers and carbon nanotubes are very promising for the detection of the phenolic compounds [38, 44-47].

Another remarkable and reasonably new approach is based on the effort to change traditionally electrodes with composite materials containing nanoparticles of suitable electrocatalysts. Thus, a lot labor has been carried out in order to obtain and characterize various types of composites and it appears that these materials guarantee not only enhanced analytical performances (mostly due to higher active surface area) but also, in several cases, improved resistance to fouling [48-51].

2.1. References

[1] M.L. Davi, F. Gnudi, Water Res. 33 (1999) 3213.
[2] M. Knutsson, J.A. Jonsson, Marcel Dekker, NewYork 18 (2000) 347.
[3] American Public Health Association: New York, 1997 (5530 method).
[4] J. Farino, G. Norwitz, W.J. Boyko, P.N. Keliher, Talanta 28 (1981). 705.
[5] S. Kjellstrom, O.N. Jensen, Anal. Chem. 75 (2003) 2362.
[6] S.X. Peng, C. Henson, M.J. Strojnowski, A. Golebiowski, S.R. Klopfenstein. Anal. Chem. 72 (2000) 261.
[7] X.W. Wang, L.Y. Luo, G.F. Ouyang, L. Lin, N.F.Y. Tam, C.Y. Lan, T.G. Luan, J. Chromatog. A 1216 (2009) 6267.
[8] Z. Es'haghi, Am. J. Anal. Chem. 2 (2011) 1.
[9] H. Xu, Y. Liao, J. Yao, J. Chromatogr. A. 1167 (2007) 1.
[10] A.H. El-Sheikh, A.A. Insisi, J.A. Sweileh, J. Chromatogr. A 1164 (2007) 25.
[11] W. Buchberger, P. Zaborsky Sorptive Acta Chim. Slov. 54 (2007) 1.
[12] M.N. Sarrion, F.J. Santos, M.T. Galceran, J. Chromatogr. A 947 (2002) 155.
[13] F. Augusto, E. Carasek, R.G.C. Silva, S. R. Rivellino, A. D. Batista, E. Martendal, J. Chromatogr. A1217 (2010) 2533.

[14] J. Regueiro, E. Becerril, C. Garcia-Jaresa, M. Llompart, J. Chromatogr. A 1216 (2009) 4693.
[15] K. Choi, S.J. Kim, Y.G. Jin, Y.O. Jang, J.S. Kim, D.S. Chung, Anal. Chem. 81 (2009) 225.
[16] Q. Zhou, Y. Gao, J. Xiao, G. Xie, Anal. Method. 3 (2011) 653.
[17] C.M. Santana, Z.S. Ferrera, M.E.T. Padron, J.J.S. Rodríguez, Molecules 14 (2009) 298.
[18] J.L.M. Vidal, A.B. Vega, A.G. Frenich, F.J.E. Gonzalez, F.J.A. Liebanas, Anal. Bioanal. Chem. 379 (2004) 125.
[19] T.J. Boyd, J. Chromatogr. A 662 (1994) 281.
[20] R.A. Ketola, T. Kotiaho, M.E. Cisper, T.M. Allen, J. Mass. Spectrom. 37 (2002) 457.
[21] M. Ojala, R.A Ketola, T. Mansikka, T. Kotiaho, R. Kostiainen, Talanta 49 (1999) 179.
[22] S. Satienperakul, S.Y. Sheikheldin, T.J. Cardwell, R.W. Cattrall, M.D. Luque de Castro, I.D. McKelvie, S.D. Kolev, Anal. Chim. Acta 485 (2003) 37.
[23] R.M. Alberici, R. Sparran, W.F. Jardin, M.N. Elberlin, Environ. Sci. Technol. 35 (2001) 2084.
[24] Z. Demianová, H. Sirén, R. Kuldvee, M.L. Riekkola, Electrophoresis 24 (2003) 4264.
[25] T.D. Mai, S. Schmid, B. Müller, P.C. Hauser, Anal. Chim. Acta 665 (2010) 1.
[26] M.A. Hossain, S.M. Salehuddin, As. J. Energy. Env. 10 (2009) 91.
[27] H. Qi, J. Lv, B. Li, Spectrochim. Acta A 66 (2007) 874.
[28] H.T. Björkman, P.O. Edlund, S.P. Jacobsson, Anal. Chim. Acta 468 (2002) 263.
[29] J.L.M. Vidal, A.B. Vega, A.G. Frenich, F.J.E. Gonzalez, F.J.A. Liebanas, Anal. Bioanal. Chem. 379 (2004) 25.
[30] C.R. Daniels, E.P. Swan, J. Chromatogr. Sci. 17 (1979) 628.
[31] C. Mardones, J. Palma, C. Sepulveda, A. Berg, D. von Baer, J. Sep. Sci. 26 (2003) 923.
[32] R.S.K. Buisson, P.W.W. Kirk, J.N. Lester, J. Chromatogr. Sci. 22 (1984) 339.
[33] M. Guidotti, M. Vitali, J. High Resol. Chromatogr. 21 (1998) 137.
[34] M.L. Menezes, A.C.C.O. Demarchi, J. Liq. Chromatogr. R.T. 21 (1998) 2355.
[35] J.M. Diserens, J AOAC Int 84 (2001) 853.
[36] C. Domeno, G. Munizza, C. Nerın, J. Chromatogr. A 1095 (2005) 8.
[37] M.S.P. Francisco, W.S. Cardoso, L.T. Kubota, Y. Gushikem, J. Electroanal. Chem. 602 (2007) 29.
[38] A.Bebeselea, F. Manea, G. Burtica, L. Nagy, Geza Nagy, Talanta 80 (2010) 1068.
[39] L. Codognotoa, V.G. Zuinb, D. de Souzaa, J.H. Yariwakeb, S.A.S. Machadoa, L.A. Avac, Microchem. J. 77 (2004) 177.
[40] P. Cannizares, J. Garciia-Goomez, C. Saaez, M.A. Rodrigo, J. Appl. Electrochem. 34 (2004) 87.
[41] Z. Mojovic, A. Milutinovic, N.S. Mentus, D. Jovanovic, Chem. Eng. Technol. 32 (2009) 738.
[42] C. Berrıos, R. Arce, M.C. Rezende, M.S. Ureta-Zanartu, C. Gutierrez, Electrochim. Acta 53 (2008) 2768.
[43] E.C. Guijarro, P. Yanez-Sedeno, J.M. Carrazon, L.M.P. Diez, Fresen. J. Anal. Chem. 339 (1991) 193.
[44] W.Q. Zhang, G.B. Zhu, J.Y. Ma, X.H. Zhang, J.H. Chen, Indian J. Chem. 50A (2011) 15.

[45] B. Sljuki, C.E. Banks, A. Crossley, R.G. Compton, Anal. Chim. Acta 587 (2007) 240.
[46] E.C. Guijarro, P. Yafiez-Sedefio, J.M.P. Carrazon, L.M.P. Diez, Analyst 113 (1988) 625.
[47] **A. Baciu,** F. Manea, A. Remes, S. Motoc, G. Burtica, R. Pode, Environ. Eng. Manag. J. 9 (2010) 1555.
[48] T. Spataru, N. Spataru, J. Hazard. Mater. 180 (2010) 777.
[49] T. Spataru, M. Marcu, A. Banu, E. Roman, N. Spataru, Electrochim. Acta 54 (2009) 3316.
[50] C.H. Tzang, C.W. Li, J. Zhao, M. Yang, Anal. Lett. 38 (2005)1735.
[51] J. Manso, M.L. Mena, P. Yanez-Sedeno, J. Pingarron, J. Electroanal. Chem. 603 (2007) 1.

CHAPTER 3. ANALYTICAL DETERMINATION OF ARSENIC

3.1. Introduction

Arsenic is cited the second main inorganic contaminant after lead in the National Priority List (NPL) of hazardous substances, [1] and in the Resource Conservation and Recovery Act (RCRA) it is regulated as one of the toxic materials, [2], and also according to the World Health Organization, inorganic arsenic has been classified as a potent human carcinogen [3].

As opposed to organic pollutants, arsenic cannot be transformed into a non-toxic material, and it cannot be easily destroyed, only can be transformed into different forms or converted into insoluble compounds in combination with other elements, having a form that is less toxic to organisms in the environment [4].

Since arsenic occurs naturally in the environment and many impurities such as lead, iron and selenium may be mixed up together with arsenic wastes, there is an urgent need for regular monitoring which imposes to develop simple, reliable, sensitive, and inexpensive equipment for field measurement [5, 6]. A range of analytical field-tests for pollutants such as arsenic provide valuable tools to support enhanced site characterization [7].

The utilization of the analytical methods for determination of the arsenic from water may be considered an integrated approach with respect to the public health, environmental protection and of a safe and economical alternative.

Generally, the laboratory instrumentations are utilized for an accurately determination of arsenic in drinking water within the range of parts per billion (ppb) concentrations. The laboratory methods for the measurement of arsenic imply pretreatment, either acidic extraction or acidic oxidation digestion of the environmental sample, by which the arsenic from the sample is transformed into an arsenic acid solution, and then is measured using analytical methods.

These analytical techniques include: atomic absorption spectroscopy (AAS) [8], atomic fluorescence spectrometry (AFS) [9], inductively coupled plasma (ICP) [10], ICP/mass spectrometry (MS) [11], and inductively coupled plasma-atomic emission spectrometry (ICP-AES) [12], graphite furnace atomic absorption (GFAA), hydride generation atomic absorption spectroscopy (HGAAS) [13]. Such techniques provide limits of detection well below the WHO arsenic guideline (10 ppb), but are fixed laboratory instrumentation. They are also time consuming, expensive to operate and maintain, bulky, and they require fully equipped and staffed laboratories to maintain and operate, and not suitable for routine monitoring of large numbers of samples [14].

3.2. Hydride generation

The current baseline methodology involves a variety of technologies that are all variations of the "Gutzeit" method, developed over 100 years ago [15]. This method involves the transformation of the arsenic compounds presents into the water sample into arsine gas with reducing reagents like sodium or potassium

tetrahydroborate. This procedure can differentiate As (III) from As (V) since As (III) reacts with tetrahydroborate at a higher pH than As (V). Thus, tetrahydroborate is acting as a reductant for As (V) as well as a hydride source. However, sulfur, selenium, and tellurium compounds have the potential of interfering with the determination of arsenic due to reaction of the interfering transition metal ions with the sodium borohydride reductant [16].

A considerable amount of research has been dedicated to developing an arsenic-detection colorimetric method that matches or exceeds the sensitivity of the "Gutzeit" method while improving safety, accuracy, and reproducibility. Thus, the main purpose of the one group of the researches was to reduce electrochemically the arsenite ion into arsine gas, and to rich low detection limits, down to 50 ppb arsenite using this method [17, 18].

Another research direction has been concentrated on the reducing the arsenic compounds in arsine gas by chemical reaction between the arsenic and a dye. This system has been shown to be an effective method for measuring arsenate, with limits of detection for arsenic as low as 30 ppb [19-21].

Another strategy for improving the sensitivity and selectivity of an assay uses the inclusion of on-line HG separation and reduces the possible interferences from the sample matrix. Hydride generation (HG) based sample introduction is particularly beneficial to atomic fluorescence spectrometry (AFS) detection, where the interferences had previously been the major problem due to scattering and sample matrix [22, 23].

Furthermore, the inclusion of the flow injection (FI) technique allowed the elimination of transition metal interferences. It has been reported that by using the FI system instead of the batch system, the concentration of the reluctant is usually lower and formation of the interfering precipitates, *e.g*. borides, is decreased [24-27].

Hydride generation (HG) combined with atomic absorption spectrometry (AAS) and atomic fluorescence spectrometry (AFS) and also coupled with different separation techniques such as liquid–liquid extraction [28], resin based low pressure ion exchange chromatography [29, 30], cold trapping [31], selective derivatisation [32] and HPLC [34-35] have brought a high level of sensitivity to speciation of arsenic compared to the colorimetric detection techniques often used for environmental samples.

3.3. Graphite furnace atomic absorption spectrometry (GFAAS)

It has been reported for the determination of arsenic without hydride generation, spectrometric methods, graphite furnace absorption spectrometry (GFAAS) or electro-thermal atomic absorption spectrometry (ETAAS). The technique is based on the absorption of free atoms produced from the sample deposited in a small graphite tube, which can be heated by the application of high temperatures. On the other hand, for arsenic detection using this technique is required a pre-concentration in order to increase sensitivity. Thus, one of the reported method based on GFAAS proposed before determination of the trace amounts of arsenic in water, using electro-thermal atomic absorption spectrometry (ETAAS) a soluble membrane filter technique for the solid-phase extraction of arsenic elements. This simple and rapid method provides similar limit of detection to FI-HG-AAS method and successfully applied in river water analysis [36, 37]. Another reported method is based on the formation and extraction of the As (III)—ammonium pyrrilidinedithio-

carbonate complex, with further dispersion in nitric acid containing Ni (II) species and injection of the obtained suspension to a graphite furnace. The possible interferences of Cu (II), Pb (II) and Sn (II) could be removed by extraction at the higher pH where no As (III) is extracted, but where the respective ammonium pyrrilidinedithio-carbonate complexes can be extracted [38].

3.4. Laser induced breakdown spectroscopy (LIBS)

Laser-induced breakdown spectroscopy can determine the elemental composition of aerosols, liquids, gases, and solids qualitatively and quantitatively in real time with a single laser pulse. A high-powered, pulsed laser beam is focused directly into the targeted sample to form a small laser-induced breakdown, called a laser spark. The resulting high-temperature plasma is sufficient to vaporize, atomize, and electronically excite a small amount of the sample matter. The electrons within these atoms gain energy, and subsequently emit light at characteristic wavelengths as the plasma cools and the electrons relax to their original condition (*i.e.*, ground state). Thus, it can be said that the analytical technique for LIBS is the atomic emission. The resulting emission's frequency spectrum is a fingerprint of the elemental composition of the sample but not its speciation. After calibration, the intensity of each peak in the spectrum can be used to quantify elemental concentrations. Detection limits for LIBS depend on the intensity of the emission line(s) for a specific metal, plasma temperature, soil moisture, and grain size, and the detector signal to noise [39]. It has been reported poor detection limits for arsenic using this technique in comparison with other analytical technique, the technique vaporizes the arsenic sample, and the speciation is not possible. Thus, the technology requires considerable research to improve the detection limits for arsenic [40, 41].

3.5. Surface-enhanced Raman spectroscopy (SERS):

Raman spectroscopy identifies and quantifies the concentration of molecules by measuring the wavelength and intensity of the laser light scattering. A molecule is adsorbed onto a metal surface (usually silver), and laser light is reflected off the adsorbed molecule. The change in wavelength of the scattered light is dependent on the vibrational spectrum of a target molecule. Raman spectra of arsenite and arsenate in solution are known, although minimum detection limits have not been determined. This technology can be miniaturized with recent advances in laser and micro-fabrication. Therefore, it could be developed into a possible field portable detection system, which can provided good sensitivity and selectivity for arsenic compounds [42-44].

3.6. Electrophoresis techniques

Capillary electrophoresis is only a technique that can extract and separate ion species from an environmental matrix. It cannot detect or measure the concentration of these species. However, when combined with a sensitive detection technique, it has potential as an analytical technique. Often, this technique that is combined with a tool, as ICP-MS, is used for arsenic speciation in the laboratory.

CE has been used to detect arsenic by direct absorbance of the arsenic species with detection limits in the ppm range whereas indirect laser-induced florescence detection shows detection limits for arsenic in the range of 250 ppb. The technology has been applied successfully to arsenic spiked water samples and soil extracts. The size, durability, and ease of use make CE a strong candidate for sensor technologies, provided greater sensitivity in comparison with other detection schemes. [45-48].

3.7. Inductively coupled plasma (ICP) techniques

3.7.1. ICP-AFS and ICP-Mass Spectrometry (MS)

The ICP technique uses the plasma to ionize components, through which the sample is acidified and sprayed into the plasma, and then, the plasma at high temperature, atomizes and ionizes all forms of arsenic, and the response does not vary with species as in the more traditional AAS methods. Often, ICP is used in combination with other analytical techniques, such as MS [49] and AES [50], because ICP eliminates any sample preparation time. ICP–AES is a less used technique and normally applied for a comparison and more accurate analysis of a multi-element sample. The ICP-MS technique is one of the most widely applied analytical technique for arsenic detection [51-53]. The main advantages of ICP-MS over ICP-AES are isotope analysis capability of high precision and lower detection limits. In order to overcome the possible interference from high levels of chloride due to the formation of argon chloride, which has the same mass as arsenic, the sample introduction should be carried via electrothermal vaporisation (ETV), which exhibits the advantages of small sample sizes, increased sensitivity and low absolute detection limits [54, 55]. On the other hand, the low sensitivity obtained in the determination of low concentrations of arsenic in real samples is due to the poor ionization efficiency in ICP. Thus, to solve this issue, a cold vapour mercury sample introduction technique combined with hydride generation and with some ICP-MS protocols have been applied for arsenic determination [56, 57].

3.7.2. High performance liquid chromatography (HPLC) and ICP-MS

A combination of a chromatograph with a spectrometer acting as a selective detector allows the determination of non-volatile species of elements such as arsenic on the level of their occurrence in the natural environment and identification of particular compounds.
By applying a coupled system with an HPLC and ICP-MS, result a suitable method for the determination of arsenic speciation in natural samples [58]. In addition, it has been reported another combination between HPLC and AAS [59] used for arsenic determination, but with a poor detection limits, which could be improved by using a combination of HPLC-ICP-MS. Therefore, using the directly coupled ion-pair reversed-phase (RP) HPLC-ICP-MS for the identification of various arsenic species, including As (III) and As (V) in spring waters improve the selectivity of the assay [60]. It was found that by using an ion exchange HPLC column rather than a reverse phase column, it could be achieved an enhanced separation and selectivity of arsenic species. At the same time, it has reported that using an anion-exchange column incorporated in an ICP-MS, the sensitivity was shown to be improved by 10-fold [61].

Also, other researcher group has been used one chromatographic run in a mixed mode column, and has succeeded in the separation of arsenic species [62]. In addition, the use of an aqueous mobile phase with low buffer salt concentration minimizes the problems associated with the coupling of HPLC and ICP-MS.

A comparison between using HPLC-HG-AFS and HPLC-HG-ICP-MS performance has been reported [63] for the speciation of arsenite, arsenate and other arsenic compounds in fresh water, and it was found that the limit of detection were similar for both techniques, however AFS presented the advantage regarding at a lower time consuming, uncomplicated handling, and cheep operation costs [64]

3.8. Electrochemical methods

An analytical technique to be practical in environment analysis, it must be sensitive, to have precision, accuracy, dynamic range, ease of pretreatment/sample preparation, ease of automation, cost, suitability for studies in the field, applicability to a wide range of substances, and the capability of determining more than one species. In addition, it is also a requirement that a method to be approved by the regulatory authorities. Thus, EPA has approved an analytical method, SW-846- 7063 for ASV capable of measuring from 0.1 to 300 µg/L of free arsenic [65]. Therefore, the electrochemical detection techniques fall into these universal requirements and in particular, the most suitable techniques for determining arsenic are polarographic techniques, cathodic stripping voltammetry (CSV) and anodic stripping voltammetry (ASV), and furthermore these methods labour best for liquid samples [66].

3.8.1. Polarographic techniques

Polarography or linear-sweep voltammetry at the hanging mercury drop electrode (HMDE) is the oldest electrochemical method for the determination of trace inorganic metals [67-69], which presents low limits of detection due to high capacitive currents. Polarography is not suitable technique for arsenic determination due to its low sensitivity for its detection at low concentrations in drinking water. Although, by differential pulsed polarography was achieved a better sensitivity, though the selectivity is low. On the other hand, these methods are based on processes that occurring at a mercury-dropping electrode, which itself have a hazardous potential for human health.

Other polarographic techniques for arsenic determination include ac/dc polarography [70], oscillography [71], square-wave polarography [72], fast linear-sweep polarography, [73] etc. Typical limits of detection reached by these techniques range between 10 ppb and several ppm. In the literature, it has been published only few articles that used differential-pulsed polarography (DPP) for the sequential trace determination of As (III) and As (V) [74-77].

3.8.2. Cathodic stripping voltammetry (CSV)

Generally, the stripping analysis is better suited than the direct polarography for trace determinations in 'real' samples because the substance of interest is pre-concentrated on the working electrode, obtaining sub-µg/L detection limits due to the enhancement of the analyte during the deposition step. Cathodic stripping voltammetry (CSV) at a hanging mercury drop electrode (HMDE) is a promising method for arsenic determination because it is simple and the instrumentation can be used both for laboratory and field applications. Also, using the fresh working

electrode surface, it can be removed the memory effects of the electrode surface and is avoided the electrode preparation [78].

The principle of arsenic speciation using CSV is to determine the electroactive As (III) species first and then, sequentially to convert other arsenic species to As (III) species for the measurement [79]. Electroactive species, As (III), is electrochemically reduced to As (0), which is insoluble in Hg. However, in order to increase sensitivity, intermetallic complexes of arsenic are stripped from HMDE, whereby As (III) reacts with copper or selenium to form AsH_3, which can be stripped cathodically [80].

3.8.3. Anodic stripping voltammetry (ASV)

ASV is able to detect and quantify both arsenite and arsenate according to the method SW-846-4063 described by EPA [65], but the studies have shown that only the arsenite can be measuring in an environmental sample with this technique. Thus, the arsenate had to be chemically reduced to arsenite and then, electrochemically measured to obtain the total arsenic. It was reported a considerable number of articles that used this technique for arsenic determination in different aquatic media and at various suitable electrodes. Different solid bare electrodes such as: glassy carbon, carbon paste, diamond, gold, silver, iridium, platinum and bismuth electrodes have been used as possible alternatives to mercury for investigative anodic process. Carbon based electrodes are the most use materials in electroanalytical stripping techniques. Successful application of carbon based electrodes, such as: glassy carbon, carbon paste, pyrographite, impregnated graphite, carbon fiber, boron doped diamond, carbon nanotubes etc. in the stripping methods result from the high chemical and electrochemical stability of carbon materials, a relatively high hydrogen and oxygen over-voltage on these materials, a wide working range for both directions, simplicity of mechanical renewal of the electrode surface [81- 83].

Thereby, the determination of arsenic by this technique in the groundwater from Bangladesh and Nepal was extensively studied because it is well-known the hazardous effect cause by this heavy metal ion on the population from this zone. By using this technique, the determination of arsenic was possible at μg/L concentration [84-87].

Otherwise, the anodic stripping voltammetry technique for trace arsenic analysis is based on the deposition of metal arsenic on the electrode surface followed by the anodic stripping. In this respect, various electrodes materials were investigated exhaustively for the determination of arsenic in water. Thus, the determination of arsenic by this technique employed at the different electrodes with variations in design allowed to obtain good reproducibility results with limits of detection accordingly to the current legislation regarding this toxic heavy metal ion [88-93].

3.9. References

[1] A. Davis, D. Sherwin, R. Ditmars, K.A. Hoenke, Environ. Sci. Technol. 35 (2001) 2401.
[2] **http://www.epa.gov/epaoswer/hazwaste/test/sw846.htm**.
[3] **http://www.who.int/inf-fs/en/fact210.html**.
[4] D.M. Crumbling, C. Groenjes B. Lesnik, K. Lynch, J. Shockley, J. Vanee, R. Howe, L. Keith, J. McKenna, D. Peck, Environ. Sci. Technol. 33 (2001) 3686.

[5] T.S.Y. Choong, T.G. Chuah, Y. Robiah, F.L. Gregory Koay, I. Azni, Desalination 217 (2007) 139.
[6] U.S. Environmental Protection Agency, May 1–3 (2001) **http://www.epa.gov/ttbnrmrl/arsenictech.htm**.
[7] U.S. Environmental Protection Agency, EPA-542-R-04-002, April 2004.
[8] S. Cabredo, J. Galban, J. Sanz, Talanta 46 (1998) 631.
[9] Z. Mester, P. Fodor, Spectrochim. Acta 52 B (1997) 1763.
[10] H.T. Delves, C.E. Sieniawska, J. Anal. Atom. Spectrom. 12 (1997) 387.
[11] J.L. Gomez-Ariza, D. Sanchez-Rodas, I. Giraldez, E. Morales, Talanta 51 (2000) 257.
[12] B.A. Fernandez, C.V.H. Temprano, M.R.C. de La Fernandez, A. Sanz-Medel, P. Neil, Talanta 39 (1992) 1517.
[13] J. Moreda-Pineiro, M.L. Cervera, M. de La Guardia, J. Anal. Atom. Spectrom. 12 (1997) 1377.
[14] U.S. Environmental Protection Agency, EPA-815-R-00-010, December (1999).
[15] D.G. Kinniburgh, W. Kosmus, Talanta 58 (2002) 165.
[16] W.R. Cullen, K.J. Reimer, Chem. Rev. 89 (1989) 713.
[17] M.H. Arbab-Zavar, M. Chansaz, T. Heidari, Anal. Sci. 26 (2010) 107.
[18] M.H. Arbab-Zavar, M. Hashemi, Talanta 52 (2000) 1007.
[19] S. Kundu, S. K. Ghosh, M. Mandal, T. Pal, New J. Chem. 26 (2002) 1081.
[20] S. Kundu, S. K. Ghosh, M. Mandal, T. Pal, New J. Chem. 27 (2003) 656.
[21] S. Kundu, S. K. Ghosh, M. Mandal, T. Pal, A. Pal, Talanta 58 (2002) 935.
[22] E.H. Evans, J.A. Day, A.F.W.J. Price, C.M.M. Smithd, J.F. Tyson, J. Anal. Atom. Spectrom. 19 (2004) 775.
[23] S. Karthikeyan, S. Hirata, Anal. Lett. 36 11 (2003) 2355.
[24] L.D. Tsalev, M. Sperling, B. Welz, Talanta 51 (2000) 1059.
[25] M. Murillo, N. Carrión, J. Colmenares, J. Romero, G. Alvarado, M. Ríos, F, Angulo, Quim. Nova. 31 (2008) 1315.
[26] B. Welz, M. Šucmanová, Analyst 118 (1993) 1417.
[27] B. Welz, M. Šucmanová, Analyst 118 (1993) 1425.
[28] P. Niedzielski, M. Siepak, J. Siepak, J. Przybyłek, Pol. J. Environ. Stud. 11 (2002) 219.
[29] M. Pantsar-Kallio, A. Korpela, Anal. Chim. Acta 410 (2000) 65.
[30] M Vilanó, A. Padró, R. Rubio, Anal. Chim. Acta 411 (2000) 71.
[31] A.G. Howar, C. Salou, Anal. Chim. Acta 33 (1996) 89.
[32] A.G. Howard, C. Salou, J. Anal. Atom. Spectrom. 13 (1998) 683.
[33] A.G. Howard, J. Anal. Atom. Spectrom. 12 (1997) 267.
[34] M.V. Gallardo, Y. Bohari, A. Astruc, M. Potin-Gautier, M. Astruc, Anal. Chim. Acta 441 (2001) 257.
[35] M.C. Villa-Lojo, E. Alonso-Rodrıguez, P. Lopez-Mahıa, S. Muniategui-Lorenzo, D. Prada-Rodrıguez, Talanta 57 (2002) 741.
[36] N. Hata, H. Yamada, I. Kasahara, S. Taguchi, Analyst 124 (1999) 23.
[37] L. Husakova, T. Cernohorsky, J. Sramkova, L. Vavrusova, Food Chem. 105 (2007) 286;
[38] K. Anezaki, I. Nukatsuka, K. Ohzeki, Anal. Sci. 15 (1999) 829.
[39] U.S. Department of Energy, Summary Report (2000).
[40] J. Kwak, C. Lenth, C. Salb, E.J. Ko, K.W. Kim, K. Park, Spectrochim. Acta B 64 (2009) 1105.
[41] B.T. Fisher, H.A. Johnsen, S.G. Buckley, D.W. Hahn, Appl. Spectrosc. 55 (2001) 1312.
[42] A. Campion, P. Kambhampati, Chem. Soc. Rev. 27 (1998) 241.

[43] S.A. Wood, C.D. Tait, D.R. Janecky, Geochem. Trans. 3 (2002) 31.
[44] E.A. Rochette, B.C. Bostick, G. Li, S. Fendorf, Environ. Sci. Technol .34 (2000) 4714.
[45] **http://www.epa.gov/ogwdw/arsenic/pdfs/methods.pdf**.
[46] Z.L. Chen, J.M. Lin, R. Naidu, Anal. Bioanal. Chem. 375 (2003) 679.
[47] B. Sun, M. Macka, P.R. Haddad, J. Chromatogr. A 1039 (2004) 201.
[48] J.Z. Wu, P.C. Ho, J Chromatogr A 1026 (2004) 261.
[49] K.J. Stetzenbach, M. Amano, D.K. Kreamer, V.F. Hodge, Ground Water. 32 (1994) 976.
[50] A. Menendez Garcia, M.C. Perez Rodriguez, J.E. Sanchez Uria, A. Sanz-Medel, Fresen. J. Anal. Chem. 353 (1995) 128.
[51] M. Niemela, P. Peramaki, H. Kola, J. Piispanen, Anal. Chim. Acta 493 (2003) 3.
[52] J. Bowman, B. Fairman, T. Catterick, J. Anal. Atom. Spectrom.12 (1997) 313.
[53] K. Van Den Broeck, C. Vandecasteele, J. M. C. Geuns, J. Anal. Atomic. Spectrom. 12 (1997) 987.
[54] D. Beauchemin, Anal. Chem. 78 (2006) 4111.
[55] Y.C. Sun, Y.S. Lee, T.L. Shiah, P.L. Lee, W.C. Tseng, M.H. Yang, J. Chromatogr. A 1005 (2003) 207.
[56] X. Wei, C.A. Brockhoff-Schwegel, J.T. Creed, J. Anal. Atom. Spectrom. 16 (2001) 12.
[57] S. Saverwyns, X. Zhang, F. Vanhaecke, R. Cornelis, L. Moens, R. Dams, J. Anal. Atom. Spectrom. 12 (1997) 1047.
[58] P. Thomas, J. K. Finnie, J. G. Williams, J. Anal. Atom. Spectrom. 12 (1997) 1367.
[59] C. Demesmay, M. Olle, M. Porthault, Fresen. J. Anal. Chem. 348 (1994) 205.
[60] S.H. Hansen, E.H. Larsen, G. Pritzl, C. Comett, J. Anal. Atom. Spectrom. 7 (1992) 629.
[61] P. Thomas, K. Sniatecki, J. Anal. Atom. Spectrom. 10 (1995) 615.
[62] Y.W. Chena, N. Belzile, Anal. Chim. Acta 671 (2010) 9–26.
[63] M. Moldovan, M.M. Gomez, M.A. Palacios, C. Camara, Microchem. J. 59 (1998) 89.
[64] J.L. Gomez-Ariza, E. Morales, I. Giraldez, D. Sanchez-Rodas, A. Velasco, J. Chromatogr. A 938 (2001) 211.
[65] Environmental Protection Agency. SW-846.
http://www.epa.gov/epaoswer/hazwaste/test/sw846.htm
[66] A.W. Bott, Curr. Separat. 14 (1995) 24.
[67] J.J. Lingane, Ind. Eng. Chem. Anal. Ed. 15 (1943) 583.
[68] J.E. Page, Nature 154 (1944) 199.
[69] H. Wohlgemuthová, J. Kuta, J. Dolezal, Collect Czech Chem. Commun. 37 (1972) 706.
[70] R. Kannan, T.V. Ramakrishna, S.R. Rajagopalan, Talanta 32 (1985) 419.
[71] J. Zhi-Liang, L. Ai-Hui, Talanta 37 (1990) 1077.
[72] J. Wang, E. Ouziel, C. Yarnitzky. M. Ariel, Anal. Chim. Acta 102 (1978) 99.
[73] G.C. Whitnack, R.G. Brophy, Anal. Chim. Acta 48 (1969) 123.
[74] T. Ferri, R. Morabito, B.M. Petronio, E. Pitti, Talanta 36 (1989) 1259.
[75] D.J. Myers, J. Osteryoung, Anal. Chem. 45 (1973) 267.
[76] J.H.T. Luong, E. Majid, K.B. Male, Open Anal. Chem. J 1 (2007) 7.
[77] A.A. Ferreira, A.A. Barros, Anal. Chim. Acta 459 (2002) 151.
[78] G. Henze, W. Wagner, S. Sander, Fresen. J. Anal. Chem. 358 (1997) 741.
[79] Y. He, Y. Zheng, D.C. Locke, Microchem. J. 85 (2007) 265.
[80] S.A. Ozkan, Curr. Pharm. Anal. 5 (2009) 127.

[81] S.B. Rasul, A.K.M. Munir, Z.A. Hossain, A.H. Khan, M. Alauddin, A. Hussam, Talanta 58 (2002) 33.
[82] S. Motoc, F. Manea, A. Pop, **A. Baciu**, G. Burtica, R. Pode, Environ. Eng. Manag. J. accepted for publication on february 2012;
[83] S. Motoc, F. Manea, A. Pop, **A. Baciu**, G. Burtică, R. Pode, WIT. Trans. Ecol. Envir. 164 (2012) 323.
[84] M.D.M. Karim, Wat. Res. 34 (2000) 304.
[85] J.K. Thakur, RK Thakur, A. Ramanathan, M. Kumar, S.K. Singh, Water 3 (2011) 1.
[86] D. Melamed, Anal. Chim. Acta 532 (2005) 1.
[87] R. Piech, B. Bas, E. Niewiara, W.W. Kubiak, Talanta72 (2007) 762.
[88] A.O. Simm, C.E. Banks, S.J. Wilkins, N.G. Karousos, J. Davis, R.G. Compton, Anal. Bioanal. Chem. 381 (2005) 979.
[89] S. Laschi, G. Bagni, I. Palchetti, M. Mascini, Anal. Lett. 40 (2007) 3002.
[90] N. Daud, N.A. Yusof, T.W. Tee, A.H. Abdullah, Int. J. Electrochem. Sci. 7 (2012) 175.
[91] Y. Liu, W. Wei, Electrochem. Commun. 10 (2008) 872.
[92] G. Forsberg, J.W. O'Laughlin, R.G. Megargle, S.R. Koirtyohann, Anal. Chem. 47 (1975) 1586.
[93] D.Q. Hung, O. Nekrassova, R.G. Compton, Talanta 64 (2004) 269.

CHAPTER 4. ELECTROANALYTICAL METHODS FOR VOLTAMMETRIC / AMPEROMETRIC DETECTION OF POLLUTANTS FROM WATER

4.1. Cyclic voltammetry (CV)

Cyclic voltammetry (CV) is a very versatile electrochemical technique, which allows probing the mechanics of redox and transport properties of a system in solution. This technique provides rapid information on the thermodynamic redox processes, on the kinetics of heterogeneous electron- transfer reactions, and on coupled chemical reactions or adsorption processes. This is accomplished with a three-electrode arrangement whereby the potential relative to some reference electrode is scanned at a working electrode, while the resulting current flowing through a counter (or auxiliary) electrode is monitored in a supporting electrolyte. The technique is ideally suited for a quick search of redox couples present in a system, and once located a couple may be characterized by more careful analysis of the cyclic voltammogram. More precisely, the controlling electronics is designed such that the potential between the reference and the working electrode can be adjusted, but the big impedance between these two electrodes effectively forces any resulting current to flow through the counter electrode. Usually, the potential is scanned back and forth linearly with time between two extreme values using a triangular potential waveform (Figure 4.1.). When the potential of the working electrode is more positive than that of a redox couple present in the solution, the corresponding species may be oxidized (*i.e.* electrons going from the solution to the electrode) and produce an anodic current. Similarly, on the return scan, as the electrode potential of the working electrode is more positive than that of a redox couple, reduction (*i.e.* electrons flowing away from the electrode) may occur to cause a cathodic current. By 'International Union of Pure and Applied Chemistry' (IUPAC) convention, anodic currents are positive and cathodic currents negative [1-5].

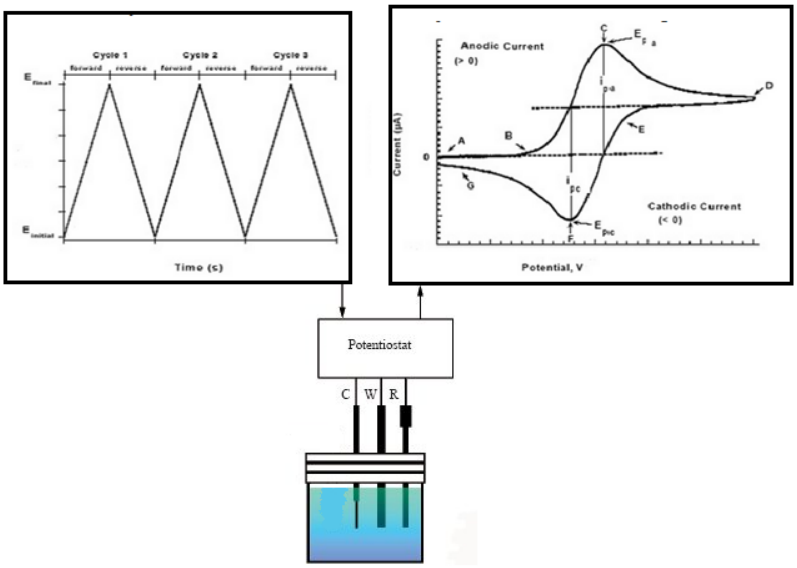

Figure 4.1. CV potential waveform with switching potentials (left), and the expected response of a reversible redox couple during a single-potential cycle (right), connected with the experimental CV set-up: counter electrode (C), working electrode (WE) and reference electrode (R) in an electrochemical cell [5].

The magnitude of the observed faradaic current can provide information on the overall rates of the many processes occurring at the working electrode surface. As is the case for any multi–step process, the overall rate is determined by the slowest step.

For a redox reaction induced at a working electrode, the rate determining step may be any one of the following individual steps depending on the system:

- rate of mass transport of the electro-active species;
- rate of adsorption or de-sorption at the electrode surface;
- rate of the electron transfer between the electro-active species and the electrode, or rates of the individual chemical reactions, which are part of the overall reaction scheme.

For the oxidation reaction involving n electrons:

$$Red \rightarrow Ox + ne^{-}?$$

The Nernst Equation gives the relationship between the potential and the concentrations of the oxidized and reduced forms of the redox couple at equilibrium (at 298 K):

$$E = E^{0'} + \frac{0.059}{n}\log_{10}\frac{[Ox]}{[Red]} \qquad (4.1)$$

where:

E is the applied potential, $E^{o'}$ is the formal reduction potential, $[O_x]$ and [Red] are the surface concentrations at the electrode/aqueous electrolyte interface, and n is the number of electrons involved in the redox reaction. It must be noticed

that the Nernst equation may or may not be valid depending on the system or on the experimental conditions.

A typical voltammogram is shown in Figure 4.2. The scan starts at a slightly negative potential, (A) up to a positive switching value, (D) at which the scan is reversed back to the starting potential. The current is first observed to peak at E_{pa} (with value i_{pa}) indicating that an oxidation is taking place and then drops due to depletion of the reducing species from the diffusion layer. During the return scan the processes are reversed (reduction is now occurring) and a peak current is observed at E_{pc} (corresponding value, i_{pc}) [1-6].

Reversible System

Providing that the charge–transfer reaction is reversible, that there is no surface interaction between the electrode and the reagents, and that the redox products are stable (at least in the time frame of the experiment), the ratio of the reverse and the forward current (in Figure 4.2 $i_{pa} = i_{pf}$ and $i_{pc} = i_{pr}$). In addition, for such a system it can be shown that:

-the corresponding peak potentials E_{pa} and E_{pc} are independent of scan rate and concentration;

-the formal reduction potential for a reversible couple $E^{o'}$ is centered between anodic and cathodic peak potentials:

$$E^{o'} = \frac{E_{pa} + E_{pc}}{2} \tag{4.2}$$

the peak separation ΔE_p for a reversible couple is given by:

$$\Delta E_p = E_{pa} - E_{pc} = \frac{0.059}{n} \tag{4.3}$$

at all scan rates (however, the measured value for a reversible process is generally higher due to uncompensated solution resistance and non-linear diffusion. Larger values of ΔE_p, which increase with increasing scan rate, are characteristic of slow electron transfer kinetics).

To distinguish between reversible (diffusion-controlled) and irreversible (charge-transfer controlled) kinetics of an electrode process potential scan rate is used as diagnostic tool, the rate of reagent transport being proportional to the square root of the scan rate. Thus, analysis of ΔE_p vs. $v^{1/2}$ gives information on reversibility and applicability of further calculations.

In simple terms, the working electrode may be regarded as a "reagent" of adjustable oxidizing or reducing strength. However, this is a purely conceptual image. In fact, the electrochemical processes are occurring at the interface of two different phases, the electrode and the electro-active species in solution. In other words, the processes under studies are heterogeneous in nature.

For the electron transfer to occur, the molecules in solution have to approach the electrode. In a cyclic voltammetry experiment, the solution is kept unstirred and in this situation, mass transport can occur only by diffusion due to concentration gradients created around the electrode surface. Such concentration–distance profiles at different steps of a cyclic voltammogram scan are illustrated in

Figure 4.2. The magnitude of the observed signal will be very much a function of the diffusion properties of the system. Intuitively, the current intensity (*i.e.* the flow of electrons) is expected to depend on the surface area of the working electrode and the concentration of the electro-active species. Also, one can expect the voltage scanning rate to affect the concentration profile around the electrode, which itself directly affects the rate of charge transport, and for this matter the diffusion coefficient appears explicitly. The expression of the peak current (A) for the forward sweep in a reversible system at 298 K is given by the Randles–Sevcik equation:

$$I_{pf} = (2.69 \times 10^5) n^{3/2} A D^{1/2} C^* v^{1/2} \qquad (4.4)$$

Where n is the number of electrons involved in the redox process, A is the active area of the working electrode (cm^2), D is the diffusion coefficient ($cm^2\ s^{-1}$), C* is the bulk concentration of the electroactive species (mol cm^{-3}), and v is the potential scan rate ($V\ s^{-1}$).

In the present experiment, the dependence of i_{pf} on scan rate and concentration will be examined.

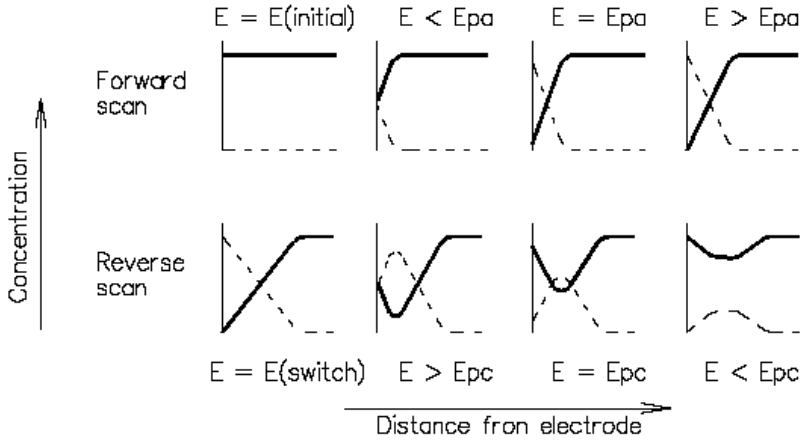

Figure 4.2. Qualitative diagrams showing concentration-distance profile at various stages of the cyclic voltammogram the solid lines correspond to the reducing species and the dotted lines to the oxidizing species.

A similar indicator of reversible electron transfer is called the current function, whose value is given by ($i_p/v^{1/2}$). The current function should be constant for all scan rates for which the electron transfer is fast enough to maintain the equilibrium ratio between the reduced and the oxidized forms of the redox couple predicted by the Nernst equation.

At this point, it is instructive to note that when describing electrochemical reversibility it is important to consider not only the value of k^o (standard rate constant), but the scan rate for which Nernstian equilibrium cannot be maintained at the electrode surface. At these scan rates, the observed voltammetry will display characteristics of quasireversible or irreversible behaviour, such as the spreading

out of voltammetric peaks over wider potential ranges, decreased peak currents, and increased values for ΔE_p^2 [1-6].

4.1.1. Irreversible and Quasi-reversible Systems

For irreversible processes (those with sluggish electron exchange), the individual peaks are reduced in size and widely separated. Totally irreversible systems are characterized by a shift of the peak potential with the scan rate:

$$E_p = E^\circ - \frac{RT}{\alpha n_a F}[0.78 - \ln\frac{k^\circ}{D^{1/2}} + \ln(\frac{\alpha n_a F \upsilon}{RT})^{1/2}] \quad (4.5)$$

where α is the transfer coefficient, and n_a is the number of electrons involved in the charge-transfer step. Thus, E_p occurs at potentials higher than E^o, with the overpotential related to k^o (standard rate constant) and α. Independent of the value k^o, such peak displacement can be compensated by an appropriate change of the scan rate. The peak potential and the half-peak potential (at 25°C) will differ by $48/\alpha n$ mV. Hence, the voltammogram becomes more drawn-out as αn decreases.

The peak current, given by

$$i_p = (2.99 * 10^5) n(\alpha n_a)^{1/2} A C^* D^{1/2} v^{/2} \quad (4.6)$$

is still proportional to the bulk concentration, but will be lower in height (depending upon the value of v). Assuming a value of 0.5, the ratio of the reversible-to-irreversible current peaks is 1.27 (*i.e.* the peak current for the irreversible process is about 80% of the peak for a reversible one). For quasi-reversible systems, the current is controlled by both the charge transfer and mass transport. The shape of the cyclic voltammogram is a function of the ratio $k^o / (\pi v n F D / RT)^{1/2}$. As the ratio increases, the process approaches the reversible case. For small values of it, the system exhibits an irreversible behaviour. Overall, the voltammograms of a quasi-reversible system are more spreaded out and exhibit a larger separation in peak potentials compared to a reversible system [1-6].

4.2. Differential-Pulse Voltammetry (DPV)

Differential-pulsed voltammetry is a very important technique in chemical analysis and is based on its superior elimination of the capacitive/background current. This is achieved by sampling the current twice: once before pulse application and then, at the end of the pulse. The current sampling is indicated by filled circles in Figure 4.3.

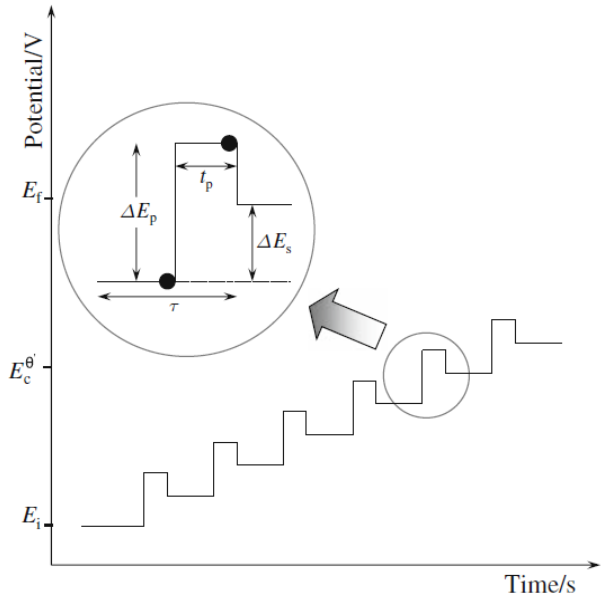

Figure 4.3. Potential diagram for DPV

The system of this measurement is usually the same as that of standard voltammetry. The potential between the working electrode and the reference electrode is changed as a pulse from an initial potential to an interlevel potential and remains at the interlevel potential for about 5 to 100 milliseconds. Then, it changes to the final potential, which is different from the initial potential. The pulse is repeated, changing the final potential, and a constant difference is kept between the initial and the interlevel potential. The value of the current between the working electrode and auxiliary electrode before and after the pulse are sampled and their differences are plotted versus potential.

The DPV technique can be used to study the redox properties of extremely small amounts of chemicals because of the following features:

- the effect of the charging current can be minimized, so high sensitivity is achieved;
- background current is extracted, so electrode reactions can be analyzed more precisely.

The main characteristics of DPV are:

- reversible reactions show symmetrical peaks, and irreversible reactions show asymmetrical peaks.
- the detection limit is about 10^{-8} M [1-6].

4.3. Square-Wave Voltammetry (SWV)

Square-wave voltammetry (SWV) is one of the fastest pulsed techniques that can be applied in both electrokinetic and analytic measurements. In square-wave voltammetry, a square-wave is superimposed on the potential staircase

sweep. Oxidation or reductions of species are registered as a peak or through in the current signal at the potential at which the species begins to be oxidized or reduced. In staircase voltammetry, the potential sweep is a series of stair steps (Fig. 4.4).

The current is measured at the end of each potential change, right before the next, so that the contribution to the current signal from the capacitive charging current is minimized. The differential current is then plotted as a function of potential, and the reduction or oxidation of species is measured as a peak or through. Due to the less contribution of capacitive charging current the detection limits for SWV are within the order of nanomolar concentrations. The major advantage of the square-wave voltammetry is its speed [1-6].

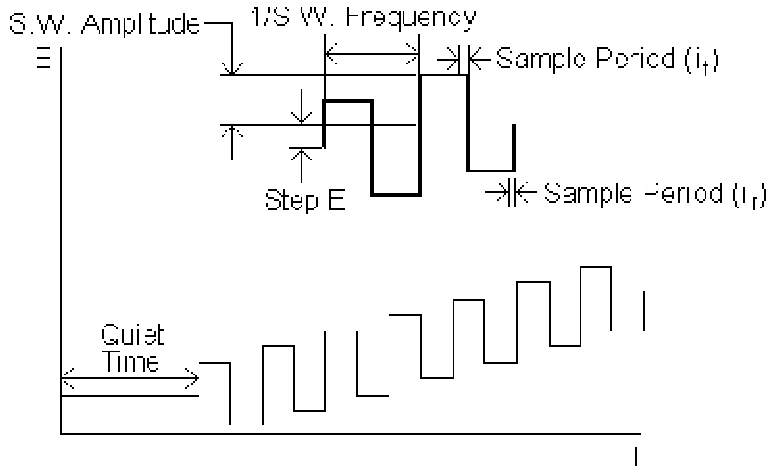

Figure 4.4. Square-wave form showing the amplitude of SWV

4.4. Chronoamperometry (CA)

Chronoamperometry (CA) is an electrochemical technique in which the potential of the working electrode is stepped and the resulting current from Faradic processes occurring at the electrode (caused by the potential step) is monitored as a function of time. A stationary working electrode and unstirred solution are used. The resulting current-time dependence is monitored.

Chronoamperometry is often used for measuring the diffusion coefficient of electroactive species or the surface area of the working electrode. It can also be applied to study the mechanisms of the electrode processes [1-6].

4.5. Pulsed amperometric detection (PAD)

Johnson and co-workers [7, 8] were the first to introduce pulsed amperometric detection as an electroanalytical technique (PAD) using platinum electrodes. They used it for the detection of alcohols, formic acid, and cyanide in flow-injection systems [9]. Later, Johnson and other researchers also, developed

PAD methods for amino acids, aldehydes, carbohydrates, sulphite, and sulphide [10-12]. Following the first reports [7, 8], a number of interesting and important articles appeared in the literature discussing different aspects and applications of the triple-pulse potential waveform or pulsed amperometric detection (PAD) [13-21].

Pulsed amperometric detection (PAD) is an excellent method for quantitative detection of numerous organic compounds that adsorb at noble metal electrodes but cannot be detected satisfactorily by conventional amperometry at constant applied (dc) potential. PAD relies on repeated applications of a multiple-pulse (mostly triple pulse) waveform consisting of regeneration/ detection, oxidation and reduction potentials. The last two of those three steps are designed for electrode cleaning. The first of the three steps usually combines regeneration of the electrode surface with a short period of signal acquisition by integration of currents resulting from the detection enabling electrode reaction. The second step should remove all reaction products and the third step restores the oxidation state of electrode surface for the detection enabling electrode reaction of analytes of interest. Many different waveforms have been reported for the detection with platinum electrodes. Fig. 4.5 presents a schematic diagram of PAD waveform.

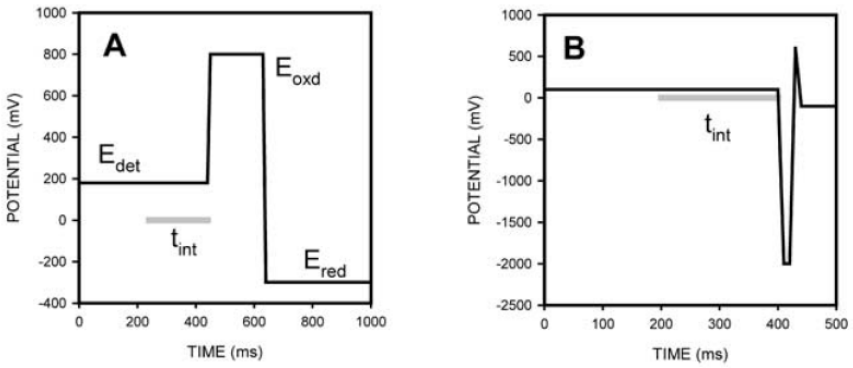

Figure 4.5. Schematic of the PAD waveform

4.6. Stripping analysis

Stripping voltammetry has been known to specialists for more than half a century, being part of well-known group of electroanalytical techniques. This technique of stripping voltammetry has been used in trace analysis, being declared the most sensitive technique among all currently electroanalytical methods available (*i.e.*, 10^{-11} M). Electroanalytical methods, particularly the stripping voltammetry methods combine excellent the characteristics provided by the electroanalytical technique, *i.e.* instrumental simplicity, the availability of low-cost portable equipment, ability of sensing, monitoring and detection of broad types of analytes with the advantages of stripping methods, *i.e.* high sensitivity, low detection and determination limits and rapidity of the measurements [22, 23].

By electrochemical stripping it means that the redox-active species are oxidative or reductive remove from an electrode surface. The electroanalytical stripping methods consist of two steps: first, the electrochemical deposition or

accumulation of a chemical species onto, or in, the working electrode at a constant potential, thus, this steps can involve either an anodic or cathodic process. The second steps consist of stripping or dissolution of the investigated analyte from the electrode surface by the voltammetric technique.

Stripping voltammetry is used mostly in trace analysis due to the general condition of this technique which consists from two independent linear relationships. One is refers at the dependence between the activity of the chemical species that are deposited and the concentration of the analyte in the sample, and the other is related to the link between the deposited substance activity and the maximum stripping current. Actually, it can be said that it is also a linear relationship between the concentration of the analyte and the maximum response, but this linearity is conditioned by limiting the ability of the electrode to deposit the analyte, yet, the condition of linearity can be satisfied at significantly below the electrode saturation.

In other words, it can be said that the stripping analysis is used for trace metals due to its remarkable sensitivity attributable to the preconcentration that takes places during which the chemical active species are accumulated onto the working electrode by specific electroanalytical procedures resulting an exceptionally good signal-to-background ratio.

The limit of detection depends on the factor of proportionality between the activity of the accumulated compound and the concentration of the analyte.

The value of the proportionality between the maximum stripping current and the analyte concentration is frequently ignored, and it is enough to establish this correlation empirically, because the slope between these two factor could be different from one target active compound to another due to diverse influences caused by the various type of electrode surface used. Thus, for this reason, the concentration of the analyte can be determined by the method of standard additions [4, 5, 24-27].

Stripping analysis imply two distinct steps, as described previously above, thus, the deposition it as the first step and involve the electrolytic deposition of a small part of the metal ions in solution into the working electrode to preconcentrate the metal, then, the second step called the measurement step or the stripping step involves the stripping or the dissolution of the deposit. Therefore, it can be employed different version of stripping analysis depending of the nature of its preconcentration and stripping steps [4].

4.6.1. Anodic stripping voltammetry (ASV)

Anodic stripping voltammetry (ASV) is the most widely used from stripping analysis for determination of metals. In this method the potential is held at a negative potential and then, it is scanning in a positive direction. In this case, the preconcentration is based on the reduction of the metal ion to electrode surface called electrodeposition and then, by an anodic potential scan it is reoxidized from the electrode surface. The preconcentration is usually done at the potential more negative than standard potential (0.3 – 0.5V), to facilitate the reduced metal ion that must to be determined. The metal ions reach to the electrode surface by diffusion or convection where they are reduced and concentrated on the electrode. Thus, under this condition, the deposition step is controlled by mass transport, hence, the convection transport is achieved by solution stirring or electrode rotation

and the diffusion is found where the solid electrodes are used, obtaining a linear diffusion when the mass transfer increased.

$$M^{n+} + ne^- \rightarrow M \qquad (4.6)$$

The concentration of the metal deposit on the electrode surface is given by the Faraday's law:

$$C = \frac{i_l t_d}{nFV} \qquad (4.7)$$

Where i_l is the limiting current for the deposition of the metal, td is the length of the deposition period, n is the number of electron transferred, F is the faraday constant, and V is the volume of the working electrode.

The concentration of the metal ions reduced on the electrode surface is influenced on the duration of the deposition step. Thus, for concentration of the order of 10^{-7} a time deposit up to 5 minutes is proper, and for high level of concentration of about 10^{-10}, a time of deposit of approximately 20 minutes is adequate. The total quantity of the metal coated represents only a part of the metal present in the volume of the solution, so the deposit current is depending of the fluctuation of the metal ion at the electrode surface.

After the selection of the suitable time of the deposition, the potential is scanned anodically and linearly with the concentration of the metal ions present on the electrode surface, forming a waveform that is distinguished from the waveform of the charging background current, and, occurring the recovering the electrode surface with the analyte from the solution and a reduced oxygen interferences. During this anodic scan the metals are reoxidized, stripped out of the electrode, and an oxidation (stripping) current is generated:

$$M \rightarrow M^{n+} + ne^- \qquad (4.8)$$

The potential–time series used in ASV, along with the resulting stripping voltammogram, is shown in Figure 4.6.

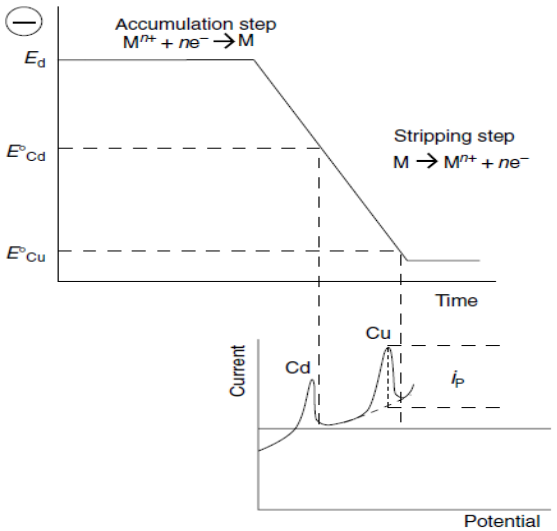

Figure 4.6. Anodic stripping voltammetry: the potential-time waveform (top), along with the resulting voltammogram (bottom).

The peak current depends on various parameters of the deposition and stripping steps, on the characteristics of the metal ion and the electrode geometry. For example, for a solid electrode, the peak current is given by [4]:

$$I_p = 2.69 \times 10^5 A D^{1/2} n^{3/2} v^{1/2} C \quad (4.9)$$

where: A represents the area of the electrode (cm^2), n is the number of electrons participating in the reaction and is equal to 1, D is the diffusion coefficient of the molecule in solution, C is the concentration of the probe molecule in the solution, and v is the scan rate ($V\ s^{-1}$) [4, 5, 27, 28].

4.6.2. Cathodic Stripping Voltammetry

Cathodic stripping voltammetry (CSV) is similar to ASV method and is the classical analysis of anions. In this case, the preconcentration of the analyte implies an anodic deposition, thus the coating step is based on the oxidation of the metal ion from the electrode surface and then, by sweeping the potential negatively the oxidized species are stripped from the electrode surface.

$$A^{n-} + Hg \xleftarrow[stripping]{deposition} HgA + ne^- \quad (4.10)$$

In cathodic stripping voltammetry the most widely used working electrode is the mercury electrode with the all forms of this. However, because the use of Hg as electrode material provides potential hazardous on human health an environment, and the innovative alternative is the use of solid electrode or/and carbon-based electrodes in the trace analysis alike CSV [27, 28].

For above-described stripping analysis, the analytical signal can be exemplified by various electrochemical techniques, according to the schemes of these processes, such as linear sweep, differential pulse, and square wave techniques. In all of these techniques, the analytical signal can be measured as the quantity of current, corresponding to the amount of the concentrate of the electroactive compound that is electrochemically changed [4, 22, 29-33].

Both ASV and CSV are suitable for a wide range of organic/inorganic compound that can be measurement by voltammetry. But these stripping voltammetric techniques are still the most used methods in the routine trace metal analysis of water. Moreover, besides that these analysis techniques are suitable for all the environmental significant trace elements, they can be used as sensitive, precise and reliable methods for the verification of the results obtained by other analytical technique, like chromatography [5, 34, and 35].

Technique	Imposed function	Recorded function	Conc. range (mole L)
Linear sweep voltammetry (LSV) (cyclic voltammetry dotted line)	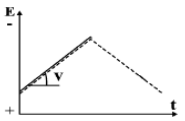	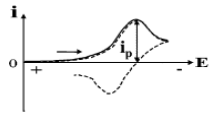	$10^{-2} - 10^{-6}$
Differential pulse voltammetry (DPV)	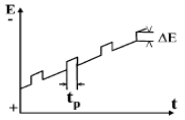	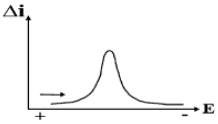	$10^{-4} - 10^{-7}$
Square wave voltammetry (SWV)	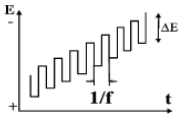	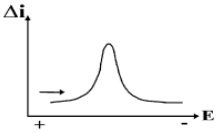	$10^{-4} - 10^{-8}$
Anodic Stripping Voltammetry (ASV) with linear scan (full line) or modulations (e.g. DP → DPASV or SW → SWASV; dotted line)	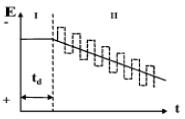	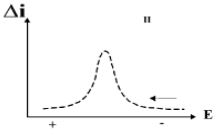	$10^{-6} - 10^{-11}$
Adsorptive stripping voltammetry (AdSV) (with or without modulation)	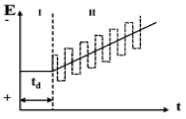	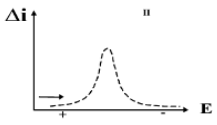	$10^{-6} - 10^{-12}$
Stripping Chronopotentiometry (SCP)	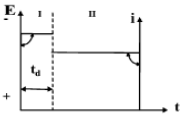	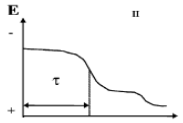	$10^{-5} - 10^{-9}$

Figure 4.7. The major voltammetric techniques used for trace-metal analysis and their typical concentration ranges. v = Potential scan rate; DE = Pulse amplitude; f = Frequency; td = Preconcentration time; ip = Peak current; Ep = Peak potential [35].

4.7. References

[1] L. Codognoto, S.A.S. Machado, L.A. Avaca, Diam. Relat. Mater. 11 (2002) 1670.
[2] V.A. Pedrosa, L. Codognoto, L.A. Avaca, Quim. Nova. 26 (2003) 844.D. Souza,
[3] S.A.S Machado, L.A. Avaca, Quim. Nova. 26 (2003) 81.
[4] J. Wang, Wiley-VCH, New-York, (2000) 75-85.
[5] F. Scholz, Springer-Verlag (2010).
[6] P. Zanello, The Royal Soc. Chem. (2003).
[7] S. Hughes, P.L. Meschi, D.C. Johnson, Anal. Chim. Acta 132 (1981) 1.
[8] S. Hughes, D.C. Johnson, Anal. Chim. Acta 132 (1981) 11.
[9] J.A. Polta, D.C. Johnson, Anal. Chem. 57 (1985) 1373.

[10] D.S. Austin, J.A. Polta, T.Z. Polta, A.P.-C. Tang, T.D. Cabelka, D.C. Johnson, J Electroanal. Chem. 168 (1984) 227.
[11] D.C. Johnson, D. Dobberpuhl, R. Roberts, P. Vandeberg, J. Chromatogr. 640 (1993) 79.
[12] J. Cheng, P. Jandik, X. Liu, C. Pohl, J. Electroanal. Chem. 608 (2007) 117.
[13] S. Hughes, D.C. Johnson, J. Agric. Food Chem. 30 (1982) 712.
[14] S. Hughes, D.C. Johnson, Anal. Chim. Acta 149 (1983) 1.
[15] G.G. Neuburger, D.C. Johnson, Anal. Chem. 59 (1987) 150.
[16] W.R. LaCourse,D.C Johnson, Carbohydr. Res. 215 (1991) 159.
[17] D.C. Johnson, W.R. LaCourse, Electroanal. 4 (1992) 367.
[18] R.E. Roberts, D.C. Johnson, Electroanal. 6 (1994) 269.
[19] R.D. Rocklin, T.R. Tullsen, M.G. Marucco, J. Chromatogr. A 671 (1994) 109.
[20] R.E. Roberts, D.C. Johnson, Electroanal. 7 (1995) 1015.
[21] J. Wen, R.M. Cassidy, A.S. Baranski, J. Chromatogr. A 811 (1998) 181.
[22] K.Z. Brainina, N.A. Malakhova, N.Y. Sjko, Fresen J. Anal. Chem. 368 (2000). 307.
[23] A. Cavicchioli, M.A. La-Scalea, I.G.R. Gutz, Electroanal. 16 (2004) 697.
[24] M.G. Paneli, A. Voulgaropoulos, Electroanal. 5 (1993) 355.
[25] A.G. Fogg, J. Wang, Pure Appl. Chem. 71 (1999) 891.
[26] P. Vanysek, John Wiley, New York, (1996) 151-185.
[27] R. Cornelis, H. Crews, J. Caruso, K. Heumann, John Wiley & Sons, Ltd, (2003) 427-460.
[28] S.A. Ozkan, Curr. Pharm. Anal. 5 (2009) 127.
[29] A.J. Bard, L.R. Faulkner, John Wiley & Sons Inc., New York (2001) 458-470.
[30] S.A. Ozkan, B. Uslu, H.Y. Aboul-Enein, Crit. Rev. Anal. Chem. 33 (2003) 155.
[31] J. Wang, Electroanal. 17 (2005) 1341.
[32] D. Harvey, McGrawHill Company, Boston (2000) 515-520.
[33] J. Buffle, M.L. Tercier-Waeber, Trend. Anal. Chem. 24 (2005) 172.
[34] J. Barek, J. Fischer, T. Navratil, K. Peckova, B. Yosypchuk, Sensor. 6 (2006) 445.
[35] J. Barek, J.C. Moreira, J. Zima, Sensor. 5 (2005) 148.

CHAPTER 5. NANOSTRUCTURED CARBON-BASED COMPOSITE ELECTRODES USED FOR ELECTROANALYSIS

5.1. Introduction in electrochemical sensors

Electrochemical sensors and detectors are important keys in environmental monitoring of a certain target pollutants. These pollutants can be found in different and significant area from industrial and recycling, effluents and wastewater preceded from agricultural and municipal sites. Thus, due to the tremendous increased of the toxic effects of these priority pollutants, their continuous monitoring in the field is necessary. The portable-electrochemical devices can satisfy the requirements that imply such type of monitoring due to the main advantages of these, like the essentially sensitive and selective towards electroactive species, the fast response and accuracy, low cost, and long lifetime [1, 2].

The most important criteria of a good sensor are high sensitivity, fast response, low cost, high volume production, and high reliability. Some of the requirements to be taken into consideration are shown in Figure 5.1.

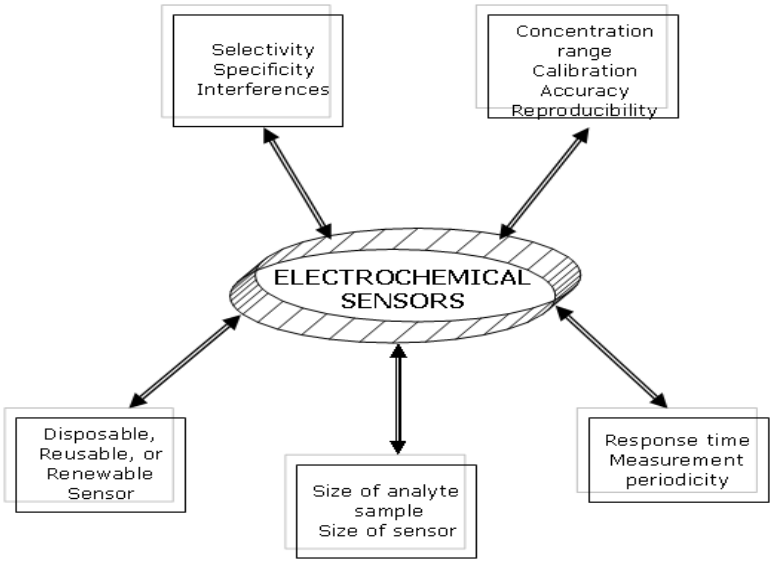

Figure 5.1. Important aspects for choosing electrochemical sensors for environmental monitoring [2].

The principle of an electrochemical sensor is to offer real-time reliable information about the chemical composition of its enclosing environment, ability of

responding continuously and reversibly and does not perturb the sample. In the electrochemical sensors, the analytical information is achieved from the electrical signal that results from the interaction of the target analyte and the electrode surface. Depending on the nature of the analyte, the character of the sample matrix, and sensitivity or selectivity requirements diverse electrochemical devices can be used for the assignment of environmental monitoring. Therefore, in agreement with the nature of the electrical signal, in general exist three main categories of sensors, *e.g.*, conductimetric, potentiometric and voltammetric.

Conductiometric detectors can be useful in electroremediation where is necessary to establish, if the total ion concentration is below a certain allowable maximum level or to be apply as an on-line detector after separation of a mixture of ions by ion chromatography.

The potentiometric sensors rely on the use of ion selective electrodes for obtaining the potential signal. The response is measured using a high-impedance voltmeter, under conditions of essentially zero current. Such sensors are very attractive for field operations because of their high selectivity, simplicity and low cost. They are, however, less sensitive and often slower than their voltammetric/amperometric complements.

Volammetric/amperometric sensors are based on the detection of electroactive species involved in the chemical or biological identification process. The current is recorded as a function of applied potential, more information and lower detection limits can usually be achieved. Using such devices and by preconcentration of the analyte on the electrode surface can be reached very low detection limits of down to the picomolar level, and also, can be determined simultaneously several species that react at different applied potentials. The sensors detectors like amperometric sensors at fixed potential can be employed as well after separation by high-pressure liquid chromatography or capillary electrophoresis, or in detectors in continuous flow, and subsequent to the voltammetric section that has been investigated.

Using these types of the electrochemical measurements described above it may bring improvements in the context of the environmental monitoring since they have a good specificity in comparison with other analytical technique. Each chemical species, element or oxidation state has an associated potential for oxidation and reduction, thus using the voltammetric sensors at an applied potential high selectivity and specificity can be reached. Also, as a consequence the speciation of the certain species can be determined.

The choosing the electrode material is very important for voltammetric sensors because at some electrode materials certain species do not react, avoiding interference problems, and improving their selectivity.

The modern electrochemical analysis methods combine with the voltammetric sensors can lead to high sensitivity and low detection limits, due to the fusions in the same time of the analytical complex programs and capability of measured the accumulation of the species at the electrode surface. Based on the nanotechnology development, it can be construct miniaturized sensors for application in specific situations where other probes may not be usable, leading to reduced weight, lower power consumption, and low cost.

As a sensor to be characterized by a high performance, it must comply with certain criteria related to how it is design, which in turn are linked with its potential benefits. Most important are suitable for amperometric and voltammetric sensors. For example, the specie to be determined is electroactive within the sensor's potential range; the concentration of electroactive species can be determined with

sufficient accuracy and precision; the measurements are sufficiently reliable and repeatable; the response time of the sensor is sufficiently fast; the sensor response with time owing to electrode degradation or surface fouling is reduced; calibration is simple and easy to perform; the detection limit is low enough for the purpose envisaged. The relative importance of these factors depends on the monitoring necessities in direct relation to the technique employed, the electrode and cell configuration. In addition, there are other advantages that arising from usage of the electrochemical sensors, *e.g.*, self-contained test modules specific assays, miniaturization, no external pretreatment or necessity of reagent addition [1, 2].

5.2. Composite materials for electroanalysis

In the last years, the composite based electrodes have been developed as the electrochemical sensors. The combination of two or more constituent materials that posses significantly different physical or chemical properties and each component remain separate and distinct forms the composite. All the composites posses different properties versus each component. In general, the reinforcements of one or more conductive fillers within the insulating matrix generate the composite material [3].

A general classification of the matrices of the composite materials used in electroanalysis, particularly for electrochemical sensors is described in the following figure.

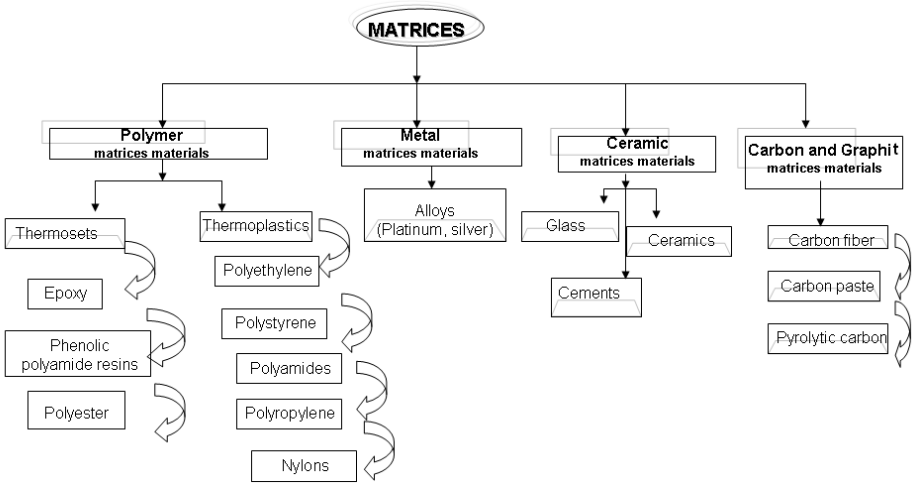

Figure 5.2. Schematically classification of various type of matrix composite [4, 5, 6].

Reinforcements for composite materials can be fibers, particles, filler, etc. The type, distribution, size, shape, orientation, and arrangement of the reinforcement will determine the properties of the composites material and its anisotropy. In figure 5.3 are represented a general description of type of reinforcement used for composite.

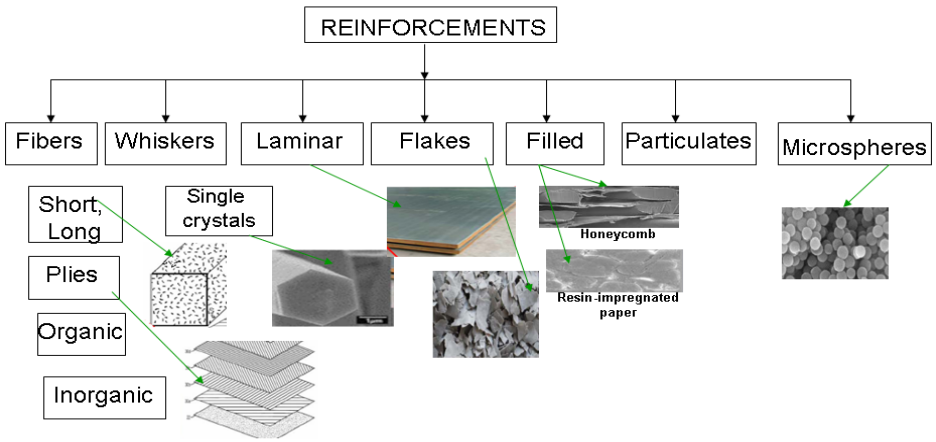

Figure 5.3. Type of reinforcements for composite materials. [4, 5, 6].

Thermosetting epoxies are most frequently used as a matrix for advanced composites due to their high thermal, excellent mechanical and electrical properties; dimensional stability and chemical resistance. Epoxy belongs to the thermosetting epoxies polymer group that are produced from a reaction between epichlorohydrin and bisphenol-A. Epoxy resins are widely used as high-quality synthetic resins, in structural application, like in the electronics, aeronautics and astronautic industries. In industrial finishing stage, the epoxy film is used for covering metallic substrates, providing superior adhesion, flexibility and corrosion resistance. Epoxy resins are also used with various curing agents, diluents and modifiers to create products with an almost unlimited range and variety of performance properties [7, 8].

However, epoxy resins are electrical insulators, and the widespread use of the epoxy resins for many high-performance applications is constrained because of their inherent brittleness, delamination and fracture toughness limitations. There were few approaches to enhance the properties of epoxy resins [9, 10], but, these methods lead to a decrease in other desirable mechanical and physical properties.

A newly developed strategy offering promising results is to reinforce epoxy matrices with nano-sized organic and inorganic particles such as carbon nanotubes (CNTs), carbon nanofibers (CNFs), nanoclays, metal oxide nanoparticles, etc. [11-14] to obtain new materials with enhanced properties. The unique properties of the nanoparticles such as nanometric size, high specific surface areas and the possibility of combining them with conventional reinforcements have caused intense research in the field of nanocomposites [15].

5.3. Chemically modified electrodes for electroanalysis

Chemically modified electrode (CME) can be defined as "electrode made of a conducting or semiconducting material that is coated with a selected monomolecular, multimolecular, ionic, or polymeric film of a chemical modifier and that by means of faradaic (charge-transfer) reactions or interfacial potential differences (no net charge transfer) exhibits chemical, electrochemical, and/or optical properties of the film [16]

Chemically modified electrodes (CMEs) have attracted considerable interest over the past two decades due to numerous important applications *e.g.*, solar

energy conversion and storage, selective electro-organic synthesis, molecular electronics, electrochromic display devices, corrosion protection, and electroanalysis. Actually, chemically modifies electrodes offer powerful opportunities, especially in the field of electrocatalysis, electroanalysis and surface sciences, due to the unique well-known advantages arises from the capability to join the electrochemical technique with the chemical, structural properties of the modifying layers [17].

The chemically modified electrodes utilized for analytical application can be designed as great sensing devices, by modification of the surface or volume matrix material of the electrode with a polymeric reagent that influence its electrochemical properties. This purpose is to improving sensitivity, selectivity and/or stability of its response in agreement with the analytical requirements [18].

To prepare the CME, most often is use as the modifying agents the inorganic materials, mainly thin film of selected chemical [19]. This is based on the physical or electrochemical deposition of an inorganic polymer film on the electrode surface, the codeposition of the inorganic particles with an organic polymer or the incorporation of inorganic materials directly into a conductive (polymeric) matrix acting as the working electrode. The most common inorganic species used to modify electrochemical interfaces include metal oxides [20, 21], Prussian Blue and related transition metal cyanides [22], metal phtalocyanines and porphyrins [23], fumed silica [24], clays [25] and zeolites [26-29]. Among these, zeolites offer the most complete range of interesting properties required at an electrochemical interface, including shape, size and charge selectivities, physical and chemical stabilities, high ion exchange capacity in a microstructured environment and hydrophilic character [30].

5.3.1. Zeolite-modified electrodes (ZMEs)

Zeolites make part from the new class of silicate minerals that include a vast number of natural and synthetic minerals with general structural characteristic. The natural ones are formed in diversity of geological sites, such as volcanic ash, clay, biogenic silica and different forms of quartz. The most common natural zeolites are mordenite, clinoptilolite, chabaxite, erionite and phillipsite [31].

Except natural zeolites all the crystalline aluminosilicates employed for modifying an electrode surface are synthetic zeolites. Zeolites A and Y are the most commonly used aluminosilicates to modify an electrode surface, due to they can demonstrate the size selectivity properties of ZMEs, and because these two zeolites present different molecular sieving properties. Based on their properties, the synthetic zeolites have been widely studied for industrial applications [55, 56]. Mordenite and zeolite X was used, especially those exchanged with transition metal cations [32-35].

Zeolites are hydrated crystalline aluminosilicates belonging to the family of the tectosilicates, with a 4-connected tetrahedral framework structure cavities occupied by large cations and water molecules, both of which have considerable freedom of movement, allowing ion exchange and reversible dehydration [36].

Aluminosilicates zeolites present interest for electrochemistry due to principal advantage of those, such as, low cost of extraction, their availability in great volumes, and their excellent stability in chemical and thermal processes. These properties makes them to be a versatile material in numerous applications, *e.g.*, petro chemistry, environmental science, agriculture, water treatment, radioactive waste storage, desiccation or gas separation and purification [37-40].

Therefore, zeolite-modified electrodes (ZMEs) have attracted considerable attention within the last decades because they combine in a sensor device the specificity of charge transfer reaction with the intrinsic properties of the aluminosilicates zeolites.

Thus, the interest for the zeolite-modified electrodes (ZMEs) can be divided in three main reasons. First, they combine the advantage of ion exchange voltammetry with the unique molecular sieving properties of the zeolites. Consequently, it can be make a distinguish between the reactants that are very small and can diffuse liberty within the zeolite framework, and those that not take part at mass transport process. Another reason is related to the development of new electroanalytical devices. Therefore, it can be gain improvements in comparison with the classical chemically modified electrodes by the combination of the attractive properties of the zeolites with the high sensitivity and selectivity of modern electrochemical techniques. However, not the least, they are interesting for the analytical investigation, particularly in electrocatalyst due to the given selectivity of zeolites based on the size and shape of the reactants. Also, because of the tridimensional lattice that made of interconnected cages of molecular dimension, the zeolite can be a support sites for a variety of catalysts [41].

A critical point in applying ZMEs in electrochemical science is their preparation. Thus, the electrochemical response is associated to the type of zeolite incorporated, and hence by its properties, as well as the way of zeolite is confinement at an electrode surface.

The various ways reported in the literature for the preparation of ZMEs may be classified in four main groups. Thus, a strategy is concerns to the dispersion of zeolite particles within solid matrices. Another manner may be the compression of zeolites on conductive substrates. Also, there has been reported the proposal relates to coating of zeolite incorporated in polymeric films on solid electrodes. Other style to design a ZMEs is refers to the covalent attachment of zeolite particles to an electrode surface. Figure 3 represent a synthesis of all the modality to prepare ZMEs retrieved in the literature.

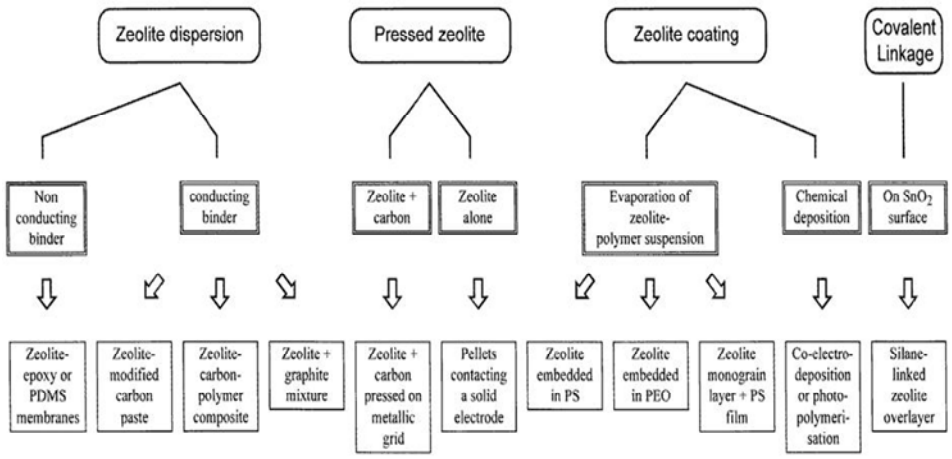

Figure 5.4. Strategies commonly applied to prepare zeolite-modified electrodes; (PDMS: polydimethylsiloxane; PS: polystyrene; PEO: polyethylene oxide). [42].

The main analytical application of ZMEs is divided in: direct amperometric detection, voltammetric detection after accumulation at open circuit, indirect amperometric detection of nonelectroactive species, amperometric biosensors, and potentiometry using zeolite membranes. All these applications are directly correlating with the intrinsic properties of zeolites. The direct detection of electroactive species was achieved either by exchanging charge transfer mediators within the zeolite or by using the microporous solid as a support for the electrode itself. The voltammetric detection after accumulation involves the ion exchange properties of zeolites. This has been applied to determine the metal cations and some organic species [41, 43].

The indirect amperometric detection of nonelectroactives species combined the exchange capacity of the zeolites with their unique size and charge selectivity. In such a way, it is possible to distinguish between size-excluded species acting like as the supporting electrolyte and no size excluded analytes. This has been exploited for the detection of alkali metal ions and water in methanol or dimethylformamide (DMF) by using silver-doped zeolites [44, 45]. Finally, the ion exchange capacity and selectivity were exploited by using zeolite membranes for potentiometric detection [46]

Consequently, the analytical performance of ZMEs is strongly connected with all these properties, which can be very different from one zeolite to another and can differ significantly as a function of the solution composition. Therefore, using several kinds of zeolites, electroactive species and different electrode configuration the electroanalytical response may be strongly influenced by each of them [47-52].

5.4. Nanostructured carbon-based composite electrodes

The evolution of length scales from meters, micrometers, sub-micrometers to nanometers presents remarkable opportunities for many disciplines of science and the development of innovative approaches in the processing, characterization, and analysis/modeling this new generation of composite materials.

The most representative and extremely used of this new generation of composite materials are nanostructured materials *e.g.*, nanofibers, nanotubes, and nanoparticles [53, 54].

Similarly, carbon-based nanostructured materials present a great interest in their preparation and application, and currently have been widespread used in electrochemical analysis due to their outstanding properties [55].

The development of composites based on conductive carbon phases dispersed in polymeric matrices has led to important advances in analytical electrochemistry and sensor devices. These new materials combine the electrical properties of graphite with the ease of processing of plastics and show attractive electrochemical, physical, mechanical, and economical features [56-59].

There are at least three general experimental methods to produce polymer nanocomposites: mixing in the liquid state, solution-mediated processes and *in-situ* polymerisation techniques. The direct melt-blending approach is much more commercially attractive than the latter two methods, as both solvent processing and *in-situ* polymerisation are less versatile and more environmentally contentious [60].

When using thermosetting matrices, as-received nanotubes/nanofibers are often directly mixed with the liquid matrix (especially epoxy) precursors. Mechanical mixing can be aided by ultrasonication and vacuum-assisted processing is often applied to ensure defect-free composite samples for mechanical testing. Chemically

treated nanotubes are often first dispersed in surfactants or solvents to which the epoxy is added [60-62].

Carbon nanofibers (CNFs) are of special interest because they promise to provide solutions to the problems encountered in composite applications. Unlike conventional composites, they are electrically conductive and thus, are suitable for applications that require the ability to discharge electrostatic potentials, provide sufficient conductivity for electrostatic painting, or even shield from radio frequency interference or lightening strike. Moreover, their thermal conductivity is excellent [63, 64].

They have diverse structure, such as platelet, herringbone, and tubular axis [65], that is derived from the anisotropic alignment of grapheme layers. The wide ranging morphology of CNF and their associated properties results in a broad range of disseminate for experimental results on processing and characterization of their with several application ranging from catalysts [66], electrode materials for supercapacitors [67], gas sensors [68], novel electrode supports for redox liquid electrodes [69], to substrates for enzyme immobilization [70].

From the point of practical importance, carbon nanofibers have been used to reinforce a variety of polymer including polypropylene [71], polycarbonate, nylon, poly (methyl methacrylate), polyester, polyethylene, and epoxy [13, 64] matrices. [72-74].

From the various nanofillers used to modify polymer matrices, CNTs have attracted great interest recently as structural reinforcements because of their unique properties *e.g.*, amazing mechanical properties, phenomenal electrical and thermal conductivity, nanoscopic size and high aspect ratio [75-78], and also, this combination of properties can also lead to electrical percolation at low concentrations. This low loading is advantageous because the effects on resin properties are minimal and the same processing equipment can be used with pure resins and nanocomposites. Thus, the resulting carbon-based polymer nanocomposites are expected to achieve high properties at low filler volume fractions due to the high aspect ratio and high surface area to volume ratio of the nano-sized particles [79-81].

In addition, different types of polymer composites have been synthesized by incorporating CNTs into various polymer matrices such as polyamides [82], epoxy [83, 84], polyurethane [85], polypropylene [86], and others [87]. The synthetic methods for CNTs include the carbon arc-discharge method [88], laser vaporization of a graphite electrode [89] and the chemical vapour-deposition methods from various carbon precursors [90]

There are two main types of CNTs: single-walled CNTs (SWCNTs) and multi-walled CNTs (MWCNTs). The MWCNTs are the most wildly used because they exhibit a fantastic property of mechanical strength allowing be used as reinforcing material. Thus, due to these properties of carbon-based composite nanostructured have been attracted a lot of interest from the scientific community for the fabrication and application of these advanced materials for electrochemical sensing and some other many areas.

Due to extraordinary properties of CNTs, they can be used in sensors, detectors and other devices. The development of such smart nanoscale materials, which can detect, convert, process, has the potential of revolutionizing the sensors industry. Thus, several studies have been reported the use of CNTs for sensors and detection application, *i.e.*, CNT-based biosensors [91], pressure sensors [92], gas sensors [93], electrochemical biosensors [94], CNT-based pH sensors [95], amperometric biosensors [96], nano-electro-mechanical- sensors and switches [97].

Potential practical applications of carbon nanotubes have been reported, *e.g.*, chemical sensors, field emission materials, catalyst support, electronic devices, high sensitivity nanobalance for nanoscopic particles reinforcements in high performance composites, nano-probes in meteorology, biomedical and chemical investigations, anode for lithium ion in batteries, nano-electronic devices, supercapacitors, and hydrogen storage [98, 99].

Recent studies demonstrated that CNT exhibits strong electrocatalytic activity for a wide range of compounds, *e.g.*, neurotransmitters, [100], NADH, [101], hydrogen peroxide, [102], ascorbic acid, [103], cytochrome *c,* [104], and DNA [105], pentachlorophenol [106, 107], glucose [108].

5.4.1. Metallic nanocomposites modified nanostructured carbon-based composite electrodes

Other types of nanostructured carbon based composite electrodes with enhanced electrocatalytical properties are based on metallic nanoparticles-modified nanostructured carbon composite electrodes. Metallic nanoparticles represent a tremendous interest in the synthesis and application in the field of electrochemistry, in particular in electroanalysis due to their interesting optical, electronic, magnetic and catalytic properties. Also, in terms of electroanalysis the metallic nanoparticles materials are suited to modify electrodes due to many advantages, *e.g.*, high active surface area, improved the selectivity, enhanced the mass transport, and provide control over the local micro-environment [109-111].

Various preparation methods have been development to modify metal nanoparticles on diverse substrates of electrodes to emphasize the electrocatalytic and electron-conducting characteristics of metal nanoparticles useful for electrochemical analysis. The most common metal nanoparticles used are silver, gold, and platinum, and as well as the most frequently methods encountered in literature are in respect to the synthesis of metallic nanoparticles and by deposition on electrodes surfaces. Thus, the chemical synthesis is referred at the reduction with different reagents, UV light or electron-beam irradiation [112- 114]. Also, the deposition of metallic nanoparticles can be performed by electrochemical techniques. [115]. The latter method provides an easy and rapid alternative for the preparation of metallic nanoparticle based electrodes within a short period of time. In addition, present some advances over chemical method such as high purity of the particles, higher control over the dimension, lower particle size distribution, more control over the density. [116-118].

The nature of substrate plays an important role in electrocatalytic properties of metal nanoparticles. In fact, the nanoparticle microenvironment is greatly influenced by the support on which it is deposited because it affects the morphologies of nanoparticles as well as their electrocatalytic properties. [119-121].

Thus, the electrodeposition of silver, which are one of the most common metallic nanoparticles used for this purpose, on carbon-based electrodes has been widely investigated [122-123]. Because carbon materials appropriately modified with silver can be used not only in electrocatalysis [124] and catalysis [125] but also, as antibacterial agents [126], the study of the properties of these materials is highly significant in theory and practice.

In prolonged contact with Ag (I) ion solution, carbon materials acquire a large percentage of zero-valence silver on the surface and in the near-surface region. The following phenomena may occur on the carbon surface, *e.g.*, cation exchange and/or complex formation of metal ions, spontaneous reduction of cations

connected with carbon surface oxidation, diffusion and/or intercalation of metal, and growth of hemispherical silver nuclei on the surface. All these phenomena have occurred at varied extents on different carbon materials [127-129].

Since, the metal nanoparticles in combination with carbon-based composite electrodes by electrodeposition have been extremely investigated as new advance composite materials for electrochemical sensing. Moreover, because of their outstanding properties of such nanoarhitectures in the field of nanostructured-based sensors many analytes were determined electrochemically using various designs of electrodes with different metal nanoparticles [130-134].

5.5. References

[1] J. Wang, K. Rogers, Las Vegas, Nev.: U.S. EPA (1995) 1.
[2] C.M.A. Brett**,** Pure Appl Chem 73 (2001) 1969.
[3] K. Gong, Y. Yan, M. Zhang, L. Su, S. Xiong, L. Mao, Anal Sci 21 (2005) 1383.
[4] T. Sabu,J. Kuruvilla, Wiley-VCH (2012).
[5] B. Harris, Maney Materials Science, 2 edition (1999).
[6] Composite Materials Handbook, MIL-HDBK-17 / 1F / 2F / 3F / 4A / 5 (2002).
[7] J. Njjuguna, K. Pielichowski, J.R. Alcock, Adv Eng Mater 9 (2007) 835.
[8] S. Barrau, P. Demont, A. Peigney, C. Laurent, C. Lacabanne, Macromolecules 36 (2003) 5187.
[9] S. Dirlikov, I. Frischinger, Z. Chen, Washington DC: American Chemical Society (1996) 95.
[10] A.J. Kinloch, F.J. Guild, Washington DC: American Chemical Society (1996) 3.
[11] D. Puglia, L. Valentini, J.M. Kenny, J Appl Polym Sci 88 (2003) 452.
[12] D. Puglia, L. Valentini, J.M. Kenny, Diamond Related Mater 2003; 12: 827–32;
[13] M.H. Al-Saleh, U. Sundararaj, Carbon 47 (2009) 2.
[14] B.C. Kim, S.W. Park, D.G. Lee, Compos Struct 86 (2008) 69.
[15] S.K. Pillai, S. Ray, InTechOpen (2011) 727.
[16] R. A. Durst, A. J. Baumner, R. W. Murray, R. P. Buck, C. P. Andrieux, Pure Appl Chem 69 (1997) 1317.
[17] W. Kutner, J. Wang, M. L'her, R.P. Buck, Pure Appl Chem 70 (1998) 1301.
[18] J.M. Zen, A.S. Kumar, D.M. Tsai, Electroanal 15 (2003) 1073.
[19] J.A. Cox, R. Jaworski, P.J. Kulesza, Electroanal 3 (1991) 869.
[20] L. G. Shaidarova, G. K. Budnikov, J Anal Chem 63 (2008) 922.
[21] C.G. Granqvist, Sol Energ Mat Sol C 60 (2000) 201.
[22] M. Arvand, S. Sohrabnezhad, M.F. Mousavi, M. Shamsipur, M.A. Zanjanchi, Anal Chim Acta 491 (2003) 193.
[23] K. Araki, L. Angnes, C.M.N. Azevedo, H.E. Toma, J Electroanal Chem 397 (1995) 205.
[24] J. Wang, N. Naser, Electroanal 6 (1994) 571.
[25] Y. Shih, J.M. Zen, Anal Chim Acta 412 (2000) 63.
[26] A. Walcarius, S. Rozanska, J. Bessière, Joseph Wang, Analyst 124 (1999) 1185.
[27] F. Manea, A. Remes, C. Radovan, R. Pode, S. Picken, J. Schoonman, Talanta 83 (2010) 66.
[28] A. Nezamzadeh, M.K. Amini, H. Faghihian, Int J Electrochem Sci 2 (2007) 583.
[29] M. Földesová, P. Hudec, P. Dillinger, Petrol Coal 49 (2007) 60.
[30] A. Walcarius, Electroanal 8 (1996) 971.
[31] J. Ceijka, H. van Bekkum, A. Corma, F. Schuth, 3rd revised edition, Elsevier (2007) 1-13.

[32] C.J. Rhodes, Sci Prog 93 (2010) 223.
[33] B. Bogdanov, D. Georgiev, K. Angelova, Y. Hristov, International Science Conference, Stara Zagora, Bulgaria "Economics and Society development on the Base of Knowledge", 4th - 5th June (2009).
[34] C. Orha, A. Pop, C. Lazau, P. Sfirloaga, I. Grozescu, V.l Tiponut, F. Manea, International Semiconductor Conference, Sinaia, Romania, CAS 2011 Proceedings, October 17-19 (2011) 299.
[35] HERA Risk Assessment of Sodium Aluminium Silicate, Zeolite A, Version 3.0, January (2004) 1-53.
[36] J. Ceijka, H. van Bekkum, A. Corma, F. Schuth, 3rd revised edition, Elsevier, (2007) 659-701.
[37] C. Colella, Stud Surf Sci Catal 125 (1999) 641.
[38] M.W. Ackley, S.U. Rege, H. Saxena, Micropor Mesopor Mat 61 (2003) 25.
[39] M. Rehakova, S. Cuvanova, M. Dzivak, J. Rimar, Z. Gavalova, Curr Opin Solid St 8 (2004) 397.
[40] M. G. Valdes, A.I. Perez-Cordoves, M.E. Diaz-Garcia, Trend Anal Chem 25 (2006) 24.
[41] S.M . Auerbach, K.A. Carrado, P.K. Dutta, Marcel Dekker, Inc (2003) chapter 14.
[42] A. Walcarius, Anal Chim Acta 384 (1999) 1-16.
[43] A. Walcarius, Anal Chim Acta 388 (1999) 79.
[44] A. Remes, F. Manea, D. Sonea, G. Burtica, S. Picken J. Schoonman, Ovidius University Annals of Chemistry 20 (2009) 61.
[45] F. Manea, A. Pop, C. Radovan, P. Malchev, A. Bebeselea, G. Burtica, S. Picken, J.Schoonman, Sensor 8 (2008) 5806.
[46] A. Badri, P. Pouladsaz, Highly, Int J Electrochem Sci 6 (2011) 3178.
[47] Alain Walcarius, J Solid State Electrochem 10 (2006) 469.
[48] A. Walcarius, P. Mariaulle, L. Lamberts, J Solid State Electrochem 7 (2003) 671
[49] A. Walcarius, S. Rozanska, J. Bessièrea, J.Wang, Analyst 124 (1999) 1185.
[50] R.H. Carvalho, F. Lemos, M.A.N.D.A. Lemos, J.M.S. Cabral, F. Ramoa Ribeiro, J Mol Catal A-Chem 248 (2006) 48.
[51] R.H. Carvalho, M.A.N.D.A. Lemos, F. Lemos, J.M.S. Cabral, F. Ramoa Ribeiro, J Mol Catal A-Chemical 253 (2006) 170.
[52] R.H. Carvalho, M.A.N.D.A. Lemos, F. Lemos, J.M.S. Cabral, F. Ramoa Ribeiro, Catal Today 133–135 (2008) 855.
[53] F. Husssain, M. Hojjati, M. Okamoto, R. E. Gorga, J Compos Mater 40 (2006) 1151.
[54] M. Trojanowicz, Trend Anal Chem 25 (2006) 480.
[55] B. Uslu, S. A. Ozkan, Anal Lett 40 (2007) 817.
[56] F. Cespedes, E. Martinez-Fabregas, S. Alegret, Trend Anal Chem 15 (1996) 296.
[57] A. Merkoci, M. Pumera, X. Llopis, B. Perez, M. del Valle, S. Alegret, Trend Anal Chem 24 (2005) 826.
[58] M. Pumera, A. Merkoci, S. Alegret, Sensor Actuat B 113 (2006) 617.
[59] S. Ramirez-Garcia, S. Alegret, F. Cespedes, R.J. Forster, Analyst 127 (2002) 1515.
[60] S.G. Advani (Ed.), Processing and properties of nanocomposite, (2007), World Scientific publishing Co.Pte.Ltd. pp. 1-59, http://www.worldscibooks.com/nanosci/6317.html.
[61] K.L. White, H.J. Sue, Polym Eng Sci 51 (2011) 2245.

[62] D. Zilli, S. Goyanes, M. M. Escobar, C. Chiliotte, V. Bekeris, A. L. Cukierman, G. H. Rubiolo, Polym Composite 28 (2007) 612–617.
[63] R.D. Patton, C.U. Pittman Jr, L. Wang, J.R. Hill. Compos Part A-Appl S 30 (1999) 1081.
[64] G.G. Tibbetts, M.L. Lak, K.L. Strong, B.P. Rice, A review of the fabrication and properties of vapor-grown carbon Nanofiber/polymer composites, Composites Science and Technology 67, (2007) pp. 1709–1718].
[65] S.H. Yoon, S. Lim, S.H. Hong, W.M. Qiao, D.D. Whitehurst, I. Mochida, B. An, K. Yokogawa, Carbon 43 (2005) 1828.
[66] J.H. Zhoua, C. Chena, R. Guoa, X.C. Fangb, X.G. Zhoua, Carbon 47 (2009) 2077.
[67] A. K. Sharma, Y. Sharma, R. Malhotra, J.K. Sharma, Adv Mat Lett 3 (2012) 82.
[68] J. Jyongsik, B. Joonwon, Sensor Actuat B-Chem 122 (2007) 7.
[69] R. Mirshafian, M. R. Ganjali, P. Norouzi1, Int J Electrochem Sci 7 (2012) 1656.
[70] K.M. de Lathouder, D. Lozano-Castello, A. Linares-Solano, S.A. Wallin, F. Kapteijn, J.A. Moulijn, Micropor Mesopor Mat 99 (2007) 216.
[71] K. Enomoto, S. Fujiwara, T. Yasuhara, H. Murakamu, J. Teraki, N. Ohtake, Jpn J Appl Phys 4 (2005) L888.
[72] J.J. George, A.K. Bhowmick, Nanoscale Res Lett 3 (2008) 508.
[73] Z. Moridi, V. Mottaghitalab, A. K. Haghi, Cellulose Chem Technol 45 (2011) 549.
[74] L. Rassaei, M. Sillanp, M. J. Bonne, F. Marken, Electroanal 19 (2007) 1461.
[75] E.T. Thostenson, C. Li, T.W. Chou, Compos Sci Tech 65 (2005).
[76] E.T. Thostenson, Z. Ren, T.W. Chou, Compos Sci Tech 61 (2001) 1899.
[77] J. Sandler, M.S.P. Shaffer, T. Prasse, W. Bauhofer, K. Schulte, A.H. Windle Polymer 40 (1999) 5967.
[78] D. Srivastava, C. Wei, K. Cho, Appl Mech Rev 56 (2003) 215.
[79] N. Hu, Z. Masuda, G. Yamamoto, H. Fukunaga, T. Hashida, J. Qiu, Composites A 39 (2008) 893.
[80] A.S. Santos, T.O.N. Leite, C.A. Furtado, C. Welter, L.C. Pardini, G.G. Silva, J Appl Polym Sci 108 (2008) 979.
[81] Y. Zhou, F. Pervin, L. Lewis, S. Jeelani, Mater Sci Eng A 475 (2008) 157.
[82] H. Cai, F.Y. Yan, Q.J. Xue, Mater Sci Eng A 364 (2004) 94.
[83] N. Hu, Z. Masuda, G. Yamamoto, H. Fukunaga, T. Hashida, J. Qiu, Composites A 39 (2008) 893.
[84] Y.H. Liao, M.T. Olivier, Z.Y. Liang, C. Zhang, B. Wang, Mater Sci Eng A 385 (2004) 175.
[85] H.C. Kuan, C.M. Ma, W.P. Chang, S.M. Yuen, H.H. Wu, T.M. Lee, Compos Sci Tech 65 (2005) 1703.
[86] M.K. Seo, J.R. Lee, S.J. Park, Mater Sci Eng A 404 (2005) 79.
[87] B. Fragneaud, K. Masenelli–Varlot, A. Gonzalez–Montiel, M. Terrones, J.Y. Chem Phys Letts 444 (2007) 1.
[88] S. Iijima, Nature 354 (1991) 56.
[89] A. Thess, R. Lee, P. Nikolaev, H. Dai, H. Petit, J. Robert, C. Xu, Y.H. Lee, S.G. Kim, A.G. Rinzler, D.T. Colbert, G. Scuseria, D. Tomanek, J.E. Fischer, R.E. Smalley, Science 273 (1996) 483.
[90] J.F. Colomer, P. Piedigrosso, I. Willems, C. Journet, P. Bernier, G. Van Tendeloo, A. Fonseca, J.B. Nagy, J Chem Soc Faraday Trans 94 (1998) 3753.
[91] S. Li, P. He, J. Dong, Z. Guo, L. Dai, J Am Chem Soc 127 (2005) 14.
[92] W. Yang, P. Thordarson, J.J. Gooding, S.P. Ringer, F. Braet, Nanotechnology 18 (2007) 1.

[93] K.H. An, S.Y. Jeong, H.R. Hwang, Y.H. Lee, Adv Mater 16 (2004) 1005.
[94] G. Chiti, G. Marrazza, M. Mascin, Anal Chim Acta 427 (2001) 155.
[95] Z. Xu , X. Chen , X. Qu , J. Jia , S. Dong, Biosens Bioelectron 20 (2004) 579.
[96] X. Liu, C. Lee, C. Zhoua, J. Han, Appl Phys Lett 79 (2001) 3329.
[97] A. A. Farajian, B. I. Yakobson, H. Mizuseki, Y. Kawazoe, Phys Rev B 67 (2003) 1.
[98] P. M. Ajayan, O. Z. Zhou, Top Appl Phys 80 (2001) 391.
[99] M. Endo, M. S. Strano, P. M. Ajayan, Top Appl Phys 111 (2008) 13.
[100] J. Wang, M. Li, Z. Shi, N. Li, Electroanal 14 (2002) 225.
[101] J. Wang, M. Musameh, Anal Chem 75 (2003) 2075.
[102] J. Wang, M. Musameh, Anal Lett 36 (2003) 2041.
[103] **A. Baciu**, A. Remes, E. Ilinou, F. Manea, S.J. Picken, J. Schoonman, Environ Eng Manag J 11 (2012) 1967.
[104] J. Wang, M. Li, Z. Shi, N. Li, Anal Chem 74 (2002) 1993.
[105] J.X. Wang, M.X. Li, Z.J. Shi, N.Q. Li, Z.N. Gu, Electroanal 16 (2004) 140.
[106] **A. Baciu**, F. Manea, A. Remes, S. Motoc, G. Burtica, R. Pode**,** Environ Eng Manag J 9 (2010) 1555.
[107] A. Remes , A. Pop, Florica Manea, **A. Baciu**, S. J. Picken, J Schoonman, Sensor 12 (2012) 7033.
[108] **A. Baciu**, A. Pop, A. Remes, F. Manea, G. Burtica, Adv Sci Eng Med 3 (2011) 13.
[109] H. Chu, L. Wei, R. Cui, J. Wang, Y. Li, Coordin Chem Rev 254 (2010) 1117.
[110] M. Oyama, Anal Sci 26 (2010) 1.
[111] C.M. Welch, R.G. Compton, Anal Bioanal Chem 384 (2006) 601.
[112] L. Suna, Z. Zhang, H. Dang, Mater Lett 57 (2003) 3874–3879;
[113] M**.** Fukushima, H**.** Yanagi, S**.** Hayashia, N**.** Suganuma, Y**.** Taniguchi, Thin Solid Films 438-439 (2003) 39.
[114] R. Hidalgo-Alvarez (Ed), CRC Press Inc (2009) 339-365.
[115] O. D. Renedo, M.A. Alonso-Lomillo, M.J. A. Martınez, Talanta 73 (2007) 202.
[116] R. A. Khaydarov, R. R. Khaydarov, O. Gapurova, Y. Estrin, T. Scheper, J Nanopart Res 11 (2009) 1193.
[117] M.E. Hyde, R.G. Compton, J Electroanal Chem 549 (2003) 1.
[118] A. Safavi, N. Maleki, E. Farjami, Electroanal 21 (2009) 1533.
[119] L. Rodrıguez-Sanchez, M. C. Blanco, M. A. Lopez-Quintela, J Phys Chem B 104 (2000) 9683.
[120] M. Ueda, H. Dietz, A. Anders, H. Kneppe, A. Meixner, W. Plieth, Electrochim Acta 48 (2002) 377.
[121] M. Chikae, K. Idegami, K. Kerman, N. Nagatani, M. Ishikawa, Y. Takamura, E. Tamiya, Electrochem Commun 8 (2006) 1375.
[122] A.N. Correia, M.C. dos Santos, S.A.S. Machado, L.A. Avaca, J Electroanal Chem 547 (2003) 53.
[123] A. Serruya, B.R. Scharifker, I. Gonzalez, M.T. Oropeza, M. Palomar-Pardave, J. Appl Electrochem 26 (1996) 451
[124] V.M. Jovanovic, S. Terzic, A. Dekanski, J Serb Chem Soc 70 (2005) 41.
[125] G.W. Yang, G.Y. Gao, C. Wang, C. L. Xu, H. L. Li, Carbon 46 (2008) 747.
[126] H. L. Pape, F. Solano-Serena, P. Contini, C. Devillers, A. Maftah, Carbon 40 (2002) 2947.
[127] N.G. Sahoo, S. Rana, J. W. Cho, L. Li, S. H. Chan, Prog Polymer Sci 35 (2010) 837–867;
[128] Y. D Tretyakov, Russ Chem Rev 73 (2004) 831.
[129] S. Biniak, M. Pakula, A. Swiatkowsk, J Appl Electrochem 29 (1999) 481.

[130] T. Hezard, K. Fajerwerg, D. Evrard, V. Colliere, P. Behra, P. Gros, Electrochim Acta 73 (2012) 15.
[131] V. N. Andreev, Russ J Electrochem 42 (2006) 98.
[132] C. M. Welch, C. E. Banks, A. O. Simm, R. G. Compton, Anal Bioanal Chem 382 (2005) 12.
[133] A.O. Simm, C.E. Banks, R.G. Compton, Electranal 17 (2005) 1727.
[134] S.H. Shin, H.G. Hong, Bull Korean Chem Soc 31 (2010) 3077.

CHAPTER 6. SCOPE AND SPECIFIC OBJECTIVES OF THE THESIS

Nowadays, the main objective of most research is to improve the quality of life. The quality of life is associated with the state of environment, health and food safety control. Related to the environmental issues, increasing the amount and the toxic effects of chemical compounds released into the environment has led to the pollution levels monitoring necessity in industrial processes and key points of recycling. Also, water, air and soil pollution monitoring are required to avoid the critical situation. At this time, creating a control system for the persistent organic and heavy metals pollutants in the environment is a global priority.

These requirements motivate the further research to develop rapid, accurate and accessible methods for the quantitative determination of the pollutants from water. In this context, electroanalysis and its applications have experienced a great extent and development in recent years. The development of electroanalysis application is direct dependent on the fundamental aspects regarding the use of classical electroanalytical techniques, its continuous improvement, elaboration of new techniques, and especial, elaboration and characterization of some electrochemical sensors, characterized by high specificity or simultaneous detection possibility, high sensitivity and the lowest limit of detection.

Carbon based electrodes have attracted enormous attention in electroanalysis during the past few decades, due to their useful properties for sensing applications. Despite of the low rates of electron transfer at some carbon based electrodes, carbon type and pretreatment methods play an important role on electrode analytical performances. Carbon-based materials, *i.e.*, graphite, carbon nanotubes (CNTs), carbon nanofibers (CNFs), carbon paste, etc. are mostly used as the conductive phase in composite materials suitable for electrochemical sensors.

The use of a mixture of a certain carbon conductive phase and an insulating matrix is an attractive approach in the obtaining of electrochemical sensor with surface that can be renewed by simple mechanical cleaning. Besides this, the electrode surface modification contributes to the response improving and/or optimization of electrochemical sensor. Modification of carbon electrodes with zeolites has gained special attention from this perspective due of the synergistic combination of the zeolites characteristics with electron transfer reactions.

The specific objectives of this research are the following:

- ✓ Elaboration and manufacturing of some carbon based composite electrode materials with useful properties for the electrochemical detection of persistent organic pollutants from water;
- ✓ Elaboration and manufacturing of silver-(doped zeolite)-modified carbon based composite suitable for the electrochemical detection of arsenic from water;
- ✓ Morphological, electrical and electrochemical characterization of the electrode materials;
- ✓ The evaluation of the electrode materials behaviour in different supporting electrolytes and in the presence of the target analyte, to establish the relationship between obtained electrode material and reaction type;

- ✓ Individual detection experiments performance, which provides specific informations, *i.e.*, voltammetric/amperometric detection type, detection potential value, concentration ranges, electrode sensitivity, stability, reproducibility and lifetime, detection limits, calibration, to elaborate the detection protocol;
- ✓ Exploitation of the specific features of the pulsed voltammetric / amperometric techniques to improve the electroanalytical performance for the detection of the pollutant from water;
- ✓ Simultaneous detection experiments performance to elaborate specific simultaneous detection protocol.

Our research was directed on the study of anodic response of pentachlorophenol, commonly used as a wood preservative, based on both antifungal and insecticide properties, in order to electrochemically detect it. It was also used in a range of areas for antifungal, antibacterial, general herbicide, and slime prevention in both industrial and consumer application. Pentachlorophenol exhibits toxicity and persistence in water and soil, with a very negative impact on environment and human health, including acute toxicity and carcinogenicity. Several carbons-based composite electrodes, *i.e.*, expanded graphite-epoxy (EG-Epoxy), carbon nanofiber-expanded graphite-epoxy matrix (CNF-EG-Epoxy), carbon nanotubes-epoxy (CNT-Epoxy) in comparison with commercial conventional glassy carbon and new boron-doped diamond electrodes were studied to select the optimum detection scheme of pentachlorophenol from water. Another research direction envisaged the electrochemical detection of arsenic (III) from water, a common trace element characterized by high toxic properties and as consequence, with a very negative impact on the human health. The main pathway of human exposure to arsenic in drinking water, especially provided by the groundwater. The main inorganic species presented in water are arsenate ion (As^{V}) and arsenite ion (As^{III}, H_2AsO_4 or $HAsO_4^-$). The presence of arsenite ion is favoured by reducing media, which are very common for drinking water. Also, this form is more soluble than the arsenate ion and approximately 50 times more toxic. The main goal of this research direction is to elaborate the protocols for the individual detection of arsenic (III) in direct relation to the silver-modified nanostructured carbon composite electrodes, *i.e.*, carbon nanotubes-epoxy (CNT-Epoxy), carbon nanofibers-epoxy (CNF-Epoxy), silver-doped natural or synthetic zeolite-modified carbon nanotubes-epoxy (CNT-ZN/ZA-Ag Epoxy), silver-doped natural zeolite-modified carbon nanofibers-epoxy (CNF-ZNAg-Epoxy), silver-chemically decorated carbon nanotubes (CNF-Ag), silver-electrochemically decorated carbon nanotubes (CNT-Epoxy(Ag)). Also, the elaboration of the protocol for the simultaneous detection of arsenic (III) and lead (II) from water is aimed.

This basic study for electrode material elaboration, characterization and use for sensing is a prerequisite stage for concrete application in sensing field.

CHAPTER 7. THE NANOSTRUCTURED CARBON-BASED COMPOSITE ELECTRODES OBTAINING

7.1. Materials

Carbon nanotubes (CNTs) synthesized by catalytic carbon vapour deposition were produced by Nanocyl^{TM}, Belgium. Their main characteristics, given by the manufacturer, consist of CNT content of 90 %, carbon purity of 90 %, average diameter of 9.5 nm, average length of 1.5 μm, and surface area of 250-300 m^2/g.

Carbon nanofibers (CNFs) with average diameter of 60–150 nm and average length of 30–100 μm were purchased from Applied Sciences Inc., Cedarville, Ohio (Pyrograf III -PR24 AGLD).

Silver-modified zeolite was prepared by ion-exchange using clinoptilolite natural zeolite (NZ) / synthetic zeolite from Mirsid, Romania, with 68 % wt. clinoptilolite [1].

The epoxy resin used in the study was Araldite®LY5052/ Aradur®5052 purchased from Huntsman Advanced Materials, Switzerland.

7.2. Preparation of nanostructured carbon -based composite electrodes

7.2.1. Preparation of EG –Epoxy and CNF-EG-Epoxy composite electrodes

The expanded graphite-epoxy composite (EG-Epoxy) electrodes were prepared from two-component epoxy resin (LY5052, Araldite) mixed with conductive expanded graphite (EG) fillers powder, which represents a less dense form of graphite, made by thermal expansion of natural graphite intercalated (Applied Sciences Inc.). The carbon nanofiber-expanded graphite epoxy composite electrode (CNF-EG-Epoxy) was obtained from 20 % wt., expanded graphite (Applied Sciences Inc.) which was added within an epoxy resin (LY5052, Araldite) and from carbon nanofibers (CNF 20 % wt.). The full amount of expanded graphite to the matrix resin was not added directly due to the high surface area of the graphite flakes. The mixing was performed in a two roll-mill at room temperature. The two parts of the epoxy were mixed together with the CNF and the full amount of the obtained paste was cured in a hot press (Fontaijne, Holland) at 80^{o}C for 40 minutes. Simultaneously, the material was shaped in a plate of approximately 1 mm thickness. The plate was slowly cooled down (for about 12 h) to the room temperature without removing the applied pressure.

Before electrochemical testing of the electrodes, to improve each type of composite material and accurately to achieve electrical contacts, the composite material was coated on one side with silver and then fixed on glass, which was previously covered with a gold film. The coverage was achieved through S150 A SPUTTER COATER equipment. The epoxy resin was used to isolate the material.

The expanded graphite-epoxy composite (EG-Epoxy) electrode was prepared under the same conditions, without carbon nanofiber addition as above-

described. Figure 7.1 shows the schematic diagram for the CNF-EG-Epoxy composite preparation [2-5].

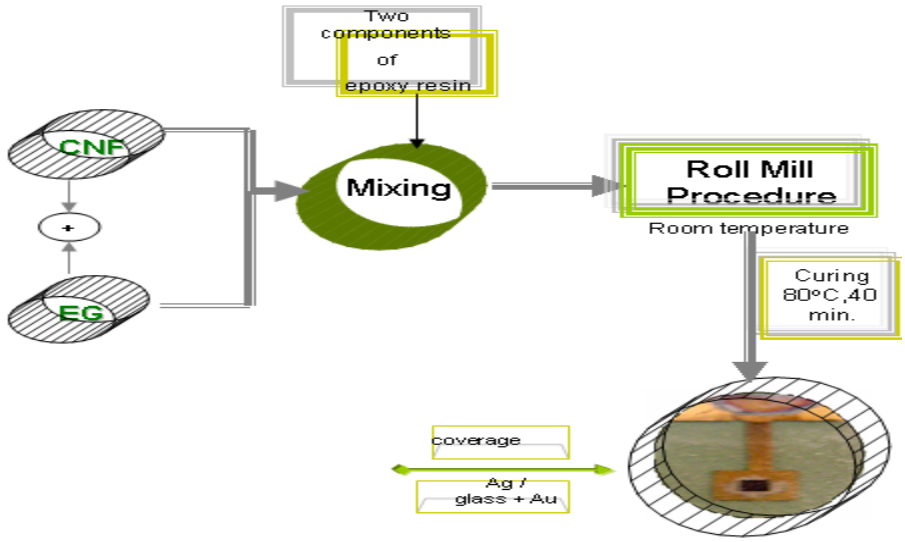

Figure 7.1. Schematically procedure of CNF-EG-Epoxy composite electrode.

7.2.2. Preparation of CNT / CNF - based composite electrodes

The dispersion of CNT / CNF in tetrahydrofuran (THF), 99.9% (Sigma Aldrich) were achieved by ultrasonication using a Cole-Parmer® 750-Watt Ultrasonic Processor for about 10 min prior to mixing with the polymer resin. After the sonication process, the solutions of CNT / CNF-THF were sonicated again with epoxy resin to obtain a more homogeneous mixture. An effective method, two roll mill (TRM) of achieving high levels of dispersion and distribution was used to prepare the electrodes. The ratio between the components was chosen to reach 20 % wt. CNT and respective, 20 % wt. epoxy resin. During processing the temperature was kept constant at 70°C, the mixing speed was maintained at 10 and 20 rpm for about 40 min, after then the curing agent (weight ratio of epoxy resin: curing agent was 100:38) was added to CNT/CNF- resin mixture and mixing was continued for an additional 20 min to ensure an uniform dispersion within the sample. The mixture was then poured into PVC tubes and cured in a vacuum oven at 80°C for 24 h, after which it was left to cool down at room temperature, and the composite electrodes with disc surface area of 19.63 mm^2 were obtained. The electrical contact of the electrode was assured using copper wire [6, 7].

In Figure 7.2 is presented schematically the procedure for the CNT/CNF-Epoxy composite preparation.

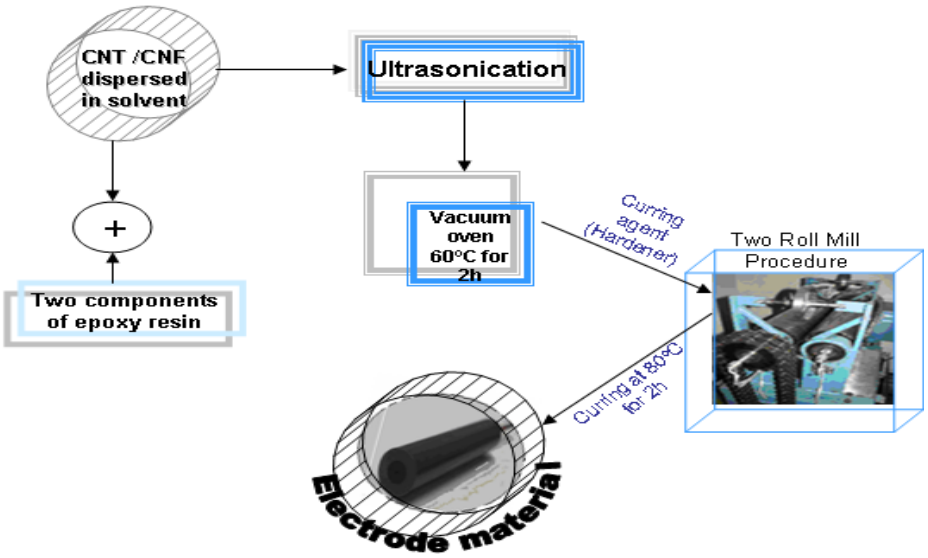

Figure 7.2. Schematically procedure of CNT / CNF-Epoxy composite electrode.

7.2.3. Preparation of the CNT – ZN / ZA – Ag composite electrodes

The same procedure applied for CNT-Epoxy electrode was also, applied for CNT-NZ/ZA-Ag-Epoxy electrodes, the natural / synthetic zeolite were mixed with CNT to reach also 20 % wt. of natural / synthetic zeolite. The mixture (ZN/ZA) was then poured into PVC tubes and cured in a vacuum oven at 80°C for 24h, after which it was left to cool down at room temperature, and the composite electrode with disc surface area of 19.63 mm^2 was obtained. The electrical contacts of the electrodes were assured using copper wire [8, 9].

7.2.3.1. Silver-modified natural/synthetic zeolite (ZN/ZA-Ag)

Silver-modified zeolite (Z-Ag) with a content of 0.008 mg Ag /g zeolite were prepared using natural zeolite from Mirsid, Romania, with 68% wt. clinoptilolite.

Synthetic zeolites (ZA) were obtained from natural clinoptilolite as Si source. Natural zeolite with high clinoptilolite content was supplied by Cemacon Company, Romania. The mass composition of powder zeolitic mineral was: 62.20% SiO_2, 11.65% Al_2O_3, 1.30% Fe_2O_3, 3.74% CaO, 0.67% MgO, 3.30% K_2O, 0.72% Na_2O, and 0.28% TiO_2.

A solution of natural clinoptilolite, sodium hydroxide and water with 1:5:50 mass ratios were mixed for 1 hour at 90°C (solution I). To prepare the aluminium solution, sodium aluminate, sodium hydroxide, sodium aluminate and water with mass ratio of 1:1.5:7.8 were mixed and heated to make a clear solution (solution II). The solutions II and I with 1:6.9 mass ratios were mixed together. Then, the mixture was heated at 90 °C and stirred with a mixing rate of 1000 rpm for 2 hours. The synthetic zeolite was thermally treated at 105 °C for 8 h to reach a good cristallinity. Because the synthetic zeolite shows a strong alkalinity that makes it unstable in water, this was soaked in a buffer solution (sodium acetate and acetic

acid). The pH of the mixture was kept around 5.5 for 4 hours and after solid-liquid separation, synthetic zeolite was drying at 130ºC for 4 hours to remove the water [10-12]. In Figure 7.3 is presented schematically the procedure for the CNT-NZ/ZA-Ag-Epoxy composite preparation.

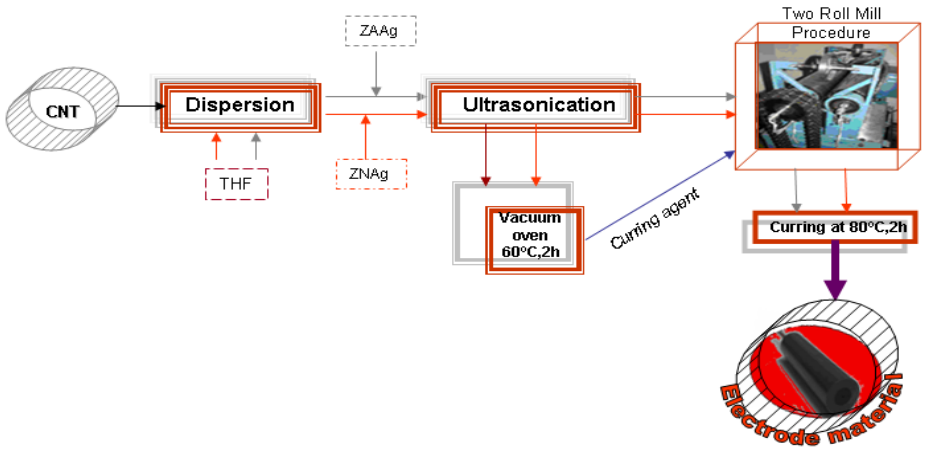

Figure 7.3. Schematically procedure of CNT-NZ/ZA-Ag -Epoxy composite electrode.

7.2.4. Preparation of the CNF with / without NZ decorated chemically with silver composite electrodes

The decoration of silver nanoparticles into CNF based composite was carried out by reducing silver ions in the presence of THF on CNF-Epoxy and respective, CNF-ZN-Epoxy composite. 1.1 g of CNF were added into 550 ml THF and the mixture was subjected to ultrasonication (Cole-Parmer 8900, USA) for 1 h. 40 ml $AgNO_3$ solution (0.02 M) was added into the mixture of 60-62°C during the stirring. After 1h heating the solution was kept without stirring at room temperature for 48 h for Ag deposition, and after filtration and sequentially washed with water, ethanol and acetone resulted silver-decorated CNF. The composite electrodes were prepared by dispersion of CNFs in THF, and epoxy resin (Araldite®LY5052) by ultrasonication, followed by the homogenization of the resulting paste with the zeolite particles and also, with the hardener using a two-roll mill. The mixture was then poured into PVC tubes and cured at 60°C for 24 h, obtaining discs electrodes with the surface area of 19.63 mm^2. The ratios were chosen to reach 20 % wt. CNFs for CNF-Ag electrode, 20 % wt. CNFs and 20 % wt. Ag-modified zeolite for CNF-ZNAg-Epoxy electrode [10-12]. Figure 7.4 show the schematic diagram for the CNF with / without NZ - Epoxy composite preparation.

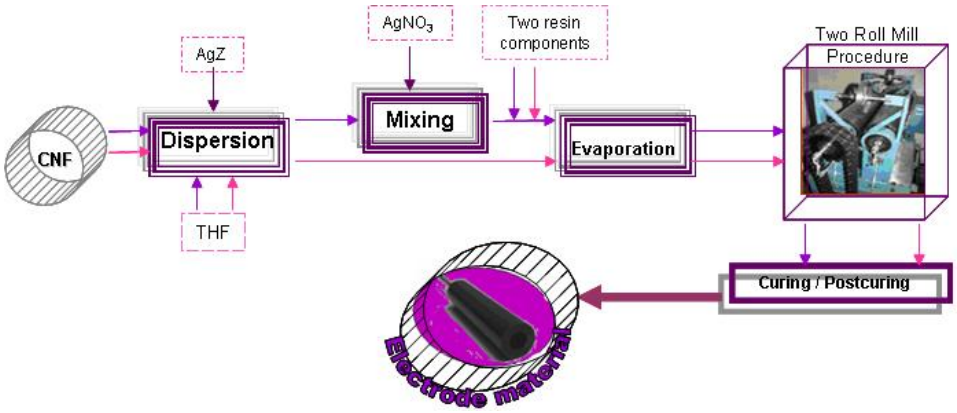

Legend: composite preparation scheme: 1. CNF-Ag
2. CNF-NZ-Ag

Figure 7.4. Schematically procedure of CNF-Ag/CNF-ZNAg-Epoxy composite preparation.

7.2.5. Preparation of the electrodeposited Ag nanoparticles on the nanostructured carbon-based composite electrodes

For the simple CNT-Epoxy composite electrode the preparation method was similarly with the one previous described (see section 7.2.2.) and the surface of the obtained electrode was decorated with silver by electrodeposition at a potential of -0.4 V/SCE for 60 s in the presence of 0.1 M AgNO3 solution. Figure 7.5 show the schematic diagram for the CNT-Epoxy (Ag) composite preparation [13].

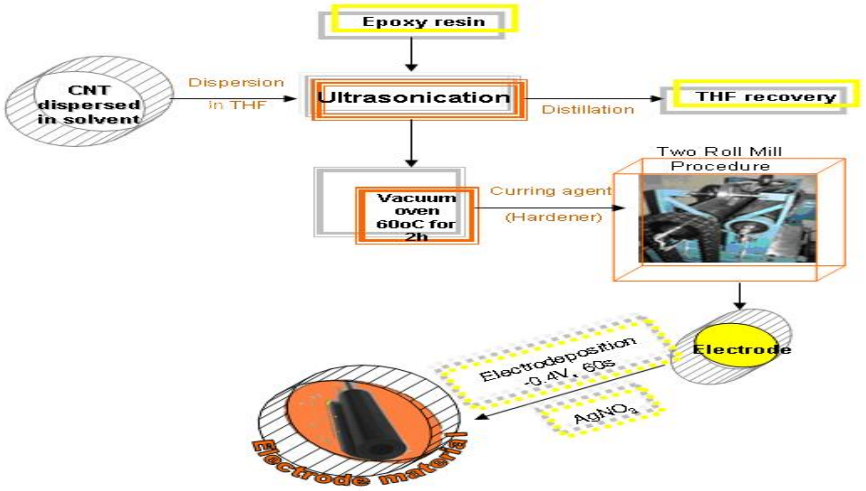

Figure 7.5. Schematically procedure of CNT-Epoxy (Ag) composite preparation.

7.3. Electrochemical measurements

Prior to use, the working electrodes were gradually cleaned, first polished with abrasive paper and then, on a felt-polishing pad by using 0.3 μm alumina powder (Metrohm, Switzerland) in distilled water for 5 minutes and rinsing with distilled water.

All electrochemical measurements performed for both electrochemical characterization and detection experiments were carried out using an Autolab potentiostat / galvanostat PGSTAT 302 (Eco Chemie, The Netherlands) controlled with GPES 4.9 software and a three-electrode cell, with a saturated calomel electrode as reference electrode, a platinum counter electrode, and the carbon-based working electrodes.

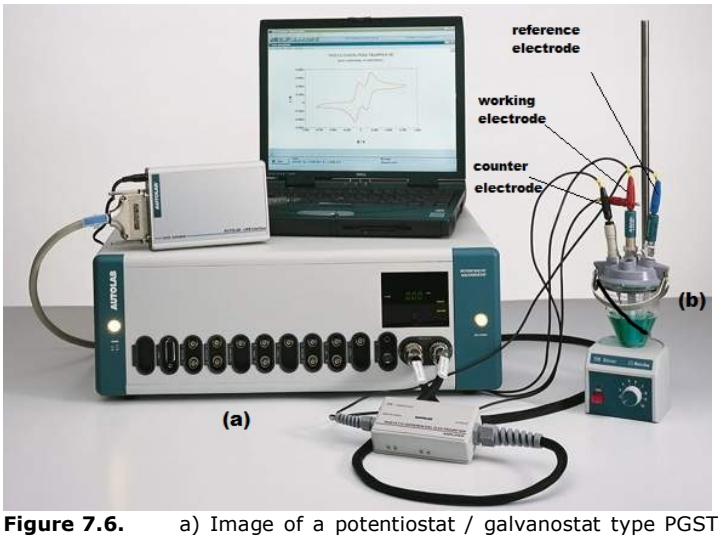

Figure 7.6. a) Image of a potentiostat / galvanostat type PGSTAT 302 (Eco Chemie), b) cell type with three electrodes

7.4. References

[1] C. Orha, A. Pop, C. Lazau, P. Sfirloaga, I. Grozescu, V.l Tiponut, F. Manea, Int. Semicond. Conf., October 17-19, Sinaia, Romania, CAS 2011 Proceedings, pp. 299-302.
[2] A. Bebeselea, F. Manea, G. Burtica, L. Nagy, G. Nagy, Talanta 80 (2010) 1068.
[3] I. Corb, F. Manea, C. Radovan, A. Pop, G. Burtica, P. Malchev, S. Picken, J. Schoonman, Sensor. 7 (2007) 2626.
[4] **A. Baciu**, F. Manea, A. Remes, S. Motoc, G. Burtica, R. Pode, Environ. Eng. Manag. J. 9 (2010) 1555.
[5] **A. Baciu**, A. Pop, F. Manea, G. Burtica, R. Pode, J. Schoonman, Third Regional Symposium on Electrochemistry South-East Europe, RSE-SEE Romania Bucuresti May 13-17 Book of Abstract (2012) 56.
[6] A. Remes, A. Pop, Florica Manea, **A. Baciu**, S. J. Picken, J Schoonman, Sensor. 12 (2012) 7033.

[7] **A. Baciu**, A. Remes, E. Ilinoiu, F. Manea, G. Burtica, J. Schoonman, 22nd European Conference on Diamond, Diamond-Like Materials, Carbon nanotubes, and Nitrides, 4-8 September, Bavaria, Gemany, Book of Abstratct (2011) p2.115.
[8] **A. Baciu**, A. Pop, A. Remes, F. Manea, G. Burtica, Adv. Sci. Eng. Med. 3 (2011) 13.
[9] A. Remes, **A. Baciu**, A. Pop, F. Manea, S.J. Piccken, J. Schoonman, TNT 2011-Trends in NanoTechnology, Tenerife-Canary Islands, Spain, November 21-25 Book of Abstract (2011).
[10] C. Orha, A. Pop, C. Lazau, I. Grozescu, V. Tiponut, F. Manea, Environ. Eng. Manag. J. 11 (2012) 641.
[11] C. Orha, A. Pop, C. Lazau, I. Grozescu, V. Tiponut, F. Manea, J. Optoelectron. Adv. M. 13 (2011) 544.
[12] F. Manea, S. Motoc, A. Pop, A. Remes, J. Schoonman, Nanoscale Res. Lett. 7 (2012), 331.
[13] A. Pop, F. Manea, C. Orha, A. Baciu, S. Motoc, N. Vaszilcsin, J. Schoonman, Third Regional Symposium on Electrochemistry South-East Europe, RSE-SEE, Romania Bucuresti May 13-17 Book of Abstract (2012) 106.

CHAPTER 8. MORPHO-STRUCTURAL AND ELECTRICAL CHARACTERIZATION OF NANOSTRUCTURED CARBON-BASED COMPOSITE ELECTRODES

The SEM images were obtained using an XL20, Philips Scanning Electron Microscope, with an acceleration voltage of 15 kV. The samples could be investigated without gold-sputtering because of their good electrical conductivity. All measurements for the electrical conductivity were performed using a digital multimeter DMM2000 and a current source 6221 DC, both provided by Keithley. Silver paste was used as electrical contacts.

8.1. Scanning electron microscopy (SEM)

SEM images of fractured surfaces of the nanostructured carbon-based composite electrodes were taken to qualify the bulk distribution and the structure of the conductive carbon filler within epoxy matrix (Figures 8.1 – 8.4).

Figure 8.1 illustrates SEM image of the cross-section of expanded graphite-epoxy (EG-Epoxy) (a) and carbon nanofiber-expanded graphite-epoxy (CNF-EG-Epoxy) (b) composite electrodes and reveals the appearance of the fractured surfaces for both composites. Generally, the graphite flakes are well-distributed within epoxy matrices. A layering of the graphite flakes parallel to the surfaces the plate is visible for both composite electrodes, due to the pressing of the plate in the hot press [1].

(a) EG-Epoxi

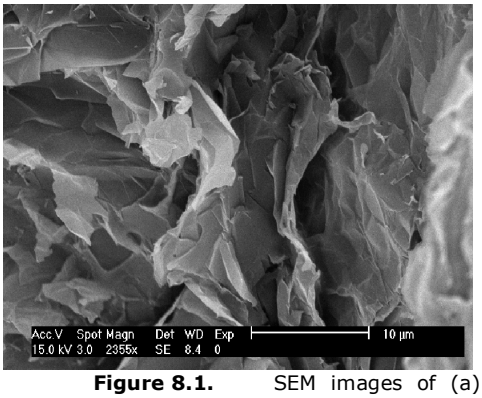

(b) CNF-EG-Epoxi

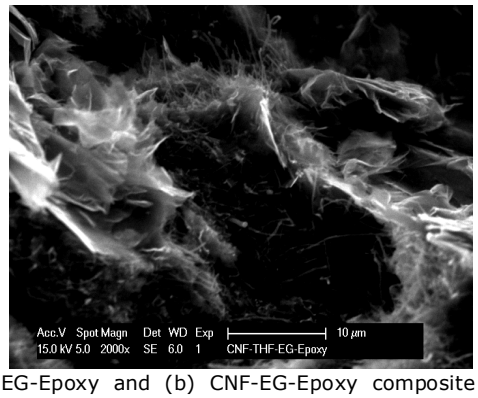

Figure 8.1. SEM images of (a) EG-Epoxy and (b) CNF-EG-Epoxy composite electrodes

In figures 8.2 (a and b) are presented the SEM images for both CNT-Epoxy and CNF-Epoxy electrodes and a homogeneous distribution of CNT/CNF within the epoxy matrix is noticed. It is well-known that due to the nanoscale diameters of CNFs, these tend to agglomerate, leading to a non-homogeneous dispersion, and also using an inappropriate solvent for the dispersion of carbon nanotubes in polymer matrix, the non-homogeneous dispersion should appear. In our case, due to the matrix was diluting with suitable solvent (tetrahydrofuran, THF) and combining mechanical mixing with sonication a good dispersion was found and thus, the particles of CNFs were not agglomerated.

(a) CNT-Epoxy (b) CNF-Epoxy

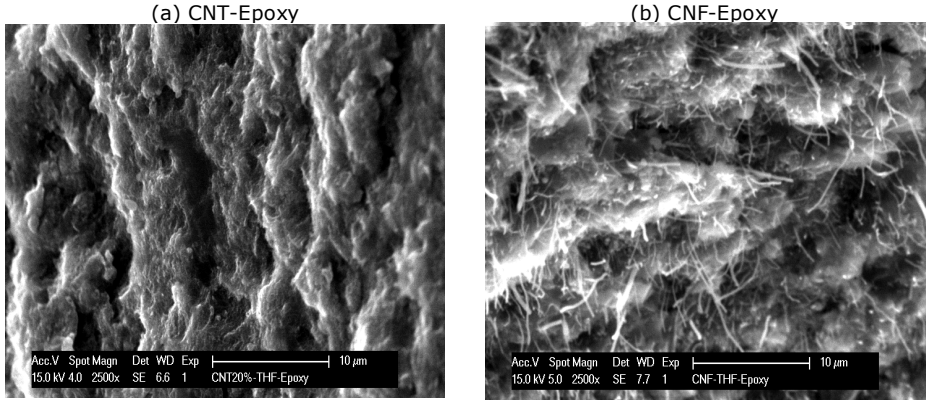

Figure 8.2. SEM images of (a) CNT-Epoxy and (b) CNF-Epoxy composite electrodes

The qualitative information about the distribution of multi-walled carbon nanotubes and Ag-modified zeolite zones in the epoxy matrix for both composite electrodes has been provided also, by SEM imaging. Figure 8.3 (a and b) shows comparatively SEM images of silver doped natural and synthetic zeolite-modified carbon nanotubes epoxy (CNT-ZAAg-Epoxy and CNT-ZNAg-Epoxy) composite electrodes and reveals a well distribution of both the multi-walled carbon nanotubes and Ag-modified zeolite particles within epoxy matrix. However, a more porous surface can be noticed in the presence of syntetic zeolite particles, which affect also the electrical conductivity. Thus, the four - points probe method has been provided the electrical conductivity for CNT-ZAAg-Epoxy of 0.982 and respective, for CNT - ZNAg-Epoxy of 1.177 Scm^{-1}. This result is in agreement with SEM result and can be explained by a better distribution of carbon nanotubes in the presence of synthetic zeolite avoiding carbon nanotubes entangling and interconnecting that decreases the electrical conductivity (See Table 8.1).

(a) CNT-ZAAg-Epoxy (b) CNT-ZNAg-Epoxy

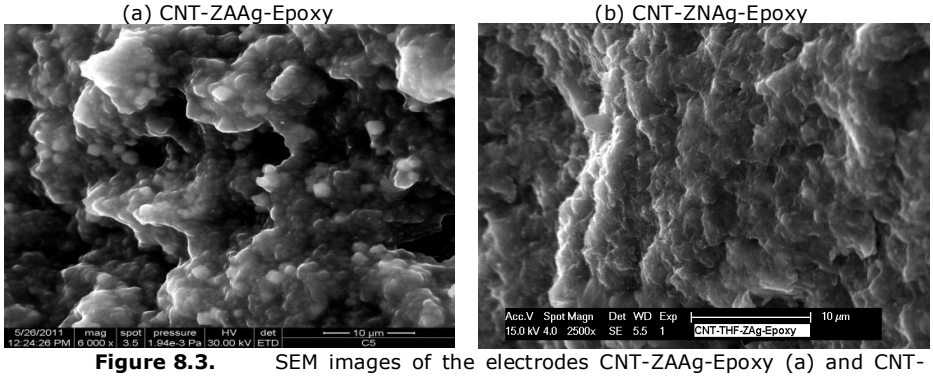

Figure 8.3. SEM images of the electrodes CNT-ZAAg-Epoxy (a) and CNT-ZNAg-Epoxy (b) composite electrodes

SEM image of silver-doped natural zeolite-modified carbon nanofibers-epoxy (CNF-ZNAg-Epoxy) composite material (Figure 8.4a) reveals a well-integrated and smooth morphology of carbon nanotubes and Ag-modified zeolite particles in the epoxy matrix. It is observed a homogeneous distribution of silver. Figure 8.4b present the SEM image of the silver-chemically decorated carbon nanotubes (CNF-Ag) electrode composite, and a homogeneous distribution of CNF within the epoxy matrix is observed. Higher content of silver particles was found for silver-modified natural zeolite-CNF-epoxy in comparison with silver-decorated CNF-epoxy composite materials.

(a)CNF-ZNAg-Epoxy (b) CNF-Ag

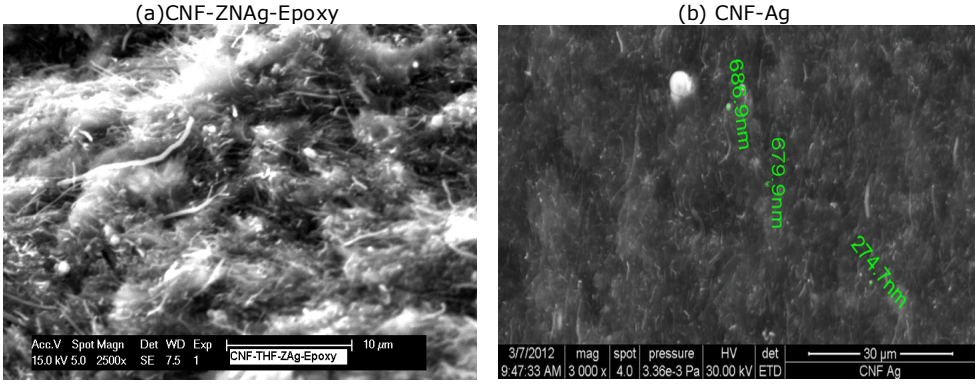

Figure 8.4. SEM images of (a) CNF-ZNAg-Epoxy and (b) CNF-Ag-composite electrodes

The electrochemical deposition of silver nanoparticles on CNT was performed by maintain the potential at -0.4 V/SCE. In this condition, the process is diffusion-controlled and, hence, spontaneous formation of silver nanoparticles on CNT surface occurred, which are deposited in aggregated form. The Ag particles were distributed randomly on the electrode surface and characterized by various sizes (see Figure 8.5).

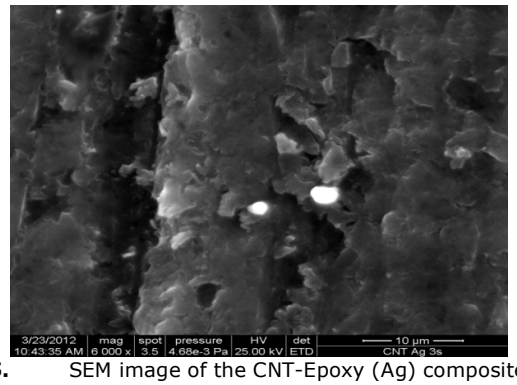

Figure 8.5. SEM image of the CNT-Epoxy (Ag) composite electrode.

8.2. Electrical conductivity

The composite electrode containing 20 % wt. for all carbon based composite electrodes were selected as optimal composition for composite preparations based on the correlation between morphology and electrical conductivity established in our previous studies [2] The results obtained by four-point probe resistance measurements (FPP) for electrical characterization of the carbon nanostructured - based composite electrodes are presented in Table 8.1.

Table 8.1. The electrical conductivity of the electrode materials containing 20 % wt. nanostructured carbon.

Nr. Crt.	Electrode type	Electrical conductivity, σ (S/cm)
1	EG-Epoxy	1.52
2	CNF-EG-Epoxy	2.27
3	CNT-Epoxy	0.596
4	CNT-ZNAg-Epoxy	1.177
5	CNT-ZAAg-Epoxy	0.982
6	CNF-Epoxy	0.247
7	CNF-Ag	0.320
8	CNF-ZNAg-Epoxy	0.409

Based on the results of the electrical conductivity measurements, it can be noticed that for the same content of the conductive filler (20 % wt.) the electrical conductivity decreased as: EG-Epoxy<CNT-Epoxy<CNF-Epoxy. This should be in direct relation with dispersion and homogenous degree of the conductive filler within the epoxy matrix.

The presence of silver modified natural/synthetic zeolite within composition improved the electrical properties due to silver presence, the natural/synthetic zeolite being an insulating material.

The differences between the electrical conductivities determined for CNT-ZNAg-Epoxy and CNT-ZAAg-Epoxy are own to silver content within natural and synthetic zeolite and the conductive filler distribution and homogeneity within zeolite and epoxy matrix.

The morphological, structural and electrical characterization results of the above-presented compositions of the carbon-based composite electrode conclude:

The conductive fillers, *i.e.*, expanded graphite, carbon nanotubes and carbon nanofibers are well distributed and dispersed within the epoxy matrix taken into account the specific preparation method involving method dispersion within suitable solvent by sonication.

Silver presence in various forms, *i.e.*, silver-modified natural/synthetic zeolite, silver particles decorated chemically and electrochemically was evidenced by SEM images.

The electrical conductivity of the composite electrode depended on the conductive filler type (expanded graphite, carbon nanotubes, carbon nanofibers) its loading and distribution within epoxy matrix. Also, silver content and distribution within composite composition enhanced the electrical properties of the composite.

All prepared carbon based composite electrode are characterized by the electrical conductivities suitable for the electrochemical applications.

8.3. References

[1] F. Manea , C. Radovan, I. Corb, A. Pop, G. Burtica, P. Malchev, S. Picken, J. Schoonman, Sensor. 7 (2007) 615.
[2] A. Remes, A. Pop, Florica Manea, **A. Baciu**, S.J. Picken, J Schoonman, Sensor. 12 (2012) 7033.

CHAPTER 9. ELECTROCHEMICAL CHARACTERIZATION OF NANOSTRUCTURED CARBON - BASED ELECTRODE COMPOSITE ELECTRODES

Cyclic voltammetry (CV) is the most frequently used electrochemical techniques, an outstanding tool for a preliminary determination of the redox properties of a given species, for understanding reaction intermediates, and for characterization of the reaction products. Above all, the most important advantage is its ability to characterize an electrode.

The ferro/ferricyanide redox couple is widely used as an example of an electrochemically reversible redox system and it is used to determine the electrochemical area of the electrode, the diffusion coefficient, and the redox potential of various analytical systems.

Ferro/ferricyanide redox system gives rise to an anodic process, which in electrochemical techniques involves one electron per molecule [1].

Given the one electron involving and chemical reversibility of the oxidation, the cyclic voltammetric analysis of the ferro/ferricyanide process envisaged the determination of the electroactive area of the carbon-based electrodes used in this study, via the apparent diffusion coefficient of this redox system on these electrodes. Thus, using cyclic voltammetry recorded at different scan rate in the presence of 4 mM $K_3Fe(CN)_6$, the electrochemical behaviour of ferrocyanide system was studied, which offers the opportunity to determine the characteristics of a cyclic voltammetric response originating from a reversible process. The reversibility of the system was estimated by the peak-to-peak separation (the separation between the anodic peak potential and the catholic peak potential, $\Delta E_p = E_{pa} - E_{pc}$). For a reversible couple the ΔE_p is equal to 0.059/n V (n, the number of electron exchanged in the reaction, and in our case is equal with 1), and it is independent of the scan rate. For quasi- and irreversible conditions, the ΔE_p depends on the voltage scan rate. Another important parameter that is relates to the electrochemical reversibility of an electrode reaction is the peak current, and more specific, the ratio between the current of the anodic peak and that of the cathodic peak (i_{pa}/i_{pc}), whose value is unity for a simple reversible couple. Above all parameters, which can predict if the study process is reversible or irreversible, the aim of the study of the electrochemical behaviour of the classical ferri/ferrocyanide system is to determine the electroactive surface of the carbon-based electrodes used [2].

Thus, in next figures (9.1) is showed the cyclic voltammograms of the all carbon based composite electrodes used in this study recorded at different scan rates (0.025, 0.05, 0.1, 0.2 and 0.3 Vs^{-1}) in 1M KNO_3 supporting electrolyte and in the presence of the 4 mM $K_3Fe(CN)_6$.

(a) GC electrode

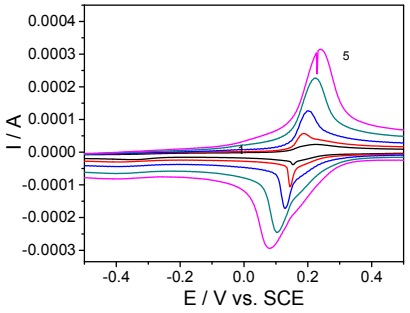

(b) EG-Epoxy electrode

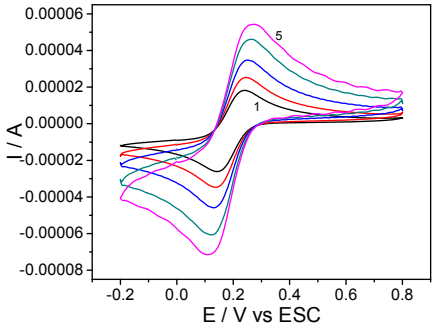

(c) CNF-EG-Epoxy electrode

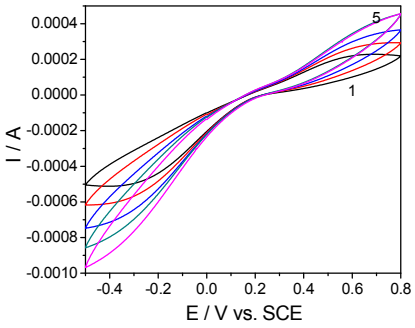

(d) CNT-Epoxy electrode

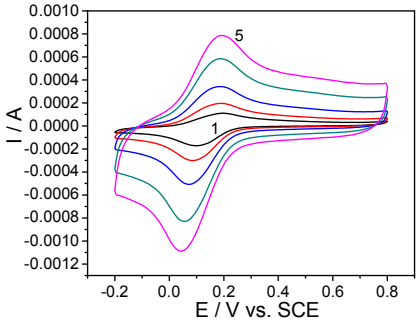

(e) CNF-Epoxy electrode

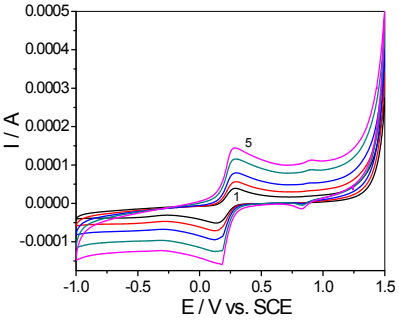

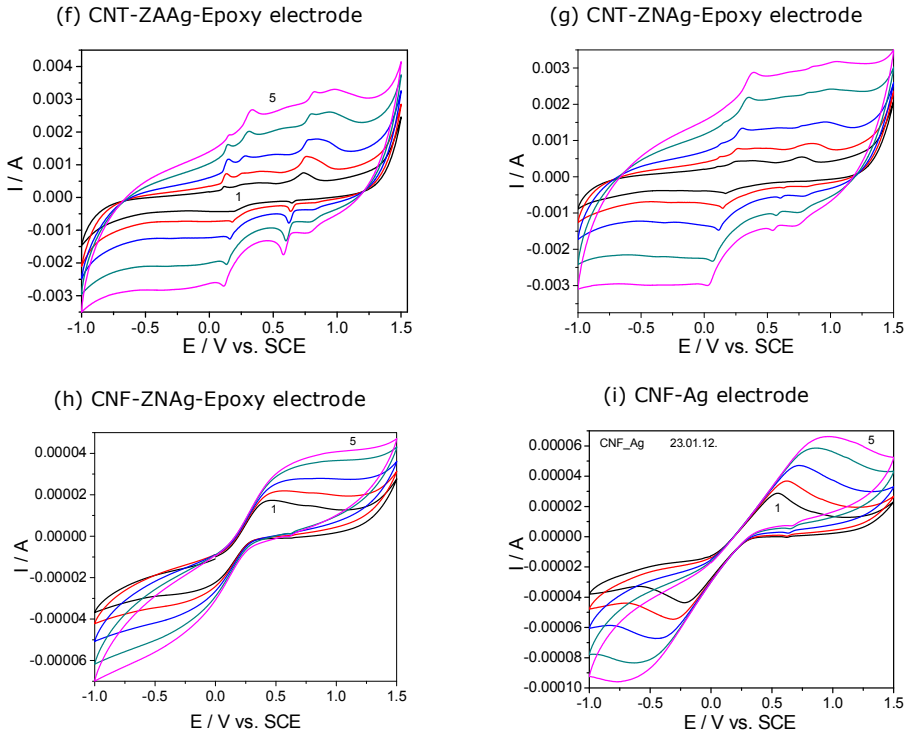

Figure 9.1. Cyclic voltammograms of carbon based composite electrode in 1M KNO_3 supporting electrolyte and in the presence of 4mM $K_3Fe(CN)_6$; at different potential scan rate 1- 0.025, 2- 0.05, 3- 0.1, 4- 0.2, 5- 0.3 Vs^{-1}; potential range: -1 ÷ +1.5V; (a) GC electrode; (b) EG-Epoxy electrode; (c) CNF-EG-Epoxy electrode; (d) CNT-Epoxy electrode; (e) CNF-Epoxy electrode; (f) CNT-ZAAg-Epoxy electrode; (g) CNT-ZNAg-Epoxy electrode; (h) CNF-ZNAg-Epoxy electrode; (i) CNF-Ag electrode.

The relationship between the peak potential and the logarithm of the scan rates corresponding to the CVs above presented are illustrated in the figures 9.2 (a-i) recorded at different scan rates (0.025, 0.05, 0.1, 0.2, 0.3, Vs^{-1}).

(a) GC electrode

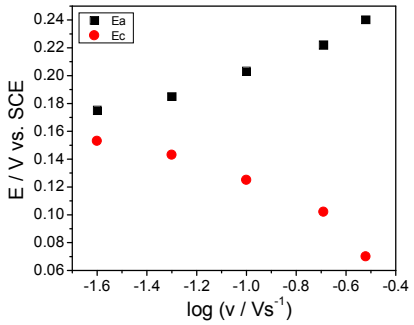

(b) EG-Epoxy electrode

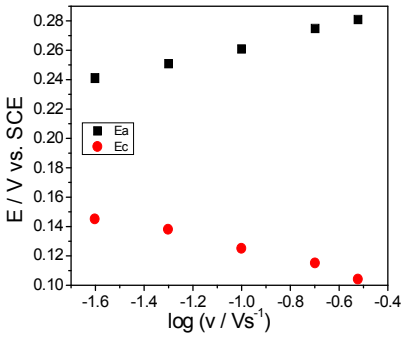

(c) CNF-EG-Epoxy electrode

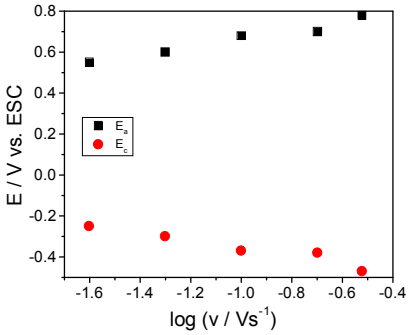

(d) CNT-Epoxy electrode

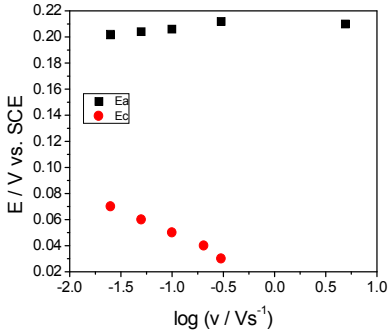

(e) CNF-Epoxy electrode

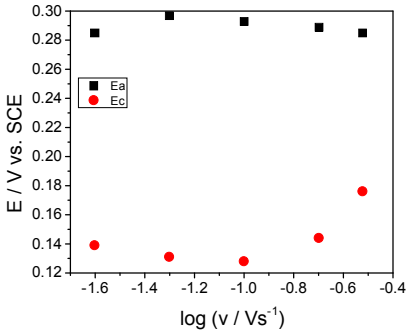

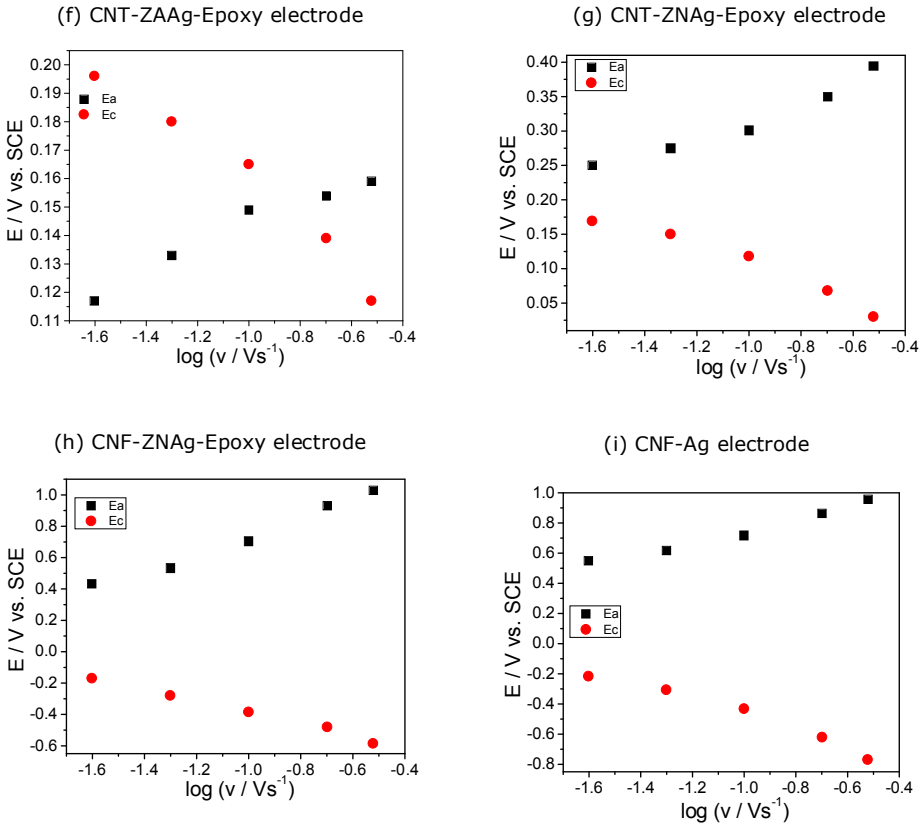

Figure 9.2. Plots of the anodic and cathodic peaks versus the logarithm of CV recorded at the scan rate: 0.025, 0.05, 0.1, 0.2, 0.3, Vs^{-1}, with CV; (a) GC electrode; (b) EG-Epoxy electrode; (c) CNF-EG-Epoxy electrode; (d) CNT-Epoxy electrode; (e) CNF-Epoxy electrode; (f) CNT-ZAAg-Epoxy electrode; (g) CNT-ZNAg-Epoxy electrode; (h) CNF-ZNAg-Epoxy electrode; (i) CNF-Ag electrode.

The height of anodic and cathodic peaks depend on the scan rate, and the dependence on the square root of the scan rate gives information about the overall mechanistic aspects of the redox couple process that occurs on the studied electrodes. The linear dependence of the anodic and cathodic peaks on square root of the scan rate is presented in the next figures (Figures 9.3).

(a) GC electrode

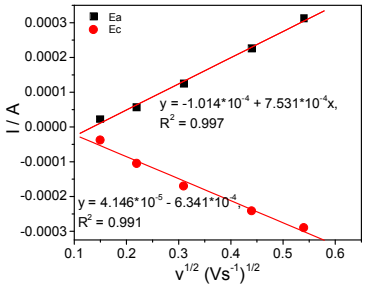

(b) EG-Epoxy electrode

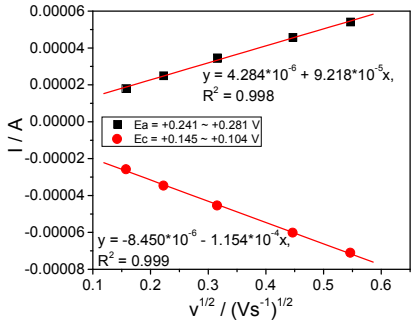

(c) CNF-EG-Epoxy electrode

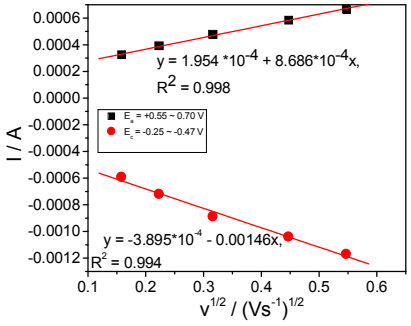

(d) CNT-Epoxy electrode

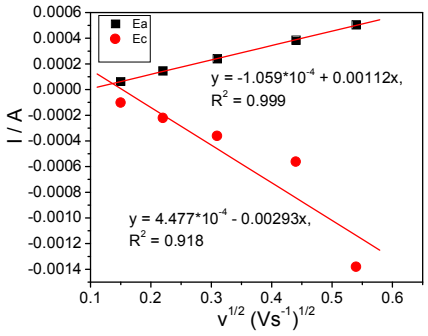

(e) CNF-Epoxy electrode

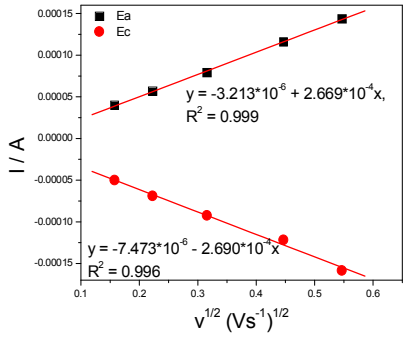

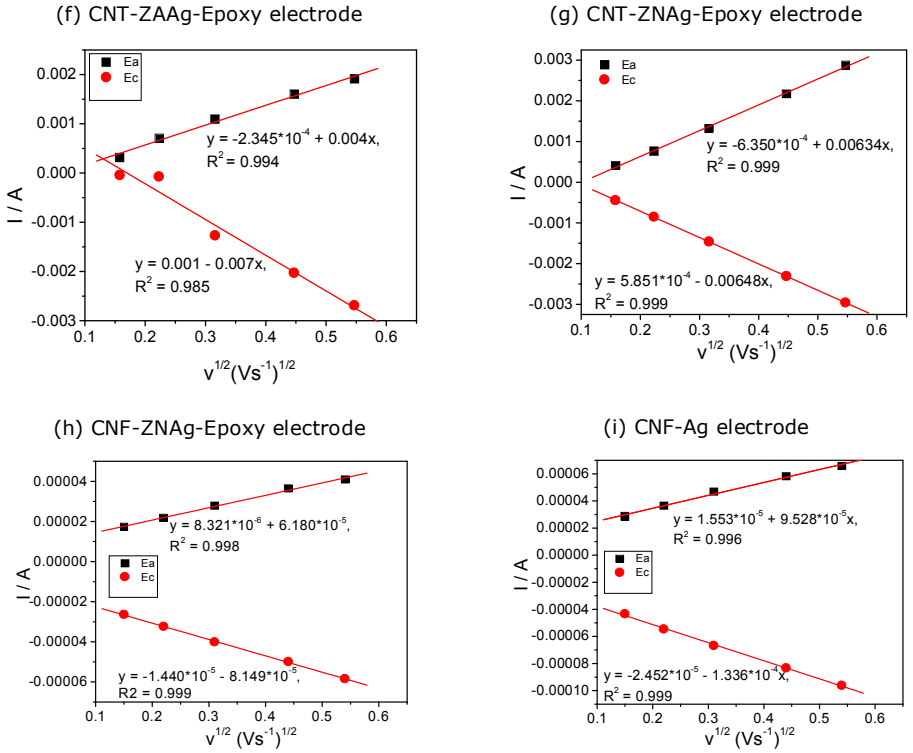

Figure 9.3. Calibrations plots of the anodic and cathodic peaks versus the square root of CV recorded at the scan rate : 0.025, 0.05, 0.1, 0.2, 0.3, Vs^{-1}, with CV; (a) GC electrode; (b) EG-Epoxy electrode; (c) CNF-EG-Epoxy electrode; (d) CNT-Epoxy electrode; (e) CNF-Epoxy electrode; (f) CNT-ZAAg-Epoxy electrode; (g) CNT-ZNAg-Epoxy electrode; (h) CNF-ZNAg-Epoxy electrode; (i) CNF-Ag electrode.

The useful characteristics to the well-known behaviour of the standard ferri/ferrocyanide oxidation process on the carbon-based composite taking into consideration the reversibility of the redox system are gathered in Table 9.1.

Table 9.1. The electrochemical parameters of the redox system (ferri/ferrocyanide) determined from the anodic and cathodic branches of CVs.

		GC		
	Scane rate / Vs^{-1}	E_a / V	I_{pa} / A	ΔI_{pa} / A
	0.025	0.240	$2.292 \cdot 10^{-5}$	$1.856 \cdot 10^{-5}$
	0.05	0.185	$5.644 \cdot 10^{-5}$	$4.968 \cdot 10^{-5}$
Anodic	0.1	0.203	$1.239 \cdot 10^{-4}$	$1.018 \cdot 10^{-4}$
	0.2	0.222	$2.256 \cdot 10^{-4}$	$2.035 \cdot 10^{-4}$
	0.3	0.240	$3.124 \cdot 10^{-4}$	$2.809 \cdot 10^{-4}$
	Scane rate / Vs^{-1}	E_c / V	I_{pc} / A	ΔI_{pc} / A
	0.025	0.153	$-3.767 \cdot 10^{-5}$	$3.278 \cdot 10^{-5}$
Cathodic	0.05	0.143	$-1.053 \cdot 10^{-4}$	$9.572 \cdot 10^{-5}$
	0.1	0.125	$-1.703 \cdot 10^{-4}$	$1.545 \cdot 10^{-4}$

	0.2	0.102	$-2.418\cdot10^{-4}$	$2.167\cdot10^{-4}$
	0.3	0.07	$-2.903\cdot10^{-4}$	$2.532\cdot10^{-4}$
		CNF-EG-Epoxy		
	Scane rate / Vs^{-1}	E_a / V	I_{pa} / A	ΔI_{pa} / A
	0.025	0.55	$3.718\cdot10^{-4}$	$3.191\cdot10^{-4}$
	0.05	0.60	$3.929\cdot10^{-4}$	$3.859\cdot10^{-4}$
Anodic	0.1	0.68	$4.796\cdot10^{-4}$	$4.657\cdot10^{-4}$
	0.2	0.70	$5.839\cdot10^{-4}$	$5.635\cdot10^{-4}$
	0.3	0.78	$6.660\cdot10^{-4}$	$6.374\cdot10^{-4}$
	Scane rate / Vs^{-1}	E_c / V	I_{pc} / A	ΔI_{pc} / A
	0.025	-0.25	$-5.918\cdot10^{-4}$	$-5.869\cdot10^{-4}$
	0.05	-0.118	$-7.205\cdot10^{-4}$	$-7.139\cdot10^{-4}$
Cathodic	0.1	-0.136	$-8.883\cdot10^{-4}$	$-8.731\cdot10^{-4}$
	0.2	-0.223	-0.00104	$-10.16\cdot10^{-4}$
	0.3	-0.182	-0.00117	$-11.41\cdot10^{-4}$
		CNT-Epoxy		
	Scan rate / Vs^{-1}	E_a / V	I_{pa} / A	ΔI_a / A
	0.025	0.202	$1.084\cdot10^{-4}$	$0.628\cdot10^{-4}$
	0.05	0.204	$1.932\cdot10^{-4}$	$1.436\cdot10^{-4}$
Anodic	0.1	0.206	$3.364\cdot10^{-4}$	$2.389\cdot10^{-4}$
	0.2	0.210	$5.75\cdot10^{-4}$	$3.861\cdot10^{-4}$
	0.3	0.212	$7.724\cdot10^{-4}$	$5.027\cdot10^{-4}$
	Scane rate / Vs^{-1}	E_c / V	I_{pc} / A	ΔI_{pc} / A
	0.025	0.07	$-1.66\cdot10^{-4}$	$-1.025\cdot10^{-4}$
	0.05	0.06	$-2.926\cdot10^{-4}$	$-2.223\cdot10^{-4}$
Cathodic	0.1	0.05	$-5.0\cdot10^{-4}$	$-3.627\cdot10^{-4}$
	0.2	0.04	$-8.229\cdot10^{-4}$	$-5.625\cdot10^{-4}$
	0.3	0.03	$1\cdot10^{-4}$	$-13.814\cdot10^{-4}$
		CNF-Epoxy		
	Scane rate / Vs^{-1}	E_a / V	I_{pa} / A	ΔI_{pa} / A
	0.025	0.285	$4.955 \cdot 10^{-5}$	$3.6 \cdot 10^{-5}$
	0.05	0.297	$5.717 \cdot 10^{-5}$	$5.045\cdot 10^{-5}$
Anodic	0.1	0.293	$7.910\cdot 10^{-5}$	$6.789\cdot 10^{-5}$
	0.2	0.289	$1.159\cdot 10^{-4}$	$9.566\cdot 10^{-5}$
	0.3	0.285	$1.437\cdot 10^{-4}$	$11.533\cdot 10^{-5}$
	Scane rate / Vs^{-1}	E_c / V	I_{pc} / A	ΔI_{pc} / A
	0.025	-0.0307	$-5.0101 \cdot 10^{-5}$	$-4.771\cdot 10^{-4}$
	0.05	-0.118	$-6.906 \cdot 10^{-5}$	$-6.467\cdot 10^{-4}$
Cathodic	0.1	-0.136	$-9.258\cdot 10^{-5}$	$-8.413\cdot 10^{-4}$
	0.2	-0.223	$-1.219\cdot 10^{-4}$	$-10.780\cdot 10^{-4}$
	0.3	-0.182	$-1.587\cdot 10^{-4}$	$-13.972\cdot 10^{-4}$
		CNT-ZAAg-Epoxy		
	Scane rate / Vs^{-1}	E_a / V	I_{pa} / A	ΔI_{pa} / A
	0.025	0.117	$3.194 \cdot 10^{-4}$	$1.193\cdot 10^{-4}$
	0.05	0.133	$7.082 \cdot 10^{-4}$	$3.252\cdot 10^{-4}$
Anodic	0.1	0.149	0.0011	$4.513\cdot 10^{-4}$
	0.2	0.154	0.00160	$5.2\cdot 10^{-4}$
	0.3	0.159	0.00191	$4.6\cdot 10^{-4}$
	Scane rate / Vs^{-1}	E_c / V	I_{pc} / A	ΔI_{pc} / A
	0.025	0.196	$-4.408 \cdot 10^{-4}$	$-1.634\cdot 10^{-4}$
	0.05	0.180	$-7.477 \cdot 10^{-4}$	$-2.827\cdot 10^{-4}$
Cathodic	0.1	0.165	-0.00127	$-5.01\cdot 10^{-4}$
	0.2	0.139	-0.00203	$-7.8\cdot 10^{-4}$
	0.3	0.117	-0.00269	$-9.9\cdot 10^{-4}$
		CNT-ZNAg-Epoxy		
	Scane rate / Vs^{-1}	E_a / V	I_{pa} / A	ΔI_{pa} / A
Anodic	0.025	0.250	$4.130 \cdot 10^{-4}$	$1.168 \cdot 10^{-4}$

	0.05	0.275	$7.666 \cdot 10^{-4}$	$2.089 \cdot 10^{-4}$
	0.1	0.301	0.00132	$4.066 \cdot 10^{-4}$
	0.2	0.350	0.00217	$6.030 \cdot 10^{-4}$
	0.3	0.394	0.00287	$8.080 \cdot 10^{-4}$
	Scane rate / Vs^{-1}	E_c / V	I_{pc} / A	ΔI_{pc} / A
	0.025	-0.0307	$-4.471 \cdot 10^{-4}$	$-1.946 \cdot 10^{-4}$
	0.05	-0.118	$-8.534 \cdot 10^{-4}$	$-3.49 \cdot 10^{-4}$
Cathodic	0.1	-0.136	-0.00146	$-5.386 \cdot 10^{-4}$
	0.2	-0.223	-0.00231	$-7.39 \cdot 10^{-4}$
	0.3	-0.182	-0.00296	$-8.72 \cdot 10^{-4}$
		CNF-ZNAg-Epoxy		
	Scane rate / Vs^{-1}	E_a / V	I_{pa} / A	ΔI_{pa} / A
	0.025	0.433	$1.723 \cdot 10^{-5}$	$1.371 \cdot 10^{-5}$
	0.05	0.533	$2.188 \cdot 10^{-5}$	$1.613 \cdot 10^{-5}$
Anodic	0.1	0.704	$2.778 \cdot 10^{-5}$	$1.788 \cdot 10^{-5}$
	0.2	0.932	$3.636 \cdot 10^{-5}$	$1.908 \cdot 10^{-5}$
	0.3	1.029	$4.095 \cdot 10^{-5}$	$1.852 \cdot 10^{-5}$
	Scane rate / Vs^{-1}	E_c / V	I_{pc} / A	ΔI_{pc} / A
	0.025	-0.170	$-2.641 \cdot 10^{-5}$	$-2.337 \cdot 10^{-5}$
	0.05	-0.280	$-3.238\ 10^{-5}$	$-2.659 \cdot 10^{-5}$
Cathodic	0.1	-0.385	$-4.011 \cdot 10^{-5}$	$-2.969 \cdot 10^{-5}$
	0.2	-0.481	$-4.994 \cdot 10^{-5}$	$-3.262 \cdot 10^{-5}$
	0.3	-0.182	-0.00296	$-8.72 \cdot 10^{-4}$
		CNF-Ag		
	Scane rate / Vs^{-1}	E_a / V	I_{pa} / A	ΔI_{pa} / A
	0.025	0.549	$2.859 \cdot 10^{-5}$	$2.613 \cdot 10^{-5}$
	0.05	0.617	$3.652 \cdot 10^{-5}$	$3.220 \cdot 10^{-5}$
Anodic	0.1	0.717	$4.677 \cdot 10^{-5}$	$3.945 \cdot 10^{-5}$
	0.2	0.863	$5.828 \cdot 10^{-5}$	$4.506 \cdot 10^{-5}$
	0.3	0.958	$6.567 \cdot 10^{-5}$	$4.825 \cdot 10^{-5}$
	Scane rate / Vs^{-1}	E_c / V	I_{pc} / A	ΔI_{pc} / A
	0.025	-0.218	$-4.345 \cdot 10^{-5}$	$-4.043 \cdot 10^{-5}$
	0.05	-0.307	$-5.466\ 10^{-5}$	$-4.901 \cdot 10^{-5}$
Cathodic	0.1	-0.433	$-6.684 \cdot 10^{-5}$	$-5.665 \cdot 10^{-5}$
	0.2	-0.622	$-8.337 \cdot 10^{-5}$	$-6.389 \cdot 10^{-5}$
	0.3	-0.770	$-9.619 \cdot 10^{-}$	$-6.869 \cdot 10^{-5}$

The reversibility parameters of the standard ferri/ferrocyanide redox system determined by CV analysis for all studied carbon-based electrodes are gathered in Table 9.2.

Table 9.2. The reversibility parameters of the ferri/ferrocyanide redox system on tested carbon-based electrodes.

Electrode	$\Delta E_{p\ (theoretical)}$	i_{pa} / i_{pc} (theoretical)	$\Delta E_{p\ (experimental)}$	$i_{pa\ (exp)}$ / $i_{pc\ (exp)}$
GC	0.059	1	0.1	0.86
EG-Epoxy			0.136	0.746
CNF-EG-Epoxy			0.843	0.565
CNT-Epoxy			0.156	1.05
CNF-Epoxy			0.146	0.85
CNT-ZAAg-Epoxy			0.039	0.78
CNT-ZNAg-Epoxy			0.207	0.79
CNF-ZNAg-Epoxy			1.106	0.695
CNF-Ag			1.210	0.684

Analyzing the data in according with Figures 9.1 – 9.3, and Table 9.1 and 9.2, it can be deduced that:

The current ratio between the anodic and the cathodic peaks is the parameter that allows judge the chemical reversibility of an electrode reaction. An electrode process is defined as electrochemically reversible when the rate of the electron transfer is higher that the rate of the mass transport. In the present case the values of the i_{pa}/i_{pc} are close to the theoretic value for a reversible process (under the limits of the experimental conditions). Getting these values that are not in the limits of the diagnostics criteria for an electrochemically reversible one-electron process can be mostly attributed to the non-compensated resistance given by the supporting electrolyte, but can suggest the electrochemical reversibility of the electron transfer on the cyclic voltammetric time-scale [3].

Also, it can be seen that the dependences of the Ip value with the square root of the scan rate in KNO_3 solutions on all electrodes are linear but do not pass the origin of coordinates. The intercepts in the ordinate depend principally on the nature and the concentration of the supporting electrolyte. This behaviour can be explained by the fact that the ion pairs of the ferricyanide and the cation of the supporting electrolyte influence the shapes of these dependences, and therefore the rate of the electrode processes is controlled both by the diffusion and adsorption of these components at the electrode surface [4].

The reversibility of the system was estimated by the difference in the potentials of anode and cathode peak ΔEp = Ea – Ec in the cyclic voltammograms (CVs) at the carbon-based composite electrodes in the presence of solutions containing $K_3F_e(CN)_6$.

The closed values of ΔEp with that of the theoretical value 0.59 V at 25°C for the one electron transfer reaction suggesting an ideal reversibility, and show that the electron transfer occurs faster. With a peak potential separation higher than the theoretical value suggesting that the electron transfer rate is slow, and thus the cyclic voltammetric curves is quasi-reversible [5]. This may be explained by the fact that the thickness of the diffusion layer surrounding the electrode increases during the voltammogram is swept from the E_a to E_c. At slow scan rate, the diffusion layer is larger and reverse, at faster scan rate the diffusion layer is thinner. The thickness of the diffusion layer controls the rate of mass transport to the electrode, it follows that at faster scan rate the process can be called quasi-reversible, and the slower scan rate is the greater the peak-to-peak separation is, and consequently the competition between the redox kinetics of ferri/ferrocyanide system at the electrode and the mass transport results if the overall process is reversible or irreversible [6].

The differences between experimental and theoretical values are noticed for all electrodes. The experimental values close to the theoretical ones were achieved for CNT-ZAAg-Epoxy composite, for which the electron transfer is faster.

Based on Randles-Sevcik equation (1) [7]:

$$I_p = 2.69 \times 10^5 A D^{1/2} n^{3/2} v^{1/2} C \qquad (1),$$

where: *A* represents the area of the electrode (cm^2), *n* is the number of electrons participating in the reaction and is equal to 1, *D* is the diffusion coefficient of the molecule in solution, *C* is the concentration of the probe molecule in the solution (4 mM), and *v* is the scan rate ($V\ s^{-1}$);

The apparent diffusion coefficient and the electroactive surface area of the nanostructured carbon-based composite electrodes from this study were determined

(see Table 9.3). For all composite electrodes we obtained an electroactive surface higher than the geometrical ones for each electrode.

Table 9.3. Apparent diffusion coefficient and the electroactive surface area of the nanostructured carbon-based composite electrodes.

Electrode	Apparent diffusion coefficient/ (cm^2 s^{-1})	Electroactive surface area/ cm^2	Geometric area/ cm^2	Electroactive surface area/ Geometrical area
GC	$3.394 \cdot 10^{-6}$	0.132	0.049	1.46
EG-Epoxy	$1.804 \cdot 10^{-6}$	0.091	0.09	1.01
CNF-EG-Epoxy	$0.353 \cdot 10^{-6}$	0.110	0.09	1.23
CNT-Epoxy	$2.668 \cdot 10^{-5}$	0.473	0.196	2.41
CNF-Epoxy	$1.349 \cdot 10^{-6}$	0.352	0.196	1.8
CNT-ZAAg-Epoxy	$3.963 \cdot 10^{-5}$	0.372	0.196	1.9
CNT-ZNAg-Epoxy	$4.3 \cdot 10^{-5}$	0.411	0.196	2.1
CNF-ZAAg-Epoxy	$0.153 \cdot 10^{-5}$	0.313	0.196	1.6
CNF-Ag	$0.569 \cdot 10^{-6}$	0.346	0.196	1.75

Based on the above presented results, it can be concluded that all tested carbon-based composite electrode exhibited the electroactive surface area at least or quite higher equal to the geometrical one.

Expanded graphite-epoxy composite electrode exhibited the lowest electrode area and the presence of nanostructured carbon within the composite composition enhanced the electroactive area. The best electroactive area was achieved for carbon nanotubes-epoxy composite electrodes.

9.1. References:

[1] J.E. O'Reilly, Biochim. Biophys. Acta 292 (1973) 209.
[2] J. Wang, Ed. John Wiley & Sons, Inc. (2006) 29-41.
[3] P. Zanello, Ed. The Royal Society of Chemistry, ISBN: 978-1-84755-114-6, (2003) 49-67.
[4] V.N. Kiryushov, L.I. Skvortsova, T.P. Aleksandrova, J. Anal. Chem. 66 (2011) 510.
[5] J.M. Nugent,K. S.V. Santhanam, A. Rubio, P.M. Ajayan, Nano. Lett. 1 (2001) 87.
[6] R.G. Compton, C. E. Banks, Ed. Imperial College Press (2011) 107-127.
[7] **A. Baciu**, A. Remes, E. Ilinoiu, F. Manea, , S.J. Picken, J. Schoonman, Environ. Eng. Manag. J. 11 (2012) 1968.

CHAPTER 10. ELECTROCHEMICAL DETECTION OF PCP USING CARBON-BASED COMPOSITE ELECTRODES

10.1. Pentachlorophenol (PCP)

PCP (pentachlorophenol) is commonly used as a wood preservative, based on both antifungal and insecticide properties. It was also used in a range of areas for antifungal, antibacterial, general herbicide, and slime prevention in both industrial and consumer applications [1]. PCP exhibits toxicity and persistence in water and soil, with a very negative impact on environment and human health, including acute toxicity and carcinogenicity [2 - 5]. The determination of PCP in water for monitoring water quality is higher desired. The methods most frequently described in the literature for the determination of phenolic and related compounds of environmental interest are based on chromatographic and spectrophotometric analysis [6 - 10]. Also, based on the good sensitivity, selectivity, simplicity and low-cost, several electrochemical detection methods for PCP determination have been developed [5, 11 – 15].

The use of the electroanalytical methods for the determination of a variety of organic and inorganic substances is steadily growing due to several improvements in techniques and instrumentation that has allowed the attainment of detection limits (DL) compatible with environmental regulations. Meanwhile, those methods are usually based on processes occurring at a mercury surface but its hazardous potential for human health strongly indicates the necessity of seeking alternative electrode materials. Such useful alternatives have been proposed for the determination of PCP by oxidation on carbon paste and vitreous carbon surfaces [12, 14]. Also, successful application of chemically modified electrodes and boron doped diamond electrodes in combination with different electrochemical methods was reported for the determination of phenol derivates. Recently, carbon-based materials such as graphite, carbon fibers etc. have been used most often as the conductive phase in preparing composite working electrodes [15-20].

Although phenol derivates in general, can be oxidized at many electrode materials, the oxidation at carbon-based solid electrodes produces phenoxy radicals, which couple to form an insulating polymeric film fouling the surfaces of the electrodes. A simple method of renewing the electrode surfaces is based on the anodic treatment. This relies on adjusting the working electrode potential high enough to oxidize the insulating film and making it water soluble without damaging the electrode [21 - 23].

This study aims to characterize the electrochemical behaviour of pentachlorophenol on three types of carbon-based composite electrodes, *i.e.*, expanded graphite-epoxy (EG-Epoxy), carbon nanofiber-expanded graphite-epoxy (CNF-EG-Epoxy) and carbon nanotubes-epoxy (CNT-Epoxy) composite electrodes, by cyclic voltammetry envisaging its detection in aqueous solution. For each electrode, the optimum detection operating conditions were established in relation with the specific electrochemical techniques and their operating parameters. Various

electrochemical techniques were applied for the detection measurements: cyclic voltammetry (CV), linear-sweep voltammetry (LSV), differential-pulsed voltammetry (DPV), square-wave voltammetry (SWV), chronoamperometry (CA), and multiple-pulsed amperometry (MPA). In addition, some mechanistic aspects regarding PCP oxidation on each type of electrode were discussed based on the results of the scan rate influence to improve the performance of the electrode in the detection application. Several detection schemes for PCP determination were proposed in relation with the electrode type, electrochemical technique and optimum operating variables linked to specific practical requirements.

10.2. Experimental

10.2.1. Reagents

Pentachlorophenol (PCP) was purchased from Merck. An aqueous 10 mg/L PCP stock solution was prepared daily by dilution the solid PCP in double distilled water and 0.1 M NaOH. Supporting electrolyte for the characterization and application of electrode material in detection process was 0.1 M Na_2SO_4 solution, which was freshly prepared from Na_2SO_4 of analytical purity (Merck) with distilled water.

10.2.2. Working electrodes

The carbon-based composite working electrodes used for the detection of PCP are gathered in Table 10.1.

Table 10.1 Carbon-based composite working electrode tested for the electrochemical detection of PCP.

Carbon-based composite electrode	Geometrical area/cm^2	Electroactive surface area/cm^2	Electroactive surface area/ Geometrical area
EG-Epoxy	0.09	0.091	1.01
CNF-EG-Epoxy	0.09	0.110	1.23
CNT-Epoxy	0.196	0.473	2.41

For comparison, commercial glassy carbon (GC) electrode, which was supplied by Metrohm, Switzerland, was also used for the electrochemical detection of PCP. Also, for GC electrode the electrochemical surface area was determined and the ratio between electroactive surface area and geometrical surface was 1.46.

10.2.3. Apparatus and procedures

The electrochemical performances of the carbon-based composite electrodes were studied by cyclic voltammetry (CV), differential-pulsed voltammetry (DPV), square-wave voltammetry (SWV), and multiple-pulsed amperometry (MPA).

Electrochemical measurements were performed in unstirred solutions using a computer controlled Autolab potentiostat/galvanostat PGSTAT 302 (EcoChemie, The Netherlands), with a standard three electrodes configuration (Figure 10.1). The three-electrode system consisted of a carbon-based working electrode, a platinum wire as counter electrode and a saturated calomel reference electrode (SCE). Before each voltammogram, each composite electrode was carefully polished with abrasive

paper and then on a felt-polishing pad by using 0.3 μm alumina powder (Metrohm, Switzerland). All experiments were carried out with a typical cell of 50 mL at room temperature (25 C).

(a) (b)

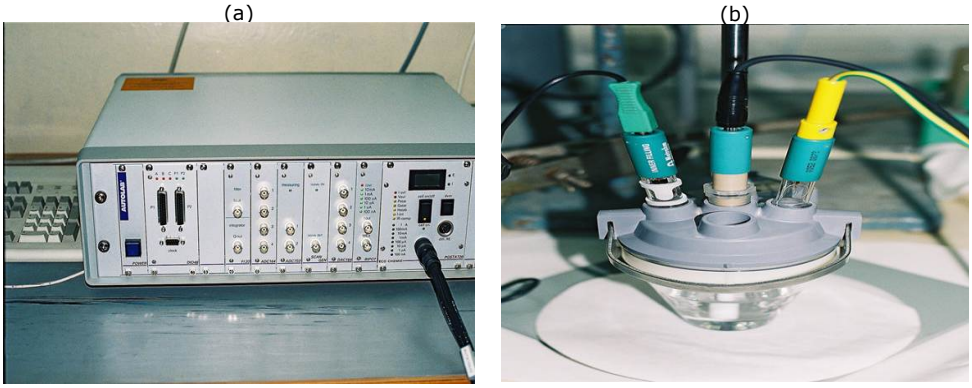

Figure 10.1 (a) Potentiostat/galvanostat PGSTAT 302 (EcoChemie); (b) Metrohm cell with 3 electrodes configuration.

10.3. Results and discussion

The selection of the carbon-based electrode, the electrochemical technique and the operation parameters to design a detection procedure requires a detailed study on each electrode. The electrochemical behaviour of each electrode in the presence of PCP and the results of PCP detection will be presented in the future three subsections.

10.3.1. EG-Epoxy composite electrode

10.3.1.1. Electrochemical behaviour of PCP on EG-Epoxy composite electrode

Figures 10.2 a and b shows the cyclic voltammograms (CVs) recorded at scan rate of 0.05 Vs^{-1} in 0.1 M Na_2SO_4 supporting electrolyte and in the presence of 7.5 μM and 15 μM PCP concentrations, on EG-Epoxy composite and respective, GC electrodes. Cyclic voltammograms recorded at GC electrode in the presence of the PCP (Figure 10.2a) shows that PCP oxidation starts from the potential value of about 0.5 V/SCE, while for the GE-Epoxi composite electrode the oxidation process starts much earlier (about -0.3 V/SCE) (Figure 10.2b).

It is well-known that, in general, the electrooxidation process of phenolic derivatives at carbon-based electrode is a very complex process that assumes adsorption and electropolymerization of the oxidation products, generally leading to the electrode fouling, in direct relation with the carbon electrode material.

No proportional increase of the anodic current recorded on GC electrode with the concentration of PCP was noticed, which informed about a rapid electrode fouling, aspect that denotes that GC electrode is not suitable for PCP detection. A better behaviour was found for EG-Epoxy electrode, for which a proportional increase of anodic current density with PCP concentration was found (see Figure

10.3) giving information about the possibility of controlled oxidation process by mass transfer, aspect desired in amperometric / voltammetric detection application. The linear proportionality between the current densities of the anodic peaks and PCP concentration was achieved for three potential values, *i.e.*, -0.2, +0.6 and + 1V/SCE with the good correlation coefficients. It must be noticed that for the anodic oxidation peak recorded at potential value of -0.2 V/SCE the corresponding reduction cathodic one occurred, which should be owns to the electrode surface-controlled redox process.

Based on the previously reported electroactive area results correlated with the electrochemical behaviour of PCP, the EG-Epoxy composite electrode was selected for further electrochemical studies.

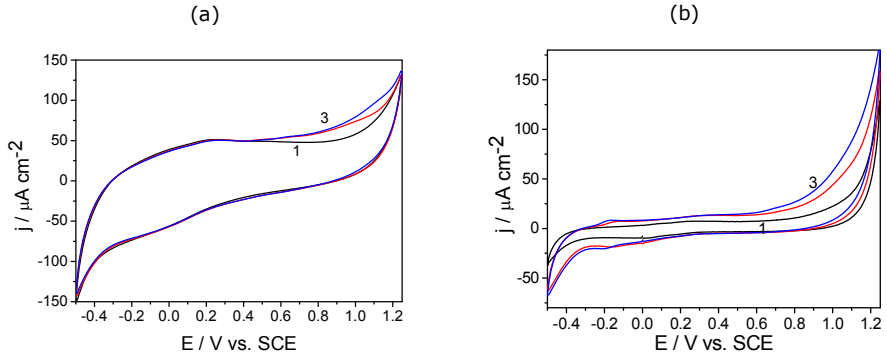

Figure 10.2 Cyclic voltammograms in 0.1 M Na_2SO_4 supporting electrolyte (curve 1) and in the presence of 7.5 μM (curve 2) and 15 μM (curve 3) PCP at : (a) GC electrode and (b) EG-Epoxy electrode

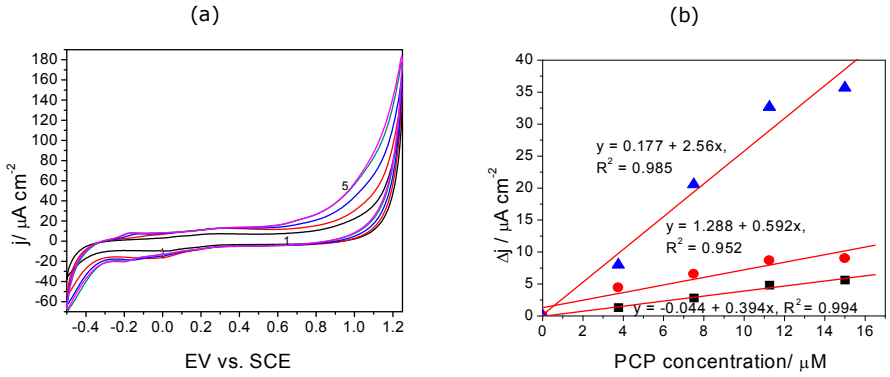

Figure 10.3 (a) Cyclic voltammograms recorded at EG-Epoxy electrode in 0.1 M Na_2SO_4 supporting electrolyte (1) and in the presence of 3.75, 7.5, 11.25, 15 μM PCP (curves 2-5); potential scan rate: 0.05 Vs^{-1}; potential range: -0.5 to +1.25 V/SCE; (b) Calibration plots of the currents recorded at E= -0.2, +0.6 and +1.0 V/SCE vs. pentachlorophenol concentrations

In order to investigate the mechanistic aspects of the overall oxidation process of PCP on EG-Epoxy composite electrode, the influence of various scan rates (0.01-0.2 Vs^{-1}) on the CVs recorded in the presence of 5.62 μM PCP was studied

(Figure 10.4). The linear increase of the current density corresponding to pentachlorophenol anodic oxidation at each prior established potential value of -0.2, +0.6 and +0.1 V/SCE with the square root of the scan rate suggested that a mass transfer controlled process, and no zero intercept informed that the adsorption and surface interaction processes are not neglected. Based on the slope value determined for each potential value, it can be seen that the diffusion process is favored as follows: +1V > +0.6 V > -0.2 V/SCE. For all potential values, the peak potential shifted towards positive potential when increasing v indicates that the electrooxidation process of pentachlorophenol is irreversible.

However, for the potential value of -0.2 V/SCE the cathodic peak occurrence corresponding to the anodic one, informed about a reversible process (see results from Figure 10.4).

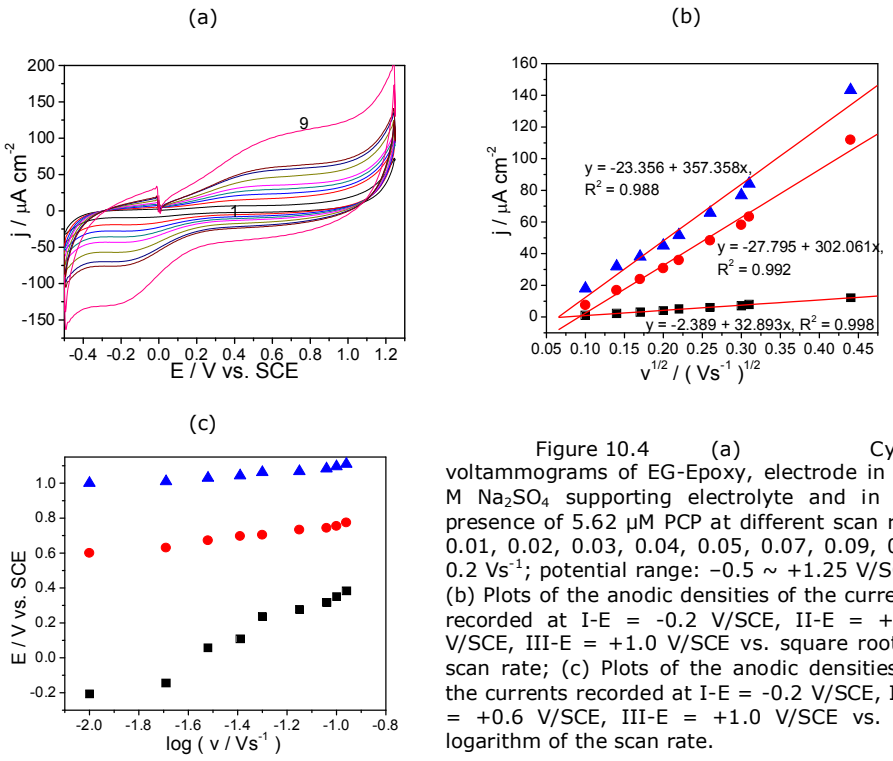

Figure 10.4 (a) Cyclic voltammograms of EG-Epoxy, electrode in 0.1 M Na_2SO_4 supporting electrolyte and in the presence of 5.62 μM PCP at different scan rate 0.01, 0.02, 0.03, 0.04, 0.05, 0.07, 0.09, 0.1, 0.2 Vs^{-1}; potential range: –0.5 ~ +1.25 V/SCE; (b) Plots of the anodic densities of the currents recorded at I-E = -0.2 V/SCE, II-E = +0.6 V/SCE, III-E = +1.0 V/SCE vs. square root of scan rate; (c) Plots of the anodic densities of the currents recorded at I-E = -0.2 V/SCE, II-E = +0.6 V/SCE, III-E = +1.0 V/SCE vs. the logarithm of the scan rate.

10.3.1.2. Detection measurements

The detection measurements were performed using cyclic voltammetry (CV), linear-scan voltammetry (LSV), differential-pulsed voltammetry (DPV) and chronoamperometry (CA).

CV results were presented in the previous section and the electroanalytical parameters determined using this technique is gathered in Table 10.2

-Linear-scan voltammetry results

Figure 10.5 shows linear-scan voltammograms recorded at EG-Epoxy composite electrode in the presence of different PCP concentrations and it can be observed a linear dependence of the anodic oxidation current densities recorded at the potential values of -0.15, +0.7 and +1V/SCE. A slight more positive shifting of the oxidation potential was noticed based on the LSV peculiarities, but the appearance of the anodic oxidation peak at very negative potential value (-0.15 V/SCE) is confirmed. The appearance of the anodic oxidation peak at the negative potential value is very unusually and may be explained by the changes at electrode surface with the oxidation products resulting from the previous oxidation process at higher oxidation potential value, products that are more easily readily oxidisable. Although this electropolymerization phenomenon is undesirable because it produces the electrode fouling following by its electrochemical activity loss, under these working conditions of small concentrations the electrochemical activity of the electrode was not lost. The major advantage of this behavior is the negative potential value used for PCP oxidation, which gives a real potential to this electrode to be selectively towards PCP detection.

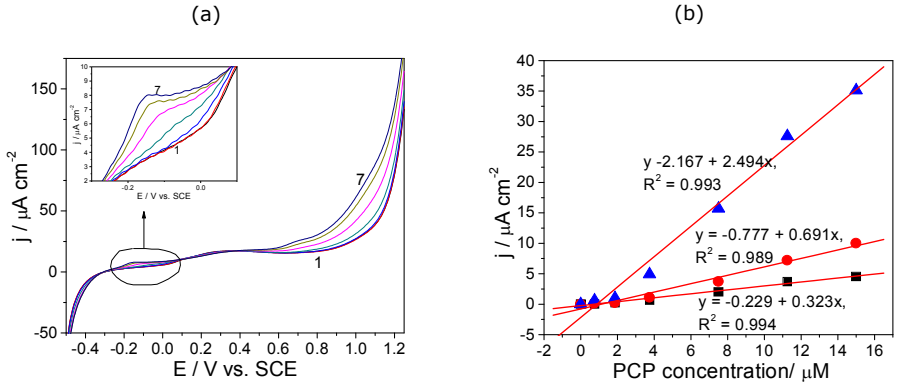

Figure 10.5 (a) Linear- sweep voltammograms at EG-Epoxy electrode in 0.1 M Na_2SO_4 supporting electrolyte (1) and in the presence of different PCP concentrations: 2- 0.75 μM, 3- 1.87 μM, 4- 3.75 μM, 5- 7.5 μM, 6- 11.25 μM, 7- 15 μM; potential scan rate: 0.05 Vs^{-1}; potential range: -0.5 to +1.25 V/SCE. Inset: detail of the potential range near to -0.2 V/SCE; (b) Calibration plots of the densities of the currents recorded at E = -0.15 V/SCE, E = +0.70 V/SCE, E = +1.0 V/SCE vs. pentachlorophenol concentrations.

-Differential-pulsed voltammetry results

In order to achieve better electroanalytical performance, it has been tested differential-pulsed voltammetry, technique that achieves a minimization of the effects of background noise, in particular of the brought the capacitive current, allowing the improvement the useful signal. Using this specific technique requires the establishment of optimum operating conditions on the step potential, which represents the potential increment between two subsequent current measurements and modulation amplitude.

The operating conditions for DPV technique are presented in Table 10.2 and the corresponding DPV results are shown in Figures 10.6 - 10.8. Also, the calibration plots are presented in Figures 10.6 – 10.8. It must be mentioned that the optimization of DPV variables was achieved in relation to the enhancement of the sensitivity for the PCP detection at the lowest oxidation potential value of -0.2 V/SCE.

Table 10.2 The operating parameters for DPV testing in relation with the sensitivity for PCP detection at the potential value of -0.2 V/SCE.

Step potential/mV	Modulation amplitude/mV	Potential range/V vs. SCE	Sensitivity/$\mu A cm^{-2} \mu M^{-1}$
0.01	0.1	-0.5→+1.25	17.973
0.01	0.2	-0.5→+1.25	7.358
0.01	0.2	-0.5→+0.1	4.522

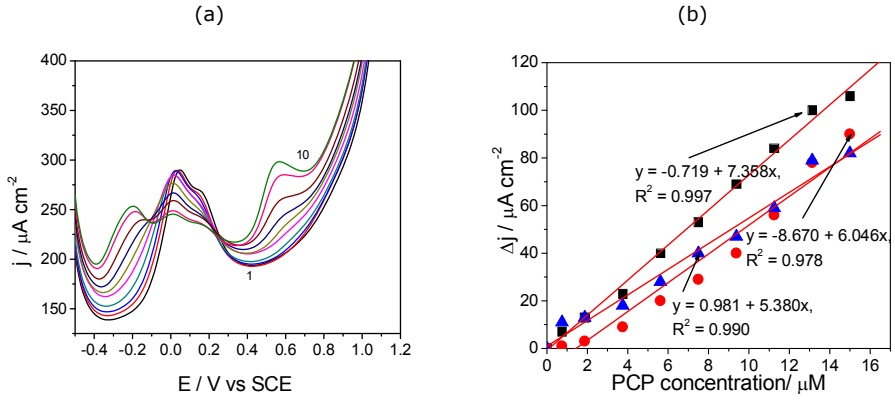

Figure 10.6 (a) Differential-pulsed voltammograms recorded on EG-Epoxy electrode with a modulation amplitude of 0.2V, a step potential of 0.01V and scan rate of 0.05 Vs^{-1} between -0.5 and +1.25 V/SCE in 0.1 M Na_2SO_4 supporting electrolyte (1) and in the presence of different PCP concentrations: 2- 0.75μM, 3- 1.87 μM, 4- 3.75 μM, 5- 5.62 μM, 6- 7.5 μM, 7- 9.38 μM, 8-11.25 μM, 9- 13.13 μM, 10- 15 μM. (b) Calibration plots of the densities of the currents recorded at E = -0.20 V/SCE, E = +0.60 V/SCE, and E = +1. 0 V/SCE vs. pentachlorophenol concentrations.

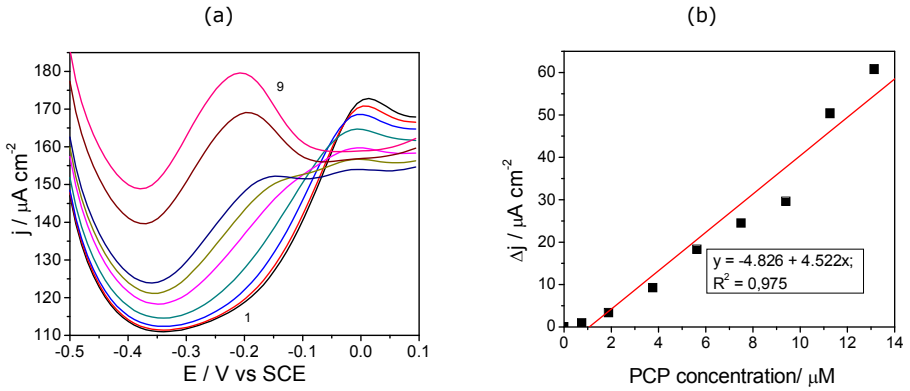

Figure 10.7 (a) Differential-pulsed voltammograms recorded on EG-Epoxy electrode with a modulation amplitude of 0.1V, a step potential of 0.01V and scan rate of 0.05 Vs^{-1} between -0.5 and +1.25V vs. SCE in 0.1 M Na_2SO_4 supporting electrolyte (1) and in the presence of different PCP concentrations: 2- 0.75 μM, 3- 1.87 μM, 4- 3.75 μM, 5- 5.62 μM, 6- 7.5 μM, 7- 9.38 μM, 8-11.25 μM, 9- 13.13 μM, 10- 15 μM. (b) Calibration plots of the densities of the currents recorded at E = -0.20 V/SCE, E = +0.60 V/SCE, and E = +1. 0 V/SCE vs. pentachlorophenol concentrations.

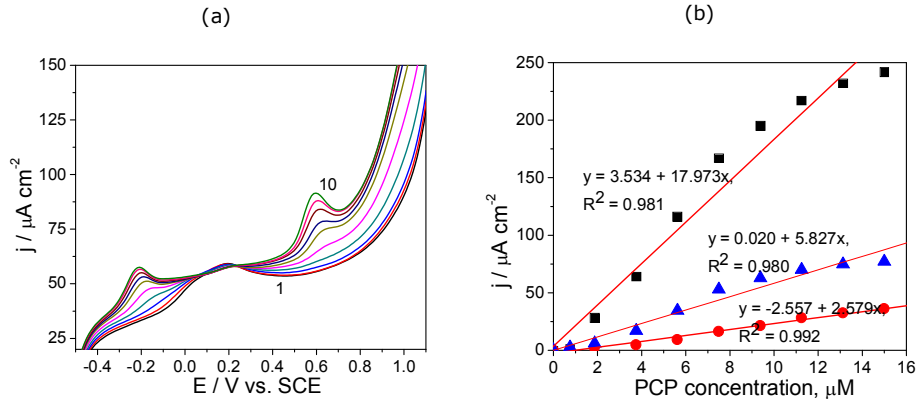

Figure 10.8 (a) Differential-pulsed voltammograms recorded on EG-Epoxy electrode with a modulation amplitude of 0.1V, a step potential of 0.01V and scan rate of 0.05 Vs^{-1} between -0.5 and +1.25V vs. SCE in 0.1 M Na_2SO_4 supporting electrolyte (1) and in the presence of different PCP concentrations: 2- 0.75μM, 3- 1.87 μM, 4- 3.75 μM, 5- 5.62 μM, 6- 7.5 μM, 7- 9.38 μM, 8-11.25 μM, 9- 13.13 μM, 10- 15 μM. (b) Calibration plots of the densities of the currents recorded at E = -0.20 V/SCE, E = +0.60 V/SCE, and E = +1.0 V/SCE vs. pentachlorophenol concentrations.

As we expected, for all tested DPV conditions better sensitivities were achieved for each oxidation potential value, and the optimum DPV variables were selected as 0.1 V modulation amplitude and 0.01 V step potential for the potential range of -0.5 to +1.25 V/SCE. Because the most negative oxidation potential value

represents the major interest for PCP detection envisaging its selective detection from phenolic class, the narrower potential range was selected that included the oxidation potential value (see Figure 10.8). Under these conditions, the sensitivity was worse than the one reached under the same DPV conditions but for a larger potential range, which informed that at the potential value of -0.2 V/SCE occurred the oxidation process of the oxidation products generated at the higher oxidation potential value corresponding to the PCP oxidation.

The adsorption property of the carbon-based electrode towards PCP is not generally desired because of the electrode fouling generation. However, these phenomena could be exploited to preconcentrate PCP at the electrode surface improving the local PCP concentration followed by the oxidation process. In a preconcentration based detection scheme, the extent of preconcentration is a function of accumulation time, which represents the time of maintaining at open circuit potential (OCP). The effect of accumulation time on the useful signal at each oxidation potential value of -0.2, +0.6 and + 1 V/SCE corresponding to the oxidation of PCP and its oxidation products. The enhancement factor was determined as ratio of the current densities recorded at different accumulation time to those recorded without a preconcentration scheme. The useful oxidation peak current and the enhancement factor determined for 5.6 μM PCP using preconcentration-voltammetric detection procedure at different accumulation time are shown in Figure 10.9a. No significant enhancement of the useful signal was reached with the accumulation time increasing, which suggested that no preconcentration based scheme is suitable for PCP detection.

(a) (b)

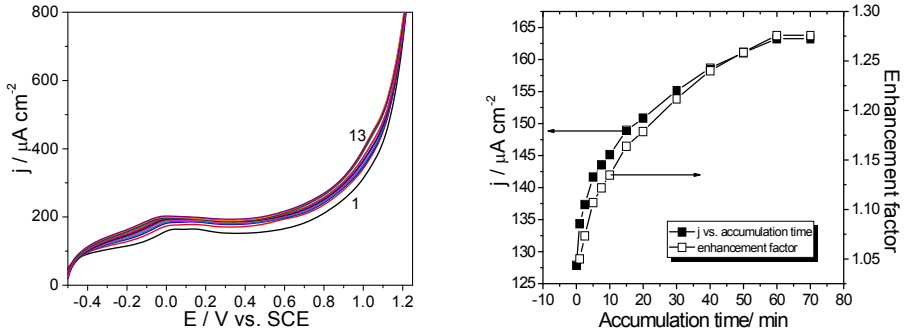

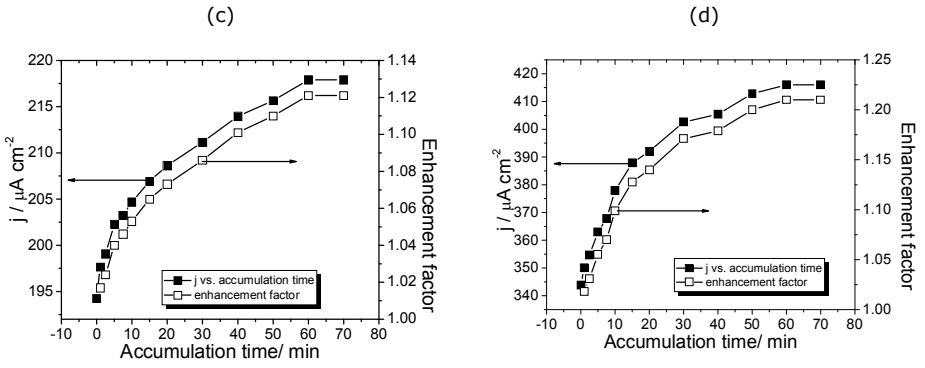

Figure 10.9 (a) Differential-pulsed voltammograms recorded on EG-Epoxy electrode in 0.1 M Na_2SO_4 supporting electrolyte (1) for detection of the PCP 5.6 μM at different accumulation times: 2-0min; 3-1 min; 4-2.5 min; 5-5 min; 6-7.5 min; 7-10 min; 8-15 min; 9-20 min; 10-30 min; 11-40 min; 12-50 min; 13-60 min. Evolution of current responses recorded obtained by DPV with accumulation time obtained to detect 5.6 μM PCP at: -0.2 V (b); +0.6 V (c) and +1 V/SCE (d)

-Chronoamperometric results

The chronoamperometry is considered as the easiest detection method envisaging the practical application. Based on the cyclic voltammetry results as the reference for operating parameters, the chronoamperometry was tested for the three potential values above-established. Figure 10.10 presents the chronoamperograms recorded at potential values of -0.2, +0.6 and + 1 V/ SCE in the presence of various PCP concentrations. The useful current signals recorded after 50 seconds depended linearly on PCP concentration within the explored concentration range between 1.87 μM and 9.38 μM only at the potential values of +0.6 and +1 V/SCE, and no current increasing was noticed at the potential value of -0.2 V/SCE. The electroanalytical parameters determined for the both potential values are gathered in Table 10.3. The sensitivity was worse versus the voltammetric tested techniques but the lowest limit of detection and quantification are similar to CV.

No amperometric signal noticed for the potential value of -0.2 V/SCE confirmed our supposition that at this potential occurred the oxidation process of the oxidation products generated at higher potential values. No amperometric detection of PCP at the potential value of -0.2 V/SCE can be operated.

The electroanalytical parameters determined for all electrochemical techniques using EG-Epoxy composite electrode are gathered in Table 10.3. The reproducibility of the electrode using the above-mentioned techniques was evaluated for three replicates measurements of PCP detection as relative standard deviation (RSD). Based on RSD values ranged from 0.900 to 4.990 it should concluded that the PCP detection at EG-Epoxy composite electrode is reproducible. Also, it can be noticed that the best electroanalytical parameters were reached by differential-pulsed voltammetry at the potential value of -0.2 V/SCE, which is very promising for practical application for selective determination of PCP from aqueous solution.

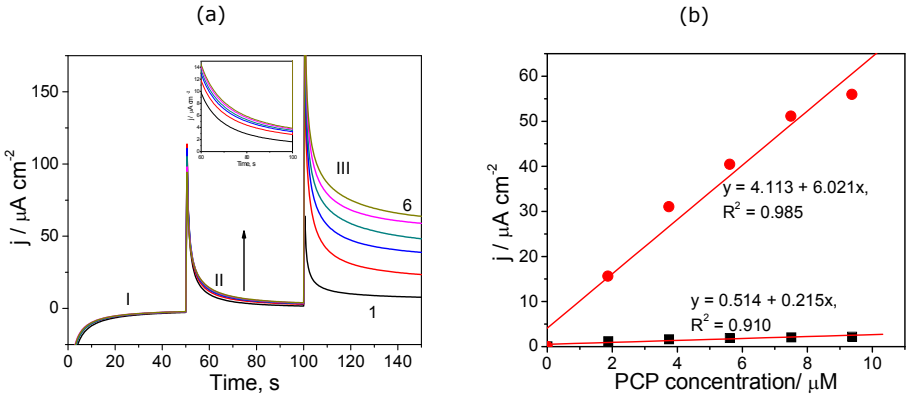

Figure 10.10 (a) Chronoamperograms recorded at EG-Epoxy electrode in 0.1 M Na_2SO_4 supporting electrolyte and in the presence of different PCP concentrations: 1.87, 3.75, 5.62, 7.5, and 9.38, μM, recorded at E= -0.2 V/SCE, E= + 0.6 V/SCE and E= +1.0 V/SCE; (b) Calibration plots of the densities of the currents recorded at E= +0.6 V/SCE, and E= +1.0 V/SCE vs. pentachlorophenol concentrations.

Table 10.3 The electroanalytical parameters of amperometric detection of PCP at an EG-Epoxy composite electrode using electrochemical techniques.

Technique	Potential value V / SCE	Sensitivity μA / μMcm^2	Correlation coefficient, R^2	Relative standard deviation, RSD, %	The lowest limit of detection, LOD/ μM	Limit of quantification, LQ/ μM	Concentration range, μM
CV	-0.2	0.394	0.994	4.980	1.335	4.451	0.75 – 7.5
	+0.68	0.592	0.952	2.717	1.447	3.491	
	+1.0	2.56	0.985	1.538	0.426	1.421	
LSV	-0.15	0.323	0.994	4.990	1.826	4.755	0.75 - 15
	+0.7	0.691	0.989	2.327	1.510	3.036	
	+1.0	2.49	0.993	1.234	0.52	1.401	
DPV	-0.2	17.9	0.981	4.015	0.218	0.726	0.75 - 15
	+0.6	2.58	0.992	1.723	1.097	3.658	
	+1.0	5.80	0.980	0.9	1.920	7.067	
CA	+0.6	0.215	0.910	2.412	1.088	3.627	1.87 – 9.38
	+1.0	6.021	0.985	2.773	0.542	1.809	

10.3.2. CNF-EG-Epoxy composite electrode

Besides carbon nanotubes (CNTs), carbon nanofibers (CNFs) are one of the most promising reinforcing materials for epoxy-based composites for the carbon-based electrode obtaining with the application in the electroanalysis due to their excellent mechanical, electrical and electrocatalytical properties. In comparison with CNTs, CNFs are advantageous from the economical point of view, being less expensive. In this study, CNFs were incorporated to replace 50%, wt. of expanded graphite to improve the electroanalytical parameters for PCP detection.

10.3.2.1. Cyclic voltammetric measurements

Figure 10.11 shows CVs recorded in 0.1 Na_2SO_4 supporting electrolyte at CNF-EG-Epoxy composite electrode in comparison with EG-Epoxy composite electrode. The presence of CNFs influenced the electrochemical behaviour of EG-Epoxy composite electrode, a higher background current and the oxygen evolution at lower potential value are noticed, which are common for the electrocatalytic behaviour. In Figure 10.12 are shown the CVs recorded in 0.1 M Na_2SO_4 supporting electrolyte in the presence of various PCP concentrations. Also, the electrochemical behaviour of PCP on CNF-EG-Epoxy composite electrode is different in comparison with EG-Epoxy, the electrochemical oxidation process of PCP started at more negative potential value, and occurred also in two steps, at +0.5 and +0.78 V/SCE versus +0.6 and +1 V/SCE for EG-Epoxy composite electrode. However, no oxidation peak appeared at -0.2 V/SCE, probably other oxidation products are generated, which are not oxidizable at this potential value. With PCP concentration increasing, the anodic peak currents increased linearly (see Figure 10.12). Based on the calibration plots, it was determined the sensitivities, which are better in comparison with those determined for EG-Epoxy electrode (see Table 10.4).

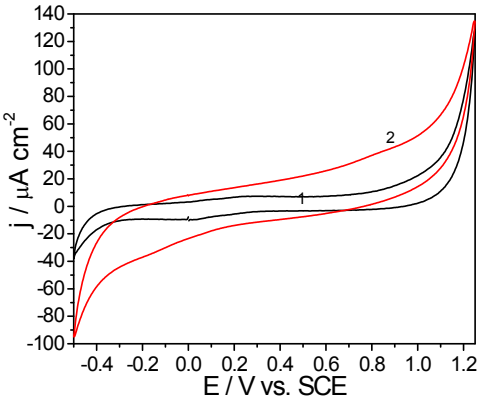

Figure 10.11 Cyclic voltammograms recorded in 0.1 m Na_2SO_4 supporting electrolyte at: EG-Epoxy electrode (curve 1) and CNF-EG-Epoxy electrode (curve 2)

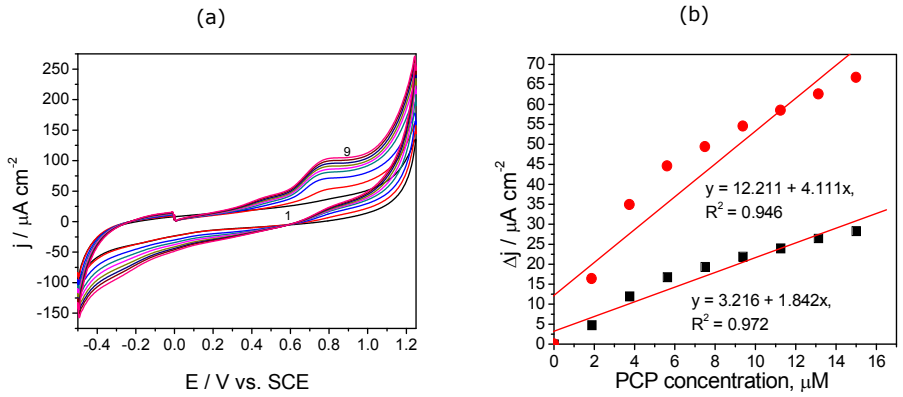

Figure 10.12 (a) Cyclic voltammograms recorded at CNF-EG-Epoxy electrode in 0.1 M Na_2SO_4 supporting electrolyte (1) and in the presence of 1.87, 3.75, 5.62, 7.5, 9.38, 11.25, 13.13, 15 μM PCP (curves 2-9); potential scan rate: 0.05 Vs^{-1}; potential range: -0.5 to +1.25 V/SCE; (b) The calibration plots of the current densities vs. pentachlorophenol concentrations recorded at E= +0.50 V/SCE and E= +0.78 V/SCE.

The effect of the scan rate on the oxidation process of PCP on the CNF-EG-Epoxy composite electrode surface was investigated, and the evolution of CVs recorded at various scan rates (0.01 – 0.2 Vs^{-1}) in the presence of 5.62 μM PCP is presented in Figure 10.13. The linear increase of current density corresponding to pentachlorophenol anodic oxidation at the both potential values of +0.5 and +0.78 V/SCE with the square root of the scan rate suggested that mass transfer controlled process, and no zero intercepts suggested that adsorption steps and surface interactions were not negligible. The slope values determined for both potential values at this electrode are slight lower than those determined for EG-Epoxy composite electrode. This aspect should be explained in relation to the microelectrode array behaviour of the composite electrode. Linear diffusion is characteristics to the macro electrode while the spherical diffusion is characteristics to microelectrode array. Under these working conditions, no spherical diffusion was determined for both electrodes, but the effect of scan rate is more significant on EG-Epoxy than CNF-EG-Epoxy composite electrode. For all potential values, the peak potential shifted towards positive potential when increasing v indicates that the electrooxidation process of pentachlorophenol is irreversible. Moreover, no cathodic reduction peaks corresponding to the oxidation ones were noticed, which confirmed the irreversibility of the PCP oxidation process (see Figure 10.13).

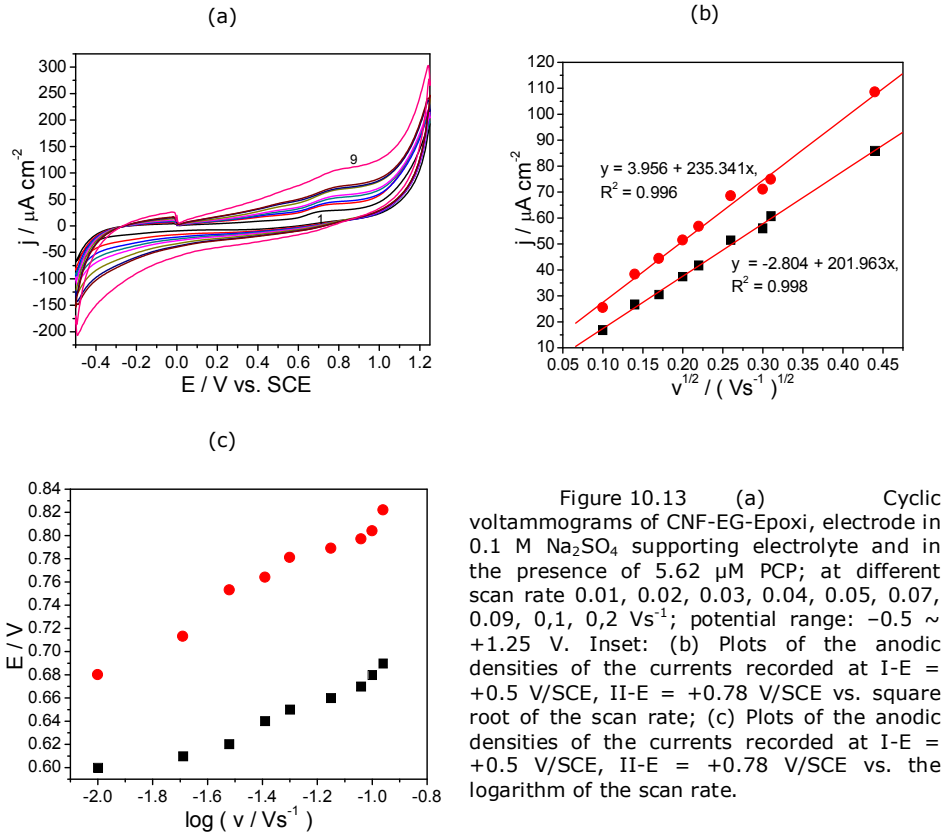

Figure 10.13 (a) Cyclic voltammograms of CNF-EG-Epoxi, electrode in 0.1 M Na_2SO_4 supporting electrolyte and in the presence of 5.62 µM PCP; at different scan rate 0.01, 0.02, 0.03, 0.04, 0.05, 0.07, 0.09, 0,1, 0,2 Vs^{-1}; potential range: –0.5 ~ +1.25 V. Inset: (b) Plots of the anodic densities of the currents recorded at I-E = +0.5 V/SCE, II-E = +0.78 V/SCE vs. square root of the scan rate; (c) Plots of the anodic densities of the currents recorded at I-E = +0.5 V/SCE, II-E = +0.78 V/SCE vs. the logarithm of the scan rate.

10.3.2.2. Detection measurements

The electrochemical behaviour of PCP on CNF-EG-Epoxy characterized by CV is promising for its electrodetection by voltammetric/amperometric techniques, and the detailed investigations are presented in the following subsections.

-Differential-pulsed voltammetry results

The operating conditions for DPV technique applied for this electrode are the optimum prior established for EG-Epoxy electrode, *i.e.*, the step potential of 0.01 V and the modulation amplitude of 0.1 V. The DPVs series recorded at various PCP concentrations are presented in Figure 10.14. It can be noticed that under these working conditions only an oxidation step is evidenced at the potential value of +0.63 V/SCE, for which the oxidation peak current increased linearly with PCP concentration (see figure 10.14b). The electroanalytical parameters, *e.g.*, the sensitivity, the lowest limit of detection, the limit of quantification and relative standard deviation are presented in Table 10.4.

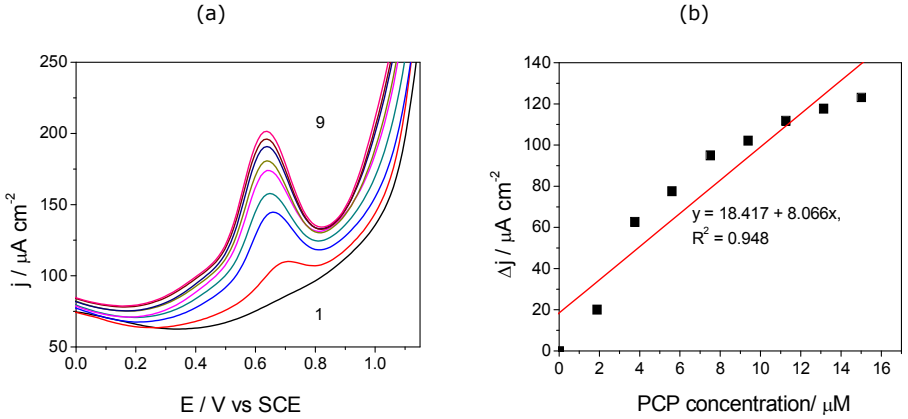

Figure 10.14 (a) Differential- pulsed voltammograms recorded on CNF-EG-Epoxy electrode with a modulation amplitude of 0.1V, a step potential of 0.01V and scan rate of 0.05 Vs^{-1} between -0.5 and +1.25V vs. SCE in 0.1 M Na_2SO_4 supporting electrolyte (1) and in the presence of different PCP concentrations: 2- 0.75μM, 3- 1.87 μM, 4- 3.75 μM, 5- 5.62 μM, 6- 7.5 μM, 7- 9.38 μM, 8-11.25 μM, 9- 13.13 μM, 10- 15 μM. (b) Calibration plots of the densities of the currents recorded at E = +0.63 V/SCE vs. pentachlorophenol concentrations.

-Chronoamperometric results

The continuous stepwise chronoamperograms were recorded at different PCP concentrations under the same conditions applied for CNF-EG-Epoxy electrode. The prior selected three potential values were applied also, for this electrode and the recorded chronoamperograms are presented in Figure 10.15. Even if the current increased with the PCP concentration at the potential value of -0.2 V/SCE, the negative values are not desired for anodic amperometric determination. The calibration plots obtained for the potential values of +0.6 and + 1 V/SCE showed the good correlation coefficients. The sensitivities are gathered also in Table 10.4 and very good sensitivity at the potential value of +0.6 V/SCE was reached in comparison with EG-Epoxy electrode. The electroanalytical parameters reached by CA were similarly with those reached by CV, informing that the electrode fouling is neglected for this electrode.

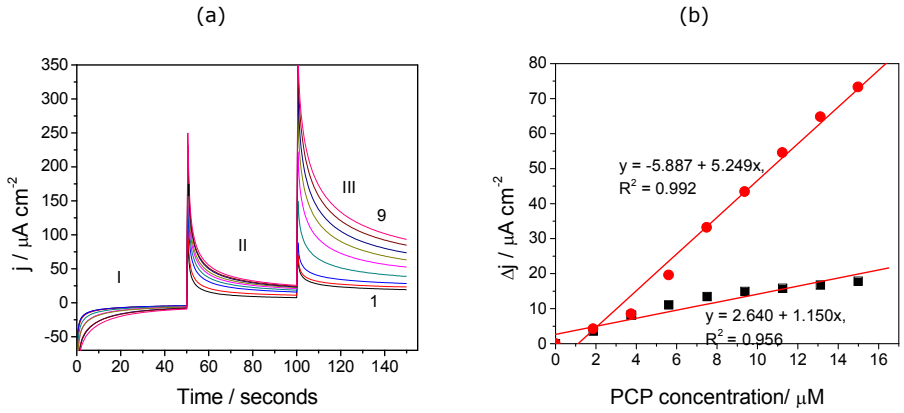

Figure 10.15 (a) Chronoamperograms recorded at CNF-EG-Epoxy electrode in 0.1 M Na_2SO_4 supporting electrolyte and in the presence of different PCP concentrations: 1.87, 3.75, 5.62, 7.5, and 9.38, μM, recorded at E= -0.2 V/SCE, E= + 0.6 V/SCE and E= +1.0 V/SCE; (b) Calibration plots of the densities of the currents recorded at E= +0.6 V/SCE, and E= +1.0 V/SCE vs. pentachlorophenol concentrations.

-Multiple-pulsed ampeormetric measurements

An alternative to the amperometric detection to improve the electroanalytical parameters and proposed in this work is the use of MPA with three potential pulses, whose values were established based on CV behaviour. The pulses were applied continuously using the following scheme:

1) +0.6 V/SCE for duration of 0.05 ms, where PCP is direct oxidized on the electrode surface,

2) +1 V/SCE for duration of 0.05 ms, where advanced oxidation of PCP occurred.

3) -0.2 V/SCE for duration of 0.05 ms, considered as reduction process of oxidation products generated from PCP electrooxidation

Figure 10.16a presents the pulsed amperograms recorded at each potential value for PCP detection. For both oxidation potential values the corresponding current depended linearly on PCP concentration (Figure 10.16b). Also, the cathodic current decreased linearly with PCP concentration (linearization results are not shown here), but in this work no cathodic response is the aim. However, the linear cathodic response confirmed that the reduction process is linked to the generation of PCP oxidation products. Alternating the advanced oxidation and the reduction processes allows the in-situ regeneration of the electrode surface. Applying MPA technique improved significantly the detection performance of the electrode for PCP detection, especial at low potential value, very desired for practical applications. These working conditions for applying MPA led to very good sensitivities, the sensitivity recorded at +1 V/SCE is better that the one reached by DPV. The best limit of detection (0.114 μM, see Table 10.4) was achieved under this technique, which can be regarded very suitable for the practical application. Also, it must be underlined that these working conditions allowed reaching very good electroanalytical parameters at a low potential value, similar with those obtained at high potential.

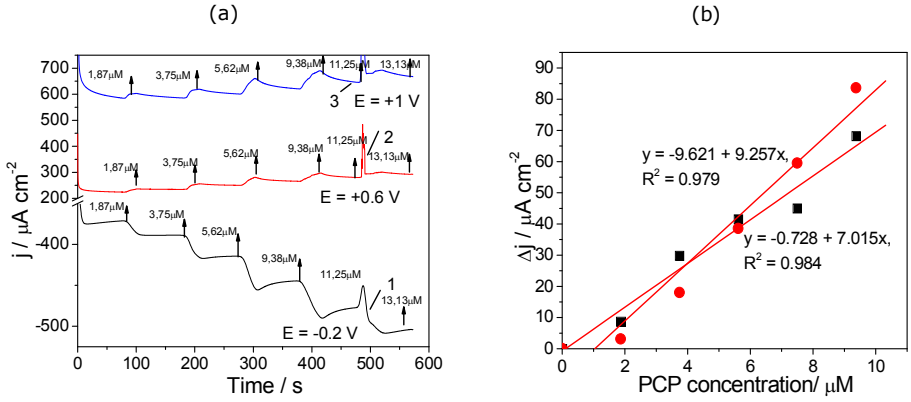

Figure 10.16 (a) Multiple-pulsed amperograms recorded at CNF- EG-Epoxy electrode in 0.1 M Na_2SO_4 supporting electrolyte and in the presence of different PCP concentrations: 1.87 μM, 3.75 μM, 5.62 μM, 7.5 μM, 9.38 μM, 11.25 μM, 13.13 μM, recorded at 1- E = -0.2 V/SCE, 2- E = +0.6 V/SCE, and 3- E = +1.0 V/SCE; (b) The calibration plots of the currents densities vs. PCP concentrations recorded at the detection potential: 1- E = +0.6 V, 2- E = +1 V/SCE.

All electroanalytical parameters obtained by applying CNF-EG-Epoxy composite electrode CV, DPV, CA and MPA are gathered in Table 10.4 and the best electroanalytical performance was achieved using pulsed techniques, as differential pulsed voltammetry and multiple-pulsed amperometry.

CNF reinforcement within epoxy matrix by replacement of 50 % EG enhanced significantly the electrocatalytic effect towards PCP oxidation, and it is more suitable for amperometric detection application in comparison with EG-Epoxy composite electrode.

Table 10.4 The electroanalytical parameters of amperometric detection of PCP at CNF-EG-Epoxy composite electrode using electrochemical techniques

Technique	Potential value V / SCE	Sensitivity μA / μMcm^2	Correlation coefficient, R^2	Relative standard deviation, RSD, %	The lowest limit of detection, LOD/μM	Limit of quantification LQ/μM
CV	+0.6	1.842	0.972	1.375	0.51	1.7
	+0.78	4.111	0.946	1.259	0.346	0.153
DPV	+0.63	8.066	0.948	0.398	0.125	0.417
CA	+0.8	1.150	0.956	2.141	0.552	1.841
	+1.1	5.249	0.992	1.378	0.158	0.529
MPA	+0.8	7.015	0.984	0.207	0.202	0.673
	+1.2	9.257	0.979	0.059	0.114	0.381

10.3.3. CNT-Epoxy composite electrode

Even if CNFs exhibit the economic advantage, CNTs are characterized by fewer defects and their properties are better. Due to the extraordinary properties of CNTs, they can be used in sensors, detectors and other devices. The development of such smart nanoscale materials, which can detect, convert, process, has the potential of revolutionizing the sensors industry. CNT-Epoxy composite electrode with 20 % wt. CNTs, was tested in order to get improved electroanalytical performance for PCP detection. The working conditions for each electrochemical technique used in this study were established for CNT-Epoxy composite electrode with 25 % wt. CNTs by our group and previously published [24].

10.3.3.1. Voltammetric measurements

The electrocatalytic behaviour of CNTs in 0.1 M Na_2SO_4 supporting electrolyte is evidenced from CVs recorded comparatively at the three carbon-based composite electrodes, *e.g.*, EG-Epoxy, CNF-EG-Epoxy and CNT-Epoxy electrodes (see Figure 10.17). A very large background current corresponding to the capacitive effect is noticed at CNT-Epoxy composite electrode. Also, the oxygen evolution occurred at the lower potential in comparison with the other carbon-based composite electrode. These aspects are characteristics to the electrocatalytic electrode materials.

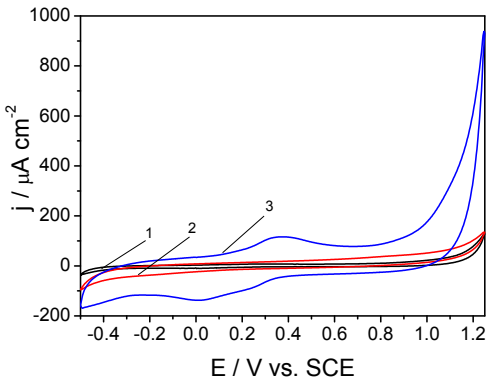

Figure 10.17 Cyclic voltammograms recorded in 0.1 M Na_2SO_4 supporting electrolyte at: EG-Epoxy electrode (curve 1), CNF-EG-Epoxy electrode (curve 2) and CNT-Epoxy electrode (curve 3).

Figure 10.18 shows the CVs recorded on CNT-Epoxy composite electrode in the presence of various concentrations of PCP at the scan rate of 0.05 Vs^{-1}. Even if the oxidation process of PCP starts at about 0 V vs. SCE, the highest defined current peak is recorded at +0.96 V/SCE, which increased linearly with PCP concentration. In general, a proportional increase of anodic current with concentration gives information about the possibility of controlled oxidation process by mass transfer [25], aspect desired in amperometric/voltammetric detection application. As we mentioned before, the oxidation process of phenols on carbon based electrodes is a

very complex process. It was reported that during the anodic oxidation of PCP at lower potentials, the reaction products became complex and an chain reaction polymerization took place leading to the electrode fouling, while at higher potentials the reaction product quickly couple and forming the oligomer products of oxidation process on their surface [1, 26]. This aspect was proven by decreasing the current corresponding to anodic oxidation peaks recorded at +0.96 V/SCE after repeating the cyclic voltammetry scanning, while the anodic current within the potential range between 0 and +0.6 V/SCE increased slightly. No significant effect on the cathodic current was noticed under these conditions. The electrode surface was renewed by easy mechanical polishing, washing and electrochemical treatment by cyclic voltammetry scanning between -0.5 and +1.25 V/ SCE in 0.1 M Na_2SO_4 supporting electrolyte [27].

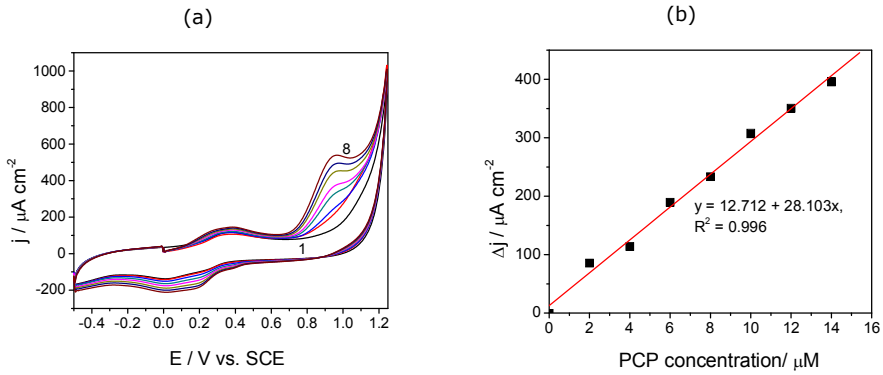

Figure 10.18 (a) Cyclic voltammograms at CNT-Epoxy electrode in 0.1 M Na_2SO_4 supporting electrolyte (1) and in the presence of 2, 4, 6, 8, 10, 12, 14μM PCP (curves 2- 8); potential scan rate: 0.05 Vs^{-1}; potential range: -0.5 to +1.25 V/SCE. (b) Calibration plot of the densities of the currents recorded at E= +0.96 V/SCE vs. pentachlorophenol concentration.

Further experiments were performed to study deeply some mechanistic aspects of the overall oxidation process of PCP on the CNT-Epoxy composite electrode surface. The evolution of CVs recorded on CNT-Epoxy composite electrode at various scan rates (0.01 – 0.2 Vs^{-1}) in the presence of 8 μM PCP was investigated (Figures 10.19 a-c).

The linearity of the anodic oxidation peak current recorded at +0.96 V/SCE in the presence of pentachlorophenol with the square root of the scan rate (Figure 10.19 b, curve 2) suggested that the reaction is mass transfer controlled, and no zero intercepts suggested that adsorption steps and surface interactions were not negligible. Moreover, peak potential shifted towards positive potential when increasing v, indicates that the electro-oxidation process of pentachlorophenol is irreversible. Because the linear dependence of the peaks currents recorded at +0.315 V/SCE was found, the effect of the scan rate on the CV shape of CNT-Epoxy composite electrode in 0.1 M Na_2SO_4 supporting electrolyte and no presence of the PCP was investigated within the same scan rates (the results are not shown here). The similar shapes of CV were recorded except the oxidation peak recorded at +0.96 V/SCE, which was found only in the presence of PCP. This inform about the oxidation and reduction processes at the potential value of about +0.315 V/SCE and respective, +0.065 V/SCE of multi-walled carbon nanotubes in 0.1 M Na_2SO_4

supporting electrolyte. However, the differences were noticed on the slopes of the linear plots of both anodic and cathodic peak current and the square root of the scan rate (see Figs. 10.19 b and c). It can be seen from the values of the slopes that PCP presence favoured the diffusion process.

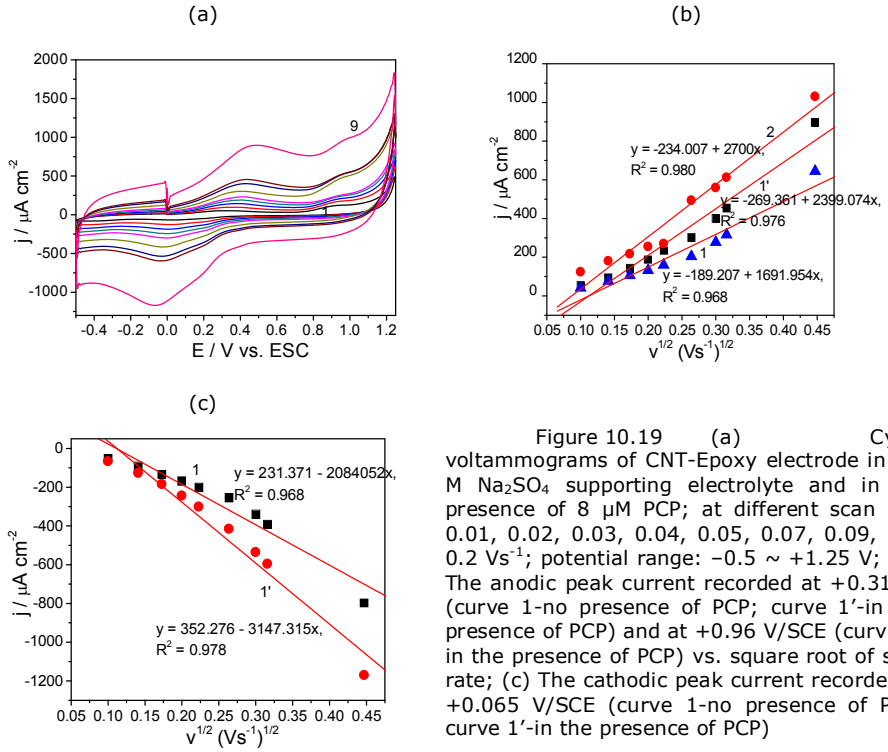

Figure 10.19 (a) Cyclic voltammograms of CNT-Epoxy electrode in 0.1 M Na_2SO_4 supporting electrolyte and in the presence of 8 μM PCP; at different scan rate 0.01, 0.02, 0.03, 0.04, 0.05, 0.07, 0.09, 0.1, 0.2 Vs^{-1}; potential range: −0.5 ~ +1.25 V; (b) The anodic peak current recorded at +0.315 V (curve 1-no presence of PCP; curve 1'-in the presence of PCP) and at +0.96 V/SCE (curve 2-in the presence of PCP) vs. square root of scan rate; (c) The cathodic peak current recorded at +0.065 V/SCE (curve 1-no presence of PCP; curve 1'-in the presence of PCP)

Analysis of the evolution of the linear-scan, differential-pulsed and square-wave voltammetric peak currents results presented in the next section for the detection measurements reveal that the oxidation peak current recorded at about +0.315V/SCE appeared in 0.1 M Na_2SO_4 supporting electrolyte and a non-linear dependence with the PCP concentration increasing was noticed. Also, the oxidation potential value shifted to the negative direction in the presence of PCP. These results suggest the selection of the potential value of +0.96 V/SCE for the detection utility.

Moreover, a corresponding analysis in square-wave voltammetry was performed by varying the frequency of the signal within the frequency range between 10 and 100 Hz at the same modulation amplitude of 0.1 V/SCE. No linear relationship between peak currents recorded at +0.96 V/SCE and the frequency was reached, which is a consequence of the specific properties of the surface processes [28].

10.3.3.2. Detection measurements

-Linear-scan voltammetry

Figure 10.20 shows linear-scan voltammograms recorded at CNT-Epoxy composite electrode in the presence of different PCP concentrations ranged between 2 and 16 μM. During the scanning from 0 to +1.25 V vs. SCE, the anodic oxidation current recorded at the potential value of +0.98 V vs. SCE increased with the PCP concentration, and a linear dependence of the current peak height vs. PCP concentration was reached.

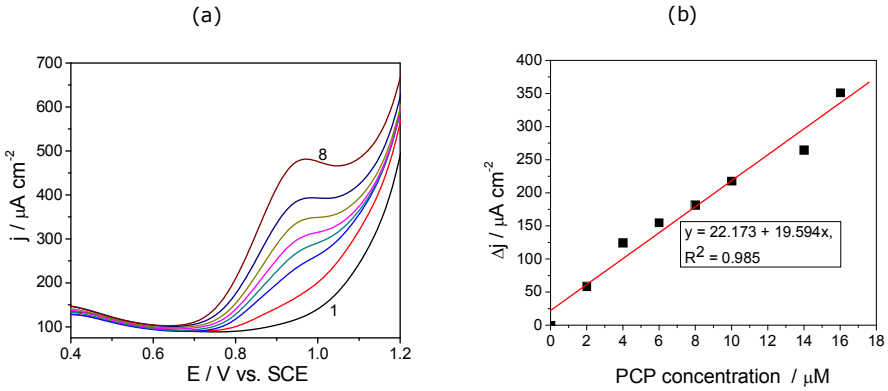

Figure 10.20 (a) Linear-scan voltammograms recorded at CNT-Epoxy electrode in 0.1 M Na_2SO_4 supporting electrolyte (1) and in the presence of different PCP concentrations: 2- 2 μM, 3- 4 μM, 4- 6 μM, 5- 8 μM, 6- 10 μM, 7- 14 μM, 8- 16 μM; potential scan rate:0.05 Vs^{-1}; potential range: -0.5 to +1.25 V/SCE; (b) Calibration plots of the current of the densities recorded at E= +0.98 V/SCE vs. pentachlorophenol concentrations.

-Differential-pulsed voltammetry

Differential-pulsed voltammetry, the technique that achieves a minimization of the effects of background noise, in particular of the brought the capacitive current, allowing the improvement the useful signal, and consequently to enhance the electroanalytical performance for PCP detection with CNT-Epoxy composite electrode was also tested.

Based on the results obtained for different operating conditions (the results are not shown here), the best results were achieved under the conditions of step potential of 0.01 and 0.02 V and modulation amplitude of 0.1 and 0.2 V.

Thus, the DPV performance of PCP oxidation at the CNT-Epoxy composite electrode was investigated in the potential range between 0 and 1.25 V/SCE, with modulation amplitude of 0.1V, a step potential of 0.01V at different concentration of PCP, and the corresponding results are shown in Figure 10.21. Under these conditions, the well-defined anodic peak appears at around of +0.83 V/SCE and a linear relationship of anodic peak currents versus PCP concentration were reached.

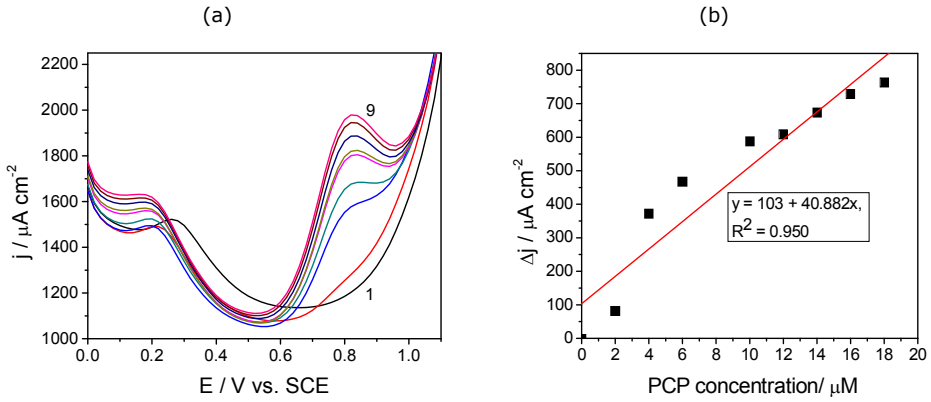

Figure 10.21 (a) Differential-pulsed voltammograms recorded CNT-Epoxy electrode with a 0.1V modulation amplitude, a 0.01V step potential and potential scan rate 0.05 Vs^{-1} between 0 and +1.25V vs. SCE in 0.1 M Na_2SO_4 supporting electrolyte (1) and in the presence of different PCP concentrations: 2- 2 μM, 3- 4 μM, 4- 6 μM, 5- 8 μM, 6- 10 μM, 7- 12 μM, 8- 14μM; (b) Calibration plots of the current densities recorded at E= +0.82 V/SCE vs. pentachlorophenol concentrations.

Better DPV results in relation with the sensitivity and the correlation coefficient were obtained under operating variables of 0.2 V modulation amplitude and 0.02 step potential (see Figure 10.22). These operating conditions are considered as optimum for DPV application.

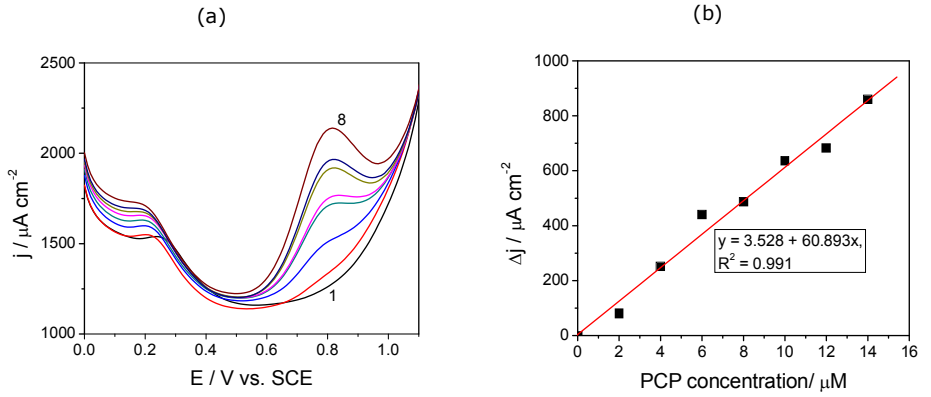

Figure 10.22 (a) Differential-pulsed voltammograms recorded CNT-Epoxy electrode with a 0.2V modulation amplitude, a 0.02V step potential and potential scan rate of 0.05 Vs^{-1} between 0 and +1.25V vs. SCE in 0.1 M Na_2SO_4 supporting electrolyte (1) and in the presence of different PCP concentrations: 2- 2 μM, 3- 4 μM, 4- 6 μM, 5- 8 μM, 6- 10 μM, 7- 12 μM, 8- 14μM; (b) Calibration plots of the current densities recorded at E= +0.82 V/SCE vs. pentachlorophenol concentrations.

The lower detection potential value and a better sensitivity were achieved using DPV in comparison with CV and LSV (see Table 10.5).

-Square-wave voltammetry

To provide data that could be compared with the DPV results, a square-wave voltammetric study of PCP electrochemical oxidation was performed. To achieve a more sensitive peak current, the optimum conditions in relation with the step potential, the modulation amplitude and the frequency were studied. Two values of step potentials, *i.e.*, 0.01 and 0.02 V were applied for the modulation amplitude of 0.1 V and the frequency of 10 Hz, and the results are presented in Figure 10.23 a-d. For both values of the step potential, the anodic peak current increased linearly with PCP concentrations, and the best results were achieved for the step potential of 0.01 V, which was selected as optimum.

Various modulation amplitude values ranged between 0.1-1 V/SCE were applied at the 0.01 step potential and the best peak shape was reached for the modulation amplitude of 0.1 V, selected as the optimum. Applying the modulation amplitude beyond 0.2 V the negative currents were reached.

The frequency was varied between 10 and 100 Hz. Although the current response corresponding to the PCP oxidation increased with frequency, the useful signal that represents the difference between current recorded in the presence of PCP and the current recorded only in supporting electrolyte (background current) decreased.

The best sensitivity and the lowest limit of detection were recorded under operating conditions of 0.1 V pulse amplitude, 0.01 steps potential and 10 Hz frequency, which were selected as optimum operating conditions using SWV voltammetry at CNT-Epoxy composite electrode.

In comparison with CV, LSV, and DPV, SWV technique operated under the optimum conditions allowed to achieve better electroanalytical performance regarding the sensitivity, the relative standard deviation, the lowest limit of detection and the limit of quantification of PCP on CNT-Epoxy composite electrode (Table 10.5).

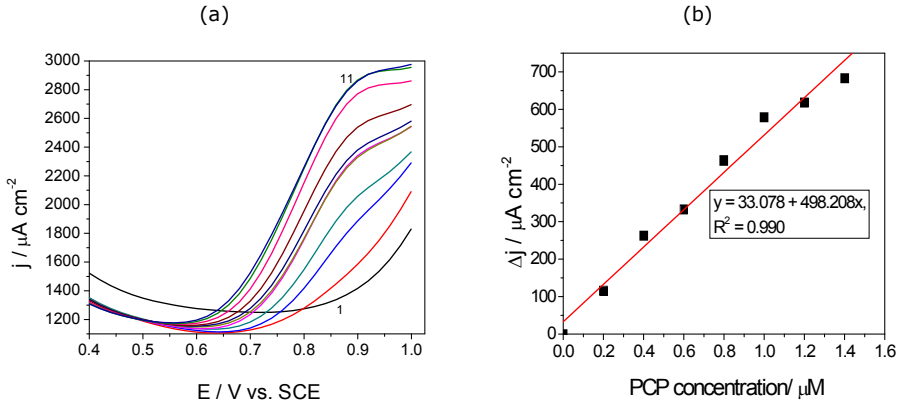

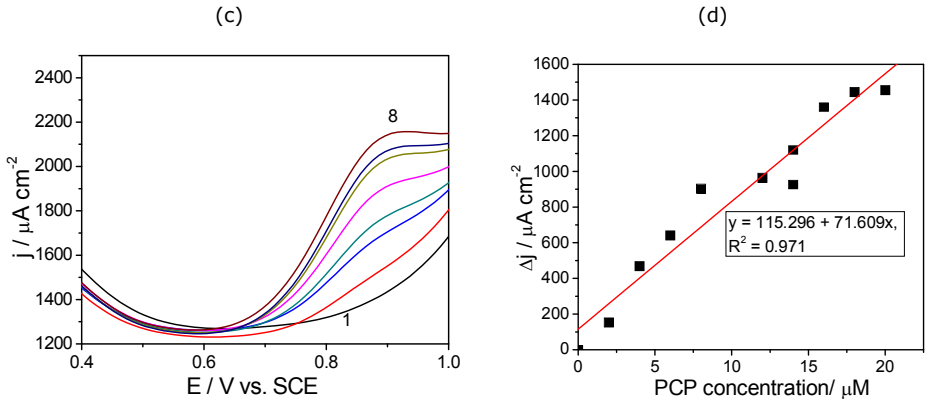

Figure 10.23 Square-wave voltammograms recorded at CNT-Epoxy composite electrode with a 0.1V modulation amplitude, 10 Hz frequency, potential scan rate of 0.05 Vs^{-1} between 0 and +1 V/SCE in 0.1 M Na_2SO_4 supporting electrolyte (curve 1) and in the presence of different PCP concentrations: 2-14 μM (curves 2-8) at the step potential: 0.01V (a) and 0.02 V (c) Calibration plots of the current densities recorded at E= +0.9 V/SCE vs. pentachlorophenol concentrations for step potential of 0.01 V (b) and 0.02 V (d)

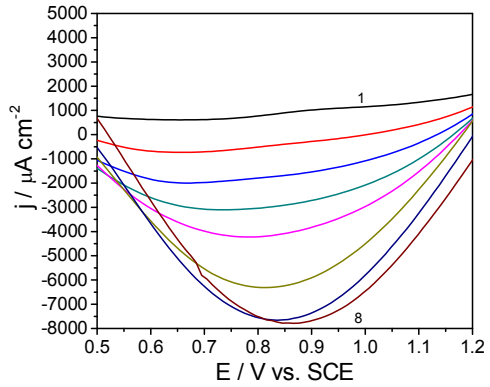

Figure 10.24 Square-wave voltammograms recorded at CNT-Epoxy electrode with a 0.01V step potential, 10 Hz frequency in 0.1 M Na_2SO_4 supporting electrolyte and 8 μM PCP at different modulation amplitudes: 0.5 - 1.2 V.

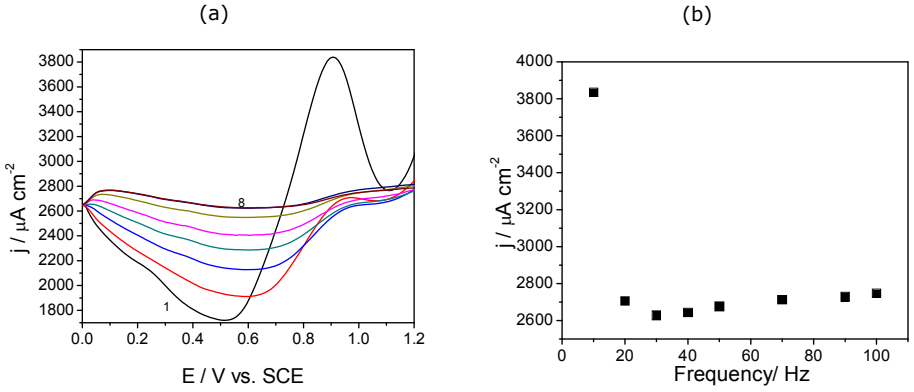

Figure 10.25 (a) Square-wave voltammograms recorded at CNT-Epoxy electrode with a 0.01V step potential, 0.1 modulation amplitude in 0.1 M Na_2SO_4 supporting electrolyte and 8 μM PCP at different frequencies: 10 - 100 Hz; (b) The peak of the current densities recorded at +0.9 V/SCE vs. frequency.

-Chronoamperometry and multiple-pulsed amperometry

Based on the voltammetric results, the chronoamperometry technique used for detection and with the practical utility potential was applied at +0.9 V/SCE detection potential values. The amperometric response of the CNT-Epoxy composite electrode obtained for successive and continuous addition of 2 μM PCP to 0.1 M Na_2SO_4 supporting electrolyte solution under batch system analysis is shown in Figure 10.26 a. The calibration plots of current vs. PCP concentration was linear over the concentration ranged from 2μM and 14 μM (Figure 10.26 b), and the electroanalytical parameters obtained by this technique are gathered in Table 10.5. This detection method exhibited the worse sensitivity compared to other techniques used, probably due to electrode fouling occurred.

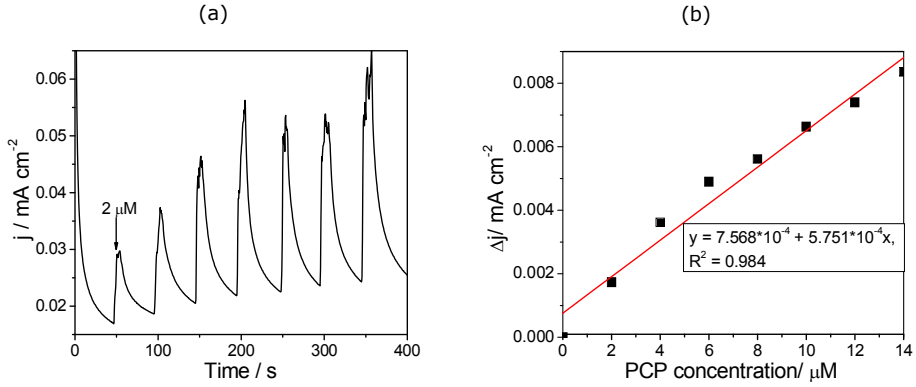

Figure 10.26 10.26 (a) Chronoamperograms recorded at CNT-Epoxy electrode in 0.1 M Na_2SO_4 supporting electrolyte and in the presence of different PCP concentrations:, 2, 4, 6, 8, 10, 12, 14 μM, recorded at E=+0.96 V/SCE; (b) The calibration plots of the current densities vs. PCP concentrations.

The use of MPA as an alternative to the amperometric detection for the in-situ cleaning of the electrode surface during the detection process and to improve the sensitivity, was applied also for this electrode. Thus, in Figure 10.27 the results of multiple-pulsed amperograms (MPAs) recorded at CNT -Epoxy composite electrode at the three detection potentials are presented. The pulses were applied continuously using the following scheme:

a) -0.1 V/SCE for a duration of 0.05 ms, where a reduction process occurred,

b) +0.96 V/SCE for a duration of 0.05 ms, where PCP oxidation occurred without oxygen evolution,

c) +1.25 V/SCE for duration of 0.05 ms, with oxygen evolution involving, that assures an advanced oxidation process that allows the reactivation of the electrode surface. These working conditions for MPA applying were chosen for comparison with CA results, and taking into account CV results. MPA applying led to both cathodic and anodic amperometric responses (no cathodic response is shown here).

Due to a linear dependence of cathodic responses versus PCP concentration was reached and this potential value could be used for an indirect detection based on the reduction of the oxidation product of PCP. However, at this potential value no calibration was determined because of cathodic response, and it was used only for the electrode surface reactivation during the detection.

At the two positive potential value of +0.96 and +1.25 V/SCE the linear dependences of current versus PCP concentration were reached. Even if a better sensitivity is reached at +1.25 V/SCE, for real practical utility this potential value is not suitable because of the possible interference potential, due to the high oxidation potential.

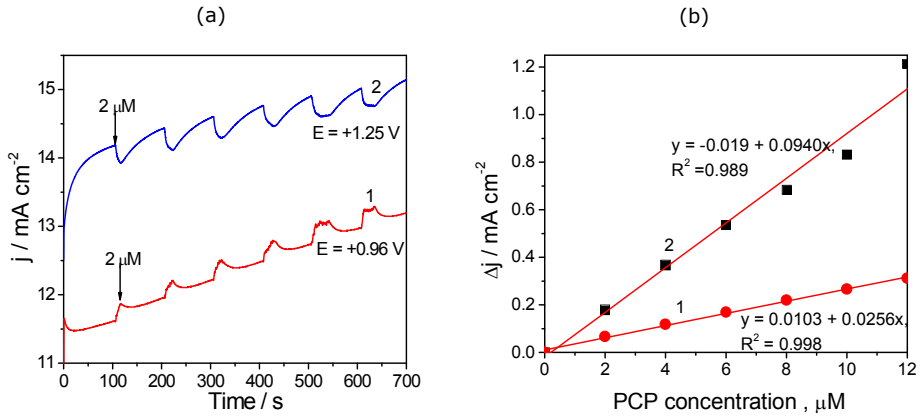

Figure 10.27 (a) Multiple-pulsed amperograms recorded at CNT-Epoxy electrode in 0.1 M Na_2SO_4 supporting electrolyte and and in the presence of different PCP concentrations: 2, 4, 6, 8, 10, 12, 14μM, recorded at: 1- E = +1.25 V/ SCE, 2- E = +0.96 V/SCE; The calibration plots of the current densities vs. PCP concentrations at both selected potentials.

All electroanalytical parameters obtained for PCP detection on CNT-Epoxy composite electrode using CV, LSV, DPV, SWV, CA and MPA are gathered in Table 10.5 and the best electroanalytical performance was achieved using square-wave voltammetry.

Table 10.5 The electroanalytical parameters of amperometric detection of PCP at a CNT-Epoxy composite electrode using electrochemical techniques

Technique	Potential value V / SCE	Sensitivity mA / μM cm^{-2}	Correlation coefficient, R^2	Relative standard deviation, RSD, %	The lowest limit of detection, LOD/μM	Limit of quantification/μM
CV	+0.96	0.0281	0.987	0.175	0.023	0.079
LSV	+0.98	0.0195	0.985	0.805	0.162	0.540
DPV	+0.83	0.040	0.950	0.983	0.159	0.530
CA	+0.96	$5.751 \cdot 10^{-4}$	0.984	0.938	0.809	2.698
MPA	+1.25	0.094	0.989	0.349	1.456	4.854
	+0.96	0.0256	0.998	0.146	0.373	1.245
SWV	0.92	0.498	0.990	0.042	0.003	0.012

A recovery test was performed by analyzing three parallel tap water samples, which contain 0.5 $mg \cdot dm^{-3}$ PCP. This test was run in 0.1 M Na_2SO_4 supporting electrolyte and a recovery of 97 % was found with a RSD of 0.9 % using SWV under optimized conditions. Finally, the results obtained by this method were compared with that obtained by means of a UV-VIS spectrophotometric method, and can be concluded that the results obtained by the two methods are very closely and the accuracy of the proposed voltammetric method is excellent.

The most representative comparative results regarding PCP detection at carbon-based composite electrode using the electrochemical technique regarding the best results in relation with the lowest detection potential value, the sensitivity, the lowest limit of detection and the lowest limit of quantification are presented in Table 10.6**.**

Table 10.6 The comparative electroanalytical parameters of amperometric detection of PCP at carbon-based composite electrode using electrochemical techniques

Electrode type	Technique	Potential value V / SCE	Sensitivity μA / μM cm^{-2}	Correlation coefficient, R^2	Relative standard deviation , RSD, %	The lowest limit of detection, LOD/μM	Limit of quantification, LQ/μM
EG-Epoxy	CV	-0.2	0.394	0.994	11.808	1.335	4.451
		+0.68	0.592	0.952	2.717	1.447	3.491
		+1.0	2.560	0.985	1.538	0.426	1.421
	DPV	-0.2	17.90	0.981	4.015	0.218	0.726
		+0.6	2.580	0.992	1.723	1.097	3.658
		+1.0	5.800	0.980	0.900	1.920	7.067
	CA	+0.6	0.215	0.910	2.412	1.088	3.627
CNF-EG-Epoxy	CV	+0.5	1.842	0.972	1.375	0.510	1.700
		+0.78	4.111	0.946	1.259	0.346	0.153
	DPV	+0.63	8.066	0.948	0.398	0.125	0.417
	CA	+0.8	1.150	0.956	2.141	0.552	1.841
		+1.1	5.249	0.992	1.378	0.158	0.529
	MPA	+0.8	7.015	0.984	0.207	0.202	0.673
		+1.2	9.257	0.979	0.059	0.114	0.381
CNT-Epoxy	CV	+0.96	28.103	0.987	0.174	0.023	0.079
	DPV	+0.82	60.893	0.991	0.068	0.061	0.203
	SWV	0.92	498.208	0.990	0.079	0.007	0.023

CA	+0.96	0.575	0.984	0.925	0.798	2.660
MPA	+0.96	94.023	0.989	0.068	0.047	0.157
	+1.25	25.601	0.998	0.032	0.502	1.675

Based on the presented results, the detection scheme for PCP determination could be proposed in direct relation to the best electroanalytical parameters achieved for each electrode using a specific technique.

EG-Epoxy composite electrode, the detection potential value of -0.2 V/SCE recorded by DPV application under operating parameters of modulation amplitude of 0.2 V, a step potential of 0.01 V, potential range: -0.5 to +1.25 V/SCE.

CNF-EG-Epoxy composite electrode, the detection potential value of +0.8 V/SCE and +1.1 V/SCE recorded by CA application. Also, MPA applying under operating parameters of +0.8 V/SCE for duration of 0.05 ms, and +1.1 V/SCE for duration of 0.05 ms.

CNT-Epoxy composite electrode, the detection potential value of 0.92 V/SCE recorded by SWV application under operating parameters of modulation amplitude of 0.1 V, a step potential of 0.02 V, a frequency of 10 Hz, potential range: 0 to +1.0 V/SCE. Also by MPA application under operating parameters of +0.96 V/SCE for duration of 0.05 ms, and +1.25 V/SCE for duration of 0.05 ms.

10.4. Partial conclusions

All tested electrodes, *i.e.,* EG-Epoxy, CNF-EG-Epoxy and CNF-Epoxy composite electrodes exhibited the availability for the direct anodic oxidation of pentachlorophenol (PCP), giving them a real potential for the amperometric/voltammetric detection of PCP.

Even if several characteristics regarding the direct electrooxidation of pentachlorophenol are common for all carbon-based composite electrodes, specific peculiarities linked to carbon structure gave them different performances for PCP detection.

The electrode performance for PCP detection in relation with the sensitivities increased as: CNT-Epoxy > CNF-EG-Epoxy > EG-Epoxy. Also the best limit of detection and quantification were achieved for CNT-Epoxy electrode.

However, the detection potential value of -0.2 V/SCE determined for EG-Epoxy is very promising for practical application for selective determination of PCP from aqueous solution by voltammetric technique. This detection potential value was found only for EG-Epoxy electrode based on the PCP anodic oxidation peak that increased linearly with its concentration. This detection potential value did not appear due to the electrode electrocatalytic activity, but the electrode surface modification during PCP electrooxidation process. The electrode surface modification is not desired during the detection process, but in this case it was exploited in a positive way envisaging the selective detection of PCP.

The replacement of a part of EG with CNF improved slightly sensitivity and the lowest limit of detection and quantification, while the full replacement of EG with CNT enhanced the electroanalytical parameters for PCP detection.

The exploitation of pulsed voltammetric / amperometric techniques allowed enhancing the electroanalytical parameters for PCP detection.

Nanostructured carbon reinforcement within the composite composition exhibited the enhanced electrocatalytic activity only by background and useful signal improvement and not by shifting the oxidation potential to lower potential values.

The selection of the electrode type, the electrochemical technique, and the operating conditions will be made taking into account the specific requirements imposed by the practical utility.

10.5. References:

[1] M. Gattrell, B. MacDougall, J. Electrochem. Soc. 146 (1999) 3335.
[2] R.E. Apreutesei, C. Catrinescu, C. Teodosiu, Environ. Eng. Manag. J. 8 (2009) 651.
[3] G. Barjoveanu, C. Teodosiu, Environ. Eng. Manag. J 8 (2009) 277.
[4] A. Bebeselea, C. Proca, F. Manea, C. Radovan, G. Burtica, J. Schoonman, Environ. Eng. Manag. J 8 (2009) 817.
[5] Y. Wu, Sensor Actuat. B-Chem 137 (2009) 180.
[6] J.M. Diserents, J. AOAC Int. 84 (2001) 853.
[7] W. Fischer, O. Bund, H.E. Hauck, Fresen. J. Anal. Chem. 354 (1996) 889.
[8] Y.G. Leblance, R. Gilbert, J. Hubert, Anal. Chem. 71 (1999) 78.
[9] C. Mardones, J. Palma, C. Sepulveda, A. Berg, D. von Baer, J. Sep. Sci. 26 (2003) 923.
[10] A.A. Mufeed, H.J. Harmon, Biosens. Bioelectron. 20 (2005) 1595.
[11] M.N. Abbas, G.A.E. Mostafa, A.M.A. Homoda, Talanta 55 (2001) 647.
[12] M.A.R .Barrio, J.M.P. Carrazón, Fresen J. Anal. Chem. 344 (1992) 34.
[13] L. Codognoto, V.G. Zuin, D. de Souza, J.H. Yariwake, S.A.S. Machado, L.A. Avaca, Microchem. J. 77 (2004) 177.
[14] E.C. Guijarro, P. Yanez-Sedeno, J.M.P. Carrazon, L.M.P. Díez, Analyst 113 (1998) 625.
[15] T. Spataru, N. Spataru, J. Hazard. Mater. 180 (2010) 777.
[16] W. Lu, G.G. Wallace, M.D. Imisides, Electroanal. 14 (2002) 325.
[17] P. Canizares, J. Garcia-Gomez, C. Saez, M.A. Rodrigo, J. Appl. Electrochem. 33 (2003) 917.
[18] C. Terashima, T.N. Rao, B.V. Sarada, D.A. Tryk, A. Fujishima, Anal. Chem. 74 (2002) 895.
[19] F. Liu, G. He, M. Zhao, M. Qu, L. Huang, The Open Mater. Sci. J. 5 (2011) 35.
[20] L. Codognoto, S.A.S. Machado, L.A. Avaca, J. Appl. Electrochem. 33 (2003) 951.
[21] B.M. Keith, S. Coralie, H.T.L. John, Anal. Chem. 70 (1998) 4134.
[22] A. Bebeselea, F. Manea, G. Burtica, L. Nagy, G. Nagy, Talanta, 80 (2010) 1068.
[23] M. Pumera, A. Merkoci, S. Alegret, Sensor. Actuat. B-Chem 113 (2006) 617.
[24] A. Remes , A. Pop, Florica Manea, **A. Baciu**, S.J. Picken, J Schoonman, Sensor. 12 (2012) 7033.
[25] S. Ramirez-Garcia, S. Alegret, F. Cespeses, R.J. Forest, Analyst 127 (2002) 1512 .
[26] O.M. Azzam, M. Al-Tarazi, Y. Tahboub, J. Hazard. Mater. B 75 (2000) 99.
[27] M.S. Ureta-Zanartu, P. Bustos, C. Berrios, M.C. Diez, M.L. Mora, C. Gutierrez, Electrochim. Acta 47 (2002) 2399.
[28] B. Nigovic, Anal. Bioanal. Chem. 384 (2006) 431.

CHAPTER 11. ELECTROCHEMICAL DETECTION OF ARSENIC (III) USING NANOSTRUCTURED CARBON -BASED COMPOSITE ELECTRODES

11.1. Introduction

Arsenic (As) is a common trace element characterized by high toxic properties and as consequence, it exhibits a very negative impact on the human health. The main pathway of human exposure to arsenic is drinking water, especially provided by the groundwater. The main inorganic species presented in water are arsenate ion (As^{V}) and arsenite ion (As^{III}, H_2AsO_4 or $HAsO_4^-$). The presence of arsenite ion is favoured by reducing media, which are very common for drinking water. Also, this form is more soluble than the arsenate ion and approximately 50 times more toxic. The toxicity character of arsenic led to that the World Health Organization to impose 10 μgL^{-1} maximum allowable concentration of arsenic in drinking water [1, 2].

Several well-known analytical methods have been used for arsenic determination, *e.g.*, chemiluminescence [3], chromatography [4, 5], spectroscopic methods [6, 7]. These methods are expensive and require certain skills for operating [8-10].

The electrochemical methods for arsenic detection have been attracted considerable attention due their simplicity, rapidity and high sensitivity. In addition, these methods are very suitable for *in-field* determination.

Most electrochemical methods involve anodic stripping voltammetry (ASV), which suppose two steps: first corresponding to reduction of arsenic (III) at the electrode surface for a certain time followed by the second step of electrochemically stripping from the electrode surface resulting a faradic response that is direct proportionally with arsenic concentration. The processes corresponding to these steps can be schematically represented by:

Step 1-Deposition: $As^{3+}+3e^-\rightarrow As^0$

Step2-Anodic stripping: $As^0 \rightarrow As^{3+}+3e^-$

Over 50 years ago, it was studied for the first time the electrochemical detection of arsenic by stripping voltammetry at mercury electrodes, but their practical application is limited by the mercury toxicity. This is the reason for which the mercury-free voltammetric methods have received a growing interest.

Unmodified electrode like bare carbon, gold, and platinum, silver have been used as possible alternative to arsenic detection instead of mercury based electrodes [11-14]. Starting with 1990s, the carbon-based composite electrodes involving different polymer matrices were reported for the first time as amperometric sensors by Wang [15]. These materials exhibit very attractive electrochemical, physical, mechanical and economical features compared with classic conductors.

Carbon nanotubes and carbon nanofibers reinforced within the polymeric matrix (*e.g.*, resin) enhance the composite properties due to the unique electrocatalytic, electrical and mechanical properties of nanotructured carbon-based composite.

Carbon nanotubes-based electrodes have been reported for anodic stripping voltammetric detection method for various heavy metals determination [16-21]. A variant to the carbon-based electrodes that do no exhibit electrocatalytic effect towards target analyte or to improve its performance is chemically modifying the carbon substrate. An alternative approach is to support or decorate the metal nanoparticles on the carbon nanotubes and nanofibers for electroanalysis application.

Also, metal-doped zeolite modified electrode have been reported to enhance the detection performance [22-24].

Several electrochemical methods involving metal nanoparticles supported by carbon-based electrodes have been reported for arsenic (III) detection [25-29].

11.2. Experimental

11.2.1. Reagents

Sodium arsenite was purchased from Merck. An aqueous 0.01 mM stock solution was prepared daily by dilution the aqueous $NaAsO_2$ in double distillate water. Supporting electrolyte for the characterization and application of electrode material in detection process was 0.09 M Na_2SO_4 + 0.01 M H_2SO_4 solution, which was freshly prepared from Na_2SO_4 and H_2SO_4 of analytical purity (Merck) with distillate water.

11.2.2. Working electrodes

The nanostructured carbon-based composite working electrodes used for the detection of arsenic (III) are gathered in Table 11.1.

Table 11.1 Nanostructured carbon-based composite working electrode tested for the electrochemical detection of As (III).

Nanostructured carbon-based composite electrode	Geometrical area/cm^2	Electroactive surface area/cm^2
CNT-Epoxy	0.196	0.473
CNF-Epoxy	0.196	0.352
CNT-ZAAg-Epoxy	0.196	0.372
CNT-ZNAg-Epoxy	0.196	0.411
CNF-ZNAg-Epoxy	0.196	0.313
CNF-Ag	0.196	0.346

11.2.3. Apparatus and procedures

The electrochemical performances of the nanostructured carbon-based composite electrodes were studied by cyclic voltammetry (CV), differential-pulsed voltammetry (DPV), square-wave voltammetry (SWV).Electrochemical measurements were performed in unstirred solutions using a computer controlled Autolab potentiostat/galvanostat PGSTAT 302 (EcoChemie, The Netherlands), with a

standard three electrodes configuration. The three-electrode system consisted of a carbon-based composite working electrode, a platinum wire as counter electrode and a saturated calomel reference electrode (SCE). Before each voltammogram, each composite electrode was carefully polished with abrasive paper and then on a felt-polishing pad by using 0.3 μm alumina powder (Metrohm, Switzerland). All experiments were carried out with a typical cell of 50 mL at room temperature (25°C).

11.3. Results and discussion

11.3.1. Preliminary results regarding arsenic (III) electrochemical behavior on nanostructured carbon-based composite electrodes

The electrochemical behaviour of arsenic (III) on carbon nanotubes epoxy (CNT-Epoxy), carbon nanofiber epoxy (CNF-Epoxy), silver-doped synthetic zeolite-modified carbon nanotubes-epoxy (CNT-ZAAg-Epoxy), silver-doped natural zeolite-modified carbon nanotubes-epoxy (CNT-ZNAg-Epoxy), silver-doped natural zeolite-modified carbon nanofibers-epoxy (CNF-ZNAg-Epoxy), and silver-chemically decorated carbon nanotubes (CNF-Ag) was studied by cyclic voltammetry (CV) taking into account the deposition step of arsenic (III) on the electrode surface by applying a preconditioning level before CV running. No response to the arsenic (III) presence was noticed on the cyclic voltammogram recorded without preconditioning step (The results are not shown here).

Taking into account the principle of the anodic stripping voltammetry, which imposed a preconditioning step for arsenic deposition on the electrode surface by its reduction process, the optimization of the deposition potential and time is required. For 3 mM As (III), the deposition potential was varied from -1 to -0.25 V/SCE at CNT-ZAAg-Epoxy composite electrode. Useful signals corresponding to the arsenic stripping process determined as the difference between the arsenic anodic stripping peak current and the background current, for each potential value at 60 seconds deposition time are presented in Figure 11.1a. The lowest useful signal was recorded for the deposition potential of -0.25 V/SCE, at which arsenic (III) reduction process just started and the maximum signal was reached for the potential of -0.4 V/SCE, corresponding to the reduction process peak, in according with CV results (Figure 11.2). More negative potential applying lead to useful signal reducing, due to hydrogen evolution that hampered the arsenic deposition through the bubble formation at the electrode surface. From these data, the optimum deposition potential of -0.4 V/SCE was chosen for the subsequent anodic stripping voltammetry experiments. In addition, the deposition time was varied between 5 and 180 minutes to select the optimum one based on the useful response for arsenic detection. From Figure 11.1b, the optimum deposition time is 120 seconds.

The optimum operating conditions for the deposition step prior to the all anodic stripping voltammetric experiments are the deposition potential of -0.4 V/SCE for the deposition time of 120 seconds.

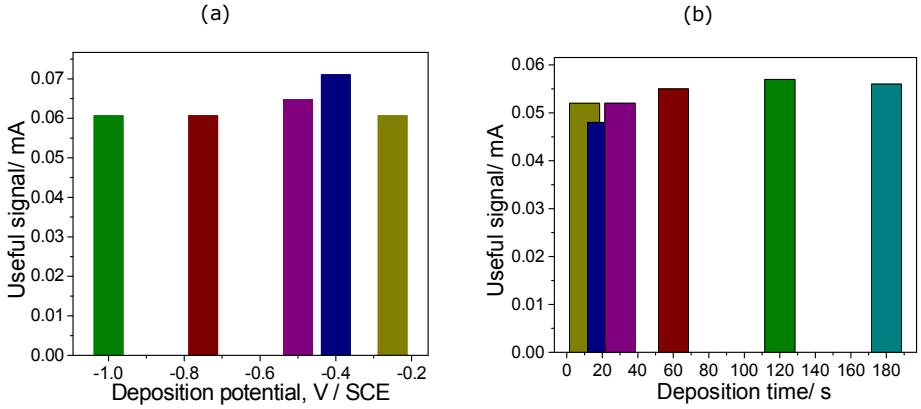

Figure 11.1 Useful signal corresponding to the 3 mM arsenic (III) anodic stripping peak recorded by CV at CNT-ZAAg-Epoxy in 0.09 M Na_2SO_4 + 0.01 M H_2SO_4 supporting electrolyte (curve 1) at: 60 seconds deposition time at various deposition potentials (a); -0.4 V deposition potential at various deposition time (b); potential scan rate: 0.05 Vs^{-1} .

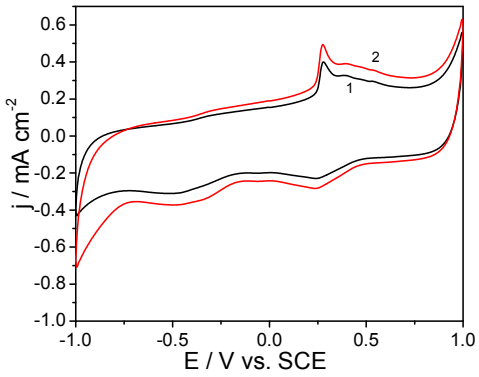

Figure 11.2 Cyclic voltammograms at CNT–ZAAg-Epoxy composite electrode in 0.09 M Na_2SO_4 and 0.01 M H_2SO_4 supporting electrolyte (1) and in the presence of 0.005 mM As (curves 2); potential scan rate: 0.05 Vs^{-1}; potential range: -1.0 to +1.0 V/SCE.

Figures 11.3 (a-f) show CVs recorded in 0.09 M Na_2SO_4+0.01 M H_2SO_4 supporting electrolyte at CNT-Epoxy (a), CNF-Epoxy (b), CNT-ZNAg-Epoxy (c), CNT-ZAAg-Epoxy (d), CNF-ZNAg-Epoxy (e), CNF-Ag (f) electrodes, after the preconditioning step, by maintaining the working electrode at the potential value of -0.4 V/SCE for 120 seconds .

Based on CV results it can be seen that neither CNTs nor CNFs exhibited the electrocatalytic effect on the electroreduction / oxidation of arsenic, no oxidation peak corresponding to arsenic oxidation to arsenic (III) appeared. For the nanostructured carbon-based electrodes containing silver supported on synthetic / natural zeolite or direct on carbon surface, a peak corresponding to arsenic stripping from the electrode surface to arsenic (III) in supporting electrolyte is evidenced.

Generally, based on the literature data [30], the silver based electrodes exhibited an anodic peak corresponding to silver oxidation. This peak was not evidenced for CNF-ZNAg-Epoxy probably due to the electrode structure, and it was evidenced very slightly for CNT-ZNAg-Epoxy and CNF-Ag. This peak is most evidenced for CNT-ZAAg-Epoxy composite electrode. Even if for CNF-ZNAg-Epoxy silver oxidation peak could not be observed, the arsenic stripping peak appeared very clearly and it was increased with As (III) concentration. For the other silver containing nanostructured carbon-based electrodes the oxidation peak corresponding to arsenic stripping appeared before silver oxidation and influenced also, this last process. The peak current corresponding to silver oxidation increased with arsenic (III) concentrations. The calibration plots determined for the silver containing nanostructured based composite electrodes for As (III) anodic stripping peak currents versus its concentration showed a good linearity with good correlation coefficients (see Figures 11.4). CNT-based composite electrode allowed reaching better sensitivity in comparison with CNF-based composite electrodes, due to the improved electrocatalytical properties of CNTs. Also, the presence of synthetic zeolite led to improve the sensitivity for arsenic (III) detection.

All electroanalytical parameters determined for each electrode using CV technique are presented in Table 11.2. The best lowest limit of detection achieved for CNT-ZAAg-Epoxy composite electrode is not sufficient to be able to detect arsenic (III) concentrations at least equal to that imposed by legislation (10 µM).

Based on these results, the further experiments will be carried out for CNT-ZAAg-Epoxy composite electrode to enhance the performance for As (III) detection.

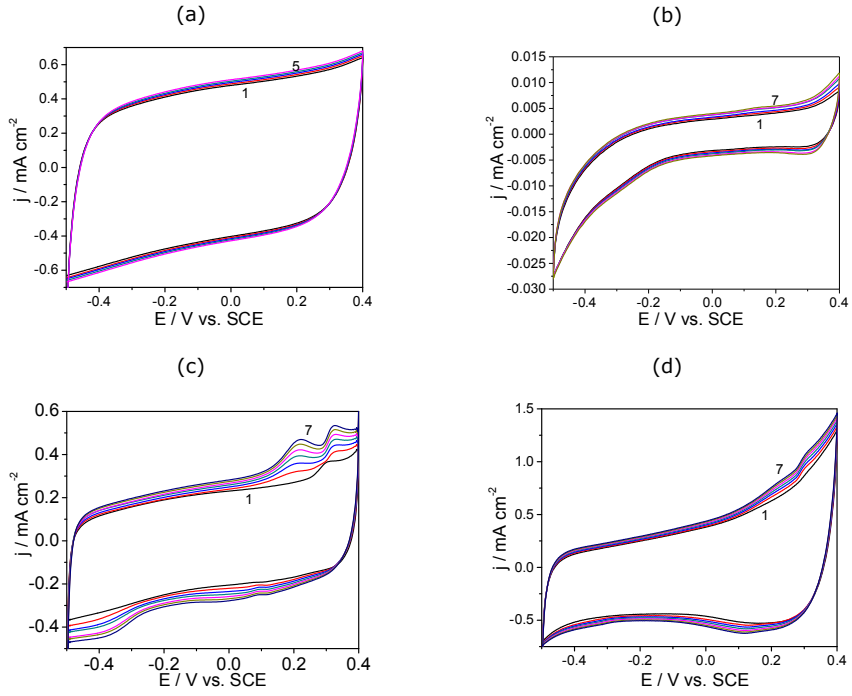

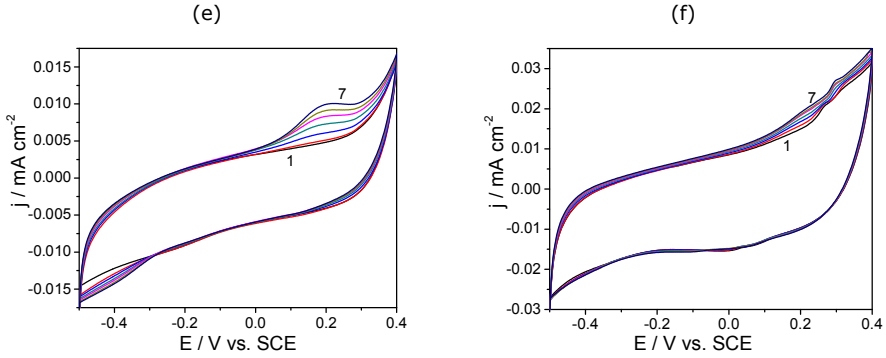

Figure 11.3 Cyclic voltammograms recorded in 0.09 M Na_2SO_4+0.01 M H_2SO_4 supporting electrolyte (curve 1) and in the presence of 1.0, 1.5, 2.0, 2.5, 3.0, 3.5 mM As (curves 2- 7) with a preconditioning of electrode at -0.4 V/SCE at deposition time of 120 s, potential scan rate: 0.05 Vs^{-1}, potential range: -0.5 to +0.4 V/SCE at the electrodes: CNT-Epoxy (a); CNF-Epoxy (b); CNT-ZAAg-Epoxy (c); CNT-ZNAg-Epoxy (d); CNF-ZNAg-Epoxy (e); CNF-Ag (f).

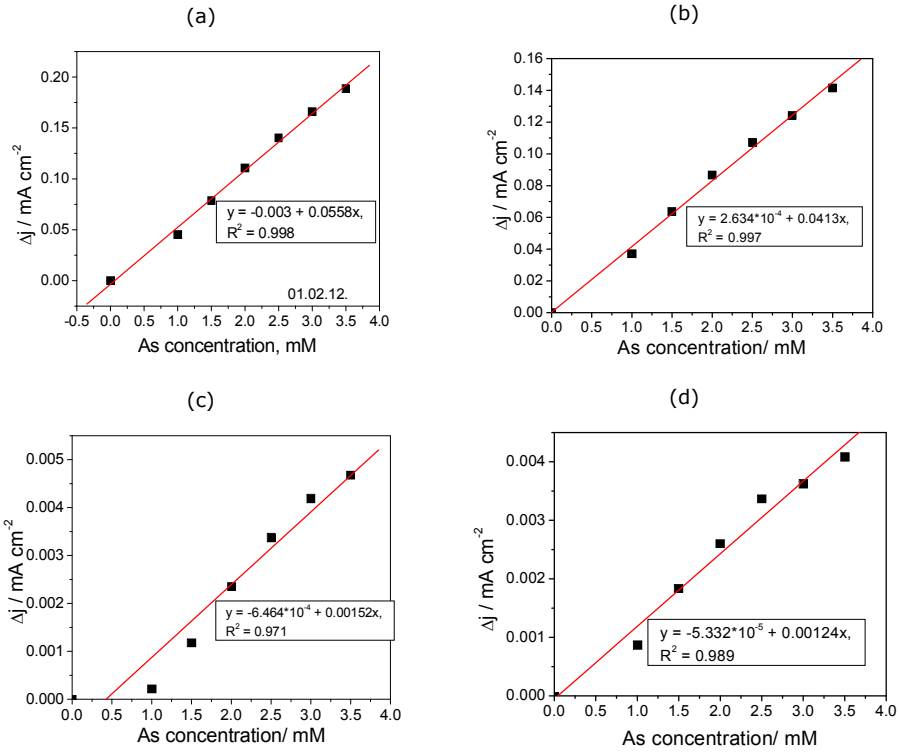

Figure 11.4 The calibration plots of the current densities corresponding to the arsenic anodic stripping peaks recorded at +0.2 V/SCE for: CNT-ZAAg-Epoxy (a); CNT-ZNAg-Epoxy (b); CNF-ZNAg-Epoxy (c); CNF-Ag (d) electrodes.

Table 11.2 The electroanalytical parameters determined for the stripping voltammetric detection of arsenic (III) at the nanostructured carbon based composite electrodes using cyclic voltammetry technique.

Electrode type	Potential value V/SCE	Sensitivity mA/mM cm^{-2}	Correlation coefficient, R^2	Relative standard deviation, RSD, %	The lowest limit of detection, LOD/mM	Limit of quantification, LQ/mM
CNT-Epoxy	-	-	-	-	-	-
CNF-Epoxy	-	-	-	-	-	-
CNT-ZAAg-Epoxy	0.22	0.0543	0.997	0.374	0.05	0.166
CNT-ZNAg-Epoxy	0.22	0.0402	0.997	2.107	0.0474	0.158
CNF-ZNAg-Epoxy	0.206	0.0016	0.979	0.509	0.918	3.061
CNF-Ag	0.2	0.0012	0.989	2.633	0.849	2.832

Some mechanistic aspects in relation with the electrochemical behaviour of arsenic (III) on CNT-ZAAg-Epoxy composite electrode were investigated by the effect of the scan rate on the cyclic voltammogram shapes. Figure 11.5 shows CVs recorded for 3 mM As (III) in 0.09 Na_2SO_4 + 0.01 H_2SO_4 supporting electrolyte at various scan rates (0.01 - 0.2 Vs^{-1}). The preconcentration step was applied before each the scan rate. The linear increase of current density corresponding to stripping anodic oxidation of arsenic to arsenic (III) with square root of the scan rate suggested a mass transfer controlled process (Figure 11.5b). Also, the current corresponding to the silver oxidation peak increased linearly with the scan rate, which informed that this process is diffusion-controlled. The peak potential shifted towards positive potential when increasing v (Figure 11.5c), but the presence of cathodic peak at -0.4 V/SCE corresponding to arsenic (III) reduction indicates the quasi-reversible electrooxidation process of arsenic.

(a) (b)

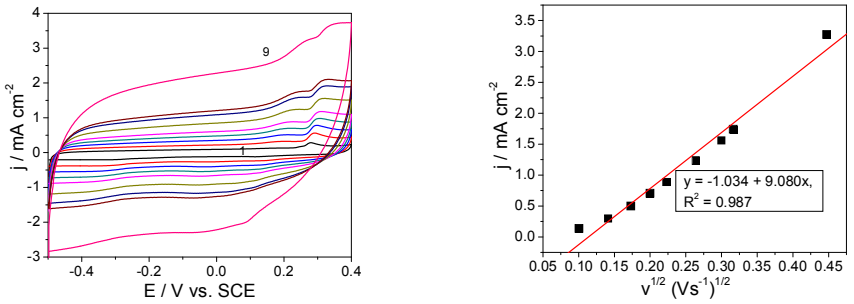

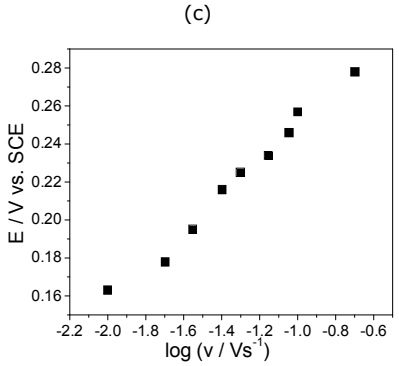

Figure 11.5 (a) Cyclic voltammograms of CNT-ZAAg-Epoxy composite electrode in 0.09 M Na_2SO_4 + 0.01 M H_2SO_4 supporting electrolyte and in the presence of 3 mM As, at different scan rate 0.01, 0.02, 0.03, 0.04, 0.05, 0.07, 0.09, 0,1, 0.2 Vs^{-1}; potential range: -0.5 ~ +0.4 V/SCE; preconditioned at -0.4 V/SCE for 120 s; (b) Plots of the current densities of the anodic peak recorded at +0.2 V/SCE vs. square root of the scan rate; (c) Plots of the anodic peak potential vs. the logarithm of the scan rate.

11.3.2. Stripping anodic voltammetric determination of As (III) at CNT-ZAAg-Epoxy composite electrode

Based on the above-presented results, the detection experiments were conducted to improve the electroanalytical parameters of arsenic (III) detection by the exploitation of the operating conditions of differential-pulsed voltammetry (DPV) and square-wave voltammetry (SWV), applied subsequently to the optimum deposition step.

The step potential and the modulation amplitude were varied. Series of DPVs at various arsenic (III) concentrations recorded at CNT-ZAAg-Epoxy composite electrode at the modulation amplitude of 0.2V and various step potential values (0.005, 0.01 and 0.02 V) are presented in Figures 11.6.

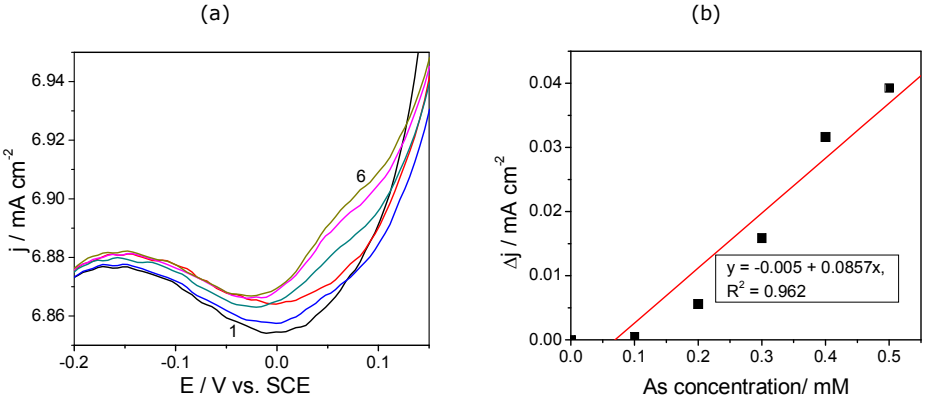

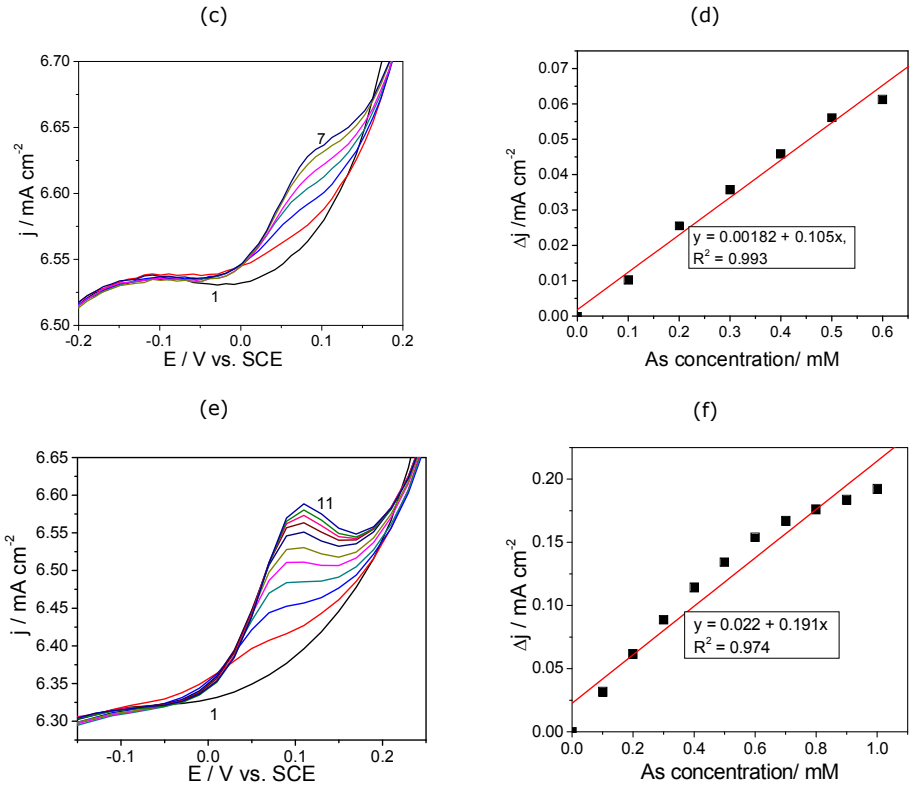

Figure 11.6 Differential-pulsed voltammograms recorded at CNT-ZAAg-Epoxy composite electrode with a 0.2V modulation amplitude, between -0.25 and +0.25 V/SCE in 0.09 M Na_2SO_4 +0.01 M H_2SO_4 supporting electrolyte (curve 1) and in the presence of different arsenic (III) concentrations: 0.1-1 mM (curves 2-11) at the step potential: 0.005V (a), 0.1 V (c) and 0.02 V (e) ; Calibration plots of the current densities recorded at E= +0.1 V/SCE vs. arsenic (III) concentration at the step potential: 0.005V (b), 0.1 V (d) and 0.02 V (f)

Also, a series of DPVs recorded at CNT-ZAAg-Epoxy composite electrode under operation conditions of 0.02 V step potential and 0.01 V modulation amplitude is presented in Figure 11.7a. The sensitivity determined based on the slope of the linear calibration between the oxidation peak current and arsenic concentrations (Figure 11.7b) is much lower than those determined for the modulation amplitude of 0.2 V.

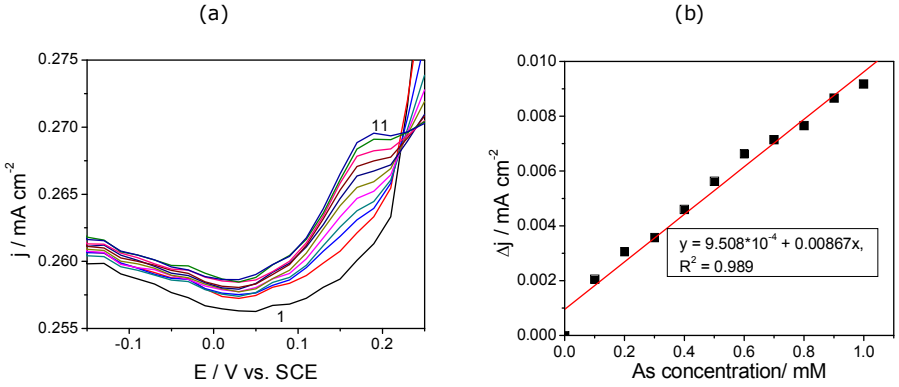

Figure 11.7 (a) Differential-pulsed voltammograms recorded at CNT-ZAAg-Epoxy composite electrode with a 0. 1V modulation amplitude and 0.02 V step potential, between -0.25 and +0.25 V vs. SCE in 0.09 M Na_2SO_4 +0.01 M H_2SO_4 supporting electrolyte (curve 1) and in the presence of different arsenic (III) concentrations: 0.1-1 mM (curves 2-11); (b) Calibration plots of the current densities recorded at E= +0.17 V/SCE vs. Arsenic (III)

The electroanalytical parameters for arsenic (III) detection using DPV technique at various steps potential values are presented in Table 11.3.

Table 11.3 The electroanalytical parameters determined for arsenic (III) anodic stripping determination at CNT-ZAAg-Epoxy composite electrode using DPV technique operated at 0.2 V modulation amplitude

Step potential value/V	Potential value V/SCE	Sensitivity mA/mM cm^{-2}	Correlation coefficient, R^2	Relative standard deviation, RSD/ %	The lowest limit of detection, LOD/mM	Limit of quantification, LQ/mM
0.05	0.07	0.0857	0.962	0.125	0.301	1.003
0.01	0.095	0.105	0.993	0.031	0.04	0.13
0.02	0.1	0.191	0.974	0.039	0.03	0. 1

In Table 11.4 are presented the electroanalytical parameters for arsenic (III) detection using DPV technique at 0.02 V step potential and 0.1 and 0. 2 V modulation amplitude.

Table 11.4 The electroanalytical parameters determined for arsenic (III) anodic stripping determination at CNT-ZAAg-Epoxy composite electrode using DPV technique operated at 0.02 V step potential

Modulation amplitude value/V	Potential value V/SCE	Sensitivity mA/m Mcm^{-2}	Correlation coefficient, R^2	Relative standard deviation, RSD, %	The lowest limit of detection, LOD/mM	Limit of quantification, LQ/mM
0.1	0.17	0.00867	0.989	0.161	0.144	0.482
0.2	0.1	0.191	0.974	0.039	0.03	0. 1

The optimized operating conditions for anodic stripping voltammetry using DPV technique are the potential step of 0.02 V and the modulation amplitude of 0.2 V. Under these conditions SWV technique was applied at various frequency values. Only for the frequency of 10 Hz the electrode response was reproducible. The results of SWV under 0.02 potential step, 0.2 V modulation amplitude and 10 Hz frequency are presented in Figure 11.8a. The sensitivity determined from the slope of the linear calibration (Figure 11.8b) was quite 10 times higher than the best reached by DPV.

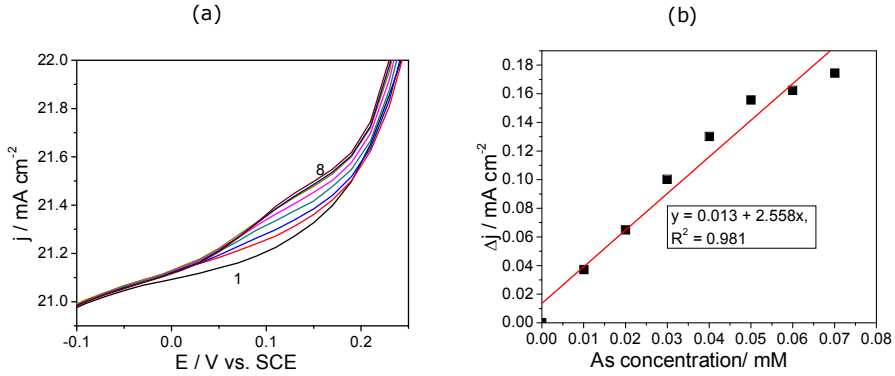

Figure 11.8 (a) Square-wave voltammograms recorded at CNT-ZAAg-Epoxy composite electrode with a 0.2V modulation amplitude, 0.02 V step potential, 10 Hz frequency between -0.25 and +0.25 V vs. SCE in 0.09 M Na_2SO_4 +0.01 M H_2SO_4 supporting electrolyte (curve 1) and in the presence of different arsenic (III) concentrations: 0.01-0.07 mM (curves 2-8); (b) Calibration plots of the current densities recorded at E= +0.14 V/SCE vs. arsenic (III)

The comparative electroanalytical parameters determined under optimized conditions using DPV and SWV are presented in Table 11.5.

Table 11.5 The electroanalytical parameters determined for arsenic (III) anodic stripping determination at CNT-ZAAg-Epoxy composite electrodes using optimized DPV and SWV techniques.

Technique	Potential value V/SCE	Sensitivity mA/mM cm^{-2}	Correlation coefficient, R^2	Relative standard deviation, RSD/%	The lowest limit of detection, LOD/mM	Limit of quantification, LQ/mM
DPV	0.1	0.191	0.974	0.039	0.03	0. 1
SWV	0.138	2.558	0.981	0.179	0.02	0.06

Anodic stripping square-wave voltammetry (ASSWV) allowed reaching the best electroanalytical parameters in relation with the sensitivity, the lowest limit of detection and quantification. Under the optimized conditions using a deposition time of 120 seconds at the potential value of -0.4 V/SCE and SWV (0.02 step potential, 0.2 modulation amplitude and 10 Hz frequency) the sensitivity of 2.558 mA / $mMcm^{-2}$ was determined and the lowest limit of detection of 0.02 mM As (III).

These results led to the following conclusions:

Carbon nanotubes (CNT) and carbon nanofibers (CNF) based composite electrodes did not exhibit the electrocatalytic effect for the reduction/oxidation process of arsenic (III) from aqueous solution under acidic medium. These electrodes are not suitable for arsenic (III) detection from aqueous solution;

Silver incorporation within CNT and CNF based composite electrode by synthetic/natural zeolite doping with silver ions or direct by chemical reducing as metallic silver directly on carbon surface led to achieving a response in the presence of arsenic (III). This response corresponding to the anodic stripping arsenic from the electrode surface applied after a deposition step in which arsenic (III) is reduced at arsenic on the electrode surface at the potential not too negative.

Even if silver incorporated CNT / CNF based composite gave a useful response for As (III) stripping, the results are not satisfactory from the point of view of the lowest limit of detection. The best limit of detection (LOD) reached under optimized SWV at CNT-ZAAg-Epoxy composite electrode exceeded the CMA imposed by legislation. Further experiments will be conducted to improve the performance of the working electrodes by the electrodeposition of Ag nanoparticles on their surface. Also, CNT-ZAAg-Epoxy will be further tested for the cathodic voltammetric determination of As (III) from the aqueous solution.

11.3.3. Cathodic voltammetric determination of As (III) at CNT-ZAAg-Epoxy composite electrode

In general, to determine arsenic (III) from aqueous solution, two approaches of the stripping techniques are employed, *i.e.*, anodic and cathodic stripping technique.

Cathodic stripping voltammetry methods for arsenic detection have usually used hanging mercury drop electrode [31-34], involving two major steps, in the first

step occurred the electrodeposition of arsenic on Hg electrode and in the second step, cathodic stripping is assured by the further reduction to AsH_3. Due to As (0) is insoluble on Hg, the presence of Cu or Se is required, which are accumulated on the Hg surface and led to Cu (Se)-As intermetallic compounds. Also, Hg electrode is limited by its toxic property and other electrode compositions have been researched to reach this aim.

Based on these considerations and also, the electrochemical behaviour of As (III) on the CNT-ZAAg-Epoxy in relation with the electrodeposition step, the electrode was tested to detect As (III) at the cathodic branch of the cyclic voltammetry. Figure 11.9 shows the CVs recorded on CNT-ZAAg-Epoxy composite electrode in 0.09 M Na_2SO_4+0.01 M H_2SO_4 supporting electrolyte and various As (III) concentrations ranged from 0.001 to 0.01 mM, for the potential window ranged from 0 to -1.25 V/SCE. A very clear reduction peak corresponding to As (III) reduction process is noticed at the potential value of -0.89 V/SCE, before to hydrogen reduction that occurred at the potential value of -1 V/SCE. The linear dependence between the cathodic peak current densities recorded at -0.89 V/SCE versus As (III) concentration was found, characterized by a good correlation coefficient (R^2=0.991).

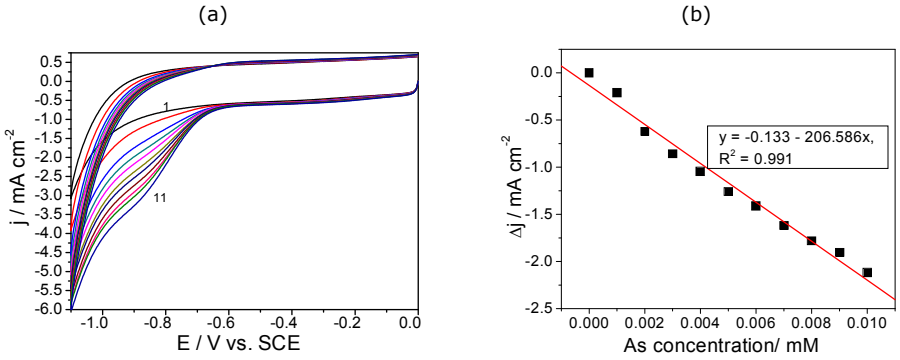

Figure 11.9 (a) Cyclic voltammograms recorded at CNT-ZAAg-Epoxy composite electrode in 0.09 M Na_2SO_4+0.01 M H_2SO_4 supporting electrolyte (curve 1) and in the presence of 0.001, 0.002, 0.003, 0.004, 0.005, 0.006, 0.007, 0.008, 0.009, 0.01 mM As (curves 2- 11), potential scan rate: 0.05 Vs^{-1}, potential range: -1.0 to 0 V/SCE; (b) The calibration plots of the current densities corresponding to the arsenic reduction peaks recorded at -0.89 V/SCE vs. As (III) concentrations

The effect of the scan rate on the cyclic voltammogram shapes was investigated to elucidate several aspects regarding the mechanistic aspects of the electroreduction of arsenic (III) on CNT-ZAAg-Epoxy composite electrode. Figure 11.10a shows CVs recorded for 0.006 mM As (III) in 0.09 Na_2SO_4+0.01 H_2SO_4 supporting electrolyte at various scan rates (0.01-0.2 Vs^{-1}) within the potential range between 0 to -1.25 V/SCE. The linear increase of the reduction peak current density corresponding to the cathodic reduction of arsenic (III) with the square root of the scan rate suggested a diffusion- controlled process (Figure 11.10b). The peak potential shifted towards more negative potential when increasing v (Figure 11.10c), indicating about an irreversible reduction process within this limited potential window.

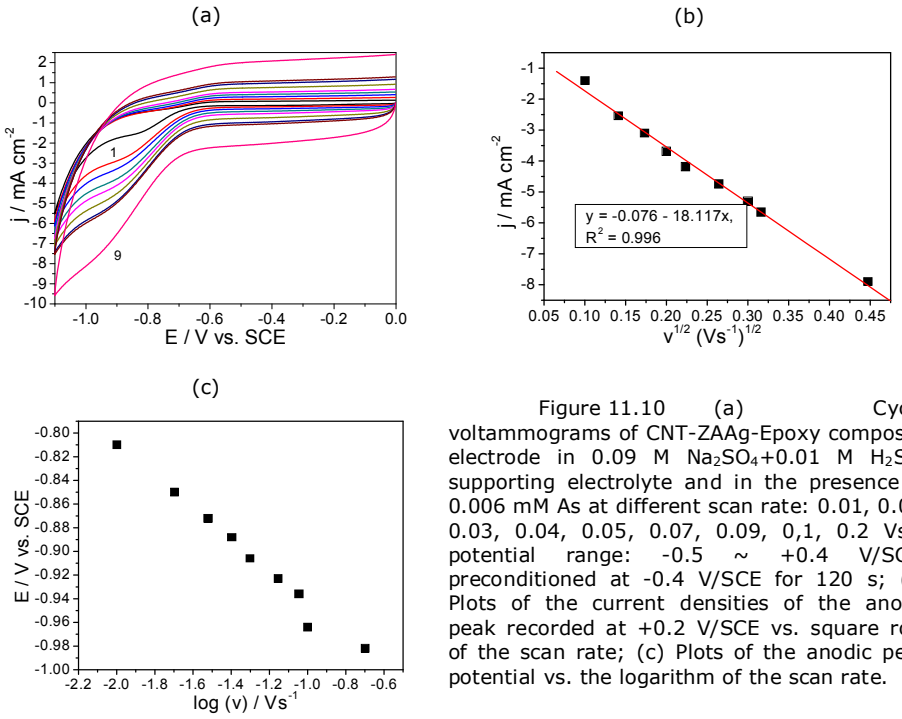

Figure 11.10 (a) Cyclic voltammograms of CNT-ZAAg-Epoxy composite electrode in 0.09 M Na_2SO_4+0.01 M H_2SO_4 supporting electrolyte and in the presence of 0.006 mM As at different scan rate: 0.01, 0.02, 0.03, 0.04, 0.05, 0.07, 0.09, 0,1, 0.2 Vs^{-1}; potential range: -0.5 ~ +0.4 V/SCE; preconditioned at -0.4 V/SCE for 120 s; (b) Plots of the current densities of the anodic peak recorded at +0.2 V/SCE vs. square root of the scan rate; (c) Plots of the anodic peak potential vs. the logarithm of the scan rate.

DPV technique operated at the parameters previously tested for the anodic stripping voltammetry, *i.e.*, 0. 1V modulation amplitude and 0.02 V step potential, led to the results presented in Figure 11.11a. Lower As (III) concentration were able to be detected with this technique, and the sensitivity determined based on the slope of the linear curve of reduction peak current densities versus As (III) concentrations was about two times higher as reached by CV. Also, the lowest limit of detection is improved using this technique (see Table 11.6).

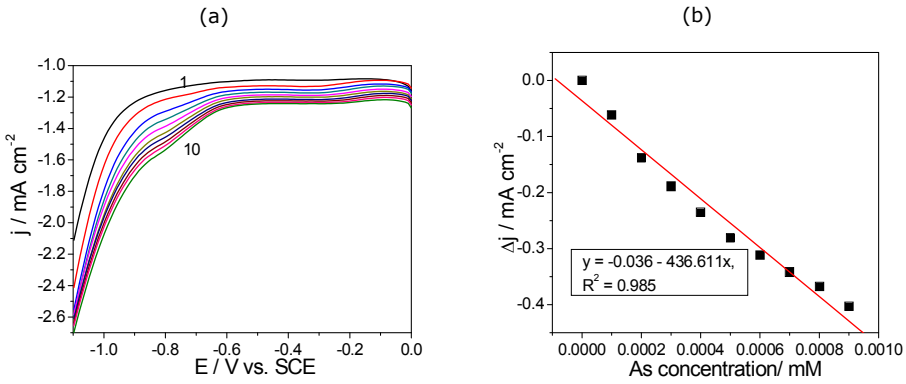

Figure 11.11 (a) Differential-pulsed voltammograms recorded at CNT-ZAAg-Epoxy composite electrode with a 0. 1V modulation amplitude and 0.02 V step potential in 0.09 M Na_2SO_4+0.01 M H_2SO_4 supporting electrolyte (curve 1) and in the presence of 0.1, 0.2, 0.3, 0.4, 0.5, 0.6, 0.7, 0.8, 0.9, 1 μM As (curves 2- 11), potential range: -1.0 to 0 V/SCE; (b) The calibration plots of the current densities corresponding to the arsenic reduction peaks recorded at -0.83 V/SCE vs. As (III) concentrations.

Applying CA technique led to the results presented in Figure 11.12. The chronoamperogram recorded at the fixed potential of -0.9 V/SCE at continuous adding of 0.001 mM As (III) by batch injection system showed a cathodic response with As (III) concentration increasing. A linear dependence of the cathodic current recorded after 50 seconds versus As (III) concentration was noticed, and the sensitivity of 58.32 $mAmM^{-1}$ was determined.

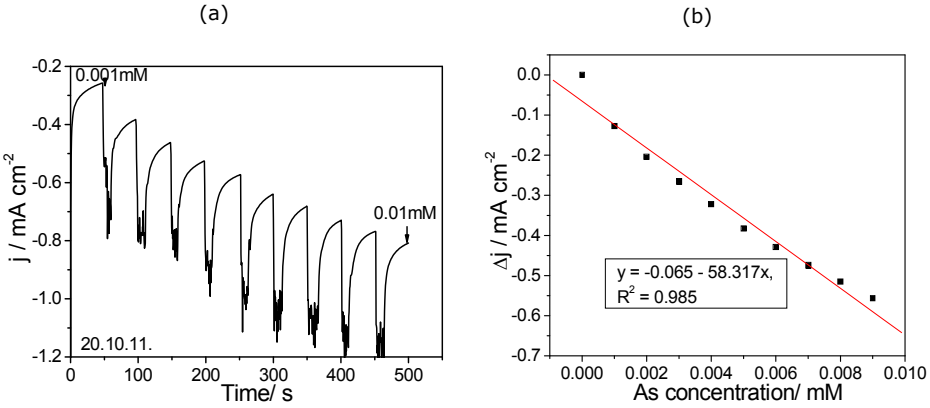

Figure 11.12 (a) Chronoamperometric response recorded at CNT-ZAAg-Epoxy composite electrode with at the potential value of -0.9 V/SCE in 0.09 M Na_2SO_4+0.01 M H_2SO_4 supporting electrolyte by adding continuously 0.001 mM As (III) concentration; (b) The calibration plots of the current densities recorded after 50 seconds from arsenic adding versus its concentrations.

All electroanalytical parameters determined for As (III) detection by the reduction process are gathered in Table 11.6.

Table 11.6 The electroanalytical parameters of voltammetric / amperometric detection of As (III) at a CNT-ZAAg-Epoxy composite electrode using electrochemical technique

Technique	Potential value V/SCE	Sensitivity mA/mM cm^{-2}	Correlation coefficient, R^2	Relative standard deviation, RSD/ %	The lowest limit of detection, LOD/ mM	Limit of quantification, LQ/mM	Concentration range, mM
CV	-0.89	206.586	0.991	0.412	$3.5 \cdot 10^{-5}$	$1 \cdot 10^{-4}$	0.001 – 0.01
DPV	-0.83	436.611	0.985	0.438	$5.2 \cdot 10^{-7}$	$1.73 \cdot 10^{-6}$	0.0001 – 0.001
CA	-0.9	58.317	0.985	1.818	$2.57 \cdot 10^{-4}$	$8.57 \cdot 10^{-4}$	0.001 – 0.01

Based on the results, it can be concluded that:

The CNT-ZAAg-Epoxy electrode exhibited the electrocatalytic activity towards the reduction process of As (III), allowing its detection by a direct and fast method in comparison with the cathodic stripping voltammetry.

The very good electroanalytical parameters for As (III) detection in relation with the sensitivity and the lowest limit of detection were achieved. Both the lowest limit of detection and the limit of quantification are below the maximum allowable concentration imposed in drinking water.

11.3.4. Electrochemical detection of As (III) on CNT-ZAAg-Epoxy composite electrode decorated electrochemically with silver nanoparticles by anodic stripping voltammetry

11.3.4.1. Cyclic voltammetry measurements

To improve the electrode performance for the electrodetection of As (III) from aqueous solution using anodic stripping voltammetry, silver nanoparticles were deposited on the CNT-ZAAg-Epoxy composite electrode by electrodeposition at the potential value of -0.4 V/SCE for 3 seconds deposition time. The electrodeposition conditions for CNT-ZAAg-Epoxy composite decoration were applied in according with our previously reported study [23]. This new electrode composition, named CNT-ZAAg-Epoxy (Ag), was tested to check its response to As (III) presence by CV under the same As (III) concentration range that was tested for unmodified CNT-ZAAg-Epoxy composite electrode. Figure 11.13 shows CVs recorded at CNT-ZAAg-Epoxy (Ag) composite electrode in 0.09 Na_2SO_4+0.01 H_2SO_4 supporting electrolyte and the As (III) concentration ranged between 0.2 and 2 mM. A linear dependence between the anodic current densities recorded at +0.2 V/SCE and As (III) concentrations was achieved, with a better sensitivity in comparison with the CV results obtained for unmodified CNT-ZAAg-Epoxy (see previous subsection).

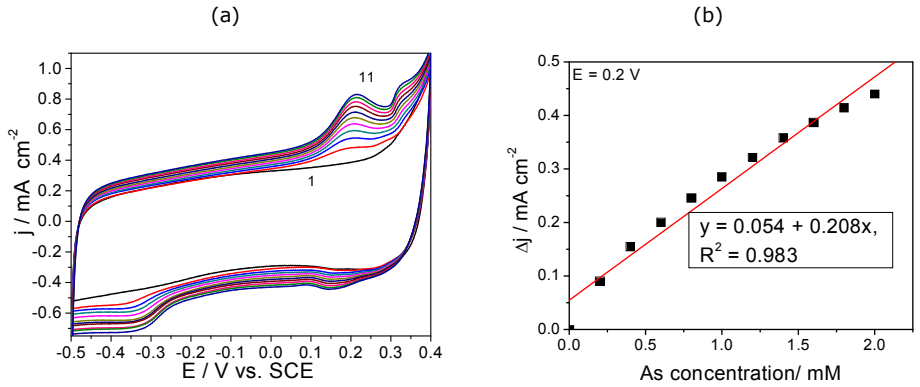

Figure 11.13 (a) Cyclic voltammograms recorded at CNT-ZAAg-Epoxy (Ag) composite electrode in 0.09 M Na_2SO_4+ 0.01 M H_2SO_4 supporting electrolyte (curve 1) and in the presence of 0.2, 0.4, 0.6, 0.8, 1.0, 1.2, 1.4, 1.6, 1.8, 2.0 mM As (curves 2- 11) with a preconditioning of electrode at -0.4 V/SCE at deposition time of 120 s, potential scan rate: 0.05 Vs^{-1}, potential range: -0.5 to +0.4 V/SCE; (b) The calibration plots of the current densities corresponding to the arsenic anodic stripping peaks recorded at +0.2 V/SCE vs. As (III) concentrations.

To compare the electrochemical behaviour of arsenic (III) on CNT-ZAAg-Epoxy (Ag) composite electrode with CNT-ZAAg-Epoxy, the effect of the scan rate on the cyclic voltammogram shapes was investigated. The same scan rate range was applied and CVs were recorded for 3 mM As (III) (see Fig. 11.14a). The similar slope was found for the linear dependence of the stripping oxidation current densities versus the square root of the scan rate, but a difference was noticed for small scan rate up to 0.03 Vs^{-1}. For this small scan rate range, no linear dependence was achieved. The current density is independent of the scan rate, which suggested a spheric diffusion, characteristics to the microelectrode array behavior (Figure 11.14b). However, at medium and high scan rate the linear diffusion controlled the oxidation anodic process for the arsenic stripping from the electrode surface to As (III) in aqueous solution. The peak potential shifted also towards positive potential when increasing v (Figure 11.14c), the quasi-reversible character of the anodic stripping process being evidenced.

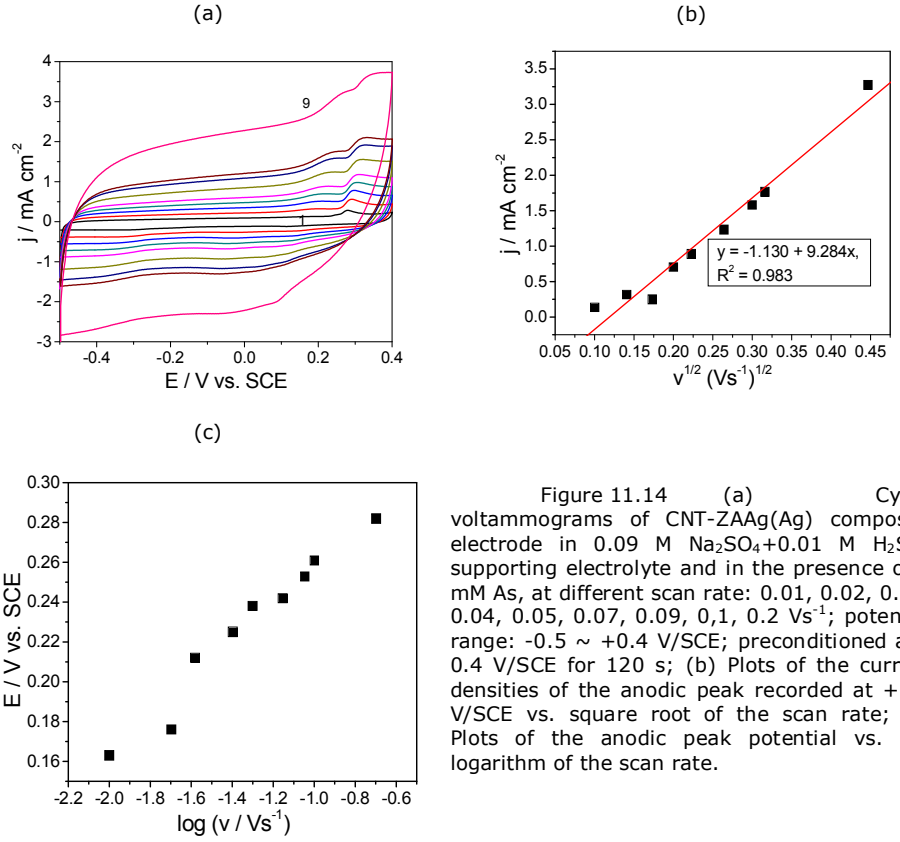

Figure 11.14 (a) Cyclic voltammograms of CNT-ZAAg(Ag) composite electrode in 0.09 M Na_2SO_4+0.01 M H_2SO_4 supporting electrolyte and in the presence of 3 mM As, at different scan rate: 0.01, 0.02, 0.03, 0.04, 0.05, 0.07, 0.09, 0,1, 0.2 Vs^{-1}; potential range: -0.5 ~ +0.4 V/SCE; preconditioned at -0.4 V/SCE for 120 s; (b) Plots of the current densities of the anodic peak recorded at +0.2 V/SCE vs. square root of the scan rate; (c) Plots of the anodic peak potential vs. the logarithm of the scan rate.

11.3.4.2. Detection measurements

Differential-pulsed voltammetry technique was applied under the operating conditions optimized for CNT-ZAAg-Epoxy, 0.02 V step potential and 0.2V modulation amplitude. Series of DPVs recorded at CNT-ZAAg-Epoxy (Ag) composite electrode at different As (III) concentrations ranges subsequently to As (III) electrodeposition at the potential value of -0.4 V/SCE for 120 seconds are presented in Figures 11.16. The slopes of the linear dependences between the anodic stripping peak currents and As (III) concentrations allowed to determine the sensitivities reached under these working conditions (Figures 11.15 b and d).

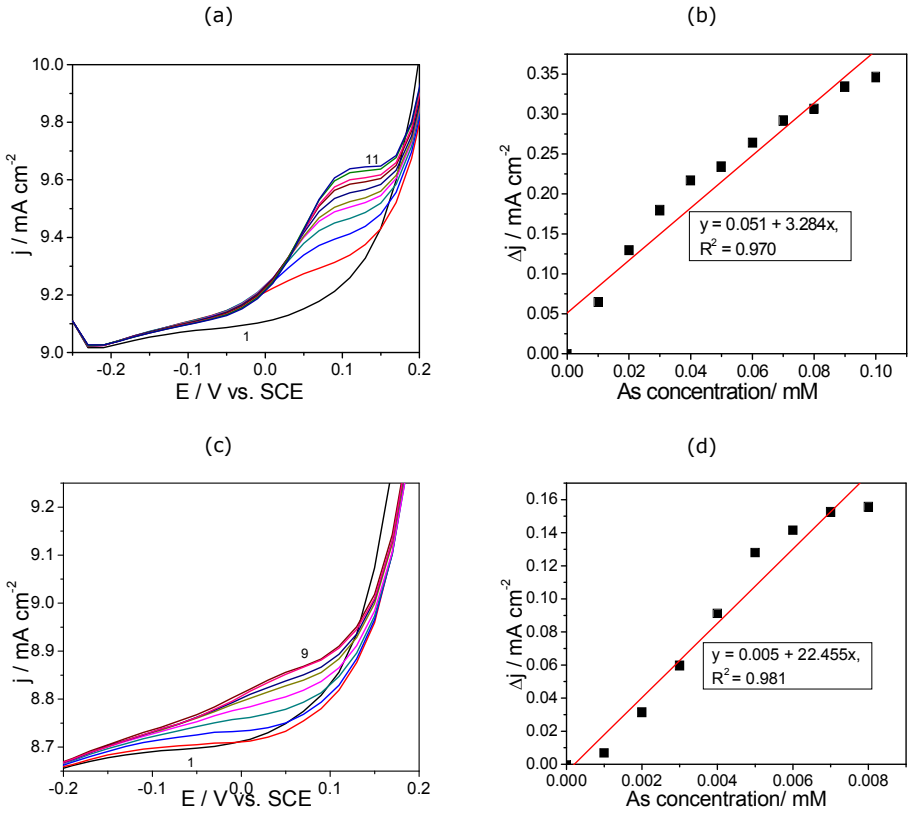

Figure 11.15 Differential-pulsed voltammograms recorded at CNT-ZAAg-Epoxy (Ag) composite electrode with 0.02 V step potential and 0.2 modulation amplitude, between -0.25 and +0.25 V/SCE in 0.09 M Na_2SO_4+0.01 M H_2SO_4 supporting electrolyte (curve 1) and in the presence of different arsenic (III) concentrations: (a) 0.01-0.1 mM (curves 2-11); (c) 0.001-0.008 mM (curves 2-9); Calibration plots of the current densities recorded at: (c) E= +0.1 V/SCE vs. arsenic (III) concentration (0.01-0.1 mM) and (d) E=0.05V/SCE vs. arsenic (III) concentration (0.001-0.01 mM)

Also, SWV technique was applied also, under optimized operation conditions previously established for CNT-ZAAg-Epoxy composite electrode for the same As (III) concentration range. Figures 11.16 (a-d) show series of SWVs recorded at CNT-ZAAg-Epoxy (Ag) composite electrode in 0.09 M Na_2SO_4+0.01 M H_2SO_4 supporting electrolyte under As (III) concentrations ranged from 0.01-0.1 mM (Figure 11.16a) and 0.001-0.01 mM (Figure 11.16c). The similar sensitivities were reached under these operating conditions of SWV applying (see Figures 11.16b, d and Table 11.6). A slight difference is noticed regarding the potential value at which the anodic stripping appeared.

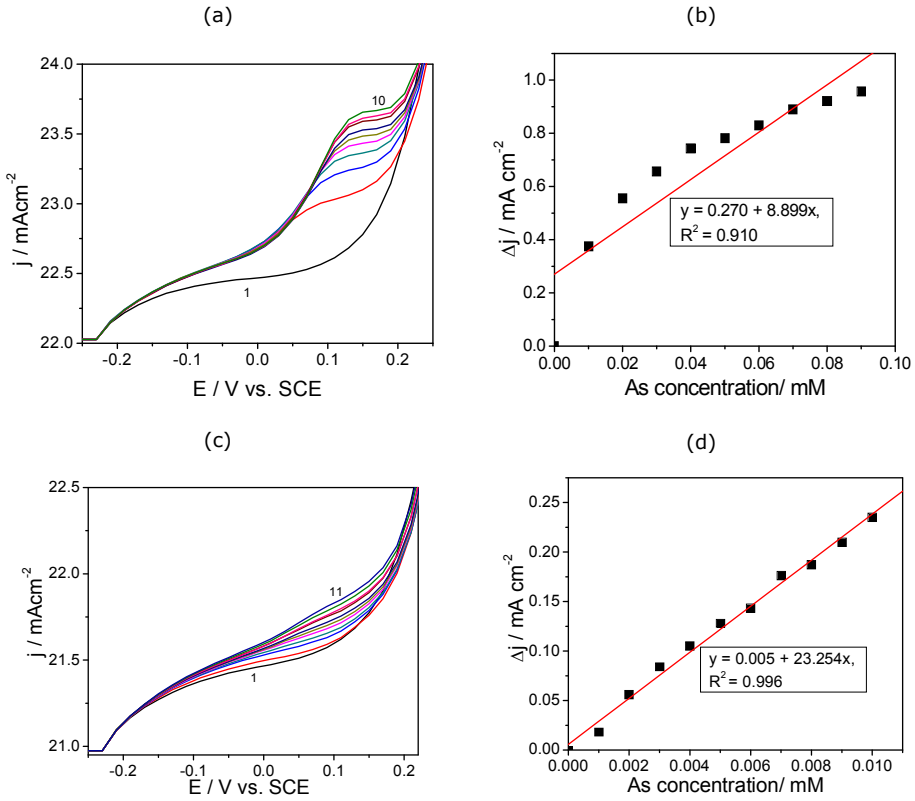

Figure 11.16 (a) Square-wave voltammograms recorded at CNT-ZAAg-Epoxy (Ag) composite electrode with 0.2V modulation amplitude, 0.02 V step potential, 10 Hz frequency between -0.25 and +0.25 V/SCE in 0.09 M Na_2SO_4+0.01 M H_2SO_4 supporting electrolyte (curve 1) and in the presence of different arsenic (III) concentrations: (a) 0.01-0.09 mM (curves 2-10); (c) 0.001-0.01 mM (curves 2-11); Calibration plots of the current densities recorded at: (c) E= +0.15 V/SCE vs. arsenic (III) concentration (0.01-0.1 mM) and (d) E=0.09V/SCE vs. arsenic (III) concentration (0.001-0.01 mM)

The electroanalytical parameters determined for this electrode composition under the optimized operating conditions of DPV and SWV techniques are gathered in Table 11.7.

Table 11.7 The electroanalytical parameters determined for arsenic (III) anodic stripping determination at CNT-ZAAg-Epoxy (Ag) composite electrode (3 seconds electrodeposition time) using DPV and SWV techniques operated under optimized conditions

Technique	Potential value V/SCE	Sensitivity mA/mM cm^{-2}	Correlation coefficient, R^2	Relative standard deviation, RSD, %	The lowest limit of detection, LOD/mM	Limit of quantification, LQ/mM
DPV	0.05	22.455	0.981	0.242	0.2	0.9
SWV	0.09	23.254	0.996	0.118	0. 3	1

11.3.5. Effect of the time electrodeposition of silver nanoparticles on the electroanalytical performance using anodic stripping square-wave voltammetry technique

The time of the electrodeposition of silver nanoparticles was varied to get optimum CNT-ZAAg-Epoxy (Ag) composite in relation with the best signal corresponding to the anodic stripping peak current obtained by SWV applying. Figure 11.7 shows the SWV recorded for 5 μM As in 0.09 Na_2SO_4+0.01 M H_2SO_4 supporting electrolyte at CNT-ZAAg-Epoxy (Ag) obtained at the time of silver electrodeposition varied from 1 to 10 seconds. Also, a time deposition of 60 seconds was tested. The useful signal determined by the difference from the anodic peak current corresponding to arsenic stripping from the electrode surface to the solution as As (III) and the background current recorded at 0.1 V/SCE is presented in Figure 11.18.

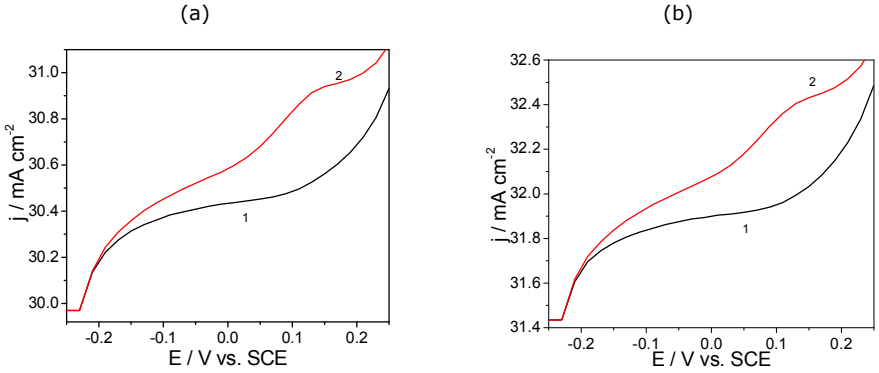

(c)

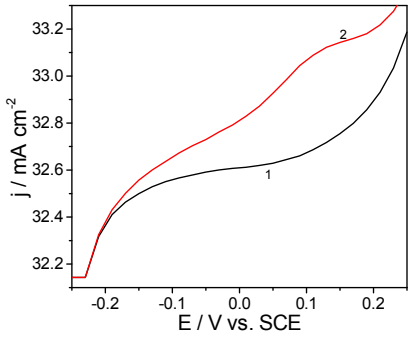
j / mA cm-2
E / V vs. SCE
1
2

(d)

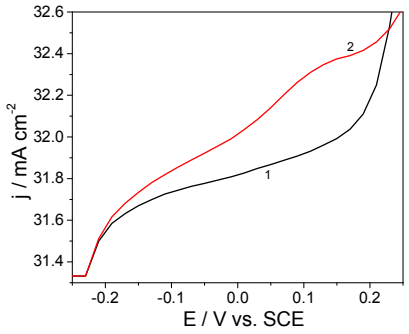
j / mA cm-2
E / V vs. SCE
1
2

(e)

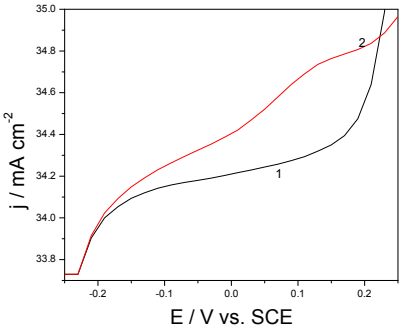
j / mA cm-2
E / V vs. SCE
1
2

(f)

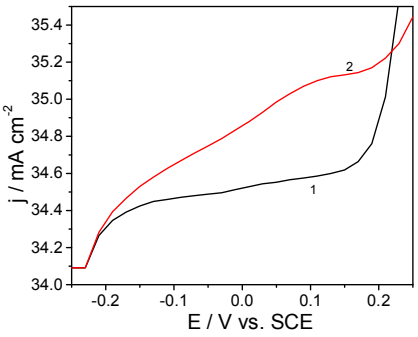
j / mA cm-2
E / V vs. SCE
1
2

(g)

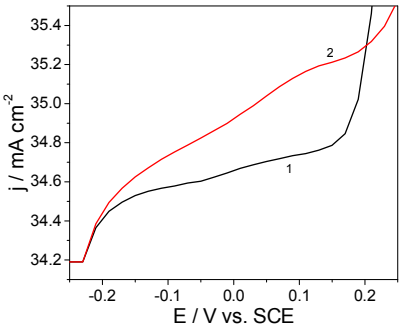
j / mA cm-2
E / V vs. SCE
1
2

(h)

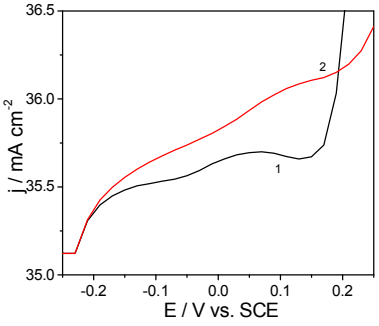
j / mA cm-2
E / V vs. SCE
1
2

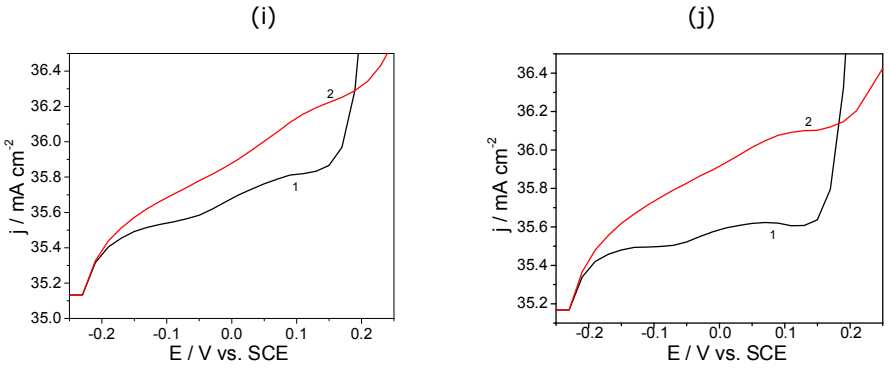

Figure 11.17 Square-wave voltammograms recorded under 0.2V modulation amplitude, 0.02V step potential, 10 Hz frequency, and potential scan rate of 0.05 Vs^{-1} between -0.25 and +0.25 V/SCE in 0.09 M Na_2SO_4+0.01 M H_2SO_4 supporting electrolyte (1) and in the presence of 0.005 mM As (2) on CNT-ZAAg-Epoxy (Ag) composite electrode obtained at different deposition time: 1-10 s (Figures a-j)

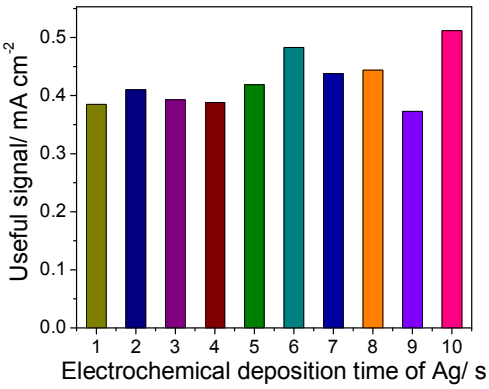

Figure 11.18 Useful signal corresponding to the 3 mM arsenic (III) anodic stripping peak recorded by SWV in 0.09 M Na_2SO_4+0.01 M H_2SO_4 supporting electrolyte (curve 1) at CNT-ZAAg-Epoxy (Ag) vs. deposition time.

Based on the above-presented results, it can be seen that the peak response increased initially until 10 seconds deposition time. At 60 seconds deposition the peak response decreased. The optimum deposition time to get CNT-ZAAg-Epoxy (Ag) composite electrode characterized by the best response signal corresponding to the arsenic anodic stripping is 10 seconds. In Figure 11.20a is shown a series of SWVs recorded at CNT-ZA-Ag (Ag) composite obtained by 10 seconds deposition time. Under this deposition condition, it was achieved the sensitivity about ten times higher than the one reached by CNT-ZAAg-Epoxy (Ag) obtained by 3 seconds deposition time of silver nanoparticles. Thus, under this optimized conditions, the sensitivity of 128.15 $mAmM^{-1}cm^{-2}$, LOD of 0.02 μM, LQ of 0.06 μM with the correlation coefficient of 0.997 were achieved.

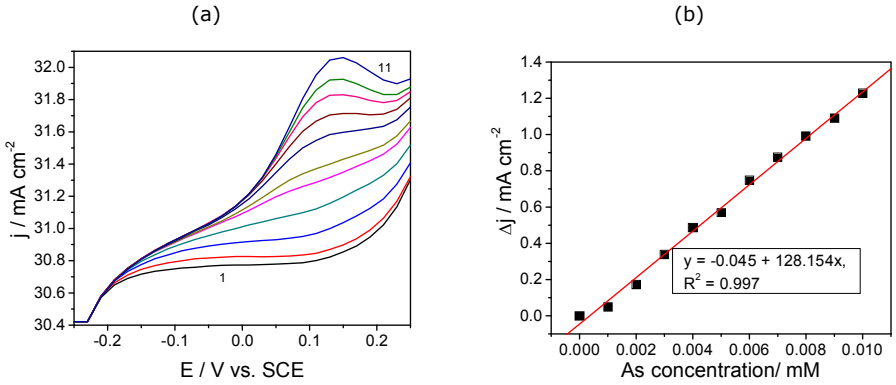

Figure 11.19 (a) Square-wave voltammograms recorded at CNT-ZAAg-Epoxy (Ag) composite electrode obtained by 10 seconds deposition time, operated by 0.2V modulation amplitude, 0.02 V step potential, 10 Hz frequency between -0.25 and +0.25 V/SCE in 0.09 M Na_2SO_4 +0.01 M H_2SO_4 supporting electrolyte (curve 1) and in the presence of different arsenic (III) concentrations: (a) 0.001-0.01 mM (curves 2-11); (b) The calibration plots of the current densities recorded at: (c) E= +0.14 V/SCE vs. arsenic (III) concentration.

11.3.6. Electrochemical detection of As (III) on CNT/CNF-Epoxy composite electrodes decorated electrochemically with silver nanoparticles

To compare the effect of the electrode substrate composition and structure on the electrodeposition of silver nanoparticles, the further experiments consist of applying the potential of -0.4 V/SCE for 3 seconds on CNT-Epoxy and CNF-Epoxy electrodes in 0.1 M $AgNO_3$ solution, followed by the voltammetric detection experiments for arsenic determination under above-presented working conditions. These new electrodes obtained by the electrochemical decoration were named CNT-Epoxy (Ag) and respectively, CNF-Epoxy (Ag) electrodes.

11.3.6.1. Cyclic voltammetry measurements

In Figure 11.21 are shown series of CVs recorded on CNT-Epoxy (Ag) (Figure 11.20a) and CNF-Epoxy (Ag) (Figure 11.20c) in 0.09 Na_2SO_4+0.01 H_2SO_4 supporting electrolyte and various As (III) concentrations, similar with working conditions applied for CNT-ZAAg-Epoxy (Ag) composite electrode. The calibration plots obtained for both silver decorated composite electrodes showed the similar results regarding the sensitivities for arsenic detection (Figure 11.20b, d). CNF-Epoxy (Ag) composite electrode exhibited the better sensitivity in comparison with CNT-Epoxy (Ag) composite, and the almost the same as the sensitivity reached for CNT-ZAAg-Epoxy (Ag) composite electrode (see Table 11.8).

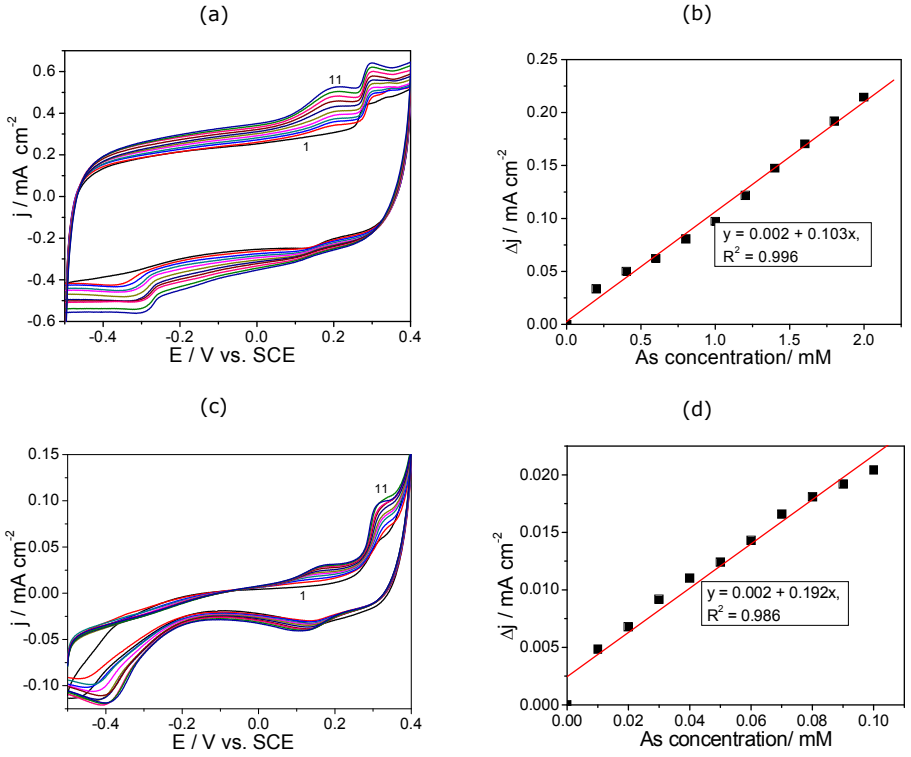

Figure 11.20 Cyclic voltammograms recorded in 0.09 M Na_2SO_4+0.01 M H_2SO_4 supporting electrolyte (curve 1) and in the presence of 0.01- 0.1 mM As (curves 2- 11) with a preconditioning of electrode at -0.4 V/SCE at deposition time of 120 s at the decorated composite electrodes: CNT-Epoxy (Ag) (a) and CNF-Epoxy (Ag) (c); The calibration plots of the current densities corresponding to the arsenic anodic stripping peaks recorded at +0.2 V/SCE vs. As (III) concentrations at the decorated composite electrodes: CNT-Epoxy (Ag) (b) and CNF-Epoxy (Ag) (d)

The electroanalytical parameters determined by CV for both composite electrodes in comparison with CNT-ZAAg-Epoxy (Ag) composite electrode are gathered in Table 11.8. Even if CNT-ZAAg-Epoxy (Ag) composite electrode allowed reaching the best sensitivity, the best LODs were achieved for CNT-Epoxy (Ag) and CNF-Epoxy (Ag) composite electrodes.

Table 11.8 The electroanalytical parameters determined for arsenic (III) anodic stripping determination using CV at the potential value of +0.2 V/SCE

Electrode type	Sensitivity mA/mMcm^{-2}	Correlation coefficient, R^2	Relative standard deviation, RSD, %	The lowest limit of detection, LOD/mM	Limit of quantification, LQ/mM
CNT-Epoxy(Ag)	0.103	0.996	3.424	0.006	0.020
CNF-Epoxy(Ag)	0.192	0.986	2.821	0.004	0.016
CNT-ZAAg-Epoxy(Ag)	0.208	0.983	0.869	0.040	0.134

The results of the investigation on the scan rate effect on the CVs recorded at both composite electrodes in 3 mM As (III). The similar behaviour was found and Fig. 11.22 shows as example the results obtained for CNT-Epoxy (Ag). The quasi-reversible and diffusion-controlled anodic oxidation process for arsenic stripping at both composite electrodes was found.

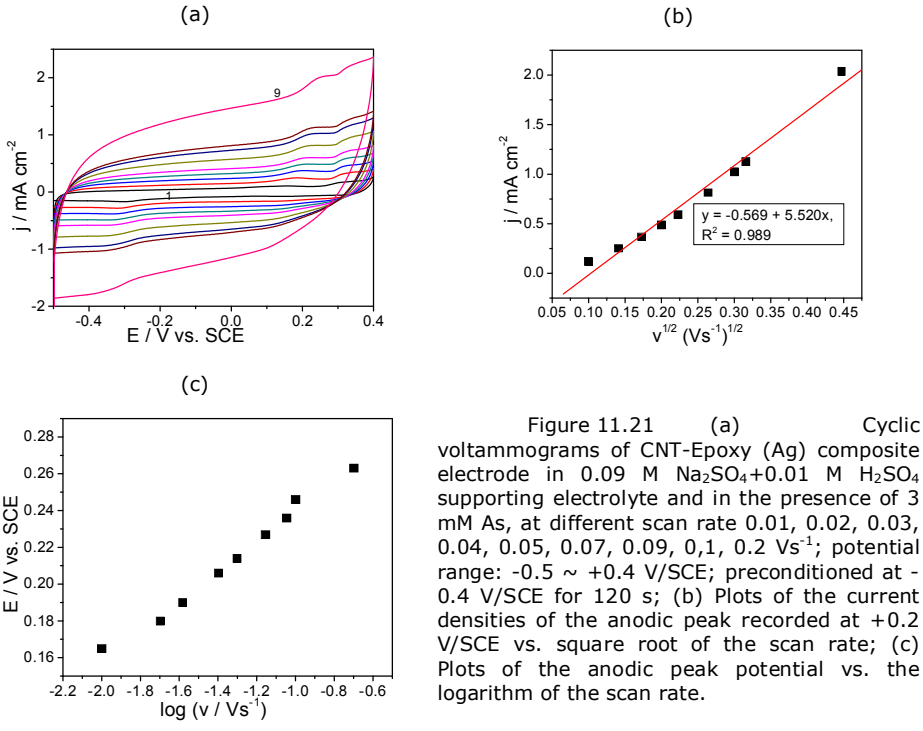

Figure 11.21 (a) Cyclic voltammograms of CNT-Epoxy (Ag) composite electrode in 0.09 M Na_2SO_4+0.01 M H_2SO_4 supporting electrolyte and in the presence of 3 mM As, at different scan rate 0.01, 0.02, 0.03, 0.04, 0.05, 0.07, 0.09, 0,1, 0.2 Vs^{-1}; potential range: -0.5 ~ +0.4 V/SCE; preconditioned at -0.4 V/SCE for 120 s; (b) Plots of the current densities of the anodic peak recorded at +0.2 V/SCE vs. square root of the scan rate; (c) Plots of the anodic peak potential vs. the logarithm of the scan rate.

11.3.6.2. Detection measurements

11.3.6.2.1. CNT-Epoxy (Ag) and CNF-Epoxy (Ag) composite electrodes obtained by electrodeposition for 3 seconds

Differential-pulsed voltammetry technique was operated under 0.02 V step potential and 0.2V modulation amplitude for both composite electrodes. Series of DPVs recorded at both composite electrodes at different As (III) concentrations ranges subsequently to As (III) electrodeposition at the potential value of -0.4 V/SCE for 120 seconds are presented in Figures 11.23. The slopes of the linear dependences between the anodic stripping peak currents and As (III) concentrations allowed to determine the sensitivities reached under these working conditions.

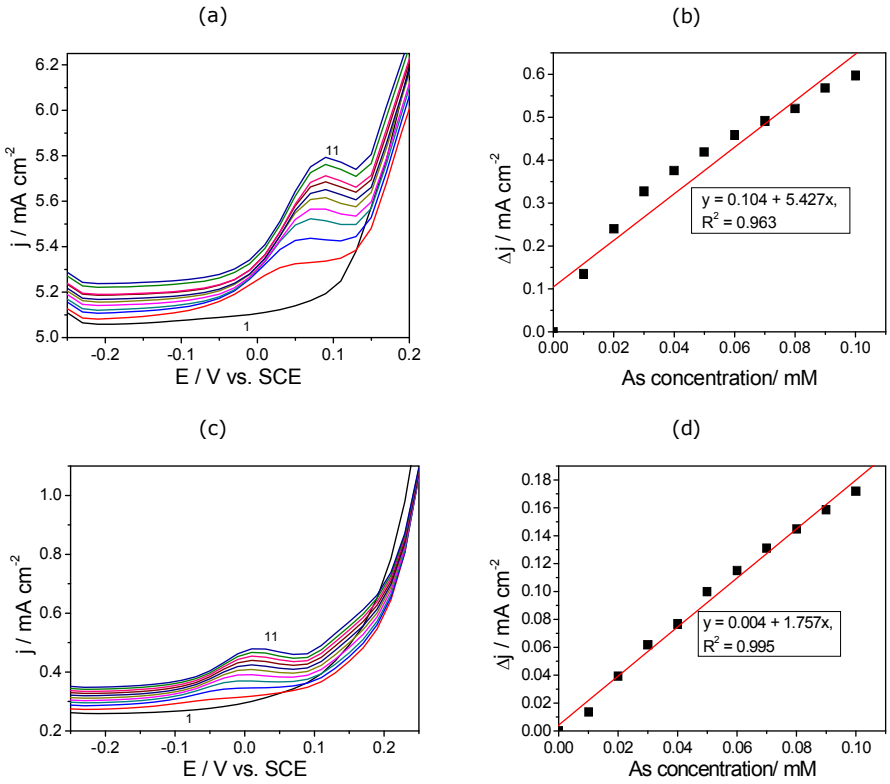

Figure 11.22 Differential-pulsed voltammograms recorded at 0.02 V step potential and 0.2V modulation amplitude, between -0.25 and +0.25 V/SCE in 0.09 M Na_2SO_4 +0.01 M H_2SO_4 supporting electrolyte (curve 1) and in the presence of 0.01-0.1 mM arsenic concentrations (curves 2-11) on the electrodes: CNT-Epoxy(Ag) (a) and CNF-Epoxy(Ag) (c); Calibration plots of the current densities recorded at: E= +0.09 V/SCE vs. arsenic (III) concentration using CNT-Epoxy (Ag) (b) and E=0.02V/SCE vs. arsenic (III) concentration using CNF-Epoxy (Ag) (d)

The electroanalytical parameters determined by DPV on both composite electrodes in comparison with CNT-ZAAg-Epoxy (Ag) composite electrode are gathered in Table 11.9. All electroanalytical parameters were worse for both CNT-Epoxy (Ag) and CNF-Epoxy (Ag) composite electrodes in comparison with CNT-ZAAg-Epoxy (Ag) composite electrode.

Table 11.9 The electroanalytical parameters determined for arsenic (III) anodic stripping determination at silver electrodecorated composite electrode (3 seconds electrodeposition time) using DPV technique

Electrode type	Potential value V/SCE	Sensitivity mA/m Mcm^{-2}	Correlation coefficient, R^2	Relative standard deviation, RSD, %	The lowest limit of detection, LOD/mM	Limit of quantification, LQ/mM
CNT-Epoxy(Ag)	0.09	5.427	0.963	0.219	0.006	0.020
CNF-Epoxy(Ag)	0.02	1.757	0.995	1.750	0.005	0.015
CNT-ZA-Ag(Ag)	0.05	22.455	0.981	0.242	0.002	0.009

SWV technique was applied using CNT-Epoxy (Ag) composite electrode under the same above-presented conditions and the results are presented in Figure 11.23 a and b. Based on the calibration plots of the current densities recorded at the potential value of +0.09V/SCE versus As(III) concentrations, the sensitivity of 26.6 $mAmM^{-1}cm^{-2}$ and LOD of 0.003 mM were achieved.

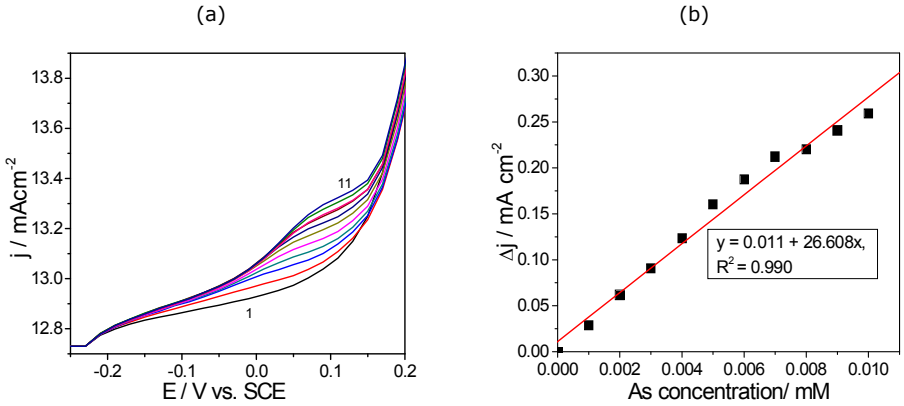

Figure 11.23 Square-wave voltammograms recorded at CNT-ZAAg-Epoxy (Ag) composite electrode obtained by 3 seconds deposition time, operated by 0.2V modulation amplitude, 0.02 V step potential, 10 Hz frequency between -0.25 and +0.25 V/SCE in 0.09 M Na_2SO_4+0.01 M H_2SO_4 supporting electrolyte (curve 1) and in the presence of different arsenic (III) concentrations: (a) 0.001-0.01 mM (curves 2-11); (b) The calibration plots of the current densities recorded at: (b) E= +0.09 V/SCE vs. arsenic (III) concentration

11.3.6.2.2. CNT-Epoxy (Ag) and CNF-Epoxy (Ag) composite electrodes obtained by electrodeposition for 60 seconds

In Figure 11.25 is shown as example series of DPVs recorded at CNT-Epoxy (Ag) composite electrode under optimized conditions above-presented. Under these conditions, the anodic stripping peak is more evidenced in comparison with other DPV recording. A very good sensitivity was reached at this electrode, about 25 times higher than the one recorded under the same conditions with the same electrode decorated with silver for 3 seconds. All electroanalytical parameters reached under these conditions are presented in Table 11.10.

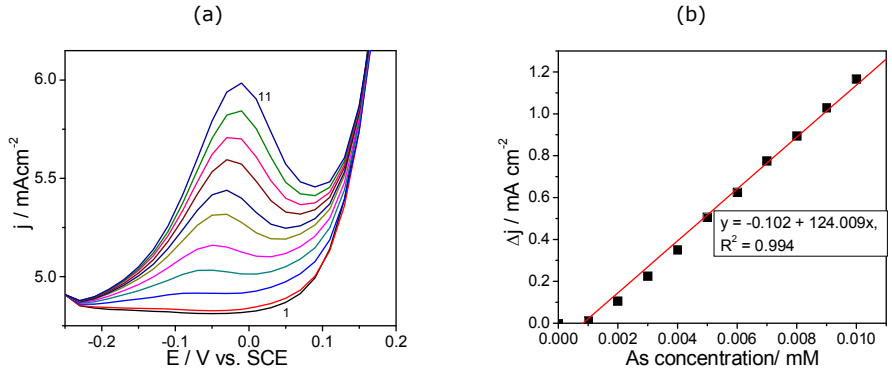

Figure 11.24 (a) Differential-pulsed voltammograms recorded at CNT-Epoxy (Ag) composite electrode (silver electrodeposition time of 60 seconds) under 0.02 V step potential and 0.2 modulation amplitude, between 0 and +1 V/SCE in 0.09 M Na_2SO_4+0.01 M H_2SO_4 supporting electrolyte (curve 1) and in the presence of 0.001-0.01 mM arsenic concentrations (curves 2-11); (b) Calibration plots of the current densities recorded at: E= -0.01 V/SCE vs. arsenic (III) concentration

The comparative results applied for both electrodes using SWV are presented in Figures 11.26 (a-d). This technique allowed achieving the best results for all electroanalytical parameters (see Table 11.10). Also, CNF-Epoxy (Ag) composite electrode exhibited the best performance for As (III) detection.

A recovery test was also performed by analyzing five parallel tap water samples, which contain 0.5 ppm arsenic (III) using CNF-Epoxy (Ag) after 60 seconds silver electrodeposition. This test was run in 0.09 M Na_2SO_4+0.01 M H_2SO_4 supporting electrolyte and a recovery of 98% was found with a RSD of 2.8 % using SWV.

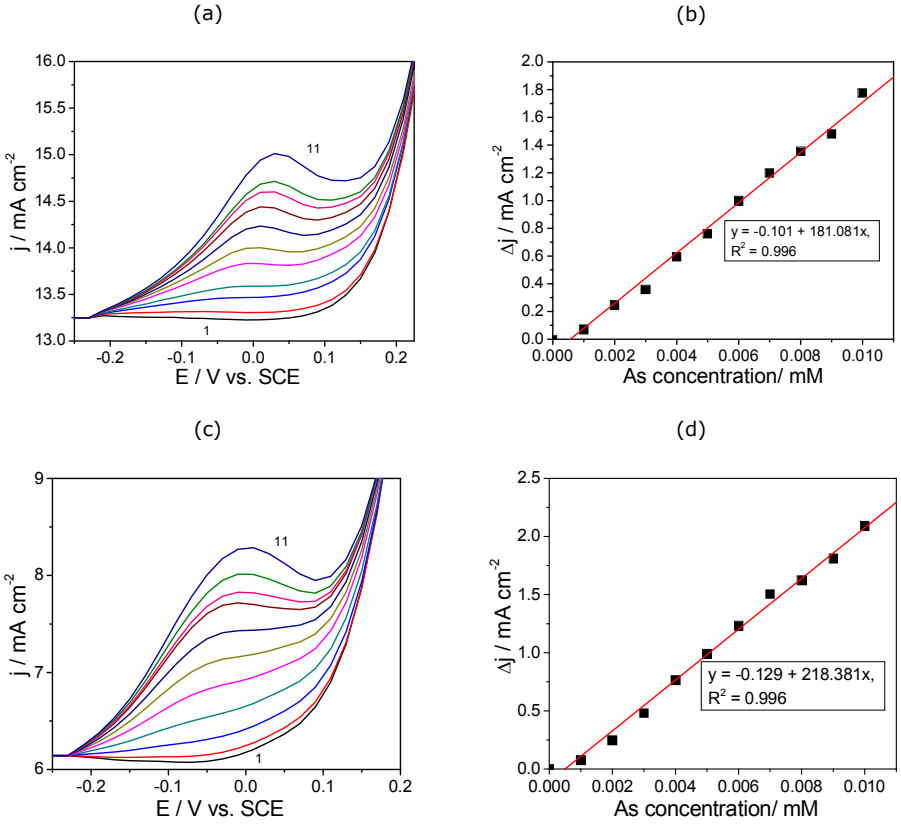

Figure 11.25 Square-wave voltammograms recorded at 0.02 V step potential, 0.2 modulation amplitude and 10 Hz frequency, between -0.25 and +0.25 V/SCE in 0.09 M Na_2SO_4+0.01 M H_2SO_4 supporting electrolyte (curve 1) and in the presence of 0.001-0.01 mM arsenic concentrations (curves 2-11) on the electrodes: CNT-Epoxy (Ag) (a) and CNF-Epoxy (Ag) (c); Calibration plots of the current densities recorded at: E= +0.03 V/SCE vs. arsenic (III) concentration using CNT-Epoxy (Ag) (b) and E=+0.009 V/SCE vs. arsenic (III) concentration using CNF-Epoxy (Ag) (d)

The electroanalytical parameters determined for arsenic (III) by anodic stripping determination at both silver electrodecorated electrode using pulsed voltammetric techniques are gathered in Table 11.10.

Table 11.10 The electroanalytical parameters determined for arsenic (III) anodic stripping determination at silver electrodecorated composite electrode (60 seconds electrodeposition time) using pulsed techniques

Electrode type	Technique	Potential value V/SCE	Sensitivity mA/m Mcm^{-2}	Correlation coefficient, R^2	Relative standard deviation, RSD, %	The lowest limit of detection, LOD/mM	Limit of quantification, LQ/μM
CNT-Epoxy(Ag)	DPV	-0.01	124.009	0.994	0.089	$9.78 \cdot 10^{-5}$	$3.26 \cdot 10^{-4}$
	SWV	0.03	181.081	0.996	0.019	$4.38 \cdot 10^{-5}$	$1.46 \cdot 10^{-4}$
CNF-Epoxy(Ag)	SWV	0.09	218.381	0.996	0.301	$1.85 \cdot 10^{-5}$	$6.18 \cdot 10^{-4}$

Based on these results, *the optimum detection scheme for arsenic (III) determination* using CNF-Epoxy (Ag) electrode can be proposed as:

Step 1 - Deposition: $As^{3+}+3e^{-} \rightarrow As^{0}$, occurred at the potential value of -0.4 V/SCE for 60 seconds;

Step 2 - Anodic stripping: $As^{0} \rightarrow As^{3+}+3e^{-}$, occurred at the potential value of +0.09 V/SCE during square-wave voltammetry running [36].

11.3.7. Application of CNF-Epoxy (Ag) composite electrode for simultaneous detection of arsenic (III) and lead (II) using Anodic Stripping Square-Wave Voltammetry technique

Taking into account that the same principle of anodic stripping using square-wave voltammetry technique (ASSWV) should be used for the detection of other heavy metals, the electrode characterized by the best performance for arsenic (III) detection was selected for testing in the simultaneous detection of arsenic (III) and lead (II) from the aqueous solutions using this technique. Though, it is very important to consider the specific deposition potential characteristics to each heavy metal. Thus, based on the literature data regarding lead detection on silver electrode [37-40] and our results of the preliminary tests regarding the influence of the potential value, which varied ranged from -1 to -0.4 V/SCE on the useful signal for lead oxidation, the potential value of -0.7 V/SCE for 60 seconds was selected as optimum for lead deposition prior to the anodic oxidation stripping. In Figure 11.27 is shown a series of SWVs recorded at CNF-Epoxy (Ag) at various lead concentrations ranged from 1 μM to 10 μM, and the calibration plots corresponding to the dependence of the anodic current densities versus Pb (II) concentration. In comparison with the sensitivity for arsenic detection, the sensitivity for Pb (II) detection is better. It must notice that by conditioning at -0.4 V/SCE that represents the optimum potential for arsenic deposition, no oxidation peak characteristics to stripping Pb(II) was noticed.

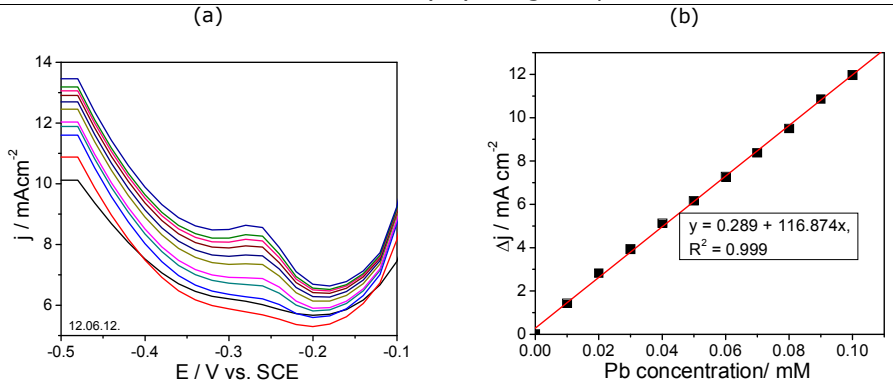

Figure 11.26 Square-wave voltammograms recorded at CNF-Epoxy (Ag) composite electrode under 0.02 V step potential, 0.2 modulation amplitude and 10 Hz frequency, between -0.5 and -0.1 V/SCE in 0.09 M Na_2SO_4+0.01 M H_2SO_4 supporting electrolyte (curve 1) and in the presence of 0.001-0.01 mM lead (II) concentrations (curves 2-11); Calibration plots of the current densities recorded at: E= -0.25 V/SCE vs. lead (II) concentration

Based on these results, *the detection scheme for lead determination* using CNF-Epoxy (Ag) electrode can be proposed as:

Step 1 - Deposition: $Pb^{2+}+2e^{-}\rightarrow Pb^{0}$, occurred at the potential value of -0.7 V/SCE for 60 seconds;

Step 2 - Anodic stripping: $Pb^{0}+2e^{-}\rightarrow Pb^{2+}$, occurred at the potential value of -0.25 V/SCE during square-wave voltammetry running.

The above-presented results suggested us to test each deposition condition for the simultaneous detection of arsenic (III) and lead (II). Neither the potential value of -0.4 V/SCE characteristics to arsenic deposition, nor the potential value of -0.7 V/SCE characteristics to lead (II) deposition, were suitable for the simultaneous detection of arsenic (III) and lead (II). This led to try to modify the detection scheme, by introduction of a new deposition step. Thus, the following schemes were applied to detect simultaneously arsenic (III) and lead (II):

Variant I:

Step 1- Deposition: $As^{3+}+3e^{-}\rightarrow As^{0}$, occurred at the potential value of -0.4 V/SCE for 60 seconds;

Step 2 - Deposition: $Pb^{2+}+2e^{-}\rightarrow Pb^{0}$, occurred at the potential value of -0.7 V/SCE for 60 seconds;

Step 3 - Anodic stripping: $As^{3+}+3e^{-}\rightarrow As^{0}$ and $Pb^{0}+2e^{-}\rightarrow Pb^{2+}$, occurred during square-wave voltammetry running.

Variant II:

Step 1- Deposition: $Pb^{2+}+2e^{-}\rightarrow Pb^{0}$, occurred at the potential value of -0.7 V/SCE for 60 seconds;

Step 2- Deposition: $As^{3+}+3e^{-}\rightarrow As^{0}$, occurred at the potential value of -0.4 V/SCE for 60 seconds;

Step3-Anodic stripping: $As^{3+}+3e^{-}\rightarrow As^{0}$ and $Pb^{0}+2e^{-}\rightarrow Pb^{2+}$, occurred during square-wave voltammetry running.

The SWVs recorded by the application of the electrodetection- variant I are presented in Figure 11.27a. Square-wave voltammograms were recorded continuously after deposition steps in 0.09 M Na_2SO_4 +0.01 M H_2SO_4 supporting electrolyte by continuous alternative adding of 0.02 mM arsenic (III) concentration and of 0.005 mM lead (II) concentration reached a mixture containing 0.14 mM As (III) and 0.035 mM Pb (II). It is very clear that the anodic stripping peak for lead (II) appeared at -0.4 V/SCE and the anodic stripping peak for arsenic (III) appeared at -0.25 V/SCE. The calibration plots of the current densities versus lead (II) and respective, arsenic (III) concentration for each potential value are shown in Figure 11.27b. The electroanalytical parameters determined for arsenic (III) and lead (II) detection for each individual/simultaneous detection scheme are presented in Table 11.11.

No reproducible results recorded by SWV were reached applying variant II.

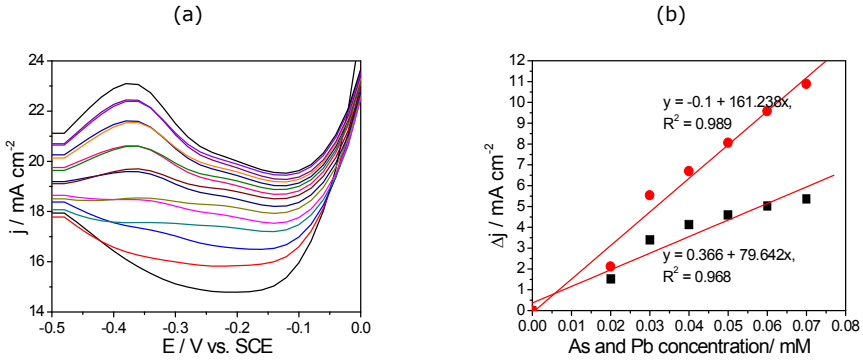

Figure 11.27 Square-wave voltammograms recorded at CNF-Epoxy (Ag) composite electrode under 0.02 V step potential, 0.2 V modulation amplitude and 10 Hz frequency, between -0.5 and 0 V/SCE in 0.09 M Na_2SO_4+0.01 M H_2SO_4 supporting electrolyte (curve 1) and in the presence of: 2- 0.02 mM As, 3- mixture of 0.02 mM As and 0.005 mM Pb, 4-mixture of 0.04mM As and 0.01 mM Pb, 5- mixture of 0.06 mM As and 0.015 mM Pb, 7-mixture of 0.08mM As and 0.02 mM Pb, 9-mixture of 0.1 mM As and 0.025 mM Pb, 11-mixture of 0.12 mM As and 0.03mM Pb, 13-mixture of 0.014 mM As and 0.035 mM Pb; Calibration plots of the current densities recorded at: E= -0.4 V/SCE vs. lead (II) concentration (curve a) and E=-0.25V/SCE vs. arsenic (III) concentration (curve b)

Table 11.11 The electroanalytical parameters determined for individual and simultaneous arsenic (III) and lead (II) anodic stripping determination at CNF-Epoxy (Ag) composite electrode using square-wave voltammetry.

Analyte	Electrodection scheme/Potential value, V vs. SCE	Sensitivity mA/m Mcm^{-2}	Correlation coefficient, R^2	Relative standard deviation, RSD, %	The lowest limit of detection, LOD/mM	Limit of quantification, LQ/μM
As (III)	Individual/0.09	218.381	0.996	0.301	$1.85*10^{-5}$	$6.18*10^{-4}$
	Simultaneous/-0.2	79.642	0.989	2.455	0.01	0.03

Pb (II)	Individual/-0.2	236.636	0.991	0.831	0.0003	0.001
	Simultaneous/-0.4	161.238	0.989	0.824	0.002	0.006

Based on these results, it can be concluded that the proposed detection scheme for simultaneous detection of As (III) and Pb (II) from aqueous solution allowed detecting each ion but the sensitivity is lower, especial for As (III) detection.

No peaks corresponding to the stripping simultaneously arsenic and lead appears for the variant II detection scheme, which informed that this scheme is not suitable for the simultaneous detection of arsenic and lead.

11.4. Partial conclusions

Several nanostructured carbon based composite electrodes were tested for arsenic (III) detection from water. No signal corresponding to the arsenic oxidation and reduction was noticed in CNT-Epoxy and CNF-Epoxy.

Silver-incorporated nanostructured carbon-based composite electrodes exhibited the electrocatalytic activity towards arsenic (III) reduction and oxidation in acidic aqueous media.

Silver incorporation within CNT and CNF based composite electrode by synthetic/natural zeolite doping with silver ions or direct by chemical reducing as metallic silver directly on carbon surface led to achieving a response in the presence of arsenic (III). This response corresponding to the anodic stripping arsenic from the electrode surface applied after a deposition step in which arsenic (III) is reduced at arsenic on the electrode surface at the potential not too negative.

All tested silver incorporated nanostructured carbon composite electrodes allowed the anodic stripping voltammetric detection of arsenic (III) from the aqueous solutions with different electroanalytical parameters in direct relation with electrode compositions and structures. CNT-ZAAg-Epoxy electrode gave the best electroanalytical performance for the anodic stripping voltammetric detection of arsenic (III) using CV, being selected for optimization of operating conditions.

The very good electroanalytical parameters for As (III) detection in relation with the sensitivity and the lowest limit of detection were achieved. Both the lowest limit of detection and the limit of quantification are below the maximum allowable concentration imposed in drinking water.

Very interesting results related to the electroanalytical parameters for arsenic detection were achieved by cathodic voltammetric determination on CNT-ZAAg-Epoxy composite electrode. However, the negative potential value of about -0.9 V/SCE limit its practical application.

Silver content is higher within the composition of CNT-ZAAg-Epoxy electrode by electrodeposition. The optimized electrodeposition of silver on CNT-ZAAg-Epoxy electrode consisted of the deposition potential of -0.4 V/SCE for deposition time of 10 seconds. Under the optimized electrodeposition and operating condition, the electroanalytical parameters for arsenic (III) detection were improved. The sensitivity of 128.15 $mAmM^{-1}cm^{-2}$ and the lowest limit of detection of 0.02 μM.

Also, silver was electrodeposited on CNT/ and zeolite-modified composite electrode and these electrodes are also suitable for arsenic (III) detection from water.

After the optimization procedure for arsenic (III) detection, the optimum detection scheme using CNF-Epoxy (Ag) electrode was proposed as:

Step 1-Deposition: $As^{3+}+3e^{-}\rightarrow As^{0}$, occurred at the potential value of -0.4 V/SCE for 60 seconds;

Step2-Anodic stripping: $As^{0}\rightarrow As^{3+}+3e^{-}$, occurred at the potential value of +0.09 V/SCE during square-wave voltammetry running.

Moreover, CNF-Epoxy (Ag) electrode was successfully used for simultaneous detection of As (III) and Pb (II) from aqueous solution based on the detection scheme:

Step 1- Deposition: $As^{3+}+3e^{-}\rightarrow As^{0}$, occurred at the potential value of -0.4 V/SCE for 60 seconds;

Step 2-Deposition: $Pb^{2+}+2e^{-}\rightarrow Pb^{0}$, occurred at the potential value of -0.7 V/SCE for 60 seconds;

Step3-Anodic stripping: $As^{3+}+3e^{-}\rightarrow As^{0}$ and $Pb^{0}+2e^{-}\rightarrow Pb^{2+}$, occurred during square-wave voltammetry running.

11.5. References

[1] http://www.epa.gov/savewater/arsenic/basicinformation.html.
[2] http://www.who.int/mediacentre/factsheet/fs210/en.
[3] K. Fujiwana, H. Tsubota, T. Kumamaru, Anal. Sci. 7 (1991) 991.
[4] Z. Gong, X. Lu, M. Ma, C. Watt, X.C. Le, Talanta 58 (2002) 77.
[5] B. Raman, V.M. Shinde, Anal. Lett. 20 (1987) 1029.
[6] W.C. Story, J.A. Caruso, J. Chromatogr. Sci. 30 (1992) 427.
[7] S.C. Shum, R. Neddersen, R.S. Houk, Analyst 117 (1992) 577.
[8] D.Q. Hung, O. Nekrassova, R.G. Compton, Talanta 6 (2004) 269.
[9] K.A. Francesconi, D. Kuehnelt, Analyst 129 (2004) 373.
[10] A.O. Simm, C.E. Banks, J. Wilkins, N.G. Karousos, J. Davis, R.G. Compton, Anal. Bioanal. Chem. 381 (2005) 979.
[11] G. Forsberg, J. W. O'Laughlin, R. Mergargle, S.R. Koirtyohann, Anal. Chem. 47 (1975) 1586.
[12] D.G. Williams, D.C. Johnson, Anal. Chem. 64 (1992) 1785.
[13] R.S. Sadana, Anal. Chem. 55 (1983) 304.
[14] M.A. Ferreira, A. Barros, Anal. Chim. Acta 459 (2002) 151.
[15] J. Wang, K. Varughege, Anal. Chem. 62 (1990) 318.
[16] J.H. Yoon, G. Muthuraman, J.E. Yang, Y.B. Shim, M.S. Won, Electroanal. 19 (2007) 1160.
[17] S. Liu, J. Li, X. Mao, P. Gao, Anal. Lett. 36 (2003) 1381.
[18] H.H. Frey, C.J. McNeil, R.W. Keay, J.V. Bannister, Electroanal. 10 (1998) 480.
[19] S.B. Khoo, J. Zhu, Analyst 121 (1996) 1983.
[20] B. Hoyer, T.M. Florence, G.E. Batley, Anal. Chem. 59 (1987) 1608.
[21] D.R. Kendall, Anal Lett 5 (1972) 867.
[22] **A. Baciu**, A. Remes, A. Pop, F. Manea, G. Burtica, The 17th Int Sympos Anal Environ Probl, Szeged, 19, September, 2011, 339.
[23] A. Pop, F. Manea, A. Remes, **A. Baciu**, C. Orga, N. Vaszilcsin, S. Picken, J. Schoonman, IEEE Sens Proceedings (2011) 581.
[24] **A. Baciu**, A. Remes, E. Ilinou, F. Manea, S.J. Picken, J. Schoonman Eviron. Eng. Manag. J. 11, (2012) 1967.
[25] S.S. Mendez, O.D. Renedo, M.L.A. Martinez, Electroanal. 21 (2009) 635.
[26] S.H. Shin, H.G. Hong, Bull. Korean Chem. Soc. 31 (2010) 3077.
[27] X. Dai, R.G. Compton, Electroanal. 17 (2005) 1325.

[28] X. Dai, R.G. Compton, Analyst 131 (2006) 516.
[29] R. Baron, B. Sljukic, C. Salter, A. Crossley, R.G. Compton, Russ. J. Phys. Chem. A 81 (2007) 1443.
[30] A.O. Simm, C.E. Banks, R.G. Compton, Electranal. 17 (2005) 1727.
[31] J. Junsomboon, P. Sooksamiti, K. Grudpan, S. Lapanantnoppakhum, P. Thavornyuthikarn, J. Jakmunee, Chiang. Mai. J. Sci 36 (2009) 369.
[32] Y. He, Y. Zheng, D.C. Locke, Microchem. J. 85 (2007) 265.
[33] G. Henze, W. Wagner, S. Sander, Fresen. J. Anal. Chem. 358 (1997) 741.
[34] H. Li, R.B. Smart, Anal. Chim. Acta 325 (1996) 25.
[35] Y. Bonfil, E. Kirowa-Eisner, Anal. Chim. Acta 547 (2002) 285.
[36] Brevet de inventie national, F. Manea, A. Pop, **A. Baciu**, A. Remes, nr. OSIM: A/00555/05.11.2012.
[37] E. Kirowa-Eisner, M. Brand, D. Tzur, Anal. Chim. Acta 385 (1999) 325.
[38] G.M.S. Alvesa, J.M.C.S. Magalhãesa, P. Salaünb, C. M.G. van den Berg, Anal. Chim. Acta 703 (2011) 1.
[39] G. Billon, C.M.G. van den Berg, Electroanal. 16 (2004) 1583.
[40] B. Bas, M. Jakubowska, Anal. Chim. Acta 615 (2008) 39.

CHAPTER 12. GENERAL CONCLUSIONS

- The original contributions of the thesis are related to the elaboration, manufacturing of several unmodified and silver-modified carbon-epoxy composite electrode materials, which involve both the detailed characterization of electrode materials and their application for the electrochemical quantitative determination of pentachlorophenol and arsenic from water. Also, the electrode materials suitable for simultaneous detection of arsenic and lead were selected.
- Several unmodified and silver-modified carbon-epoxy composite electrodes were successfully obtained by two-roll mill procedure: carbon nanotubes-epoxy (CNT-Epoxy), carbon nanofibers-epoxy (CNF-Epoxy), silver-doped natural or synthetic zeolite-modified carbon nanotubes-epoxy (CNT-ZN/ZA-Ag Epoxy), silver-doped natural zeolite-modified carbon nanofibers-epoxy (CNF-ZNAg-Epoxy), silver-chemically decorated carbon nanotubes (CNF-Ag), silver-electrochemically decorated carbon nanotubes (CNT-Epoxy(Ag)).
- The morphological, structural and electrical characterization results of the above-presented compositions of the carbon-based composite electrode conclude:
  - The conductive fillers, *i.e.*, expanded graphite, carbon nanotubes and carbon nanofibers are well-distributed and dispersed within the epoxy matrix taken into account the specific preparation method involving method dispersion within suitable solvent by sonication;
  - Silver presence in various forms, *i.e.*, silver-modified natural/synthetic zeolite, chemically and electrochemically decorated silver particles was evidenced by SEM images;
  - The electrical conductivity of the composite electrode depended on the conductive filler type (expanded graphite, carbon nanotubes, and carbon nanofibers), its loading and distribution within epoxy matrix. Also, silver content and distribution within composite composition enhanced the electrical properties of the composite.
  - All prepared carbon based composite electrode are characterized by the electrical conductivities suitable for the electrochemical applications.
- The electrochemical behaviour of the well-known ferri/ferrocyanide standard redox system allowed determining the electroactive surface area of these electrodes. All tested carbon-based composite electrode exhibited the electroactive surface area at least or quite higher equal to the geometrical one. Expanded graphite-epoxy composite electrode exhibited the lowest electrode area and the presence of nanostructured carbon within the composite composition enhanced the electroactive area. The best electroactive area was determined for carbon nanotubes-epoxy composite electrode.
- All unmodified carbon-based composite electrodes, *i.e.*, EG-Epoxy, CNF-EG-Epoxy and CNF-Epoxy composite electrodes exhibited the availability for the direct anodic oxidation of pentachlorophenol (PCP), giving them a real potential for the ampeormetric / voltammetric detection of PCP.
- Even if several characteristics regarding the direct electrooxidation of pentachlorophenol are common for all carbon-based composite electrodes,

specific peculiarities linked to carbon structure gave them different performances for PCP detection.

- The electrode performance for PCP detection in relation with the sensitivities increased as: CNT-Epoxy>CNF-EG-Epoxy>EG-Epoxy. Also the best limit of detection and quantification were achieved for CNT-Epoxy electrode.
- However, the detection potential value of -0.2 V/SCE determined for EG-Epoxy is very promising for practical application for selective determination of PCP from aqueous solution by voltammetric technique. This detection potential value was found only for EG-Epoxy electrode based on the PCP anodic oxidation peak that increased linearly with its concentration. This detection potential value did not appear due to the electrode electrocatalytic activity, but the electrode surface modification during PCP electrooxidation process. The electrode surface modification is not desired during the detection process, but in this case this situation was exploited in a positive way envisaging the selective detection of PCP.
- The replacement of a part of EG with CNF improved slightly sensitivity and the lowest limit of detection and quantification, while the full replacement of EG with CNT enhanced the electroanalytical parameters for PCP detection.
- The exploitation of pulsed voltammetric/amperometric techniques allowed enhancing the electroanalytical parameters for PCP detection.
- Nanostructured carbon reinforcement within the composite composition exhibited the enhanced electrocatalytic activity only by background and useful signal improvement and not by shifting the oxidation potential to lower values.
- The selection of the electrode type, the electrochemical technique, and the operating conditions will be made taking into account the specific requirements imposed by the practical utility.
- Several nanostructured carbon based composite electrodes, *i.e.*, carbon nanotubes-epoxy (CNT-Epoxy), carbon nanofibers-epoxy (CNF-Epoxy), silver-doped natural or synthetic zeolite-modified carbon nanotubes-epoxy (CNT-ZN/ZA-Ag Epoxy), silver-doped natural zeolite-modified carbon nanofibers-epoxy (CNF-ZNAg-Epoxy), silver-chemically decorated carbon nanotubes (CNF-Ag), silver-electrochemically decorated carbon nanotubes (CNT-Epoxy(Ag)) were tested for arsenic (III) detection from water. No signal corresponding to the arsenic oxidation and reduction was noticed in CNT-Epoxy and CNF-Epoxy.
- Silver-incorporated nanostructured carbon-based composite electrodes exhibited the electrocatalytic activity towards arsenic (III) reduction and oxidation in acidic aqueous media.
- Silver incorporation within CNT and CNF based composite electrode by synthetic/natural zeolite doping with silver ions or direct by chemical reducing as metallic silver directly on carbon surface led to achieving a response in the presence of arsenic (III). This response corresponding to the anodic stripping arsenic from the electrode surface applied after a deposition step in which arsenic (III) is reduced at arsenic on the electrode surface at the potential not too negative.
- All tested silver incorporated nanostructured carbon composite electrodes allowed the anodic stripping voltammetric detection of arsenic (III) from aqueous solutions with different electroanalytical parameters in direct relation with electrode composition and structures. CNT-ZAAg-Epoxy electrode gave the best electroanalytical performance for the anodic stripping voltammetric detection of arsenic (III) using CV, being selected for optimization of operating conditions.

- The very good electroanalytical parameters for As (III) detection in relation with the sensitivity and the lowest limit of detection were achieved. Both the lowest limit of detection and the limit of quantification are lower that the maximum allowable concentration imposed in drinking water, which makes this electrode to be appropriate for real applications of arsenic (III) electrochemical detection.
- The silver content was higher by electrodeposition resulting CNT-ZAAg-Epoxy electrode. The optimized electrodeposition of silver on CNT-ZAAg-Epoxy electrode consisted of the deposition potential of -0.4V/SCE for deposition time of 10 seconds. Under the optimized electrodeposition and operating condition, the electroanalytical parameters for arsenic (III) detection were improved, the sensitivity of 128.15 $mAmM^{-1}cm^{-2}$ and the lowest limit of detection of 0.02 μM.
- Also, silver was electrodeposited on CNT/ and zeolite-modified composite electrode and these electrodes are also suitable for arsenic (III) detection from water.
- After the optimization procedure for arsenic (III) detection, the optimum detection scheme using CNF-Epoxy (Ag) electrode was proposed as:

Step 1-Deposition: $As^{3+}+3e^{-}\rightarrow As^{0}$, occurred at the potential value of -0.4 V/SCE for 60 seconds.

Step2-Anodic stripping: $As^{0} \rightarrow As^{3+}+3e^{-}$, occurred at the potential value of +0.09 V/SCE during square-wave voltammetry running.

- Moreover, CNF-Epoxy (Ag) electrode was successfully used for simultaneous detection of As (III) and Pb (II) from aqueous solution based on the detection scheme:

Step 1- Deposition: $As^{3+}+3e^{-}\rightarrow As^{0}$, occurred at the potential value of -0.4 V/SCE for 60 seconds.

Step 2-Deposition: $Pb^{2+}+2e^{-}\rightarrow Pb^{0}$, occurred at the potential value of -0.7 V/SCE for 60 seconds

Step3-Anodic stripping: $As^{3+}+3e^{-}\rightarrow As^{0}$ and $Pb^{0}+2e^{-}\rightarrow Pb^{2+}$, occurred during square-wave voltammetry running.

- The electroanalytical performance of unmodified carbon nanotubes-epoxy composite electrode for pentachlorophenol detection using voltammetric/amperometric techniques and of silver-electromodified carbon nanofibers-epoxy composite electrode for arsenic detection using cathodic voltammetric and especial, stripping anodic voltammetric techniques gave these electrides a great potential for the practical applications. In general, these sensors can be used for certain conditions, which are not appropriate for other detection variants and must be clear defined in direct relation with the imposed practical applications. Thus, electrochemical sensors and electroanalysis should be regarded as very interesting and actual alternative analytical techniques.